SOX11 transcription factor functional analysis in aggressive MCL

Maria Carmela Vegliante

INSTITUT D'INVESTIGACIONS BIOMÈDIQUES AUGUST PI I SUNYES (IDIBAPS)

MOLECULAR PATHOLOGY, PHARMACOLOGY AND MICROBIOLOGY DEPARTMENT

HOSPITAL CLINIC OF BARCELONA

FACULTY OF MEDICINE, UNIVERSITY OF BARCELONA

SOX11 transcription factor functional analysis in aggressive MCL

Thesis presented by **Maria Carmela Vegliante**

to obtain the degree of Doctor in Medicine

Ph.D. Program in Medicine

FACULTY OF MEDICINE, UNIVERSITY OF BARCELONA

Doctoral advisors:

Prof. **Elias Campo**

Dr. **Virginia Amador**

Barcelona 2013

Doctoral advisors:

Dr. Elias Campo, M.D., Ph.D

Dr. Virginia Amador, Ph.D

This work was supported by the *Ministerio de Economía y Competitividad* (MINECO) (BFU2009-09235 and RYC-2006- 002110) (V.A.), the *Ministerio de Ciencia e Innovación* (SAF 2008-03630 and BES-2009-017958) and the *Red Temática de Investigación Cooperativa en Cáncer* (RTICC) (E.C.). Fondo Europeo de Desarrollo Regional, Unión Europea, Una manera de hacer Europa (R06/ 0020/0039).

Ai miei genitori

To my family

A Peppe

Don't wait to finish university,
to fall in love,
to find a job,
to marry,
to have children,
to see them grow up,
to lose that ten kilos,
to wait for Friday night or Sunday morning,
for it to be spring, autumn, summer or winter.
There isn't a better moment to be happy than this, happiness is the way, not the destination.
Work as if you don't need money, love as if you never have been hurt, and dance as if nobody can see you.
Remember that the skin wrinkles, hairs become white and the days become years, but the important things don't change, and your power, your belief, doesn't age.
Your spirit is the feather duster that sweeps away every web.
Behind every finishing line there is a new start.
Behind every result there is a new challenge.
Until you'll live, feel alive.
Go on, even when everybody expects you to give up.

(Mother Teresa of Calcutta)

Non aspettare di finire l'università,
di innamorarti,
di trovare lavoro,
di sposarti,
di avere figli,
di vederli sistemati,
di perdere quei dieci chili,
che arrivi il venerdì sera o la domenica mattina,
la primavera, l'estate, l'autunno o l'inverno.
Non c'è momento migliore di questo per essere felice. La felicità è un percorso, non una destinazione.
Lavora come se non avessi bisogno di denaro, ama come se non ti avessero mai ferito e balla, come se non ti vedesse nessuno.
Ricordati che la pelle avvizzisce, i capelli diventano bianchi e i giorni diventano anni. Ma l'importante non cambia: la tua forza e la tua convinzione non hanno età.
Il tuo spirito è il piumino che tira via qualsiasi ragnatela.
Dietro ogni traguardo c'è una nuova partenza.
Dietro ogni risultato c'è un'altra sfida.
Finché sei vivo, sentiti vivo.
Vai avanti, anche quando tutti si aspettano che lasci perdere.

(Madre Teresa di Calcutta)

ABSTRACT

Mantle cell lymphoma (MCL) is an aggressive subtype of non-Hodgkin lymphomas associated with poor prognosis and frequent relapses. Recently, the neuronal transcription factor SOX11 has been identified as a very specific biomarker for MCL. SOX11 is constantly overexpressed in virtually all aggressive MCLs, and at lower levels in a subgroup of Burkitt lymphoma and acute lymphoblastic leukemia but not in other lymphoid neoplasms.

SOX11 was found exclusively overexpressed in conventional MCL and totally absent in normal lymphoid cells or in MCL patients with indolent clinical course and prolonged survival. Although SOX11 function and potential target genes in lymphoid cells are poorly known, the highly specific expression in aggressive MCL suggests that it may be an important element in the development and progression of this tumor.

Two publications resulted from our studies and compose this thesis.

In paper I, we have studied the molecular mechanisms leading to the aberrant expression of SOX11 in aggressive MCL.

MCL is one of the lymphoid neoplasms with highest number of genetic aberrations but none involving the SOX11 genomic region at chromosome 2p25. As no chromosomal changes affecting SOX11 locus were identified in MCL, we hypothesized that epigenetic events could lead to SOX11 aberrant overexpression. We performed a comprehensive SOX11 gene expression and epigenetic studies. We observed that SOX11 expression was associated with unmehtylated DNA and presence of activating histone marks (H3K9/14Ac and H3K4me3) in embryonic stem cells and some aggressive B-cell neoplasms, including MCL. Conversely, the loss of SOX11 expression in adult stem cells, normal hematopoietic cells and other lymphoid neoplasms was associated with the presence of silencing histone marks H3K9me2 and H3K27me3 with or without simultaneous DNA methylation. We concluded that the pathogenic role of SOX11 is associated with its *de novo* expression in some aggressive lymphoid malignancies, which is mediated by a shift from inactivating to activating histone modifications.

In paper II, we have focused on uncovering putative biological functions of SOX11 in aggressive MCL. Using chromatin immunoprecipitation microarray analysis combined with gene expression profiling upon SOX11 knockdown, we identified target genes and

transcriptional programs regulated by SOX11 including the block of mature B-cell differentiation, modulation of cell cycle, apoptosis, and stem cell development. PAX5 stood out as one of the major SOX11 direct target genes.

SOX11 silencing downregulates PAX5, induces BLIMP1 expression, and promotes the shift from a mature B-cell into the initial plasmacytic differentiation phenotype in both MCL primary tumor cells and an *in vitro* model. Our results suggested that SOX11 contributes to tumor development by altering the terminal B-cell differentiation program of MCL cells.

Moreover, we have demonstrated the tumorigenic ability of SOX11 *in vivo,* using a xenotransplant model of MCL in CB17-SCID mice. The significant reduction on tumor growth of the SOX11-silenced cells compared to the growth of control MCL cells in the xenograft experiments highlighted the implication of SOX11 expression in the aggressive behavior of this lymphoma.

Overall our results demonstrated that SOX11 can act as oncogene in MCL.

RESUMEN

El linfoma de células del manto (LCM) es un subtipo agresivo de linfoma non Hodgkin asociado a un mal pronóstico y recaídas frecuentes. Recientemente, el factor de transcripción neuronal SOX11 se ha identificado como un marcador muy específico de LCM. SOX11 se encuentra sobreexpresado constantemente en todos los LCM agresivos y en niveles más bajos en un subgrupo de Burkitt linfoma (BL) y leucemia linfoblástica aguda (LLA) aunque no en otros neoplasmas linfoides.

SOX11 se encontró exclusivamente sobreexpresado en LMC convencionales y totalmente ausente en células linfoides normales o en pacientes LMC con un curso clínico indolente y una supervivencia prolongada.

Aunque la función de SOX11 y sus genes potenciales dianas aún se desconocen, su elevada expresión específica en LCM sugiere que puede ser un elemento importante en la progresión y desarrollo de este tumor.

Se han obtenidos dos publicaciones de los estudios que componen esta tesis. En el primer artículo hemos estudiado los mecanismos moleculares responsables de la expresión aberrante de SOX11 en LCM agresivo.

El artículo I proporciona una caracterización exhaustiva de los mecanismos epigenéticos que conducen a la desregulación de SOX11 en estas neoplasias linfoides.

En general se observó una significativa correlación inversa entre la metilación del promotor de SOX11 y la expresión de dicho gen. Sin embargo, en muchas muestras (células madre embrionarias, ESC, o adultas, células B normales y algunos LCM indolentes, leucemia linfática crónica y linfoma folicular) la expresión de SOX11 se vió reprimida a pesar de su estado no metilado. Estos hallazgos nos sugieren que la expresión de SOX11 no depende exclusivamente del estado de metilación del ADN del gen y nos llevó a estudiar mecanismos epigenéticos alternativos.

Hemos observado que la expresión de SOX11 se asocia con la presencia de marcas de activación de las histonas (H3K9/14Ac y H3K4me3) en las células madre embrionarias y algunas neoplasias de células B agresivas. Por el contrario, en las muestras que no expresan SOX11, incluidas las células madre adultas, las células hematopoyéticas normales y diversas neoplasias linfoides, se observó que el promotor de SOX11 mostraba un enriquecimiento en las marcas de silenciamiento H3K9me2 y H3K27me3. El silenciamiento de SOX11 en líneas celulares fue revertido por el inhibidor de la

histona deacetilasa (SAHA) pero no por el inhibidor de la ADN metiltransferasa (AZA). Estos datos indican que, como SOX11 no se expresa en las células linfoides normales, no metiladas, lo más probable es que la hipermetilación del ADN en algunos tumores sin expresión de SOX11 sea funcionalmente inerte, y podría estar asociada con la reducción de la plasticidad epigenética en células tumorales. También observamos que la expresión *de novo* de SOX11 se asocia con las neoplasias linfoides agresivas como el LCM, algunos subtipos de B-LLA y algunos casos de BL, siendo este efecto mediado por un "switch" entre inactivación y activación de las modificaciones de las histonas.

Además, como SOX11 se expresa fuertemente en las ESC, los datos sugieren que la expresión de SOX11 podría estar asociada con la adquisición de características de la cromatina similares a la de las células madre.

En el artículo II nos hemos centrado en identificar las posibles funciones biológicas de SOX11 en LCM. Combinando análisis de microarray de inmunopecipitación de cromatina y perfil de expresión diferencial después de silenciar SOX11, hemos identificado genes dianas y programas transcripcionales regulados por SOX11, incluyendo el bloqueo de la diferenciación de la célula B madura, la modulación de ciclo celular, apoptosis y desarrollo de célula madre.

PAX5 destacó como uno de los genes diana directos de SOX11 más significativo. El silenciamiento de SOX11 downregula PAX5, induce la expresión de BLIMP1 y promueve el cambio de fenotipo de célula B madura a la diferenciación inicial plasmacítica, tanto en células tumorales primarias de LCM como en un modelo *en vitro*.

Nuestros resultados sugieren que SOX11 contribuye al desarrollo tumoral mediante la modulación del programa de diferenciación terminal de célula B en LCM.

Además, hemos demostrado la habilidad tumorigénica de SOX11 *en vivo* mediante un modelo de xenotrasplante de LCM en ratones CB17-SCID. La reducción significativa del crecimiento tumoral de las células con expresión de SOX11 silenciada comparada con el crecimiento de células de LCM con elevados niveles de expresión de SOX11 de los xenotrasplantes, demuestra la implicación de la expresión de SOX11 en el comportamiento agresivo de este linfoma.

En conclusión, nuestros resultados demuestran que SOX11 puede actuar como oncogén en LCM.

List of Papers

This thesis has been generated by the following papers, which are referred to in the text by the Roman numerals (I and II):

I. **Vegliante MC**, Royo C, Palomero J, Salaverria I, Balint B, Martín-Guerrero I, Agirre X, Lujambio A, Richter J, Xargay-Torrent S, Bea S, Hernandez L, Enjuanes A, Calasanz MJ, Rosenwald A, Ott G, Roman-Gomez J, Prosper F, Esteller M, Jares P, Siebert R, Campo E, Martín-Subero JI*, Amador V*. Epigenetic activation of SOX11 in lymphoid neoplasms by histone modifications. *PLoS One. 2011;6(6):e21382.*

II. **Vegliante MC***, Palomero J*, Pérez-Galán P, Roué G, Castellano G, Navarro A, Clot G, Moros A, Suárez-Cisneros H, Beà S, Hernández L, Enjuanes A, Jares P, Villamor N, Colomer D, Martín-Subero JI, Campo E, Amador V. SOX11 regulates PAX5 expression and blocks terminal B-cell differentiation in aggressive mantle cell lymphoma. *Blood. 2013 Mar 21;121(12):2175-85.*

* These authors contributed equally to this work.

Other published papers by the author associated with this thesis.

1. Royo C, Navarro A, Clot G, Salaverria I, Giné E, Jares P, Colomer D, Wiestner A, Wilson WH, **Vegliante MC**, Fernandez V, Hartmann EM, Trim N, Erber WN, Swerdlow SH, Klapper W, Dyer MJ, Vargas-Pabón M, Ott G, Rosenwald A, Siebert R, López-Guillermo A, Campo E, Beà S. Non-nodal type of mantle cell lymphoma is a specific biological and clinical subgroup of the disease. Leukemia. 2012 Aug;26(8):1895-8.

2. Navarro A, Clot G, Royo C, Jares P, Hadzidimitriou A, Agathangelidis A, Bikos V, Darzentas N, Papadaki T, Salaverria I, Pinyol M, Puig X, Palomero J, **Vegliante MC**, Amador V, Martinez-Trillos A, Stefancikova L, Wiestner A, Wilson W, Pott C, Calasanz MJ, Trim N, Erber W, Sander B, Ott G, Rosenwald A, Colomer D, Giné E, Siebert R, Lopez-Guillermo A, Stamatopoulos K, Beà S, Campo E. Molecular subsets of mantle cell lymphoma defined by the IGHV mutational status and SOX11 expression have distinct biologic and clinical features. *Cancer Res. 2012 Oct 15;72(20):5307-16.*

3. Navarro A, Clot G, Prieto M, Royo C, **Vegliante MC**, Amador V, Hartmann E, Salaverria I, Beà S, Martín-Subero JI, Rosenwald A, Ott G, Wiestner A, Wilson WH, Campo E, Hernandez L. microRNA expression profiles identify subtypes of mantle cell lymphoma with different clinicobiological characteristics. Clin Cancer Res. 2013 Jun 15;19(12):3121-3129.

CONTENTS

LIST OF SELECTED ABBREVIATIONS

ABC-DLBCL	Activated B-cell–like Diffuse large B-cell lymphoma
AID	Activation-induced deaminase
ALL	Acute lymphoblastic leukemia
AZA	5-azacytidine
BCL1	B-cell leukemia/lymphoma 1
BCL2	B-cell leukemia/lymphoma 2
BCR	B-cell receptor
BL	Burkitt lymphoma
BRCA1	Breast-cancer susceptibility gene 1
CCND1	Cyclin D1
CCND2	Cyclin D2
CCND3	Cyclin D3
CDK2	Cyclin-dependent kinase 2
CDK4	Cyclin-dependent kinase 4
CDK6	Cyclin-dependent kinase 6
ChIP	Chromatin immunoprecipitation
CLL	Chronic lymphocytic leukemia
CLP	Common lymphoid progenitor
CMP	Common myeloid progenitor
CRC	Chromatin remodeling complex
DC	Dendritic cell
DLBCL	Diffuse large B-cell lymphoma
DNMT	DNA methyltransferases
ELP	Early lymphoid progenitor
ESC	Embrionic stem cell
ETP	Early T-cell-lineage progenitor
FDC	Follicular dendritic cell
FL	Follicular lymphoma
GC	Germinal center
GCB-DLBCL	Germinal center B-cell–like Diffuse large B-cell lymphoma
GEP	Gene expression profiling
GSEA	Gene set enrichment analysis
HAT	Histone acetylase
HCL	Hairy cell leukemia
HDAC	Histone deacetylase
hESC	human embryonic stem cell

HMG	High mobility group
HSC	Hematopoietic stem cell
IGH	Immunoglobulin heavy locus
IGL	Immunoglobulin light locus
INF- I	Type I Interferon
iPSC	induced Pluripotent stem cell
IRF4	Interferon regulatory factor 4
LEF1	Lymphoid-enhancer-binding factor 1
LT	Long-term
MALT	Mucosa associated lymphoid tissue
MAPC	Multipotent adult progenitor cell
MBD2	Methyl CpG-binding domain protein 2
MCL	Mantle cell lymphoma
Mi-2/NuRD	Mi-2/Nucleosome remodeling and deacetylase
miRNA	microRNA
MLL2	Mixed-lineage leukemia 2
MPP	Multipotential progenitor
MSC	Mesenchymal stem cell
MTC	Major translocation cluster
NF-κB	Nuclear factor κB
NGS	Next-generation sequencing
NHL	non-Hodgkin lymphoma
NK	Natural killer
NLS	Nuclear localization signal
PAX5	Paired box 5
PcG	Polycomb group
qRT-PCR	quantitative Real time polymerase chain reaction
RNAi	RNA interference
RNA-seq	RNA sequencing
SAHA	Suberoylanilide hydroxamic acid
sIG	Surface immunoglobulin
SMZL	Splenic marginal zone lymphoma
SOX	Sex-determining region Y (SRY) box
SOX 4	Sex-determining region Y (SRY) box 4
SOX 11	Sex-determining region Y (SRY) box 11
ST	Short-term
SWI/SNF	Switch/sucrose non-fermenting

TAD	Transactivation domain
TCF	T-cell factor
TNF	Tumor necrosis factor
UPR	Unfolded proteins
UTR	Untranslated region
VHL	von Hippel-Lindau disease
WHO	World health organization

1. INTRODUTION

MCL is an aggressive subtype of non-Hodgkin lymphoma (NHL) characterized by the hallmark translocation t(11;14)(q13;12) driving the overexpression of cyclin D1 (CCND1) and by frequent additional cytogenetic alterations (Swerdlow et al., 2008).

MCL is one of the most aggressive lymphoid neoplasms associated with poor prognosis. However, recent studies have identified a distinct clinical group of t(11;14)(q13;12)-positive MCL patients that show an indolent clinical course and prolonged survival (Orchard et al., 2003; Fernandez et al., 2010).

Contrary to conventional MCLs (cMCL), these indolent MCLs (iMCL) have very stable karyotypes with virtually no chromosomal alterations other than the classical t(11;14), they frequently carry hypermutated immunoglobulin genes and frequently have a leukemic non-nodal MCL clinical presentation (Orchard et al., 2003; Fernandez et al., 2010; Ondrejka et al., 2011). In contrast with the high levels of expression of SOX11 in classic MCL, SOX11 is not expressed in iMCLs, lymphoid progenitors and mature B-cells (Fernandez et al., 2010; Royo et al., 2012; Navarro et al., 2012). These findings suggest that SOX11 plays a relevant role in the pathogenesis of these tumors. However, the function of SOX11 and its potential target genes in lymphoid cells remain unknown.

This thesis focuses on the putative role of SOX11 in the pathogenesis and aggressiveness of MCL, deciphering its function to uncover basic mechanisms underlying the complex biology of this aggressive tumor.

1.1. B-cell lymphomas

1.1.1. B-cell differentiation process and function

The lymphoid system is traditionally divided into primary and secondary lymphoid tissues. **Primary lymphoid tissues** are the tissues in which lymphocytes are generated and differentiate into mature naive lymphocytes: these are the bone marrow for B-cells, and the bone marrow and the thymus for T cells. Mature B-cells migrate to **secondary lymphoid tissues** which include blood, spleen, lymph node and mucosa-associated lymphoid tissue (MALT)

B-cell development is a multistep process that encompasses a continuum of stages that begin in primary lymphoid tissue, with subsequent functional maturation in secondary

lymphoid tissue. The functional end point is antibody production by terminally differentiated plasma cells (LeBien and Tedder, 2008).

Hematopoietic stem cells (**HSC**s), located in the bone marrow, give rise to mature B-cells through the sequential differentiation of lymphoid progenitor cells. Long-term HSCs (**LT-HSC**s) have the ability to self-renewal and reconstitute the entire immune system by differentiating into short-term HSCs (**ST-HSC**s). ST-HSCs differentiate into multipotential progenitors (**MPP**s) which is at the bifurcation between the myeloid and lymphoid lineages: MPPs can differentiate into common myeloid progenitors (**CMP**s) and or into early lymphoid progenitors (**ELP**s) (Medina et al., 2001). CMPs further differentiate into erythrocytes and megakaryocytes (Adolfsson et al., 2005), whereas ELPs can branch into thymic precursors of the T-cell lineage (early T-cell-lineage progenitors, **ETP**s) (Allman et al., 2003) or into bone-marrow commonlymphoid progenitors (**CLP**s), which are lymphoid restricted and can generate B-cells, T-cells, dendritic cells (**DC**) and natural killer (**NK**) cells (Figure 1) (Matthias and Rolink, 2005).

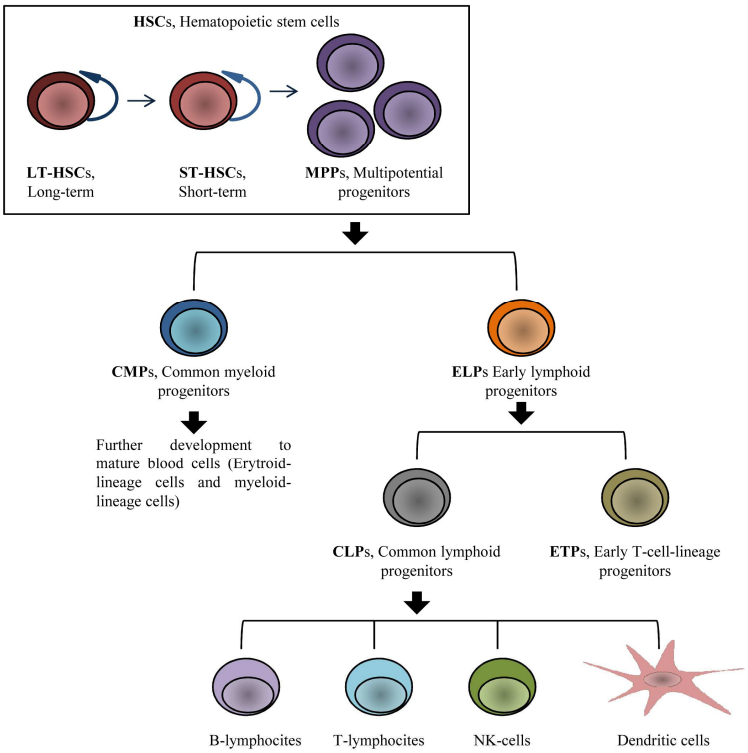

Figure 1. Development of haematopoietic stem cells. HSCs can be subdivided into long-term self-renewing HSCs, short-term self-renewing HSCs and multipotent progenitors (blue arrows indicate self-renewal). HCSs differentiate through a number of immature stages, e.g., common myeloid progenitors (**CMP**s), early lymphoid progenitors (**ELP**s) which develop to mature blood cells depicted at the far bottom.

Once committed to the lymphoid lineage, further differentiation steps lead to the formation of pro-B and pre-B-cells, which are the early B-cell precursors for mature B-cells, germinal center B-cells and the terminally differentiated plasma cells.

Normal B-cell differentiation begins in the bone marrow, with the first precursor: pro-B-cell (or CLP-2) which expresses the B-cell marker B220 and can undergo immunoglobulin (IG) VDJ (variable, diversity and joining) gene rearrangement in the heavy chain gene locus.

The next step can be identified by expression of CD19 and completion of immunoglobulin heavy chain complex (IGH) D_H-to-J_H gene-segment rearrangement by pre-BI cells. The IGH locus then continues to rearrange its variable region gene segments until productive V_H–DJ_H alleles are generated in large pre-BII cells. These cells stop to express *Rag1* and *Rag2*, and they display the product of the rearranged IGH gene at the cell surface; there, it assembles with the surrogate immunoglobulin light chains (IGL) VpreB and λ5, together with the signaling molecules Igα (which is encoded by the *MB-1* gene) and Igβ (which is encoded by the *B29* gene) to form the pre-B-cell receptor (pre-BCR) (LeBien, 2000).

At this stage the immature B-cell, defined by the appearance of the assembled BCR at the cell surface, are tested for autoreactivity. B-cells that are autoreactive can be rescued by a secondary immunoglobulin gene rearrangement, which is known as receptor editing (Nemazee and Weigert, 2000), otherwise they are eliminated or inactivated by apoptosis or anergy, respectively. After they have successfully passed this examination, immature IgM^+ B-cells leave the bone marrow. They are first found in the spleen as transitional B-cells T1 (IgM^{high}, IgD^{low}, $CD21^{low}$, $CD23^-$) which undergo several selection steps (Allman and Pillai, 2008). T1 lymphocytes responding to autoantigens can be negatively selected, this step is therefore a crucial check-point for the generation of mature B-cells; differentially they convert in T2 transitional lymphocytes (IgM^{high}, IgD^{high}, $CD21^{high}$, $CD\ 23^+$) (Loder et al., 1999; Matthias and Rolink, 2005).

Only 1-3% of splenic transitional B-cells can differentiate in naive B-cells. Naive B-cells are divided into two groups: marginal zone B-cells (IgM^{high}, IgD^{low}, $CD21^{high}$, $CD23^-$) and follicular B-cells (IgM^{high}, IgD^{int}, $CD21^{int}$, $CD23^+$). In the secondary lymphoid organs, the naive B-cells, expressing CD5, in response to a T-cell dependent antigen, are costimulated by T-cells. They give rise to immune reaction, through the

interaction with follicular dendritic cells (FDC) and form a germinal centre (GC) (Liu et al., 1991; Liu, 2005). In mature GCs two compartments are established, termed the "dark zone" and "light zone" on the basis of their histological appearance, which are surrounded by follicular mantle cells. The dark zone contains a high density of large, proliferating B-cells with downregulated surface immunoglobulin (sIg) expression known as centroblast (Nieuwenhuis and Opstelten, 1984; MacLennan, 1994). At the distal pole lies the light zone, where the density of B-cells is lower and the density of FDC network higher. Light zone B-cells, so called centrocytes, are small B-cells with lower mitotic rate and expressing higher surface immunoglobulins (Figure 2).

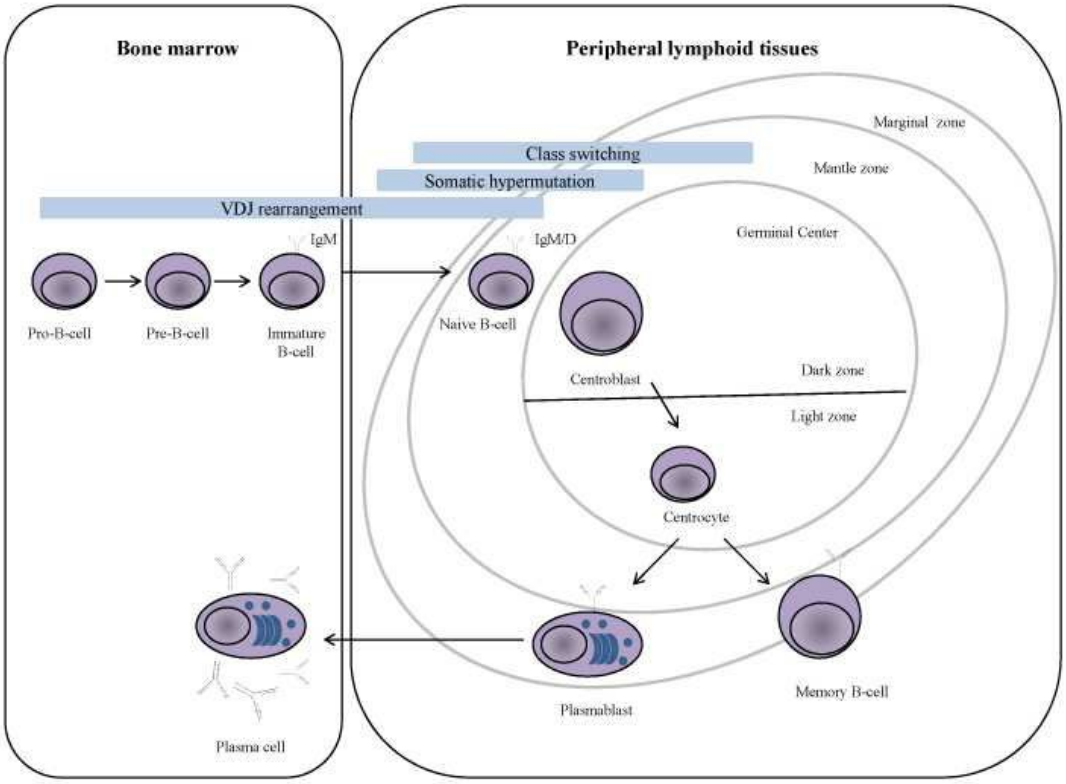

Figure 2. B-cell maturation and function in the periphery. B-cells that exit the bone marrow (left) as immature B-cell enter secondary lymphoid organs where they undergo several steps of maturation (right).

The GC B-cells also express CD10 and the transcription factor BCL-6, which are negative in naive B-cells, memory B-cells and plasma cells. Another important feature of the GC B-cells is that they switch off the expression of the anti-apoptosis protein BCL-2, thus they are susceptible to death through apoptosis. Apoptosis of the GC B-cells can be prevented by survival and proliferation-promoting signals provided by FDCs and T-cells (Liu et al., 1996).

In the GC, B-cells are involved in two different genetic processes: somatic mutation and isotype switching. Somatic mutation occurs mainly in the regions of the immunoglobulin heavy and light chain variable genes that form the antigen binding site, aiming to increase the affinity of surface IG receptors. Since this process is partially random, these mutations may result in decreased affinity of the IG receptor. Such cells can not bind to the antigen retained on the FDC and therefore do not receive survival signals. Almost 90% of the GC B-cells die through apoptosis; only those B-cells that have an increased affinity to the antigen presented by FDC will bind to the antigen and receive survival signals from FDC (Liu et al., 1996; Alt et al., 1984). The isotype switch process takes place on the IG heavy chain and the switch goes from IgM to IgG, IgA or less commonly to IgE. Importantly, somatic hypermutation may also occur in non-IG genes. A fraction of normal GC and memory B-cells carry BCL6 and CD95 (also called FAS) gene mutations (Pasqualucci et al., 1998; Gronbaek et al., 1998).

Centrocytes that survive in the GC mature into class switched plasma cells or memory cells (Harris et al., 2001). Plasma cells enter the blood and home to the bone marrow. These cells lack expression of B-cell markers, CD19, CD20 and sIG, but express the adhesion molecules CD138 and CD38 (Rawstron, 2006). In plasma cells, the production of immunoglobulin shifts from a membrane-bound form, as found in mature B-cells, to a secreted form, and after primary immunization they persist for only a few days, they are also called short-lived population cells (Matthias and Rolink, 2005). Memory B-cells comprise some of the cells in the follicular marginal zone of lymph nodes and spleen, these cells also home to the bone marrow. Memory B-cells express CD27 and strong IgM but little IgD (Gronbaek et al., 1998; Spencer et al., 1985). Conversely, memory B-cells are classified as long-lived population originated from GC B-cells and reside mainly in the bone marrow (Figure 3).

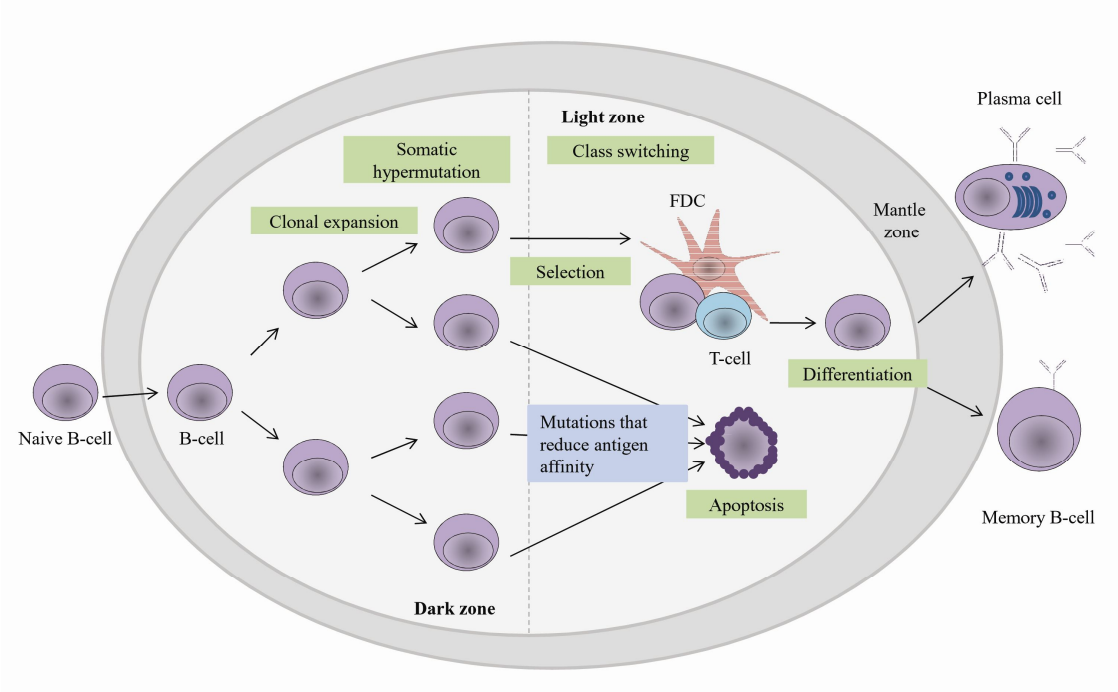

Figure 3. B-cell differentiation in the germinal-centre reaction. Mature (naive) antigen-activated B-cells that receive signals known as "T-cell help" are driven into B-cell follicles in secondary lymphoid organs such as lymph nodes, where they establish a germinal center (highest grey region). **FDC**, follicular dendritic cell. Modified from (Matthias and Rolink, 2005).

1.1.2. Key transcription factors for B-cell development

In recent years the network of transcription factors involved in all differentiation steps of B-lymphopoiesis is beginning to be understood. Every step in B-cell development is characterized by the activation of the specific genetic program of the new intermediate/progenitor generated and the repression/extinction of the genetic program of the previous cellular state. To achieve this, the distinct differentiation steps are tightly regulated at the transcriptional level. The following section sheds light on the critical transcription factors in the control of B-cell development and maturation.

IKAROS and PU.1: early specification towards the lymphoid lineage

IKAROS and **PU.1** are two transcription factors which play critical roles in the early cellular specification towards the lymphoid lineage. IKAROS was shown to be a crucial transcription factor for the commitment of ELPs into CLPs, clearly demonstrating its key role in the early cellular decision to undergo lymphocyte development. IKAROS functions either as a transcriptional activator or repressor by recruiting various chromatin remodeling complexes (CRCs) including SWI/SNF (related to the yeast switch/sucrose non-fermenting) or Mi-2/Nucleosome Remodeling and Deacetylase (Mi-

2/NuRD) to DNA regulatory elements (O'Neill et al., 2000; Kim et al., 1999; Sridharan and Smale, 2007).

IKAROS promotes B-cell identity, because it was observed that IKAROS-deficient pro-B-cells expressing EBF1 and PAX5 were uncommitted (Reynaud et al., 2008). Thus, IKAROS restricts the self-renewal program in early hematopoiesis, while it advances the B lineage program at later stages of development.

The transcription factor PU.1, an Ets family transcription factor encoded by *Sfpi1* gene, regulates the bifurcation between myeloid and B lymphoid development (DeKoter and Singh, 2000). Low concentrations of PU.1 favor the B-cell fate, while higher concentrations promote myeloid differentiation. Infact, mice deficient for PU.1 die around birth and lack B, T, NK and myelomonocytic cells (McKercher et al., 1996; Lee et al., 2002).

LEF1 and SOX4: early B-cell committed

LEF1 (lymphoid-enhancer-binding factor 1) is also expressed by developing B and T cells, as well as at many sites of organ formation during embryogenesis. LEF1 is highly related to T-cell factor 1 (TCF1), TCF2 and TCF3, which have been implicated in control of transcription in T cells (Schilham and Clevers, 1998). LEF1 and TCFs interact with β-catenin and are the downstream integrators of the WNT-signaling pathway (Schilham et al., 1996). By itself, LEF1 does not activate transcription, but it can function as an architectural protein promoting the formation of multiprotein complexes on enhancer DNA sequences by inducing DNA bending.

The transcription factors **SOX4** (sex-determining region Y (SRY) box 4) is a member of the High-Mobility Group (HMG) box family and has a crucial role at an early stage of B-cell development. In adult mice, *Sox4* is expressed mainly by immature T and B-cells, whereas during embryogenesis, expression is broader. Mice lacking Sox4 die at E14 due to a defect in cardiac formation. However, when *Sox4*–/– fetal liver cells were used to reconstitute the hematopoietic system of lethally irradiated mice, a very strong block was observed at the pro-B-cell-to pre-B-cell transition (Schilham et al., 1996).

PAX5 and BCL6: maintenance of B-cell identity

PAX5 is a paired homeodomain protein that is essential in determining and maintaining the fate of B-cells (Cobaleda et al., 2007). Its expression is first detected at the early pro-B-cell stage and increases in a stepwise manner during B-cell development until the plasma cell stage. PAX5 knockdown mice show a block in B-cell development at the pro-B stage (Urbanek et al., 1994). This factor works both as a transcriptional activator and repressor. It has been implicated in the direct transcriptional regulation of several B-cell specific genes, such as genes encoding essential components of the BCR like the costimulatory receptors CD19 and CD21, the signal-transducing chain Igα (CD79a) and the central adaptor proteins BLNK and LEF1 (Delogu et al., 2006; Nutt et al., 1998). PAX5 activated genes in pro-B-cells were found to be enriched with epigenetically active marks, including H3K9ac, H3K4me2 and H3K4me3 (McManus et al., 2011). By contrast, PAX5 represses the transcription of genes necessary for T-lymphopoiesis such as FLT-3, PD-1, NOTCH1, macrophage colony-stimulating factor receptor (M-CSFR), CCR2 and CD28 to render B-cell precursors unresponsive to myeloid cytokines (Pridans et al., 2008; Holmes et al., 2008).

PAX5 exerts its repressive function by recruiting members of the SWI/SNF chromatin remodeling complex (BRG1) and the NCoR1 repressor complex with its associated HDAC3 deacetylase activity to repress its target genes (McManus et al., 2011). PAX5 has similar relevant role in lymphocyte development promoting B-cell commitment and inhibiting plasma cell differentiation. The loss of PAX5 function is sufficient to promote IG secretion and plasma cell differentiation (Nera and Lassila, 2006). In GC B-cells, PAX5 represses the expression of XBP1, a transcription factor that is required for plasma cell differentiation (Reimold et al., 1996).

Interestingly, the conditional deletion of PAX5 in mature B-cells (Schebesta et al., 2007) also results in premature expression of genes encoding proteins involved in plasma cell differentiation and function, including BLIMP1, XBP1, J chain and secreted immunoglobulins (Nutt et al., 2011). In effect, PAX5 exerts its function as repressor of plasma cell differentiation through negative regulation of BLIMP1 that holds the position of a chief regulator that opens the way to the antibody secreting cell phenotype (Yasuda et al., 2012).

Due to its crucial role in normal B-lymphopoiesis, alteration of the *PAX5* gene is presumed to contribute to leukemogenesis.

Forced overexpression of PAX5 by t(9;14)(p13;q32) translocation has been identified in some B-cell lymphomas contributing to lymphomagenesis (Busslinger et al., 1996; Iida et al., 1996; Morrison et al., 1998).

Monoallelic deletion of *PAX5* has been observed in about 30% of children with Acute lymphoblastic leukemia (B-ALL), resulting in the loss of PAX5 protein expression or the production of a PAX5 protein lacking the DNA binding domain and/or transcriptional regulatory domain. Point mutations in *PAX5* are also observed (7–30%), and they also impair normal PAX5 function. Translocation of *PAX5* occurs in 1–2.5% of B-ALL cases, and they involve multiple partners such as *ETV6*, *ENL* and *FOXP1* (Mullighan et al., 2007; Familiades et al., 2009). The fusion transcript is thought to act as a constitutive repressor of the remaining *PAX5* allele or the fusion partner gene, which could result in a block of normal B-cell differentiation (Mullighan et al., 2007; Cobaleda et al., 2007; Nebral et al., 2009).

BCL6 is a transcriptional factor which is very highly expressed in GC B-cells and is essential for their formation. BCL6 is required during the extensive proliferation that characterizes GC B-cells and to allow somatic hypermutation (Basso and la-Favera, 2010).

The molecular mechanisms leading to induction of BCL6 expression in GC remain largely unknown. To date, IRF8 is the only transcription factor shown to be involved in BCL6 transcriptional activation (Lee et al., 2006).

BCL6 appears to modulate a very broad program in GC B-cells aiming to prevent premature activation and differentiation and to fine-tune the DNA damage response.

BCL6 acts on modulating a number of molecules involved in both BCR and CD40 signal transduction from the surface to the nucleus including Ca^{2+}-mediated signaling and the MAPK and NF-κB pathways, then ensuring that none of these pathways is prematurely activated (Saito et al., 2007; Niu et al., 1998). BCL6 has been shown to play a role in the modulation of molecules involved in the B-T cell interaction by regulating the expression of CD80 and CD274, both members of the B7-CD28 family (Niu et al., 2003; Basso, 2009). CD80 is expressed on antigen presenting cells including

B-cells, and its interaction with CD28 is required for T-cell activation, GC formation, and IG class switching (Borriello et al., 1997).

BCL6 also binds to the regulatory regions of many thousands of genes in GC including cell cycle inhibitor, CDKN1A (encoding p21), TP53 (encoding p53) and oncogenes such as MYC and BCL2 (Basso et al., 2010; Ci et al., 2009).

By contrast BCL6 also represses a number of genes required for the differentiation of B-cells into plasma cells, including BLIMP1 and IRF4 (Basso and la-Favera, 2010; Shaffer et al., 2000; Tunyaplin et al., 2004; Ci et al., 2009), two key transcription factors involved in the terminal differentiation of B-cells into plasma cells. BCL6 displays a broad control on the apoptosis pathway affecting multiple genes encoding both pro- and anti-apoptotic proteins (Basso et al., 2010; Ci et al., 2009), consistent with the observation that GC B-cells display a transcriptional profile characterized by downregulation of multiple anti-apoptotic genes and upregulation of pro-apoptotic genes (Klein et al., 2003), resulting in their high susceptibility to apoptosis.

BCL6 was identified as the target of chromosomal translocations affecting chromosome 3q27 in Diffuse large B-cell lymphoma (DLBCL) (Ye et al., 1993; Baron et al., 1993). BCL6 rearrangements were detected in approximately 40% of DLBCL and 5–10% of Follicuar lymphoma (FL) (Ye et al., 1993; Kerckaert et al., 1993; Lo et al., 1994; Butler et al., 2002). Different regulatory regions have been shown to be translocated upstream the BCL6 coding sequence, including those of the IGH and IGL loci, and the TTF, PAX5, BOB1, and H4 genes. A common feature of these promoters is their constitutive activity in the B-cell lineage, and in particular their persistent activity in post-GC cells, such as immunoblasts and plasma cells (Chen et al., 1998). Therefore, these chromosomal translocations cause deregulation of BCL6 expression by preventing its physiological downregulation in post-GC B-cells (Figure 4).

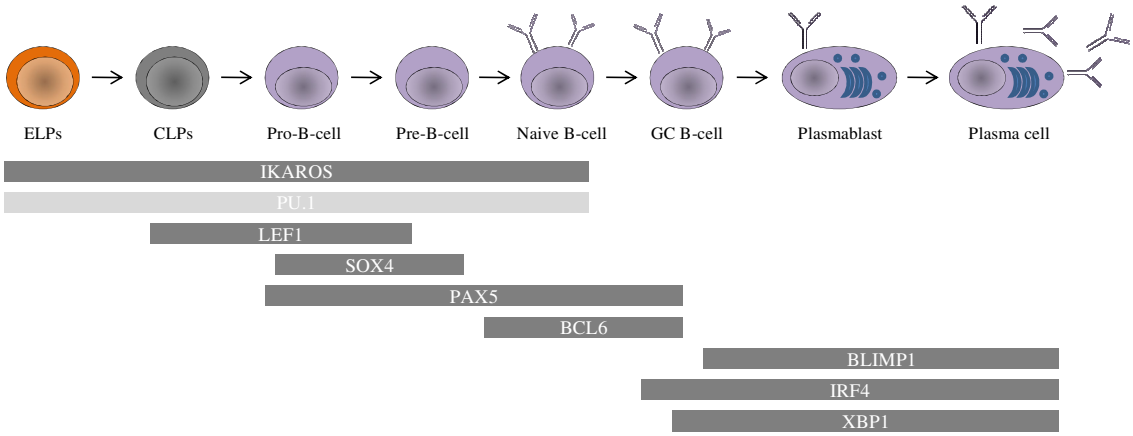

Figure 4. Transcription factors expression during B lymphopoiesis. The progression of cells from ELPs to plasma cell is shown. Grey dark bars represent high levels of gene expression of transcription factors that are important in B-cell development during the course of differentiation, shaded grey bar represents low expression. Modified from (Ramirez et al., 2010).

Terminal B-cell differentiation

Terminally differentiated B-cells are known as plasma cells. In these cells, the production of immunoglobulin shifts from a membrane-bound form, as found in mature B-cells, to a secreted form. The genesis of plasma cells is associated with the extinction of the transcriptional program that establishes the B-cell phenotype, and this transition seems to be mediated by a network of interacting transcriptional repressors.

BLIMP1 is considered the master regulator of plasma cell differentiation because it is able to induce plasmablatic features in transfected B-cells *in vitro* (Turner, Jr. et al., 1994), and its depletion in mouse B-cells prevents the development of plasma cell *in vivo* (Shapiro-Shelef and Calame, 2005).

BLIMP-1 has a major role in erasing the pre-plasma cell phenotypes by suppressing PAX5 and BCL6. This transcription factor is also responsible for the induction of expression of many genes in the plasma cell program, such as IRF4 and genes that are involved in immunoglobulin secretion like XBP1 (Shaffer et al., 2004). However, BLIMP1 is not essential for the initiation of the antibody-secreting cells program, as a pre-plasmablast population can be generated in its absence (Kallies et al., 2007). BLIMP1 is a tumor suppressor gene, it has been reported that loss of BLIMP1 by several mechanisms including deletions, gene mutations and transcriptional repression contributes to lymphomagenesis by blocking plasma cell differentiation in DLBCL (Mandelbau et al., 2010; Tam et al., 2006; Pasqualucci et al., 2006).

IRF4, a transcription factor expressed in immature B-cells and re-expressed in GC centrocytes, has been identified as a second master gene in plasma cell differentiation (Klein et al., 2006; Sciammas et al., 2006), controlling many processes such as Igκ gene recombination, immunoglobulin class switch recombination, GC B-cell formation and antibody-secreting cell differentiation (Shaffer et al., 2009). IRF4 is also broadly required for the differentiation of CD4+ T cells (Mittrucker et al., 1997). This transcription factor can bind to DNA weakly on its own, but displays strong co-operative binding in the presence of PU.1, or the closely related gene SPI-B (Brass et al., 1996; Brass et al., 1999). IRF4 is responsible for BLIMP1 induction (Nutt et al., 2011).

Two other members of the IRF family are known to be involved in B-cell differentiation. IRF8 is the closest relative of IRF4 and it is expressed very highly in GC B-cells. IRF5, instead, is involved in the type I interferon (IFN-I) and inflammatory responses (Takaoka et al., 2005; Paun et al., 2008).

XBP-1 is also essential for differentiation of plasma cells (Iwakoshi et al., 2003). This differentiation requires not only the expression of XBP-1 but the expression of the spliced isoform of XBP-1s.

XBP1 is ubiquitously expressed at low levels, but its expression is dramatically upregulated in antigen-secreting cells. Its expression is regulated by unconventional mRNA splicing, occurring predominantly in the cytoplasm, that is carried out by endonuclease IRE1 and a specific RNA ligase in response to the accumulation of unfolded proteins (UPR) in the endoplasmic reticulum, leading to the production of an active form of the transcription factor [pXBP1(S)]. Interestingly, XBP1 pre-mRNA is also translated into a functional protein [pXBP1 (U)] that negatively regulates the UPR.

Mammalian cells can quickly adapt to a change in conditions in the endoplasmic reticulum by switching proteins encoded in the mRNA from a negative regulator to an activator. This elaborate system contributes to various cellular functions, including plasma cell differentiation (Yoshida et al., 2001). In plasma cell differentiation, XBP1 seems to function downstream of BLIMP1 (Shaffer et al., 2004).

XBP-1-lacking plasma cells fail to colonize their long-lived niches in the bone marrow and to sustain antibody secretion (Hu et al., 2009). Recently a preplasmablast stage has been identified as a step preceding terminal plasma cell differentiation. This new cell

phenotype is characterized by very low immunoglobulin secretion and expression of XBP1 in the absence of detectable amounts of both BLIMP1 and IFR4 induction *in vitro* (Kallies et al., 2007). Afterwards BLIMP1, IRF4 and XBP1 are independently regulated proteins, all of which are required for terminal plasma cell differentiation downstream of PAX5 inhibition (Figure 5) (Shapiro-Shelef and Calame, 2005).

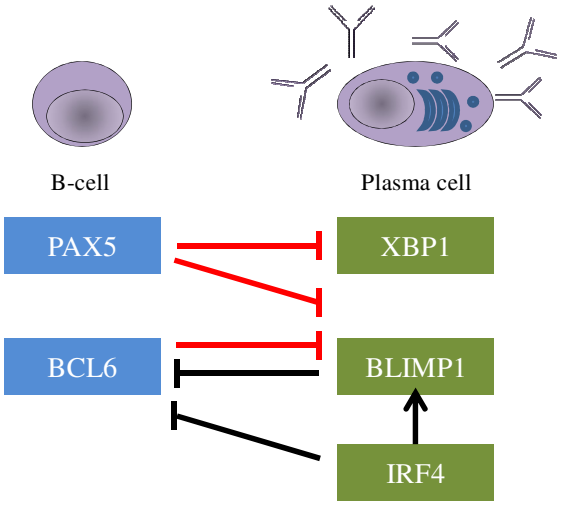

Figure 5. Model of the transcriptional network controlling B-cell terminal differentiation. ↑, indicates positive regulation of gene expression, ⊣ indicates repressive activity. Modified from (Nutt et al., 2011).

1.1.3. B-cell lymphomas

Malignancies of B-cell occur when the normal regulation of cell differentiation is disrupted and there is a subsequent accumulation of cells that have been blocked at a particular stage of normal B-cell development. Malignant lymphomas have been classified by the WHO (World Health Organization) into disease categories based on histological features, cell surface markers, cytogenetic, clinical features and pathogenic mechanisms (Swerdlow et al., 2008).

Small B-cell lymphomas comprise approximately 50% of the B-cell NHLs and include follicular lymphoma (FL; 40%), mantle cell lymphoma (MCL; 7%), marginal zone B-cell lymphoma (MZL; 12%) and B-cell chronic lymphocytic leukemia (B-CLL; 3%–4%). Diffuse large B-cell lymphoma (DLBCL) constitutes the majority of the remaining 50% of B-cell NHLs and can be sub-classified as either GC B-cell–like (GCB-DLBCL) or activated B-cell–like (ABC-DLBCL). Burkitt lymphoma (BL) represents only 2% of GC B-cell lymphomas.

B-cell chromosome translocations play an important role in lymphoma development, however these abnormalities alone do not always result in transformation, and therefore additional genetic and epigenetic alterations are required for cells to become fully malignant.

Frequently, these chromosomal translocations involve IG genes and a variety of partner genes leading either to transcription deregulation or production of chimeric proteins.

Translocations occur at three stages in B-cell development: during V(D)J recombination in the bone marrow, during somatic hypermutation and during class switch in the GC (Kuppers, 2005; Kuppers and Dalla-Favera, 2001). Two paradigms of translocation that involve naive B-cell are the t(11;14) (q13 ;q32) *BCL1-IGH* translocation in MCL and the (14;18)(q32;q21) *BCL2-IGH* translocation in FL (Tsujimoto et al., 1985; Tsujimoto et al., 1988). In MCL, the translocation leads to overexpression of cyclin D1, causing deregulation the cell cycle. In FL, the translocation causes deregulated expression of the anti-apoptotic protein BCL-2.

BCL-2 is used as a diagnostic marker since it can be used to distinguishing normal B-cell follicles from neoplastic follicles observed in FL. Translocations that occur during somatic hypermutation are characterized by breakpoints within or adjacent the rearranged V(D)J genes, and these V region are mostly somatically mutated (Kuppers and Dalla-Favera, 2001; Goossens et al., 1998). The *MYC-IG* translocations in BL and some translocations of the *BCL6* gene in DLBCL show translocation breakpoints in somatically mutated V region genes (Denny et al., 1985; Akasaka et al., 2000). The third kind of translocation was detected in the chromosome breakpoints located in *IGH* switch regions. Many different translocations have been detected involving breakpoints in the *IGH* switch regions such as *MYC* in sporadic BL (Figure 6) (Dalla-Favera et al., 1983).

Recently, next generation sequencing (NGS) techniques have enabled the comprehensive documentation of genetic lesions in numerous hematological malignancies. These powerful methods of investigation have provided insights into the mechanisms for the deregulation of known pathways (e.g. NF-κB), uncovered the importance of new pathways for oncogenesis (e.g. mRNA processing), identified disease-defining mutations, and provided meaningful new targets which are already being translated into therapeutic interventions (Bomben et al., 2013).

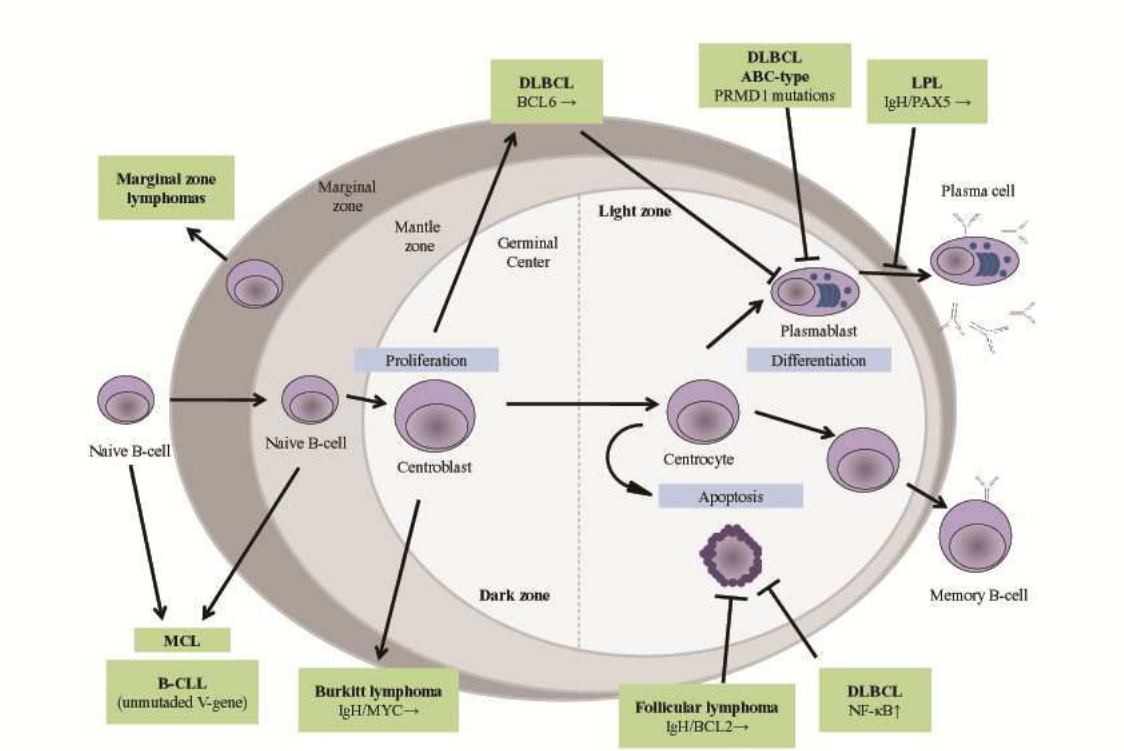

Figure 6. Cellular origin of human B-cell lymphomas. Most lymphomas are derived from germinal center or from B-cells that have passed through the GC, indicating its role in the pathogenesis of B-cell lymphomas. **LPL**, lymphoplasmacytoid lymphoma. Modified from (Klein and la-Favera, 2008).

1.2. Mantle cell lymphoma

1.2.1. Introduction

MCL accounts for 7 % of NHL predominating in male with advanced age and represents a particularly challenging disease with patient outcomes inferior to most other lymphoma subtypes (Tort et al., 2002).

Patients commonly present with disseminated disease. The clinical evolution is usually very aggressive with short response to treatment and frequent relapses, and few patients are cured with current therapies. However, recent clinical studies have identified a group of patients with a more indolent form of the disease that have a long survival even without the need for treatment (Nodit et al., 2003; Espinet et al., 2005; Orchard et al., 2003).

MCLs are CD5-positive mature B-cell lymphoid tumors derived from antigen-naive pre-germinal center B-cells located in the mantle zone surrounding normal germinal center follicles (Jares et al., 2007). Notably, contrary to what was observed in cMCL, most commonly carrying unmutated immunoglobulin genes (Swerdlow et al., 2008), iMCLs frequently carry hypermutated immunoglobulin genes, indicating an origin in cells that have experienced the somatic hypermutation machinery of the follicular germinal center (Orchard et al., 2003; Navarro et al., 2011).

The t(11;14) (q13;q32), a chromosomal rearrangement driving to overexpression of the cyclin D1 gene (Swerdlow et al., 2008), is a hallmark of this disease, although a small subset of lymphomas resembling conventional MCL but lacking the t(11;14)/CCND1 breakpoint has been identified (Mozos et al., 2009; Ondrejka et al., 2011). Nevertheless, nuclear cyclin D1 expression is routinely used as one of the most important element in the diagnosis of MCL and it is able to distinguish this lymphoma from other NHL. This genetic alteration is thought to be the primary event in the pathogenesis of the tumor, probably facilitating the deregulation of the cell cycle at the G1-S phase transition (Campo et al., 1999). In addition to the constitutive deregulation of the cell cycle, other mechanisms such as DNA damage response alteration and activation of cell survival pathways are integrated to drive MCL pathogenesis (Jares and Campo, 2008).

Furthermore, indolent and conventional MCLs differ in the expression of a small signature of 13 genes, including SOX11, which is usually not expressed in iMCLs but

in all cMCL cases (Fernandez et al., 2010). The SOX11 transcription factor has been found to be a reliable and highly specific biomarker for conventional MCLs. In addition, it is not expressed in other low-grade-B-cell lymphomas, offering a valuable practical tool to properly recognize cases of cyclin D1-negative MCLs (Mozos et al., 2009; Royo et al., 2012; Salaverria et al., 2013).

In the last years, recent studies have contributed to the substantial advances made in the comprehension of the pathogenesis of MCL, giving new perspectives for the identification of the optimal therapeutic targets and for the design of new molecular therapies that can ultimately cure this fatal disease.

Aggressive MCL (70-90%)	**Indolent MCL (10-30%)**
Median survival of 3-5 years Clinical presentation: disseminate, nodal with classical cytological variant Chromosomal instability, multiple genomic alterations Unmutaded IGHV Three-gene signature high (SOX11, HDGFRP3, DBN1)	Median survival of 7-10 years Clinical presentation: leukemic non-nodal, splenomegaly with small-cells cytological variant Stable karyotype Hypermutated IGHV Three-gene signature low (SOX11, HDGFRP3, DBN1)

Table 1. Principal features of two subtypes of MCL

1.2.2. Morphological, phenotypic and clinical features of MCL

Morphologically, MCL is characterized by a spectrum of cytological variants that are associated with different biological and clinical characteristics.

The **classical** variant occurs in 80-90% of cases and shows a monotonous proliferation of small–medium-sized lymphocytes with irregular nuclei and inconspicuous nucleoli.

The **small-cells** cytological variant has been mainly recognized in patients with a leukaemic and splenomegaly presentation without lymph nodes and a more indolent clinical course (Angelopoulou et al., 2002; Orchard et al., 2003). Although MCL proliferation activity may vary from case to case, it is generally low, with Ki-67 positive cells around 15–30%.

At the other end of the spectrum, the current WHO classification identified two cytological variants associated with more aggressive evolution, **blastoid** and **pleomorphic** MCL (Figure 7).

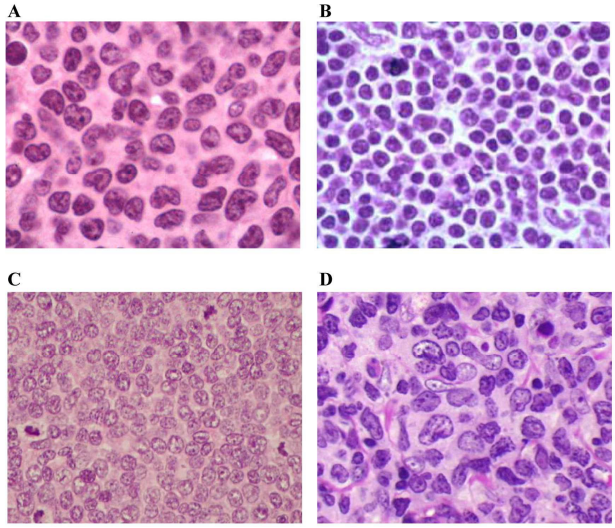

Figure 7. MCL histological variants (tissue sections staining for hematoxilin and eosin (H&E): (**A**) classical MCL, (**B**) small-cell MCL, (**C**) blastoid MCL, (**D**) pleomorphic MCL.

Blastoid MCLs show morphology with rounded nuclei, finely dispersed chromatin and inconspicuous nucleoli and may have an extremely high proliferative activity with numerous mitotic figures, high percentage of Ki-67 positive cells (>90%).

Pleomorphic MCLs are composed of a more heterogeneous population of larger cells. Although the proliferation activity is high, it is usually lower than in blastoid cases. These tumors are frequently tetraploid and it is not uncommon to observe mitotic figures highly hyperchromatic with an apparent high number of chromosomes (Ott et al., 1997).

Some tumors may have very discordant morphology with areas of pleomorphic cells intermingled with others with a classical morphology.

Blastoid variants occur usually *de novo* and less frequently in patients with previous diagnosis of classical MCL (Norton et al., 1995; Agatoff et al., 1997). However, recent data supports the view that blastoid MCL arising in patients with previous diagnosed classical MCL, represents histological transformation of the initial neoplastic clone rather than a *de novo* tumor (Yin et al., 2007).

MCL cells show a mature B-cell phenotype with moderate–strong expression of surface immunoglobulins (IgM/IgD, predominantly lambda), B-cell-associated antigens such as CD20, CD22, CD79, and the T-cell-associated antigen CD5.

MCL is usually negative for several B-cell activation and germinal center markers such as CD23, a key cell surface molecule for B-cell activation and growth, CD10 the germinal centre-associated antigen, which is a transmembrane endopeptidase, or BCL6, a transcription factor involved in lymphoid follicle germinal centre formation and maintenance (Jares et al., 2007).

MCL cells have a striking tendency to disseminate throughout the body. Most patients have generalized lymphadenopathies at diagnosis, but involvement of the bone marrow, peripheral blood, spleen, liver and the gastrointestinal tract are also very common.

During the progression of the disease the tumor may infiltrate any tissue, including the central nervous system and respiratory tract. The median overall survival of patients with MCL is 3–4 years. Complete remission of the disease with conventional therapy is obtained in 20– 80% of patients, but almost all will relapse (Swerdlow et al., 2008).

A subset of patients may follow an indolent clinical course and may not required treatment for a long period. This indolent clinical evolution was recognized initially in patients presenting with splenomegaly and a leukemic non-nodal or minimal nodal disease, suggesting that it may correspond to a different subtype of MCL (Orchard et al., 2003; Angelopoulou et al., 2002).

1.2.3. Initial ontogenetic steps

The t(11;14)(q13;q32) is considered the primary oncogenic event in the pathogenesis of MCL (Campo et al., 1999). This translocation juxtaposes the protooncogene *CCND1* locus at 11q13 to the *IGH* localized at chromosome 14q32 causing the overexpression of cyclin D1. In particular, this alteration leads to a 5'-5' fusion of the BCL-1 locus with the sequence from the IGH@ locus and brought under the control of IGH enhancer CCND1 (Jares and Campo, 2008).

The majority of breakpoint sites at 11q13 occurs in a region named the major translocation cluster (MTC) (Figure 8). Although normal B lymphocytes might express cyclin D2 and D3 (Teramoto et al., 1999), cyclin D1 is not normally expressed in these

cells, but it is overexpressed at both mRNA and protein levels in MCL, highlighting its pivotal importance in MCL lymphomagenesis (Bosch et al., 1994; de Boer et al., 1995).

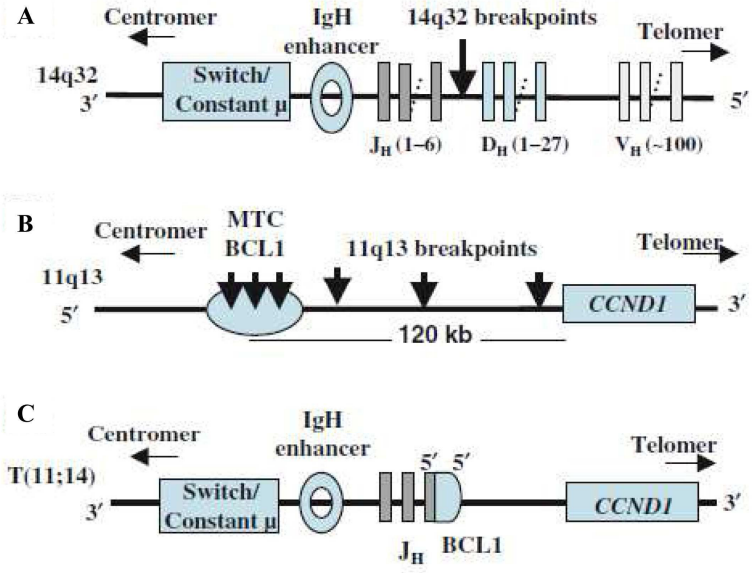

Figure 8 The translocation t(11;14)(q13;q32) in MCL. (**A**) Schematic representation of the germline immunoglobulin heavy chain (IGH) locus (IGH@) on chromosome 14q32 displaying the genomic organization of the variable (V), diversity (D), joining (J) and the constant region. The breakpoint in IGH seems to occur between the diversity and joining regions during the early steps of the V(D)J recombination. (**B**) Genomic organization of the BCL-1 (B-cell lymphoma/leukaemia 1) locus on chromosome 11q13. The majority of breakpoints (30–50%) happens at the MTC, however there is some variability and 10–20% of the breaks occur outside the MTC closer to CCND1. (**C**) The translocation leads to a 5'-5' fusion of the BCL-1 locus with sequences from the IGH@ locus and brought under the control of the IGH enhancer, CCND1 (Jares and Campo, 2008).

The cyclin D1 gene is transcribed in two major mRNA transcripts of approximately 4.5 and 1.5 kb respectively. Both isoforms contain the whole coding region of the gene and differ only in the length of their 3' untranslated region (UTR) that generates a polypeptide of 36 kDa (isoform a). About 4–10% of MCLs aberrantly express truncated forms of the 4.5 kb mRNA transcript with shorter 3'-UTR that lacks destabilizing AUUUA sequences involved in transcript instability (Seto et al., 1992; Xiong et al., 1991) and in the binding sites for different microRNAs (miR-16, miR-503, miR-15a, miR-34a, miR-195, miR-424) that negatively regulate cyclin D1 expression (Chen et al., 2008; Jiang et al., 2009). The loss of these regulatory sequences is caused by additional rearrangements in the 3' region of the gene, microdeletions or point mutations (Seto et al., 1992; de Boer et al., 1997; Komatsu et al., 1994; Rimokh et al., 1994; Wiestner et al., 2007).

These aberrant transcripts have an increased half-life and, interestingly, the tumors have very high levels of cyclin D1 expression, high proliferation and more aggressive clinical behavior (Rosenwald et al., 2003; Sander et al., 2005). An additional mechanism targeting cyclin D1 is the amplification of the translocated t(11;14) allele, which also results in very high levels of cyclin D1 expression (Bea et al., 2009). In addition to this canonical isoform a, the cyclin D1 gene also encodes a less abundant isoform (isoform b) that lacks the C-terminal region (Hosokawa et al., 1999; Betticher et al., 1995). This isoform is generated by an alternative splicing that skips the whole exon 5. This exon contains important regulatory motifs including a residue that promotes the nuclear export of cyclin when phosphorylated (Alt et al., 2000; Diehl et al., 1998). Although cyclin D1b isoform seems to have a higher transforming capacity in cultured cells, its oncogenic mechanisms are not well understood (Solomon et al., 2003).

In a recent study, a high-throughput sequencing approach allowed the identification of several mutations in CCND1 gene. These novel mutations involve the 5´-UTR and the first exon of the gene, and are highly frequent among MCL patients. The predominance of transitions over transversions, their position at 5'-end of CCDN1, and the proximity of the IGH chain locus that stems from the t(11,14) suggest that these mutations likely arise through somatic hypermutation (Kridel et al., 2012).

The role of cyclin D1 in promoting MCL lymphomagenesis is related to its function in the G1 phase of cell cycle regulating the cyclin-dependent kinases (CDK) (Hunter and Pines, 1994). Cyclin D1-CDK4 and cyclin D1-CDK6 complexes phosphorylate retinoblastoma 1 (RB1), causing the inactivation of its suppressor effect on cell cycle progression (Ewen et al., 1993). The hyperphosphorylation of RB1 by cyclin D1-CDK4 and cyclin D1-CDK6 lead to the release of E2F transcription factors and the subsequent progression of the cell into S phase. RB1 is hyperphosphorylated in MCL, particularly in highly proliferative variants (Figure 9) (Jares et al., 1996).

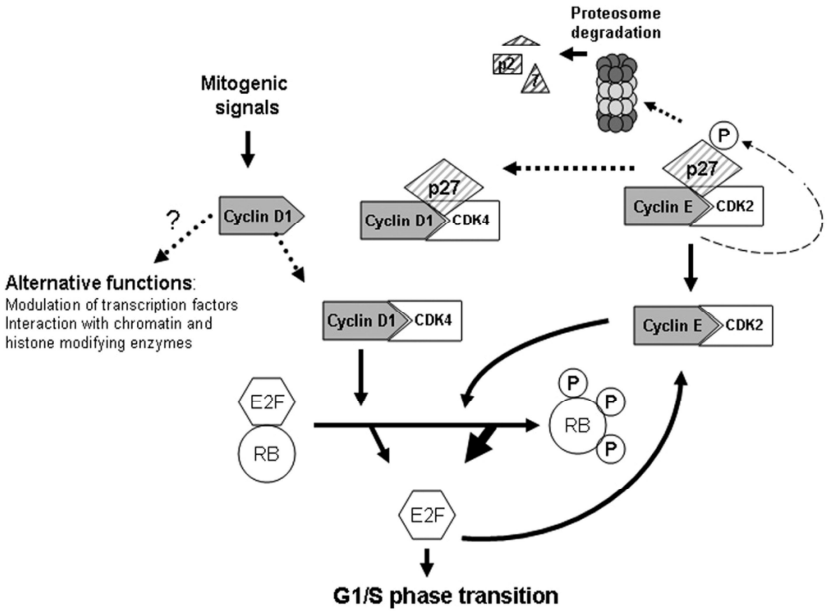

Figure 9. Role of cyclin D1 in cell cycle Cyclin D1, induced by mitogenic signals, binds to CDK4 and controls the G1/S phase transition by initiating the hyperphosphorylation of RB1 and the release of E2F. This initial activation of E2F would initiate the accumulation of cyclin E. In addition, the titration of p27 into cyclin D1/CDK4 complexes will promote the activation of cyclin E/CDK2 complexes that, in turn, will enhance p27 degradation and further phosphorylation of RB1, allowing the cell to progress into S phase. New evidence suggests that cyclin D1 might have cell cycle–independent functions (Navarro et al., 2011).

However, recent studies identified intragenic deletions of RB1 which lead to a total lack of protein expression in some cases of MCL (Pinyol et al., 2007), suggesting that cyclin D1 may also have an oncogenic role independently of RB1 in these tumors.

MCL may also have an impaired control of late G1 phase and the G1-S phase transition. This step is regulated by cyclin E-CDK2 complex and CDK inhibitor p27. The overexpression of cyclin D1 in MCL cells seems to sequester p27 into CDK4-cyclin D1 complexes rendering p27 incapable of inducing G1 cell cycle arrest (Quintanilla-Martinez et al., 2003; Qi et al., 2006).

MCL seems to also have an increased degradation of p27 by the proteasome pathway (Chiarle et al., 2000). The hypothetical higher levels of cyclin E-CDK2 could facilitate p27 phosphorylation and degradation.

Deregulation of cyclin D1 may also have oncogenic potential independently of its CDK cell cycle regulatory function. Studies in solid tumor models have shown that cyclin D1 might act as transcription regulator interacting with transcription factors, chromatin-

remodeling, and histone-modifying enzymes (Fu et al., 2004; Aggarwal et al., 2010; Bienvenu et al., 2010). Cyclin D1 may also promote chromosome instability by binding to genes that regulate chromosome segregation and chromatin reorganization (Casimiro et al., 2012). Furthermore, cyclin D1 has been implicated in promoting DNA repair by binding to RAG1 and homologous DNA recombination (Jirawatnotai et al., 2011).

These functions of cyclin D1 none related to cell cycle have not been properly investigated in MCL. However, the complete inactivation of the *RB1* by mutations and deletions in some MCLs (Pinyol et al., 2007), making cyclin D1 not essential for cell cycle functions, support the hypotesis that cyclin D1 may play additional oncogenic roles in this tumor. Interestingly, the recent description of cyclin D1 as promoting cell survival in MCL by sequestering the proapoptotic BAX protein supports this hypothesis (Beltran et al., 2011).

1.2.4. Cell origin and normal cell counterpart

The term mantle cell lymphoma reflects the idea that the normal cell counterpart of this tumor is a lymphocyte whose physiological microenvironment is the mantle zone of the secondary lymphoid follicle.

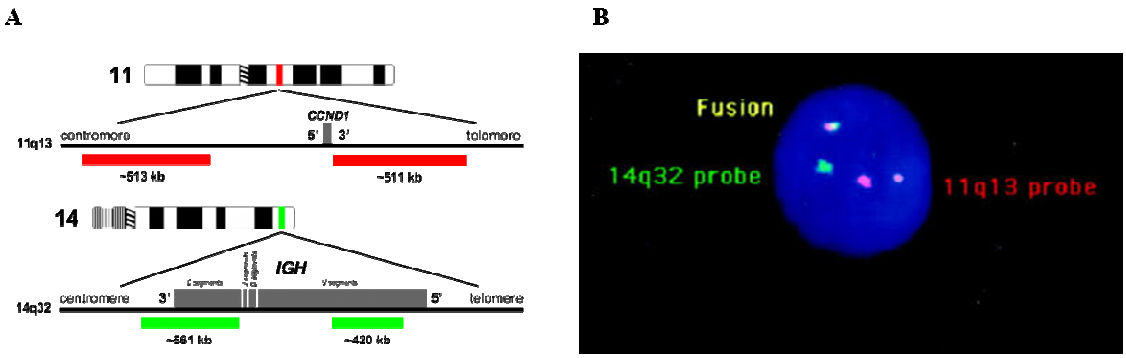

Figure 10. (**A**) Schematic representation of t(11;14) involving CCND1 and IGH genes in MCL. (**B**) Malignant cell with *IGH-CCND1* fusion and a split of the 11q13 probe (major configuration). The two red/orange signals correspond to the 11q13 probe, hybridized on the normal and derivative chromosomes 11, respectively. The green signal corresponds to the normal chromosome 14, whereas the yellow signal corresponds to the fusion of the 11q13 and 14q32 probes on the derivative chromosome 14 (Li et al., 1999).

The t(11;14)(q13;q32) translocation occurs in the bone marrow at the pre-B stage of differentiation when the cell is initiating IG gene rearrangement with the recombination of the V(D)J segment (Navarro et al., 2011). Although the translocation occurs at a very

early stage, MCL cells are mature B lymphocytes that express genes normally detected in naive B-cells, like IgD and CD5.

The phenotype and topographic distribution of these cells are similar to a small subpopulation of naive B CD5+ cells, producing low affinity polyreactive antibodies that colonize the normal mantle zone of the lymphoid follicles and tend to recirculate.

These observations and the predominance of unmutated IG genes observed in most MCL suggest that the normal counterpart of this tumor is a mature naive B-cell.

However, recent studies have shown that 15% to 40% of MCLs carry IGHV somatic hypermutations and have a strong bias in the IGHV gene repertoire with IGHV3-21, IGHV4-34, IGVHV1-8, and IGHV3-23 used by 46% of the cases (Hadzidimitriou et al., 2011).

The mutational load and the associated light chain gene also differ between the IGHV families. Thus IGHV3-21, in contrast to IGHV3-23 and IGHV4-59, is almost exclusively found in germline configuration and is commonly paired with the light chain IGLV3-19. The fact that the mutation frequency is not random and is related to the utilization of specific IGHV genes suggests that at least a subgroup of MCL is not derived from naive B-cells but from cells expanding under the stimulation of certain antigens. This idea is further supported by the recognition of a bias association of certain IGHV, IGHD and IGHJ genes with restricted VH CDR3 motifs in 10% of tumors (Navarro et al., 2011).

This scenario is similar to the stereotyped IG rearrangements observed in CLL (Murray et al., 2008). However, the family usage and clusters of the rearranged IG genes are different in the two diseases suggesting that the potential mechanisms involved in the clonal selection may be different.

Overall these data suggest that most MCLs may derive from antigen-experienced cells. However, the different levels of somatic mutations in the IGHV genes observed in MCL may indicate that different subpopulations of B-cells could be considered normal counterparts of the tumor. Thus, the fact that around 15% of the tumors have a large number of somatic mutations would suggest that these tumors originate in cells that have had strong experience through the germinal center.

Conversely, roughly 30%-50% of the cases have total homology with the germline sequence of the IGVH genes and these cases may derive from cells without any exposure to the mutational machinery (Navarro et al, 2011).

Finally, a number of cases have a low number of somatic mutations. These cases may be related to marginal zone or early germinal center cells similar to a particular subtype of B-cell called "pro-germinal center cell" which is considered as an intermediated step between both naive and germinal center cells, characterized by the expression of IgD+ CD38-CD23-CD71+, activation-induced cytidine deaminase (AID) and a few somatic IGHV hypermutations. These cells may be the normal counterparts of at least a number of MCLs cases (Kolar et al., 2007).

1.2.5. Secondary genetic alterations

Despite the important role of the t(11;14)(q13;q32) translocation and the cyclin D1 overexpression in the development of MCL, several observations suggest that this mechanism may not be sufficient for the full transformation of the cells and the aggressive behavior of the tumor.

Transgenic mice that overexpress cyclin D1 did not develop spontaneous lymphomas, and cooperation with other oncogenes like myc were required for lymphomagenesis (Lovec et al., 1994). Furthermore, a mouse model expressing a constitutively nuclear cyclin D1 in murine lymphocytes developed mature B-cell lymphomas carrying alterations similar to blastoid variants of MCL, including deregulation of the ARF/MDM2/p53 pathway and BCL-2 overexpression (Gladden et al., 2006). In addition, the identification of the t(11;14) translocation in blood cells of 1–2% of healthy individuals without evidence of disease (Hirt et al., 2004) supports the need for additional oncogenic events in the progression of MCL (Jares et al., 2012).

Compared with other lymphoma subtypes, MCL is characterized by a particularly high number of chromosomal gains and losses that are thought to occur secondarily to the underlying hallmark translocation t(11;14) involving cyclin D1. It seems probable that the secondary genetic alterations and their molecular consequences are of major importance in determining the aggressiveness of the tumor and therefore the clinical course (Jares et al., 2007) These alterations target genes involved in molecular pathways such as cell cycle control, DNA damage response, and cell survival pathways, are frequently found in aggressive MCL (Figure 11) (Jares and Campo, 2008).

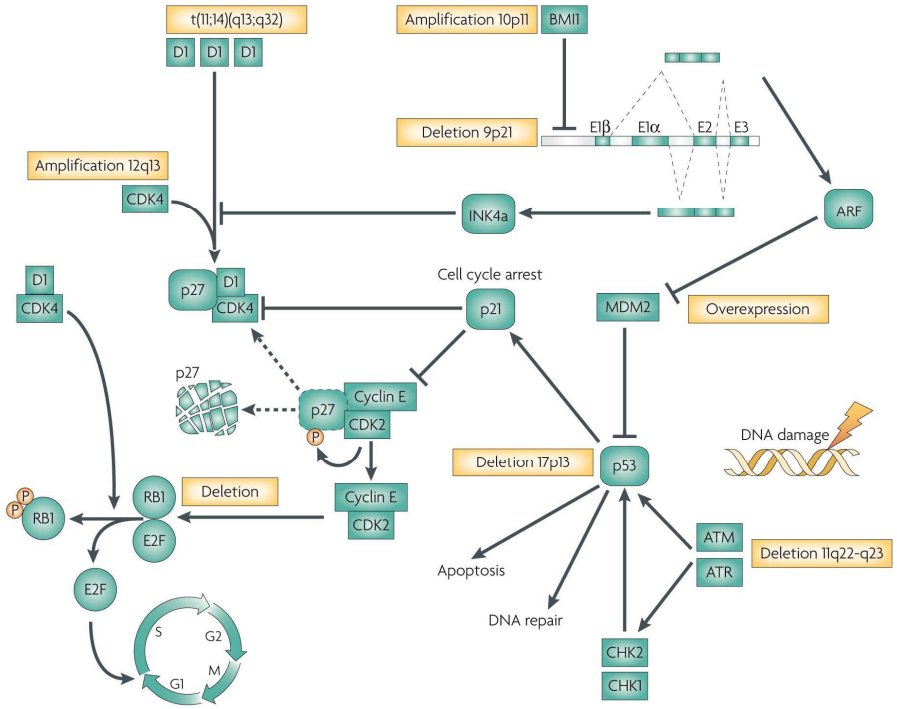

Figure 11. Cell cycle and DNA damage pathway dysregulation in MCL (Jares et al., 2007).

The INK4a/CDK4/RB1 and ARF/MDM2/p53 cell cycle pathways are very frequently targeted by secondary genetic alterations in MCL. Both pathways are connected through the *CDKN2A* locus (9p21), which encodes for both the CDK inhibitor INK4a and the positive p53 regulator ARF, and this locus is frequently deleted in MCL.

Other key elements of these pathways, such as *TP53* and *RB1*, are also frequently inactivated by point mutations or gene deletions (Pinyol et al., 2007; Hernandez et al., 1996). In addition, gene amplification events have been found to deregulate additional genes, including CDK4, polycomb ring finger gene BMI1, and MDM2 (Hernandez et al., 2005). Accordingly, the proliferation gene expression signature is the best predictor of patient survival, underscoring the importance of cell cycle dysregulation in dictating the behavior of MCL (Rosenwald et al., 2003).

Chromosome aberrations observed in MCL are consistent with an important role for deregulation of the DNA damage response in this lymphoma (Royo et al., 2011). The ataxia telangiectasia mutated (*ATM*) gene, located at 11q22-23, is frequently deleted and mutated in MCL cases with increased genomic instability (Camacho et al., 2002). Additional downstream elements of this pathway, including *CHK1* and *CHK2*, are

occasionally deregulated in MCL, suggesting that mutation of DNA damage response contributes to oncogenesis (Jares et al., 2012).

Recent studies have also shown that genes involved in cell survival are targets of recurrent genetic alterations in MCL. Amplifications and overexpression of antiapoptotic genes such as *BCL2* (18q21) (Bea et al., 2009) and homozygous deletions of proapoptotic genes such as *BCL2L11* (2q13) have been described in primary tumors (Hartmann et al., 2010).

In the last few years, NGS technology has emerged as a valuable tool in cancer research, enabling the detection of somatic mutations and gene expression changes in tumor DNA at a much higher resolution than arrays, offering greater accuracy and cost-effectiveness than ever before.

A recent study, based on whole transcriptome shotgun sequencing (RNA-seq), found *NOTCH1* mutations in 12% of MCL cases to be associated with poor survival (Kridel et al., 2012). This gene encodes for a transmembrane protein that functions as a ligand-activated transcription factor. Similar to *NOTCH1* mutations described recently in CLL (Puente et al., 2011; Gesk et al., 2006), mutations in MCL occur in the PEST domain and generate a truncated, more stable and transcriptionally active protein. Furthermore, it was observed that inhibition of NOTCH pathway reduced proliferation and induced apoptosis of MCL cell lines (Kridel et al., 2012).

Alteration (loss/gain)	Candidate genes	Pathways
Loss 1p32.3	*FAF1,CDKN2C*	Cell cycle/ cell survival
Loss1q32	*PROX1*	Proliferation
Loss 2q34	*MAP2*	Microtubules
Homozygous loss 2q13	*BCL2L11*	Cell survival
Loss 6q24/25	*LATS1*	Hippo signaling pathway
Loss 6p23	*TNFAIP3/A20*	NF-κB inhibition
Loss 8p23	*MCPH1*	DNA damage response
Loss 9p21.3	*CDKN2A/B, MTAP*	Cell cycle
Loss 19p13.3	*MOBKL2A*	Hippo signaling pathway
Loss 11q22.3	*ATM*	DNA damage response
Loss 13q14.2	*RB1*	Cell cycle
Loss 13q34	*CUL4A, ING1*	Cell cycle/ DNA damage response
Loss 17p13	*TP53*	Cell cycle/ DNA damage response
Gain 8q24.21	*MYC*	Proliferation
Gain 10p12.2-12.31	*BMI1*	Cell cycle
Gain 11q13.3-q21	*CCND1, MAP6*	Cell cycle/ microtubule dynamics
Gain 12q14	*CDK4, MDM2, CENTG1*	Cell cycle/apoptosis/ DNA damage
Gain 13q31.3	*MIR17H-g (miR-17-92)*	Cell cycle, apoptosis
Gain 18q21.33	*BCL2*	Apoptosis

Table 2. Recurrent genetic alterations and target genes detected in MCL (Royo et al., 2011).

1.2.6. Cyclin D1-negative MCLs

Despite the relevance of the t(11;14) translocation and cyclin D1 deregulation in MCL, there is a rare variant of this tumor that lacks cyclin D1 expression but resembles cMCL histologically, clinically, and molecularly (Rosenwald et al., 2003; Fu et al., 2005; Mozos et al., 2009). The lack of cyclin D1 expression is due to the absence of translocations involving cyclin D1 in the majority of patients (Klapper, 2011). Although the number of cases is still limited, a gene expression profile study on a set of these putative cyclin D1-negative MCLs showed that they had a global expression signature similar to that of conventional cyclin D1-positive tumors confirming that they corresponded to the same entity (Fu et al., 2005). This idea was further supported by the identification of a similar profile of secondary genomic alterations (Salaverria et al., 2007).

Interestingly, cyclin D1-negative MCLs frequently exhibited overexpression of other cyclins such as cyclin D2 and cyclin D3, but without evidence of chromosomal aberrations involving these loci (Fu et al., 2005). Subsequent studies have identified isolated cyclin D1-negative MCL harboring a t(2;12)(p12;p13) fusing the *CCND2* gene to the *IGK@* locus (Gesk et al., 2006), t(12;22)(p13;q22) with *IGL-CCND2* fusion (Shiller et al., 2011), cryptic t(12;14)(p13;q32) *IGH-CCND2* (Herens et al., 2008) or *CCND2* breaks with unidentified partner (Quintanilla-Martinez et al., 2009). In addition, a translocation of the *CCND3* gene has been detected in a single MCL patient (Wlodarska et al., 2008).

Furthermore, rare chromosomal translocations involving *CCND3* (which codifies for cyclin D3) and *IGH* genes have been reported in B-cell malignancies other than MCL (Shaughnessy, Jr. et al., 2001; Sonoki et al., 2001; Wlodarska et al., 2008).

In a recent study involving the largest series of cyclin D1-negative MCL patients, CCND2 rearrangements were identified as the most frequent genetic events (55% of cases) resulting in deregulation of CCND2 expression. Additionally, it was observed that CCND2, but not the CCND3 gene, predominantly translocates to IG light chain genes suggesting that these rearrangements take place in a different stage of B-cell differentiation compared with the stages where CCND1, BCL2 or BCL6 translocations occur (Salaverria et al., 2013).

These findings suggest that the deregulation of CCND2 in the absence of cyclin D1 expression may be an alternative mechanism in cyclin D1-negative MCL pathogenesis (Jares et al., 2012; Salaverria et al., 2013), however the absence of any cyclin D gene alterations in a subset of otherwise conventional MCL raises the intriguing question about the initial driver for pathogenesis in these cases.

SOX11 has been identified recently as a reliable biomarker of MCL. SOX11 is highly expressed in virtually all MCL tumors but it is not expressed in other mature lymphoid neoplasms and normal lymphocytes at any stage of differentiation (Ek et al., 2008). Interestingly, SOX11 is highly expressed in both cyclin D1–negative and –positive MCLs, suggesting that in addition to its value as a diagnostic biomarker, it may be an important factor in the pathogenesis of MCL (Mozos et al., 2009).

1.2.7. Indolent MCLs

Recent observations have suggested that the clinical behavior of MCL may not be as homogeneous as initially thought. Thus, although most patients follow a very rapid progression and die of the disease, others have an indolent clinical course and can survive more than 10 years, even without receiving immunochemotherapy. The identification of these patients is important because they may benefit from more conservative management for some time without apparently harming their global outcome (Martin et al., 2009).

Since Orchard and colleagues reported in the 2003 a subset of patients with MCL characterized by leukemic-non-nodal disease, typical phenotype, mutated IgV_H and a indolent clinical presentation with prolonged survival, there has been ongoing debate about whether the heterogeneity in the non-nodal group represents a true variation within MCL or it is due to the inclusion of other B-cell malignancies with the t(11;14) translocation (Orchard et al., 2003).

Furthermore, studies of prognostic factors in MCL have indicated that tumors with very low proliferation index, a histological growth pattern restricted to mantle zone of the lymphoid follicles (mantle zone pattern), and a limited clinical stage may have a significantly better prognosis with longer survival than the global series of patients (Navarro et al., 2011; Tiemann et al., 2005). These cases may correspond to early stages in the development of cMCL.

Most MCLs have complex karyotypes, but non-nodal tumors have very few, if any, chromosomal alterations in addition to the t(11,14) translocation. Non-nodal MCLs frequently have hypermutated *IGHV*, suggesting an origin in cells with a strong influence of the germinal center microenvironment, whereas cMCLs typically have few or no mutations in *IGHV* (Orchard et al., 2003; Royo et al., 2012; Del, I et al., 2012; Navarro et al., 2012).

In a study carried out in our laboratory, a gene expression profiling was performed to compare a group of indolent leukemic MCLs with a group of patients with conventional disease to shed light on different biological features of these two subtypes of MCL. This study also included other leukemic lymphoid neoplasias such as CLL, splenic marginal zone lymphoma (SMZL), hairy cell leukemia (HCL) and leukemic FL. Interestingly, unsupervised hierarchical clustering analysis revealed that the iMCLs were molecularly more similar to cMCLs than to any other type of lymphoid neoplasia supporting the idea that they correspond to the same molecular disease. However, they also had differential expression of a 13 genes signature including SOX11 gene (Figure 12) (Fernandez et al., 2010).

In a further study, it was confirmed by quantitative Real Time-PCR (qRT-PCR) that three genes of this signature, SOX11, HDGFRP3 and IBSN1, were highly expressed in MCLs with aggressive clinical behavior and nodal presentation, whereas MCLs with non-nodal disease and good prognosis showed low expression. These data might supply a good additional diagnostic tool to distinguish these two subtypes of MCLs (Royo et al., 2012).

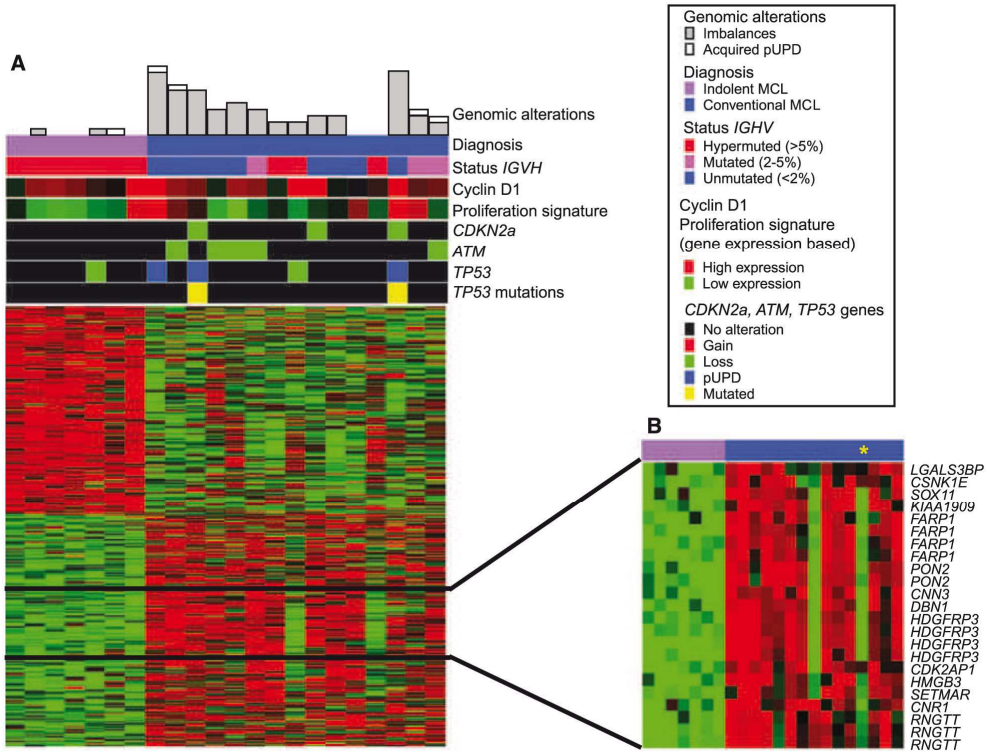

Figure 12. Gene expression profiling of several B-cell lymphomas. (**A**) Characterization of iMCL according to their genetic and molecular features. The genomic complexity is illustrated in the bar plots at the top of the panels, reflecting the number of alterations for each case. The plot below indicates the diagnosis of the cases. Violet, iMCL; blue, cMCL. IGVH gene status of all MCL cases is indicated by color (red, >5% mutations; pink, 3–5% mutations; blue, 0–2%). Bright red, high expression; green, low expression. (**B**) Differential signature between iMCL and cMCL. Probe sets that showed a highly significant differential expression between iMCL and cMCL are highlighted (Fernandez et al., 2010).

The detection of SOX11 by immunohistochemistry (Figure 13) or qRT-PCR in larger series of patients has confirmed the relationship among its lack of expression, hypermutated *IGHV*, low karyotype complexity, non-nodal leukemic disease, and longer survival with stable disease in an independent cohort of patients, suggesting that these biological and clinical features may identify a different subtype of MCL (Del, I et al., 2012; Royo et al., 2012; Fernandez et al., 2010; Ondrejka et al., 2011; Rule et al., 2011; Navarro et al., 2012).

Some patients with a non-nodal and leukemic presentation may progress to an aggressive behavior after several years of a stable disease. On the other hand, some patients with SOX11 negative MCL may present with blastoid morphology at diagnosis and a very aggressive behavior (Nygren et al., 2012). These patients may have long leukemic, non nodal phase followed in some cases by progression to an aggressive lymphoma associated with the acquisition of 17p/TP53 alterations and complex

karyotypes. Although these patients may represent the transformed and advanced phase of the SOX11-negative MCL, more studies are needed to better understand these tumors and the potential interest in the management of the patients (Jares et al., 2012).

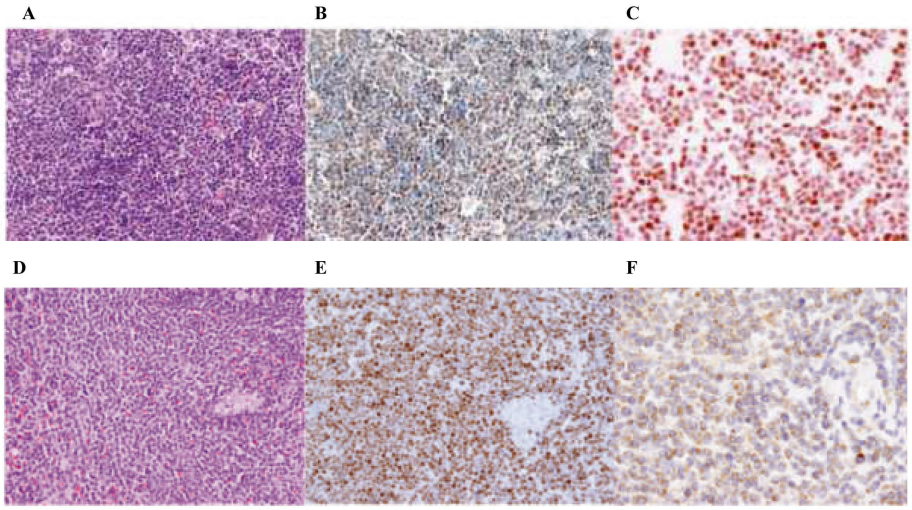

Figure 13. Immunohistochemical analysis of SOX11 gene in MCL. The cMCL (top, A, B, C) shows H&E staining (**A**), cyclin D1 expression (**B**), and a strong nuclear SOX11 immunostaining (**C**), whereas the iMCL (bottom D, E, F) is also cyclin D1 positive (**D**) but the nuclei of the tumor cells are negative for SOX11 (**F**) (Fernandez et al., 2010).

1.3. The SOX family of transcription factors

SOX genes encode a group of transcription factors that bind to the minor groove in DNA. In general, proteins containing a HMG domain with 50% or higher amino acid similarity to the HMG domain of Sry, the sex-determining gene chromosome Y, are referred to as Sox proteins (Sry-related HMG box). SOX proteins have a critical role in the determination of cell fate and differentiation in numerous processes, such as sex differentiation, skeletogenesis, and stemness (Wegner, 1999; Kiefer, 2007; Lefebvre et al., 2007). SOX family comprises 20 genes in human and mice and are divided into eight subgroups termed A to H, according to the degree of homology within and outside the HMG (Xu and Li, 2010). Individual members within a group share biochemical properties and thus have overlapping functions. In contrast, SOX factors from different groups have acquired distinct biological functions despite recognizing the same DNA consensus motifs (Sarkar and Hochedlinger, 2013).

DNA binding

SOX proteins bind sequence-specifically to DNA through a HMG domain, allowing them to function as transcription factors. HMG domain consists of approximately 80 residues that form three alpha helices in a twisted L-shape structure (Bewley et al., 1998). The concave surface of the L-shape binds the minor groove of the DNA (Figure 14) (Dong et al., 2004). This domain is highly conserved among SOX factors, and all members appear to recognize a similar binding motif of 6-8 bases, 5'-T(A/T)-(A/T)-CAA-(A/T)G-3'. Most SOX proteins also feature one to several other functional domains outside the HMG box. These domains have generally been highly conserved among orthologues as well as among members of the same group, and they are totally different among proteins from distinct groups. They include transactivation domain, transrepression and dimerization domains (Lefebvre et al., 2007).

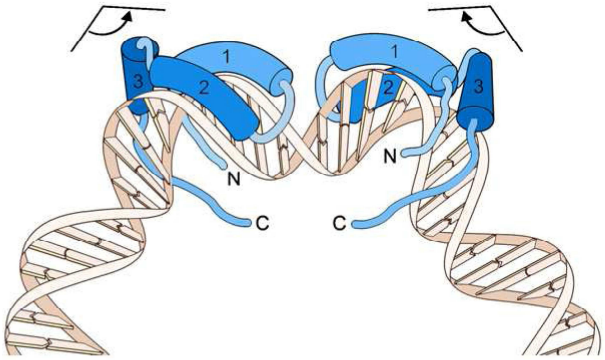

Figure 14. Unique structural and functional features of the Sox HMG box domain This domain is folded into an L-shape composed of three alpha helices. It contacts the DNA double helix in the minor groove and forces it to bend to an angle varying between 30° and 110°. Two HMG box domains are shown binding in opposite orientation on DNA. Their alpha helices are shown as cylinders. Sequences N-terminal and C-terminal to the HMG box domains and sequences linking the helices are shown as thin rods. The DNA bending angle is schematized above the HMG box domains (Lefebvre et al., 2007).

SOX proteins also have the ability to bend DNA although this role has not been demonstrated for any SOX protein yet. Supporting the hypothesis that DNA bending is an essential SOX function, mutations in human *SRY* and *SOX2* genes that selectively interfere with DNA bending have been described, and these mutation could cause a disease phenotype (Pontiggia et al., 1994; Scaffidi and Bianchi, 2001). The DNA bending angle induced by SOX proteins varies from as little as 30° up to as much as 110°, which has led to their qualification as "floppy" proteins (Weiss, 2001). This is due to the fact that the angular surface of the L-shaped HMG box domain is flexible. It becomes fixed upon binding of the SOX protein to DNA, with the SOX domain instructing DNA how to bend and DNA instructing the protein how to complete its tertiary fold (Lefebvre et al., 2007).

It has been suggested that the function of SOX protein is at least partly architectural, allowing other transcription factors to bind to the major groove and bringing together regulatory elements and thereby facilitating the formation of protein complexes (Dong et al., 2004). In addition, it has been shown that sequences outside of the HMG box may facilitate interactions and influence the specificity of SOX proteins (Kamachi et al., 1999; Wilson and Koopman, 2002).

SOX proteins bind to DNA with relatively low affinity. To increase the binding strength to DNA and refine their target gene selection in different cellular contexts, SOX proteins often interact with other transcriptional regulators (Bergsland et al., 2011).

Several transcription factor proteins from a wide range of families have been found to partner with SOX proteins, either to activate or repress transcription from target promoters (Wilson and Koopman, 2002). The first target of the SOX gene family described is *Fgf4*, a gene specifically expressed in embryonic stem cells and embryonic carcinoma cells (Yuan et al., 1995). The enhancer of *Fgf4* is characterized by adjacent recognition sites for SOX and POU domain proteins. Sox2 and the POU domain factor Oct3/4 are co-expressed in these cells and synergize in activating the enhancer of *Fgf4* gene. They form heterodimers with each other on DNA through their DNA-binding domains (Remenyi et al., 2003). Other evidence indicates that SOX proteins can also recruit transcriptional repressors to promoter sequences (Lefebvre et al., 2007).

Several SOX protein groups have a potent transactivation domain in their C-terminal region, and this domain in Sox2 and Sox9 physically interacts with the transcriptional co-activator CBP/p300 (Nowling et al., 2003; Tsuda et al., 2003). These proteins must therefore contribute to the activity of enhanceosomes not only through architectural roles, but also through direct interaction with partners of the transcriptional machinery. SOX proteins of group D preset two highly conserved leucine-zipper coiled-coil domains, which mediate protein homodimerization in the absence or presence of DNA, resulting in high-efficiency binding adjacent recognition sites on DNA (Lefebvre et al., 2007).

In addition to binding to DNA and mediating interactions with transcription factor proteins, the HMG domain also contains signals for nuclear import. In order to regulate gene expression, transcription factors must be imported into the nucleus from the cytoplasm. This active process is mediated by a family of transporter proteins called importins, which recognize a nuclear localization signal (NLS) in their cargo. NLS sequences have been identified in both the amino and carboxyl termini of the HMG domain of SOX proteins (Poulat et al., 1995; Sudbeck and Scherer, 1997). Recently it has been demonstrated that nuclear import of SRY is mediated by importin β, which requires the HMG-domain carboxy-terminal NLS of SRY. The SOX NLS is conserved (Sudbeck and Scherer, 1997), and nuclear import via importin β is likely to be common to all SOX proteins.

Summarizing three different classes of SOX protein–protein interactions can be described. Thus, SOX partners and co-factors can be divided into three groups: (a) DNA-binding proteins that partner with SOX proteins to regulate gene expression (these

interactions are likely to be specific to different SOX proteins); (b) adaptor proteins, linking SOX factors to other proteins; and (c) importins, required for the nuclear import of all SOX proteins (Figure 15) (Wilson and Koopman, 2002).

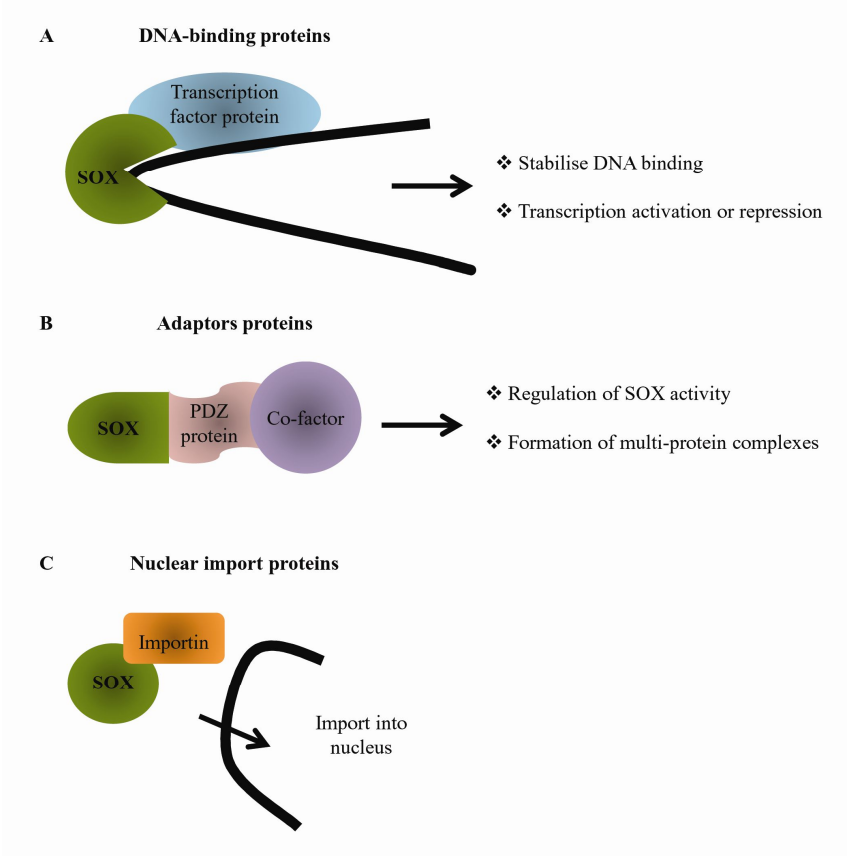

Figure 15. Three different classes of SOX protein–protein interaction. SOX partners and co-factors can be divided into three groups: (**A**) **DNA binding** proteins that partner with SOX proteins to regulate gene expression; (**B**) **adaptor proteins,** linking SOX factors to other proteins; and (**C**) **Importins,** required for the nuclear import of all SOX proteins. Modified from (Wilson and Koopman, 2002).

1.3.1. The role of SOX proteins *in vivo*

SOX family of transcription factors are well-established regulators of cell fate decision during development. Accumulating evidence documents that they play additional roles in adult tissue homeostasis and regeneration. Forced expression of SOX factors, in combination with other proteins, reprogram differentiated cells into somatic or pluripotent stem cells. SOX2 is undoubtedly the SOX gene with highest stemness profile (Lefebvre et al., 2007). This protein functions cell-autonomously in both the epiblast and the extraembryonic ectoderm of the early embryo to maintain the pluripotency of the stem cells that later give rise to all embryonic and trophoblast cell types (Avilion et al., 2003). It is also required to maintain the pluripotency of embryonic

stem cells *in vitro*. Sox2 acts in synergy with the POU domain protein Oct3/4 to directly activate essential genes in embryonic stem cells, such as *Fgf4* (Yuan et al., 1995). Moreover, it was recently shown to form a quartet of transcription factors together with Oct3/4, c-Myc, and Klf4 that is sufficient to induce pluripotent stem cell properties in embryonic and adult fibroblasts (Takahashi and Yamanaka, 2006). Thus, *Sox2* is a stemness master gene (Lefebvre et al., 2007).

Additionally, Sox2 binds to several other sites in the genome, giving rise to the hypothesis that it may also function as a pioneer factor in embrionic stem cells (ESCs). In concordance with such a function, Sox2 has recently been found in ESCs on several enhancers that become activated only later during B-cell development (Liber et al., 2010). Although Sox2 is best known for its role in ESCs, it has numerous other functions during development, including a prominent one in neurogenesis (Wegner and Stolt, 2005; Pevny and Nicolis, 2010).

The SOXC factors (SOX4, SOX11 and SOX12) are another set of SOX factors that are induced by preneuronal proteins as neuron precursor cells develop into mature neurons (Wegner, 2011). Gliogenesis (development of oligodendrocytes, astrocytes, and Schwann cells) in the central nervous system and peripheral nervous system relies on *SoxE*, and *SoxD* genes (Stolt et al., 2004; Stolt et al., 2005; Wegner and Stolt, 2005). *Sox9* and, to a lesser extent, *Sox8* specify the gliogenic fate of neuronal precursors. SOX factors are also involved in skeletogenesis, Sox9 has a master role in this process. In contrast to other developmental processes, few Sox proteins have been reported to be expressed and to have roles in hematopioiesis. *Sox4* is highly expressed in the thymus and promotes pro-B lymphocyte expansion and T-lymphocyte differentiation (Schilham et al., 1997; Schilham et al., 1996). The *SoxD* gene *Sox13* acts further downstream in the same pathway to promote delta-gamma T-cell development by TCF1 downstream of the Wnt signaling pathway, while opposing alpha-beat T-cell differentiation (Melichar et al., 2007). Sox13 works by inhibiting transactivation of lineage-specific genes. Another *SoxD* gene, *Sox6*, is expressed in mature erythroid cells (Lefebvre et al., 2007).

1.3.2. SOX C transcriptional factors

The group C of SOX transcription factors is constituted by Sox4, Sox11 and Sox12, which are single exon genes. Human SOX4, SOX11 and SOX12 proteins have 474, 441 and 315 amino acids, respectively (Figure 16).

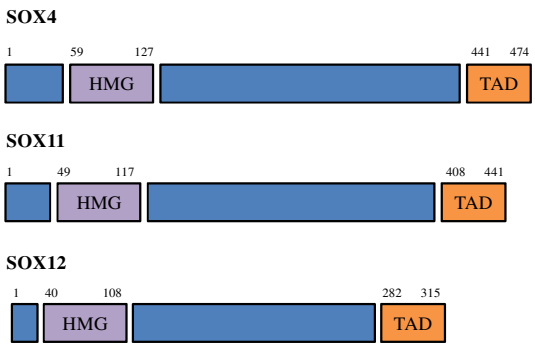

Figure 16. Schematic structure of human SOXC group proteins: SOX4 (474 aa), SOX11 (441 aa) and SOX12 (315 aa) highlighting the two functional domains in each protein. **HMG**, high mobility group; **TAD**, transactivation domain.

They have two functional domains: a Sry-related HMG box DNA-binding domain, located in the N-terminal half of the protein, and a transactivation domain (TAD), located at the C-terminus. The HMG box is 84% identical across all vertebrate SOXC proteins (Dy et al., 2008). The Sox4 HMG box binds preferentially to the AACAAAG motif in electrophoretic mobility shift assay (EMSA) (van de Wetering et al., 1993), but Sox4, Sox11 and Sox12 also bind and transactivate reporters harboring such distantly related motifs as the GACAATAG and CACAATG sequences present in a bona fide *Tubb3* target gene (Bergsland et al., 2006; Dy et al., 2008; Hoser et al., 2008). The SoxC proteins are able to cooperate with protein partners. Like the SoxB1 and SoxE proteins, they strongly synergize with the POU domain transcription factors Brn1 and Brn2 to activate an *Fgf4* enhancer that contains adjacent Sox and POU domain binding sites (Kuhlbrodt et al., 1998; Dy et al., 2008).

SOXC genes play critical roles in development. *Sox4*-null mice die at embryonic day 14 (Schilham et al., 1996). *Sox11*-null mice die immediately after birth, from similar, but less severe, heart outflow tract malformation (Sock et al., 2004). In addition, they display multiple malformations, including microphthalmia with anterior segment dysgenesis (Wurm et al., 2008), open eyelids, cleft palate, cleft lips, hypoplastic lungs, asplenia, omphalocele, undermineralized skull and split lumbar vertebrae. *Sox12*-null mice have no obvious malformations and a normal lifespan and fertility (Hoser et al., 2008).

SOX gene family transcription factors of the C group have important sequential roles in regulating the maintenance and differentiation of progenitor cells from early pluripotent stages to late steps of neurogenesis (Guth and Wegner, 2008).

RNA interference (RNAi) knockdown of *Sox4* and *Sox11* in chick embryo neural tubes blocked neuronal gene expression while forced expression of *Sox4*, *Sox11* or *Sox12* resulted in neuronal gene upregulation. Functional SoxC binding sites were also identified in the regulatory element of the pan-neuronal gene *Tubb3*, suggesting that this gene may be a direct target of the SoxC proteins (Bergsland et al., 2006; Hoser et al., 2008). On the other hand, forced expression of *Sox4* resulted in impaired oligodendrocyte differentiation in mice (Potzner et al., 2007), suggesting that the *SoxC* genes may both promote differentiation of progenitor cells into neurons and prevent differentiation into glia. Deletion of Sox4 or Sox11 in mice had little consequences on neurogenesis, arguing that SoxC proteins function redundantly in this process. On the other hand, simultaneous deletion of both SoxC factors led to massive apoptosis throughout the developing nervous system that predominantly affected immature neurons (Wegner, 2011).

Sox4 is the only gene in the Sox family that has been found to have an important role in early B- and T-cell development (van de Wetering et al., 1993; Schilham et al., 1996). Sox4 is a prominent transcription factor in lymphocytes of both B- and T-cell lineages, and is crucial for B-lymphopoiesis, as *Sox4*-null hematopoietic cells grafted into wild-type mice remain blocked at the pro-B-cell stage (Schilham et al., 1996), similar to that observed for PAX5 (Wegner, 1999).

Other studies have suggested that the *SOXC* genes may also be important in specific cell lineages to promote cell proliferation or survival. *Sox4* heterozygous adult mice develop osteopenia, with low osteoblast numbers and low-level expression of osteoblast markers, and *Sox4* knockdown results in impaired proliferation and differentiation of osteoblasts *in vitro* (Nissen-Meyer et al., 2007).

1.3.3. SOX11 biological functions

The SOX11 gene is mapped at chromosome 2p25.3. Evidences suggest that SOX11 is critical for embryonic neurogenesis and tissue remodeling. SOX11 is normally expressed throughout the developing nervous system of human embryos and is required for neuron survival and neurite growth. Recently it has been demonstrated that neurogenesis depends on the ordered succession of a defined group of Sox proteins on a set of common target gene enhancers (Bergsland et al., 2011). Genome-wide binding maps of Sox factors in neural development, revealed that active neuronal and the

inactive neural precursor cell enhancers are occupied by Sox11 in young neurons, suggesting that Sox11 is not only involved in activating the neuronal enhancers, but may also help to shut off the enhancers of neural precursor cells (Bergsland et al., 2011). Mature neurons lose SoxC expression, thus they can only be responsible for the induction and the early phases of neuronal gene expression, but not for maintenance (Wegner, 2011).

The role of Sox11 in tissue remodeling has also been studied in a knock-out mouse model, showing several malformations, indicating that Sox11 is important for tissue remodeling and that mutated SOX11 in humans may potentially be associated with malformation syndromes. Furthermore, using RNAi knock-down in a neuroblastoma cell line and in cultured mouse dorsal root glia neurons, it has been observed that Sox11 silencing modulated the levels of mRNA for several proteins related to cell survival and death, for instance increased expression of the pro-apoptotic gene BNIP3 and decreased expression of anti-apoptotic gene TANK (tumor necrosis factor, TNF, receptor-associated factor family member-associated nuclear factor κB, NF-κB activator) (Jankowski et al., 2006).

1.3.4. SOX11 in cancer

Several clinical observations have suggested a link between SOX transcription factors and oncogenesis. SOX4 and SOX11 have been shown to be both highly expressed in most medulloblastomas, which are brain tumors derived from neuronal progenitors. Increased *SOX4* expression is also associated with bladder (Aaboe et al., 2006), prostate (Liu et al., 2006), colon (Andersen et al., 2009), and non-small cell lung tumors (Medina et al., 2001). High expression of *SOX11* was detected in gliomas (Weigle et al., 2005), medulloblastoma (Lee et al., 2002), NHL (Wang et al., 2008) and epithelial ovarian tumors (Brennan et al., 2009; Sernbo et al., 2011).

High level of SOX11 expression is associated with improved survival among high-grade epithelial ovarian cancer (Sernbo et al., 2011).

Recently, SOX11 was found highly expressed in breast cancer (Lopez et al., 2012). It was observed that patients with breast cancer expressing higher levels of SOX11 showed a worse overall survival than those with tumors expressing lower levels (Zvelebil et al., 2013). It is possible that the SOX C genes have different effects on tumor cells depending on the context and primary transformation mechanism.

1.3.5. SOX11 in MCL

SOX11 expression in MCL was described for the first time in 2008 (Ek et al., 2008) in a small cohort of patients. This transcription factor was found specifically expressed in the nucleus of MCL compared with other lymphomas (CLL, BL and DLBCL) and benign lymphoid tissues. The role of SOX11 in hematological development (both normal and malignant) is unclear, although SOX4 belonging to the same SOX protein group C, is required for B-cell differentiation. Strong nuclear expression of SOX11 was also detected by immunohistochemistry in lymphoblastic lymphomas (B and T), and some BL with weaker nuclear expression present in HCL (Dictor et al., 2009; Mozos et al., 2009).

Since a subset of MCL patients with indolent clinical behavior was identified, goals of research have been to elucidate molecular pathogenesis of MCL to shed light on mechanisms driving the indolent form of MCL that occurs in a small proportion of patients and to identify the normal cell counterpart that may constitute the MCL cell of origin, thus clinical behavior of MCL may not be as homogeneous as initially thought.

Despite the differences in the genetic and clinical characteristics between conventional MCL and the indolent form, both show the t(11;14)(q13;q32) translocation with cyclin D1 overexpression and share a similar global gene expression profile (Ondrejka et al., 2011). However indolent and conventional MCLs differ in the expression of a small signature of 13 genes (Fernandez et al., 2010). SOX11 emerged as one of the best discriminatory gene between these two phenotypes. This transcription factor is usually not expressed in indolent MCLs but in all conventional MCL cases, suggesting its relevant role in the pathogenesis of the disease (Mozos et al., 2009; Ek et al., 2008; Ondrejka et al., 2011).

The detection of SOX11 by immunohistochemistry or RQ-PCR in a larger series of patients has confirmed the relationships among its lack of expression, hypermutated *IGHV*, low karyotype complexity, non-nodal leukemic disease, and longer survival with stable disease in independent cohorts of patients (Royo et al., 2012; Navarro et al., 2012; Ondrejka et al., 2011). Interestingly, SOX11 is highly expressed in both cyclin D1-negative and -positive MCLs, suggesting that this transcription factor could be a reliable biomarker that may be incorporated into routine MCL diagnosis, especially as

SOX11 can identify the rare cyclin D1-negative patients (Mozos et al., 2009; Royo et al., 2012; Salaverria et al., 2013).

The role of SOX11 in predicting MCL prognosis remains apparently controversial. Recently, it has been observed that some SOX11-negative tumors may progress rapidly after diagnosis and have a poor prognosis (Nygren et al., 2012). Interestingly, further studies have shown that the aggressive behavior of SOX11-negative MCLs seems related to an extensive nodal disease, blastoid morphology, complex karyotypes, and 17p/*TP53* alterations (Royo et al., 2012; Navarro et al., 2012). One possible explanation for this apparent discordance is that the SOX11-negative cases with aggressive disease could correspond to a progressed or transformed stage with generalized lymphadenopathy of SOX11-negative tumors, suggesting this phenotype may have an indolent phase and eventually some of the tumors could progress with a generalized lymphadenopathy and aggressive behavior associated with acquisition of *TP53* mutations or other genetics events (Jares et al., 2012).

Therefore, SOX11 expression by itself should not be considered a prognostic parameter but a biomarker that may help to recognize a particular subtype of MCL with different clinical and biological features than conventional MCLs (Jares et al., 2012).

1.4. The role of epigenetics in cancer

1.4.1. Epigenetic features of normal cells

Epigenetics encompasses hereditable alterations in gene expression and chromatin without accompanying changes in the DNA sequence. Epigenetic events are crucial in the control of both normal cellular processes and abnormal events associated with cancer development (Esteller, 2008).

Major epigenetic mechanisms include DNA methylation, covalent post-translational modification of histones proteins, and RNA-mediated gene silencing.

DNA methlylation has critical roles in the control of gene activity and the architecture of the nucleus of the cell. In humans, DNA methylation occurs in cytosines that precede guanines; these are called dinucleotide CpGs distributed in regions known as CpG islands which span the 5'-end of the regulatory region of many genes (Figure 17) (Herman and Baylin, 2003; Weber et al., 2007).

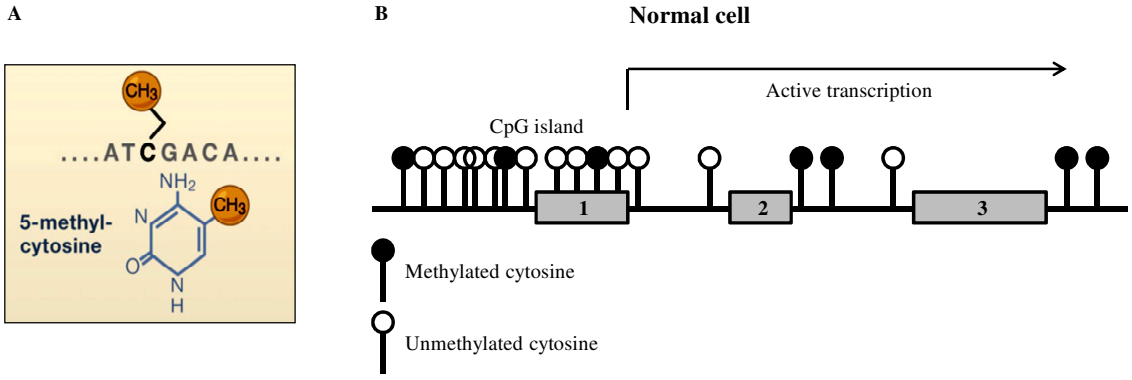

Figure 17. (**A**) DNA methylation occurs in cytosines that precede guanines, called dinucleotide CpG known as CpG islands. (**B**) In normal cells, CpG islands are localized in the 5'-end of regulatory regions of many genes. Unmethylated CpGs are associated with active transcription, whereas methylated CpGs are associated with repression of transcription.

On the other end, histones participate in the regulation of gene expression storing epigenetic information through such post-translational modifications as lysine acetylation, arginine and lysine methylation and serine phosphorylation. These modifications affect gene transcription and DNA repair. It has been proposed that distinct histone modifications form a "histone code" (Figure 18) (Jenuwein and Allis, 2001). Acetylation of histone lysines, for example, is generally associated with transcriptional activation. The functional consequences of the methylation of histones

depends on the type of residue -lysine (K) or -arginine (R) and the specific site that the methylation modifies (e.g., K4, K9, or K20) (Mack,2006; Bernstein et al., 2007). Methylation of H3 at K4 is closely linked to transcriptional activation (Karpf and Matsui, 2005), whereas methylation of H3 at K9 or K27 and H4 at K20 is associated with transcriptional repression. This pattern of DNA methylation and histone modifications is essential for the physiological activities of cells and tissues (Esteller, 2008).

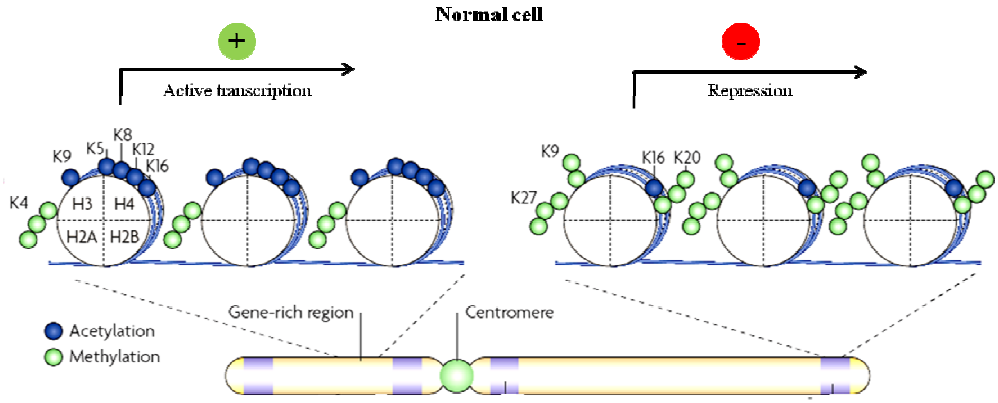

Figure 18. Histone-modification code for a typical chromosome in normal cells. Left, activating histone marks associated with active transcription, localized in a gene rich region. Right, inactivating histone marks associated with repression of transcription mapped in heterocromatin (Esteller, 2007).

DNA methylation and Histone acetylation in the control of gene transcription

Cytosine methylation plays an important role in a number of central cellular functions. Methylation is carried out by two types of DNA methyltransferases (DNMTs): *de novo* and maintenance methyltransferases. Methylation patterns are established during early development by *de novo* methyltransferases DNMT3A and DNMT3B and propagated with extreme fidelity by the maintenance methyltransferase DNMT1 (Bird, 2002; Colot and Rossignol, 1999; Reik et al., 1999). Methylation marks are concentrated in transposons and repetitive sequences but are virtually absent at gene promoter regions, except for certain imprinted genes and genes on the inactive X chromosome in female (Jaenisch and Bird, 2003). However, CpGs islands typically unmethylated in normal cells are often hypermethylated in tumor cells, a finding associated with abnormal silencing of tumor suppressor genes and other cancer associated genes. Thus, alteration of methylation patterns leads to malignant transformation (Vaissiere et al., 2008).

Histone acetylation is a reversible modification of specific residues in histone tails and is controlled by histone acetylases (HATs) and histone decetylaces (HDACs) that typically act as transcriptional co-activators and co-repressors, respectively (Vaissiere et al., 2008). While global histone aceylation correlates with general transcriptional activity, promoter-specific acetylation is a critical mechanism to control specific gene activation (Gottesfeld and Forbes, 1997). Histone acetylation affects not only chromatin structure but also the interaction of transcription-regulatory proteins with target DNA in chromatin, modulating gene expression at different levels. For instance, removal of acetyl groups by HDAC results in compactation of chromatin structure and thus repression of gene transcription. Furthermore, low levels of hystone acetylation may also induce another epigenetic modification, e.g. DNA methylation, leading to a permanent gene silencing. Deregulation of histone acetylation can lead to aberrant gene expression and tumorigenesis (Cairns, 2001; Yang, 2004).

Recent studies suggested that an intimate communication and mutual dependence exists between histone acetylation and DNA methylation in the process of gene silencing. Communication between histone acetylation and cytosine methylation may proceed in both directions. In one scenario, DNA methylation may be the pimary mark for gene silencing that triggers events leading to non-permissive chromatin state. In the other scenario, the loss of histone acetylation may serve as the initial event of gene silencing, which is followed by DNA methylase targeting and inducing local DNA hypermethylation (Vaissiere et al., 2008).

Epigenetic modification in Embrionic Stem cells

Human ESCs were shown to possess a unique DNA methylation signature when compared to differentiated cells and cancer cells. The pluripotency-associated genes OCT4 and NANOG are largely unmethylated in ESCs and in iPSCs (induced pluripotent stem cells), and methylated in differentiated cells (Mitsui et al., 2003; Okita et al., 2007). A genome-wide DNA methylation approach to map the methylation status of 11,201 proximal promoters in mouse ESCs revealed that the majority of unmethylated genes corresponded to general cellular functions, whereas the set of methylated genes was enriched for differentiation-associated genes (Fouse et al., 2008).

Histone tail modification patterns have been largely studied in developmental processes. Interestingly, the analysis of histone modifications in ESCs has generated genome-wide

location maps of H3K27me3 and H3K4me3 (Bernstein et al., 2006; Mikkelsen et al., 2007), catalyzed by Polycomb and Trithorax complexes, respectively (Schuettengruber et al., 2007). These studies indicate that many promoters exhibit a bivalent chromatin signature characterized by the joint presence of active chromatin marks, such as H3K4me3, and repressive ones, like H3K27me3 (Vastenhouw and Schier, 2012). These 'bivalent' chromatin domains often mark lineage-regulatory genes. It has been proposed that bivalent domains might repress lineage control genes (H3K27me3) during pluripotency while keeping them poised for activation upon differentiation (H3K4me3). In this model, H3K27me3-mediated repression of developmental control genes might protect cells from the aberrant expression of lineage regulators and thus help to maintain pluripotency (Zhao et al., 2007; Pan et al., 2007).

During differentiation into specific cell types, continued association with H3K27me3 might maintain the repression of the majority of developmental control genes while only a specific subset of regulators is activated in a given lineage. Conversely, it has been proposed that H3K4me3 might poise developmental regulators for activation. H3K4me3 might also protect genes from permanent silencing, for example by repelling transcriptional repressors or blocking DNA methylation (Fouse et al., 2008). Thus, it is possible that bivalent domains convey temporal and spatial precision to the expression of lineage control genes during pluripotency and differentiation (Vastenhouw and Schier, 2012).

1.4.2. Epigenetics in cancer

Hypermethylation of the CpG islands in the promoter regions of tumor suppressor genes is a major event in the origin of many cancers. Throughout epigenetic studies in the last years, aberrant DNA hypermethylation has been described in many human suppressor genes providing new insights into the molecular comprehension of mechanisms of carcinogenesis. The first gene reported was RB tumor suppressor-gene (Greger et al., 1989; Sakai et al., 1991), followed by tumor-suppressor genes VHL (associated with von Hippel-Lindau disease) (Herman et al., 1994), p16 ^{INK4a} (Merlo et al., 1995; Herman et al., 1995; Gonzalez-Zulueta et al., 1995) and BRCA1 (breast-cancer susceptibility gene 1) (Herman and Baylin, 2003; Esteller et al., 2000).

Hypermenthylation of the CpGs-island promoter can affect genes involved in cell cycle, DNA repair, metabolism of carcinogens, cell-to-cell interaction, apoptosis and angiogenesis, all of which are involved in cancer development (Esteller, 2008).

In the DNA methylation scenario, abnormal DNA hypomethylation also contributes to oncogenic transformation or tumor progression. Tumors display an overall DNA hypomethylation compared with the level of DNA methylation in their normal-tissue counterparts. The loss of methylation is mainly due to hypomethylation of repetitive DNA sequences and demethylation of coding regions and introns (Figure 19) (Feinberg and Tycko, 2004).

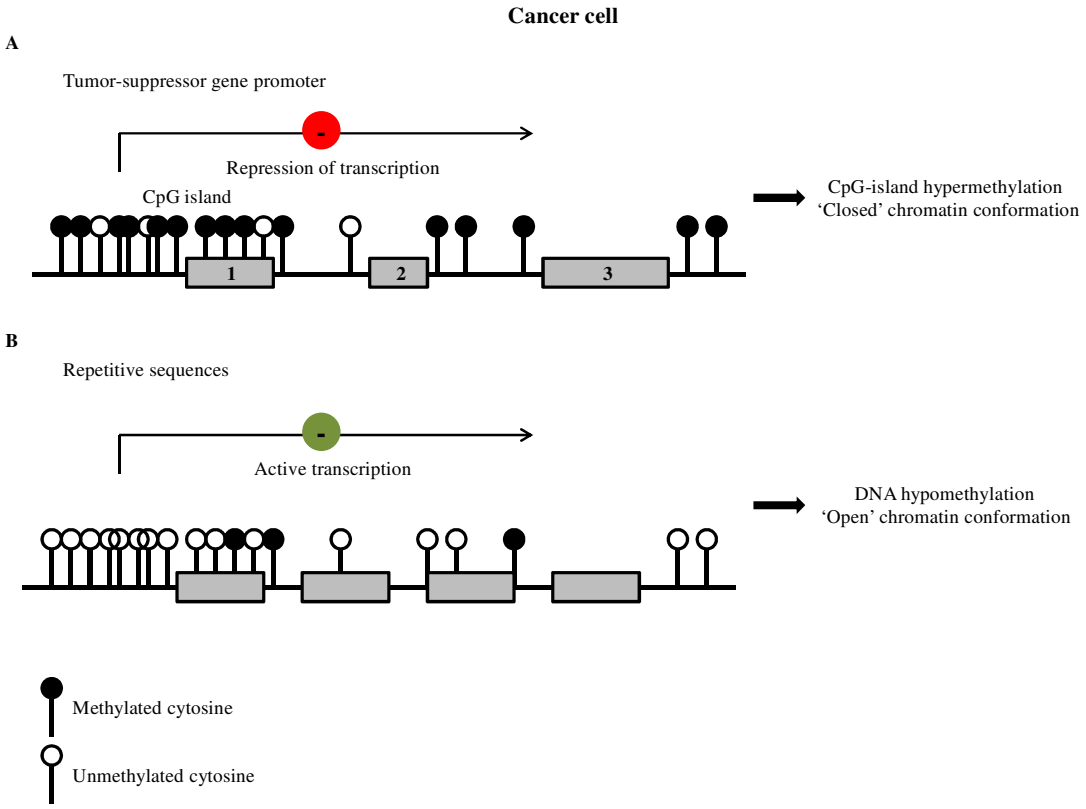

Figure 19. Altered DNA-methylation patterns in tumorigenesis. (**A**) The hypermethylation of CpG islands of tumour suppressor genes is a common alteration in cancer cells, and leads to the transcriptional inactivation of these genes and the loss of their normal cellular functions. (**B**) Global hypomethylation at repetitive sequences contribute to cancer cell phenotype by increasing genomic instability that characterizes tumors.

DNA hypomethylation can contribute to the development of a cancer cell through three main mechanisms: generation of chromosomal instability, reactivation of transposable elements, and loss of imprinting (Esteller, 2008). Undermethylation of DNA can favor mitotic recombination, leading to delections and translocations, and it can also promote

chromosomal rearrangements. This mechanism was observed in studies in which the depletion of DNA methylation by DNMTs knock-out caused aneuploidy (Karpf and Matsui, 2005).

Epigenetic landscape encompasses covalent modifications of histones that can control gene activity. Altered histone modification patterns have been implicated in many human cancers (Cairns, 2001; Wolffe, 2001; Yang, 2004). Hypermethylation of the CpG islands in the promoter regions of tumor-suppressor genes in cancer cells is associated with a particular combination of histone marks: deacetylation of histones H3 and H4, loss of H3K4 trimethylation, and gain of H3K9 dimethylation and H3K27 trimethylation (Figure 20) (Ballestar et al., 2003; Jones and Baylin, 2007).

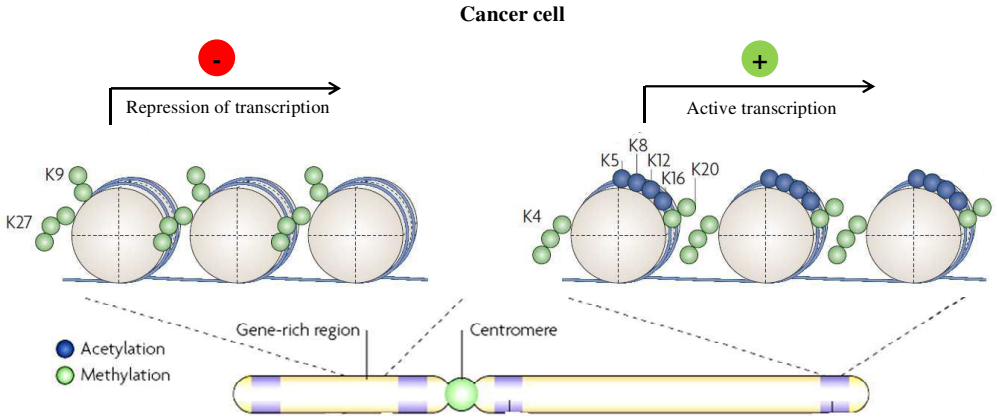

Figure 20. Histone-modification marks for cancer cells. In cancer cells histone modification patterns result altered by the loss of the 'active' histone marks on gene-rich regions, for instance at tumour-suppressor gene promoters, and by the loss of repressive marks at repeated DNA sequences (subtelomeric regions) (Esteller, 2007).

The presence of the hypo-acetylated and hypermethylated histones H3 and H4 silences certain genes with tumor-suppressor–like properties, such as *p21WAF1* (Richon et al., 2000), despite the absence of hypermethylation of the CpG island. In human tumors generally, modifications of histone H4 lead to a loss of monoacetylated and trimethylated forms. These changes appear early and accumulate during the development of the tumor (Fraga et al., 2005). The losses occur predominantly at the monoacetylated Lys16 and trimethylated Lys20 residues of histone H4 in association with hypomethylated repetitive DNA sequences (Fraga et al., 2005).

Genetic alterations in chromatin modifier genes are one of the major responsible of the aberrant epigenetic scenario of the cancer cell. Expression patterns of histone-modifying

enzymes distinguish cancer tissues from their normal counterparts, and they differ according to tumor type (Ozdag et al., 2006).

In leukemias and sarcomas, chromosomal translocations that involve histone-modifier genes, such as histone acetyltransferases (e.g., cyclic AMP response-element binding protein [CREB]-binding [*CREBBP*], protein-monocytic leukemia zinc finger [*CBP-MOZ*]) and histone methyltransferases (e.g., mixed-lineage leukemia 1 [*MLL1*], nuclear-receptor binding SET-domain protein 1 [*NSD1*], and nuclear-receptor binding SET-domain protein 3 [*NSD3*]), create aberrant fusion proteins (Esteller, 2006).

In solid tumors, there is amplification of genes coding for histone methyltransferases such as *EZH2, MLL2*, or *NSD3* (Bracken et al., 2003) or a demethylase (e.g., Jumonji domain-containing protein 2C [*JMJD2C/GASC1*]) (Cloos et al., 2006).

Gene	Alteration	Tumour type
DNA methyltransferases		
DNMT1	Overexpression	Multiple types
DNMT3b	Overexpression	Multiple types
Methyl-CpG-binding proteins		
MeCP2	Overexpression, rare mutations	Multiple types
MBD1	Overexpression, rare mutations	Multiple types
MBD2	Overexpression, rare mutations	Multiple types
MBD3	Overexpression, rare mutations	Multiple types
MBD4	Inactivating mutations in microsatellite instable tumours	Colon, stomach, endometrium
Histone acetyltransferases		
p300	Mutations in microsatellite instable tumours	Colon, stomach, endometrium
CBP	Mutations, translocations, deletions	Colon, stomach, endometrium, lung, leukaemia
pCAF	Rare mutations	Colon
MOZ	Translocations	Haematological malignancies
Histone deacetylases		
HDAC1	Aberrant expression	Multiple types
HDAC2	Aberrant expression, mutations in microsatellite instable tumours	Multiple types
Histone methyltransferases		
MLL1	Translocation	Haematological malignancies
MLL2	Gene amplification	Glioma, pancreas
MLL3	Deletion	Leukaemia
NSD1	Translocation	Leukaemia
EZH2	Gene amplification, overexpression	Multiple types

Table 3. Disrupted DNA methylation and histone-modification genes in cancer (Esteller, 2007).

In a recent study, RNA-seq technology has revealed frequent mutations in two histone-modifying genes, MLL2 and MEF2B, in non-Hodgkin lymphoma. These findings indicate that post-transcriptional modification of histones is of key importance in germinal centre B-cells. The identified mutations can likely deregulate histone modification patterns reducing acetylation and enhancing methylation, and they act as core driver events in the development of NHL (Morin et al., 2011).

In mammalians, microRNAs (miRNAs) represent another important epigenetic mechanism that regulates around 60% of the transcriptional activity of protein-encoding genes (Figure 21). These short 22-nucleotides, non-coding RNAs pair to sequence-specific base in the 3'-UTR of the target mRNAs. The result is mRNA degradation or inhibitor of translation (He and Hannon, 2004). Patterns of miRNAs expression are tightly regulated and play important roles in cell proliferation, apoptosis and differentiation (He and Hannon, 2004).

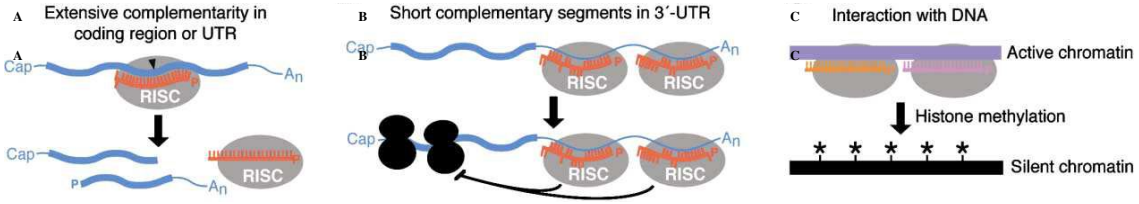

Figure 21. miRNAs are involved in transcriptional and post-transcriptional regulation of gene expression. Gene silencing may occur through three main mechanisms: (**A**) mRNA degradation, (**B**) inhibition of mRNA translation, (**C**) direct interaction with DNA (Bartel, 2009).

Some miRNAs have also been found to undergo methylation-associated silencing in cancerous cells (Chen, 2005; Calin and Croce, 2006a; Lu et al., 2005). Let-7 and miR15/16 play important roles in down-regulating RAS and BCL2 oncogenes, and their silencing has been found in cancer cells (Johnson et al., 2005; Cimmino et al., 2005). DNA hypermethylation in the miRNA 5'-regulatory region is a mechanism that can cause the down-regulation of miRNAs in tumors. In colon-cancer cells with disrupted DNMTs, hypermethylation of the CpG island does not occur in miRNAs. The methylation silencing of *miR-124a* also causes activation of the *CDK6* oncogene, and it is a common epigenetic lesion in tumors (Saito et al., 2006; Lujambio et al., 2007).

1.4.3. Epigenetics in MCL

Epigenetic changes, such as methylation of gene promoters, have been shown to contribute to the pathogenesis of both solid and hematologic malignancies (Jones and

Baylin, 2007). Single-locus studies analyzing methylation in MCL patient samples have shown hypermethylation of key genes, such as cell-cycle regulators $p14^{ARF}$ and *CDKN2A* (Hutter et al., 2006; Chim et al., 2007), protein phosphatase *SHP-1* (Chim et al., 2004) and Rho–adenosine triphosphatase *PARG-1* (Ripperger et al., 2007).

Methylation profiling of MCL revealed 252 hypermethylated genes. Five genes (SOX9, HOXA9, AHR, NR2F2 and ROBO1) correlated with higher proliferation, increased number of chromosomal alterations and shorter survival of patients (Enjuanes et al., 2011). Further studies using genome-wide HELP assay and NimblegenRoche methylation arrays reported differences in methylation between 22 primary MCLs and 10 purified fractions of IgD+ B-cell controls, the putative normal counterparts of these malignant cells (Leshchenko et al., 2010). On a global scale, primary MCLs demonstrated predominantly hypomethylation with locus-specific hypermethylation involving tumor suppressor genes. Among 1413 genes differentially methylated and correlated with gene expression data, eight genes were considered relevant to MCL cancer biology. These included four hypermethylated genes (PCDH8, MLF1, HOXD8, and CDKN2B) and four hypomethylated genes (CD37, HDAC1, NOTCH1, and CDK5), involved in key cellular regulatory pathways such as cell cycle, DNA damage response and cell cycle checkpoint activation (Leshchenko et al., 2010).

Aberrant methylation in MCL may contribute to lymphomagenesis through genomic instability, activation of oncogenes or repression of tumor suppressor genes.

Chromosomal alterations which lead to aberrant histone modification patterns can also cause genomic instability, resulting in the aberrant expression of oncogenes or repression of tumor suppressor genes, concurrently contributing to the pathogenesis of MCL.

Proteins belonging to the Polycomb group (PcG) are epigenetic silencers that regulate lymphopoiesis by forming multimeric complexes that bind and remodel chromatin, thus regulating gene activity (Sparmann and van, 2006). Some PcG genes have been implicated in lymphomagenesis (Raaphorst, 2005). Forced expression of the PcG protein BMI1 in lymphocytes was associated with lymphoma generation, whereas *BMI1* gene is amplified and over-expressed in MCL and in other B-cell lymphomas (Raaphorst, 2005; Jacobs et al., 1999; Bea et al., 2001). BMI1 has essential roles in regulating proliferation and self-renewal of both normal and leukemic stem cells

(Lessard and Sauvageau, 2003). These findings highlight a potential critical characteristic of mutated *BMI1* in lymphomagenesis by reprogramming pre-malignant lymphocytes bearing different chromosomal rearrangements into lymphoma-originating cells.

Protein arginine methyltransferase PRMT5 interacts with human SWI/SNF complexes and methylates histones H3R8 and H4R3 (Pal et al., 2007). PRMT5 is overexpressed in primary MCLs and acts concertedly with HDAC2, methyl-CpG-binding domain protein 2 (MBD2) and DNMT3a to silence genes with anti-cancer and immune modulatory activities (Pal et al., 2003). siRNA-mediated knockdown of PRMT5 in MCL cell lines led to growth arrest and apoptosis (Pal et al., 2007).

Post-transcriptional miRNAs expression deregulation has also been described in many types of neoplasms and has proven to be useful as biomarkers for diagnosis (Huppi et al., 2007; Calin and Croce, 2006b). Some cancer-related miRNAs are also casually involved in oncogenesis due to their impact in the deregulation of oncogenes and tumor suppressor genes (Fabbri and Croce, 2011). Recent studies have investigate the miRNAs profile of MCL and have identified subsets of miRNAs related to the prognosis of the patients and the potential regulation of pathogenic pathway (Di et al., 2010; Zhao et al., 2010; Iqbal et al., 2012). An additional study identified a group of 17 miRNAs differentially expressed between the conventional and indolent subtype of MCL related also to IGHV mutational status, SOX11 expression, nodal presentation and number of chromosomal alterations (Navarro et al., 2013). These differentially expressed miRNAs seem to regulate different pathways relevant for MCL pathogenesis such as DNA damage response (Navarro et al., 2013). Furthermore, miR-34a downregulation was found associated with poor prognosis jointly with high MYC expression (Navarro et al., 2013).

In recent years, studies addressing epigenetic mechanisms in MCL raised the hypothesis that epigenetic modifications, at both DNA methylation and histone modification levels, but also miRNAs may play an important and indispensable role in the pathogenesis of MCL. Epigenetic modifications imply that MCL can epigenetically silence and activate genes that support its survival. As DNA methylation and histone modification are reversible, this provides a rationale for the use of epigenetic specific drugs to treat this disease.

2. AIMS OF THE PRESENT STUDY

The overall aims of the present study were:

I. To study the epigenetic events that lead to SOX11 overexpression in MCL associated with lymphomagenesis and tumor progression.

II. To identify and to characterize signalling pathways regulated by SOX11 using different strategies, aiming for a better understanding of the pathogenesis of aggressive MCL, and to find potential candidates for targeted therapies.

Hypothesis I

Compared with other lymphoma subtypes, MCLs harbor high number of genetic aberrations but none involving the SOX11 genomic region at chromosome 2p25. As no chromosomal changes affecting SOX11 locus were identified in MCL, we hypothesized that epigenetic events could be the most likely mechanisms involved in SOX11 aberrant overexpression.

Aims of paper I

The specific aims of paper I were:

a. To perform a comprehensive study on SOX11 gene expression in stem cells, normal hematopoietic cells and different lymphoid neoplasms through gene expression array and qRT-PCR.

b. To study DNA-methylation and histone modification patterns of SOX11 promoter in a broad spectrum of normal B-cell types and different aggressive lymphomas.

c. To determine the influence of either DNA methylation or histone modification patterns in regulating SOX11 expression in B-cell lymphomas.

d. To study putative molecular mechanisms leading to SOX11 aberrant expression in B-cell lymphomas using bioinformatic analysis.

Hypothesis II

SOX11 has no known lymphopoietic function and it is neither expressed in lymphoid progenitors nor in mature normal B-cells. SOX11 upregulation has been detected in various types of human solid tumors and it is expressed in virtually all aggressive

MCLs, and at lower levels in a subgroup of BLs and ALLs but not in other lymphoid neoplasms.

In a gene expression profiling study we identified SOX11 as one of the best discriminatory genes between conventional and indolent MCL tumors. An expanded study of SOX11 protein and mRNA expression in an independent large series of MCL confirmed that its negativity was associated with a significant better outcome than SOX11-positive MCLs, suggesting that SOX11 may be an important element in the pathogenesis of this tumor. However, the function of SOX11 and its potential target genes in lymphoid cells remain unknown.

The goal of our study was to identify the spectrum of genes regulated by SOX11 in malignant lymphoid cells and provide insights on how the constitutive overexpression of SOX11 may contribute to the oncogenic development of this aggressive type of malignant lymphoma.

Aims of paper II

The specific aims of paper II were:

a. To investigate the potential tumorigenic ability of SOX11 in a MCL-xenotransplant model.

b. To identify target genes and transcription programs regulated by SOX11 in MCL combining genome-wide promoter analysis and gene expression profiling upon SOX11 silencing in MCL cell lines.

c. To study the phenotype associated to the loss of SOX11 expression in MCL cell lines.

d. To study the putative oncogenic pathways regulated by SOX11 in primary MCL tumors.

3. RESULTS

3.1. Paper I

Epigenetic activation of SOX11 in lymphoid neoplasms by histone modifications.

Abstract

Recent studies have shown aberrant expression of SOX11 in various types of aggressive B-cell neoplasms. To elucidate the molecular mechanisms leading to such deregulation, we performed a comprehensive SOX11 gene expression and epigenetic study in stem cells, normal hematopoietic cells and different lymphoid neoplasms. We observed that SOX11 expression is associated with unmethylated DNA and presence of activating histone marks (H3K9/14Ac and H3K4me3) in embryonic stem cells and some aggressive B-cell neoplasms. In contrast, adult stem cells, normal hematopoietic cells and other lymphoid neoplasms do not express SOX11. Such repression was associated with silencing histone marks H3K9me2 and H3K27me3. The SOX11 promoter of non-malignant cells was consistently unmethylated whereas lymphoid neoplasms with silenced SOX11 tended to acquire DNA hypermethylation. SOX11 silencing in cell lines was reversed by the histone deacetylase inhibitor SAHA but not by the DNA methyltransferase inhibitor AZA. These data indicate that, although DNA hypermethylation of SOX11 is frequent in lymphoid neoplasms, it seems to be functionally inert, as SOX11 is already silenced in the hematopoietic system. In contrast, the pathogenic role of SOX11 is associated with its de novo expression in some aggressive lymphoid malignancies, which is mediated by a shift from inactivating to activating histone modifications.

OPEN ACCESS Freely available online

PLoS one

Epigenetic Activation of SOX11 in Lymphoid Neoplasms by Histone Modifications

Maria Carmela Vegliante[1], Cristina Royo[1], Jara Palomero[1], Itziar Salaverria[2], Balazs Balint[3], Idoia Martín-Guerrero[2], Xabier Agirre[4], Amaia Lujambio[3], Julia Richter[2], Silvia Xargay-Torrent[1], Silvia Bea[1], Luis Hernandez[1], Anna Enjuanes[1], María José Calasanz[5], Andreas Rosenwald[6], German Ott[7], José Roman-Gomez[8], Felipe Prosper[4], Manel Esteller[3], Pedro Jares[1], Reiner Siebert[2], Elias Campo[1,9], José I. Martín-Subero[9☯], Virginia Amador[1*☯]

1 Hematopathology Section, Laboratory of Pathology, Hospital Clínic, Institut d'Investigacions Biomèdiques August Pi i Sunyer (IDIBAPS), University of Barcelona, Barcelona, Spain, **2** Institute of Human Genetics, Christian-Albrechts University Kiel and University Hospital Schleswig-Holstein, Campus Kiel, Kiel, Germany, **3** Cancer Epigenetics and Biology Program (PEBC), Bellvitge Biomedical Research Institute (IDIBELL), L'Hospitalet de Llobregat, Barcelona, Spain, **4** Hematology Service and Area of Cell Therapy, Clínica Universidad de Navarra, Foundation for Applied Medical Research, University of Navarra, Pamplona, Spain, **5** Department of Genetics, University of Navarra, Pamplona, Spain, **6** Institute of Pathology, University of Würzburg, Würzburg, Germany, **7** Department of Clinical Pathology, Robert-Bosch-Krankenhaus and Dr. Margarete Fischer-Bosch Institute of Clinical Pharmacology, Stuttgart, Germany, **8** Hematology Department, Reina Sofia Hospital, Cordoba, Spain, **9** Department of Anatomic Pathology, Pharmacology and Microbiology, University of Barcelona, Barcelona, Spain

Abstract

Recent studies have shown aberrant expression of SOX11 in various types of aggressive B-cell neoplasms. To elucidate the molecular mechanisms leading to such deregulation, we performed a comprehensive SOX11 gene expression and epigenetic study in stem cells, normal hematopoietic cells and different lymphoid neoplasms. We observed that SOX11 expression is associated with unmethylated DNA and presence of activating histone marks (H3K9/14Ac and H3K4me3) in embryonic stem cells and some aggressive B-cell neoplasms. In contrast, adult stem cells, normal hematopoietic cells and other lymphoid neoplasms do not express SOX11. Such repression was associated with silencing histone marks H3K9me2 and H3K27me3. The *SOX11* promoter of non-malignant cells was consistently unmethylated whereas lymphoid neoplasms with silenced SOX11 tended to acquire DNA hypermethylation. SOX11 silencing in cell lines was reversed by the histone deacetylase inhibitor SAHA but not by the DNA methyltransferase inhibitor AZA. These data indicate that, although DNA hypermethylation of *SOX11* is frequent in lymphoid neoplasms, it seems to be functionally inert, as SOX11 is already silenced in the hematopoietic system. In contrast, the pathogenic role of SOX11 is associated with its de novo expression in some aggressive lymphoid malignancies, which is mediated by a shift from inactivating to activating histone modifications.

Citation: Vegliante MC, Royo C, Palomero J, Salaverria I, Balint B, et al. (2011) Epigenetic Activation of SOX11 in Lymphoid Neoplasms by Histone Modifications. PLoS ONE 6(6): e21382. doi:10.1371/journal.pone.0021382

Editor: Eliana Saul Furquim Werneck Abdelhay, Instituto Nacional de Câncer, Brazil

Received April 28, 2011; **Accepted** May 26, 2011; **Published** June 27, 2011

Funding: This study was supported by the Comisión Ministerio de Ciencia e Innovación (BFU2009-09235 to VA, SAF2009-08663 to JIM-S, SAF08/3630 to EC), Instituto de Salud Carlos III Red Temática de Investigación Cooperativa de Cancer (2006RET2039 to EC), the Asociación Española Contra el Cancer (to ME), the Deutsche Krebshilfe through the network project "Molecular Mechanisms in Malignant Lymphomas subproject M2 (70-3173-Tr3 to RS and JIM-S), the Kinderkrebsinitative Buchholz/Holm-Seppensen (to RS), the Alexander von Humboldt Foundation (to IS) and the Junta de Andalucia (2009/0206 to JR-G). The funders had no role in study design, data collection and analysis, decision to publish, or preparation of the manuscript.

Competing Interests: The authors have declared that no competing interests exist.

* E-mail: vamador@clinic.ub.es

☯ These authors contributed equally to this work.

Introduction

The SRY (sex-determining region Y)-box11 (*SOX11*) gene belongs to the SRY-related high-mobility group box gene family of transcription factors, which as a whole controls cell fate and differentiation [1]. SOX11 has been shown to be particularly important for the development of nervous system and adult neurogenesis [2,3,4,5]. SOX11 upregulation has been detected in various types of solid tumors including medulloblastomas, gliomas and epithelial ovarian tumors [6,7,8]. Although SOX11 does not seem to play a role in hematopoiesis, its expression has been observed in various aggressive B-cell neoplasms, suggesting that this protein plays a role in the pathogenesis of these tumors. In particular, SOX11 is highly expressed in mantle cell lymphoma (MCL), acute lymphoblastic leukemias (ALL) and in some Burkitt lymphomas (BL) [9,10,11,12,13]. In contrast, patients with an indolent variant of MCL [14] and other mature B-cell neoplasias such as chronic lymphocytic leukemia (CLL), follicular lymphoma (FL) or diffuse large B-cell lymphoma (DLBCL) do not express SOX11 [9,10,12]. Chromosomal changes, like translocations or gene amplifications, constitute one of the main mechanisms leading to deregulated gene expression in lymphomas [15]. In the case of SOX11, chromosomal changes affecting band 2p25.2 (where *SOX11* is located) have not been identified in MCL, BL or ALL [16,17,18,19,20]. Therefore, other, non-genetic mechanisms should be responsible for its expression pattern in these lymphoid neoplasms. Epigenetic changes like DNA methylation and histone modifications, that regulate gene expression without changing the DNA sequence [21,22], could be

involved in deregulating SOX11 expression in lymphoid neoplasms. In the present study, we have performed a thorough epigenetic characterization of *SOX11*, including DNA methylation and various activating and inactivating histone marks, in several subtypes of non-malignant cells as well as a wide range of lymphoid neoplasia cell lines and primary cases. Our findings show that SOX11 expression is associated with activating histone marks whereas SOX11 repression is associated with inactivating marks with or without the simultaneous presence of DNA methylation.

Results

SOX11 gene expression in lymphoid neoplasms by microarrays and qRT-PCR

Microarray data confirm that ESCs show high SOX11 expression levels and that SOX11 was not expressed or expressed at very low levels in different hematopoietic cell lineages at various stages of differentiation (Figure 1A–1B, Table S1). Interestingly, upon induction of pluripotent stem cells (iPS) from human hematopoietic cells like CD133+ cord blood cells [23], CD34+ peripheral blood cells or peripheral blood mononuclear cells (PBMC) [24] with different transcription factors (SOX2, OCT4, KLF4 and MYC) , SOX11 is clearly re-expressed (Figure 1C).

In lymphoid neoplasms, SOX11 shows high expression levels in B-ALLs with the TEL-AML1 fusion or E2A rearrangement as well as in the great majority of cases of MCL (Figure 1A–1B). Also, approximately half BL cases express SOX11. In the rest of the neoplasms studied, including additional ALL groups and mature B-cell neoplasms such as CLL, FL, iMCL, DLBCL, primary mediastinal B-cell lymphoma and BL, *SOX11* was either not expressed or expressed at very low levels in a small subset of the cases (Figure 1A–1B).

The qRT-PCR results were in line with the data generated with microarrays. SOX11 was strongly expressed in the embryonic stem cell line NTERA-2, whereas in the two adult stem cells studied (MCS and MAPC) SOX11 was not expressed (Figure 1D). No expression of SOX11 was detected in the four different CD19+

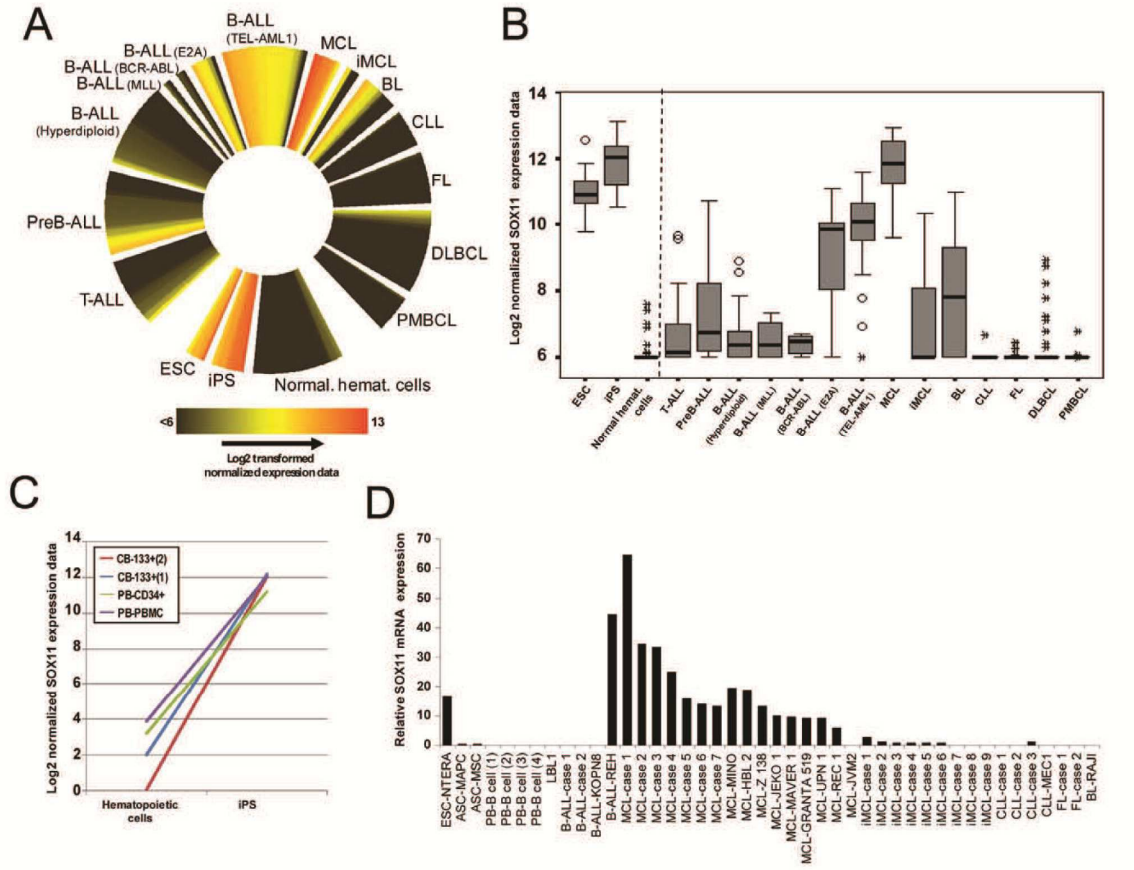

Figure 1. Gene expression analyses of SOX11. (A) Circular heatmap from microarray-data (Table S1) showing the normalized expression levels of 416 samples. SOX11 is consistently expressed in ESC, iPS, MCL as well as B-ALLs with TEL/AML1 fusion or E2A rearrangements. (B) Box-plot summarizing the data shown in panel 1A. (C) Induction of SOX11 in normal hematopoietic cells transformed to iPS by expressing OCT4, SOX2, KLF4 and MYC [23,24]. (D) Analysis of SOX11 gene expression using qRT-PCR in different lymphoid neoplasm cell lines and primary cases. T-ALL: T-cell acute lymphoblastic leukemia; PreB-ALL: PreB acute lymphoblastic leukemia; B-ALL: B-cell acute lymphoblastic leukemia; MCL: mantle cell lymphoma; iMCL: indolent variant of mantle cell lymphoma; BL: Burkitt lymphoma; CLL: chronic lymphocytic leukemia; FL: follicular lymphoma; DLBCL: diffuse large B-cell lymphoma; PMBCL: primary mediastinal B-cell lymphoma; ESC: embryonic stem cell; iPS: induced pluripotent stem cell; CB: cord blood; PB: peripheral blood; ASC: adult stem cell.
doi:10.1371/journal.pone.0021382.g001

cells purified from healthy blood and the lymphoblastoid B-cell line LBL1. In lymphoid neoplasms, SOX11 was highly expressed in *TEL-AML1*-positive ALL (cell line REH) as well as in all MCLs studied, including eight cell lines and seven primary cases. In contrast, SOX11 was absent in the MCL cell line JVM2, the indolent variants of MCL (nine cases), BCR-ABL-positive B-ALLs (the cell line KOPN8 and two primary cases), CLL (three primary cases), FL (two primary cases) and BL (cell line RAJI) (Figure 1D).

DNA methylation status of SOX11 by microarrays

To gain a global insight into the DNA methylation status of *SOX11* in hematological neoplasms and control samples (total n = 159), we used a CpG-specific microarray that includes two CpGs in the 5′ regulatory region of *SOX11* (circular heatmap shown in Figure 2A). In general, both CpGs showed similar DNA methylation values, but as some exceptions were observed, we defined the methylation status of *SOX11* as the maximum of the two values, which was subsequently used to calculate descriptive statistics and the box-plot (Figure 2B). Using this approach, we could determine that various types of normal hematopoietic cells showed low DNA methylation levels (Median/IQR = 0.23/0.22). Cases of ALL were heterogeneous. In those ALLs with the *TEL-AML1* fusion (n = 5) *SOX11* was completely unmethylated (Median/IQR = 0.04/0.04) whereas in other subtypes, like *BCR-ABL* positive (n = 15) or T-ALL (n = 9) *SOX11* exhibited a gradient of DNA methylation values, from unmethylated to methylated cases (Median/IQR of 0.49/0.41 and 0.43/0.40, respectively). MCL primary cases (n = 61) were mostly unmethylated (Median/IQR of 0.10/0.07) and cases of indolent variant of MCL (n = 9) showed a variable degree of DNA methylation (Median/IQR = 0.65/0.44). Aggressive germinal center B-cell lymphomas like DLBCL (n = 14) and molecular BL (mBL, which were defined by transcriptional and genomic profiling) [25] (n = 6) were frequently methylated. DNA methylation values in mBLs showed more heterogeneity (median/IQR = 0.50/0.43) than in DLBCL, in which they were homogeneously methylated (median/IQR = 0.58/0.12) (Figure 2B).

In MCL cell lines (n = 8), *SOX11* was mostly unmethylated (median/IQR = 0.14/0.17) whereas all non-MCL cell lines including T-ALL (n = 1), DLBCL (n = 3), BL (n = 1) and Hodgkin lymphoma (n = 4) were strongly methylated (median/IQR = 0.91/0.03).

These analyses indicate that *SOX11* is mostly unmethylated in normal controls and some types of lymphoid neoplasias like TEL-AML1 positive-ALLs or MCL. In other types of lymphoid neoplasias, however, *SOX11* tends to acquire variable levels of DNA methylation.

DNA methylation analyses by pyrosequencing and correlation with gene expression

To elucidate whether DNA methylation correlates with SOX11 gene transcription, we quantified the methylation status of six CpGs in the promoter region of *SOX11* using bisulfite pyrosequencing in the same samples used for the expression analysis of SOX11 by qRT-PCR.

The pyrosequencing primer was designed to analyze different CpG sites in the amplified promoter region, including one CpG analyzed by the Infinium array (cg20008332). Twenty six cases (14 primary cases and 12 cell lines) were analyzed by both methods and the DNA methylation values were highly concordant (Rho Spearman coefficient = 0.902, $p<0.001$, Figure S1). The six CpGs showed similar DNA methylation percentages, indicating the presence of a homogeneous methylation pattern in the *SOX11*-associated CpG island (heatmap shown in Figure 2C).

We defined the methylation status of *SOX11* as the mean of DNA methylation levels among the six CpGs. This single value was subsequently used to study the relationship between DNA methylation and SOX11 gene expression.

In general, a significant inverse correlation between *SOX11* promoter methylation and gene expression was identified (Rho Spearman coefficient = −0.676, $p<0.001$) (Figure 2D). However, in many samples (embryonic/adult stem cells, normal B cells and some iMCL, some CLL and FL) SOX11 expression was repressed in spite of its unmethylated status. Interestingly, the MCL cell line JVM2 also showed this lack of correlation. This cell line was obtained from a formerly described B-prolymphocytic leukaemia harbouring t(11;14)(q13;q32) translocation cell line. Although JVM2 is considered a MCL cell line, it has a very low number of genetic alterations compared with other MCL cell lines and presents a expression signature similar to indolent MCL, including SOX11 repression. These findings suggest that SOX11 expression does not depend exclusively on the DNA methylation status of the gene and prompted us to study alternative epigenetic mechanisms.

Detection of histone marks associated with the SOX11 promoter and correlation with gene expression and DNA methylation

To study how the pattern of histone modifications was involved in the regulation of SOX11 expression, we performed quantitative-ChIP assays in samples used for pyrosequencing studies in which at least two million of cells were available.

The relative enrichment of the different marks studied in each sample (H3K4me3, H3Ac, H3K9m2 and H3K27m3) is shown as a heatmap in Figure 3.

We observed that, consistent with expression analyses, *SOX11* promoter in NTERA-2 was enriched for activating chromatin marks (H3K4me3 and H3Ac) and did not show enrichment for repressing marks (H3K9m2 and H3K27m3). On the contrary, in the two types of adult stem cells studied (MCS and MAPC), the four different normal CD19+ cells and the LBL1 cell line, enrichment for repressing histone marks predominates over activating chromatin marks in the *SOX11* promoter, which correlates with the absent expression levels of SOX11 in these samples.

A very similar enrichment pattern as in NTERA-2 was observed in lymphoid neoplasms expressing SOX11. MCLs (GRANTA519 cell line and three primary cases) and the TEL-ALM1 positive ALL (REH cell line) were clearly enriched for activating H3K4me3 and H3Ac chromatin marks. In contrast, samples lacking SOX11 expression, i.e. the MCL cell line JVM2 and iMCL samples (n = 3) as well as the rest of the lymphoid samples (BCR-ABL1-positive ALLs (two primary cases and one cell line (KOPN8)), three CLLs (two primary cases and one cell line (MEC1)), two FL cases and one BL (RAJI)) were enriched for the silencing marks H3K9m2 and H3K27m3 but not for activating marks in *SOX11* promoter (Figure 3).

Analyzing together SOX11 expression, DNA methylation and histone marks in the same cells, our data indicate that SOX11 expression is associated with activating histone marks and absence of DNA methylation. In contrast, lack of SOX11 expression was associated with silencing histone marks, with or without the simultaneous presence of DNA methylation. These results suggest that histone marks, rather than DNA methylation, are the main epigenetic mechanism controlling SOX11 expression.

SAHA induces SOX11 gene expression in lymphoid cell lines

To confirm the role of histone modifications and DNA methylation in SOX11 gene expression, we investigated gene re-expression, DNA methylation and H3 histone acetylation status

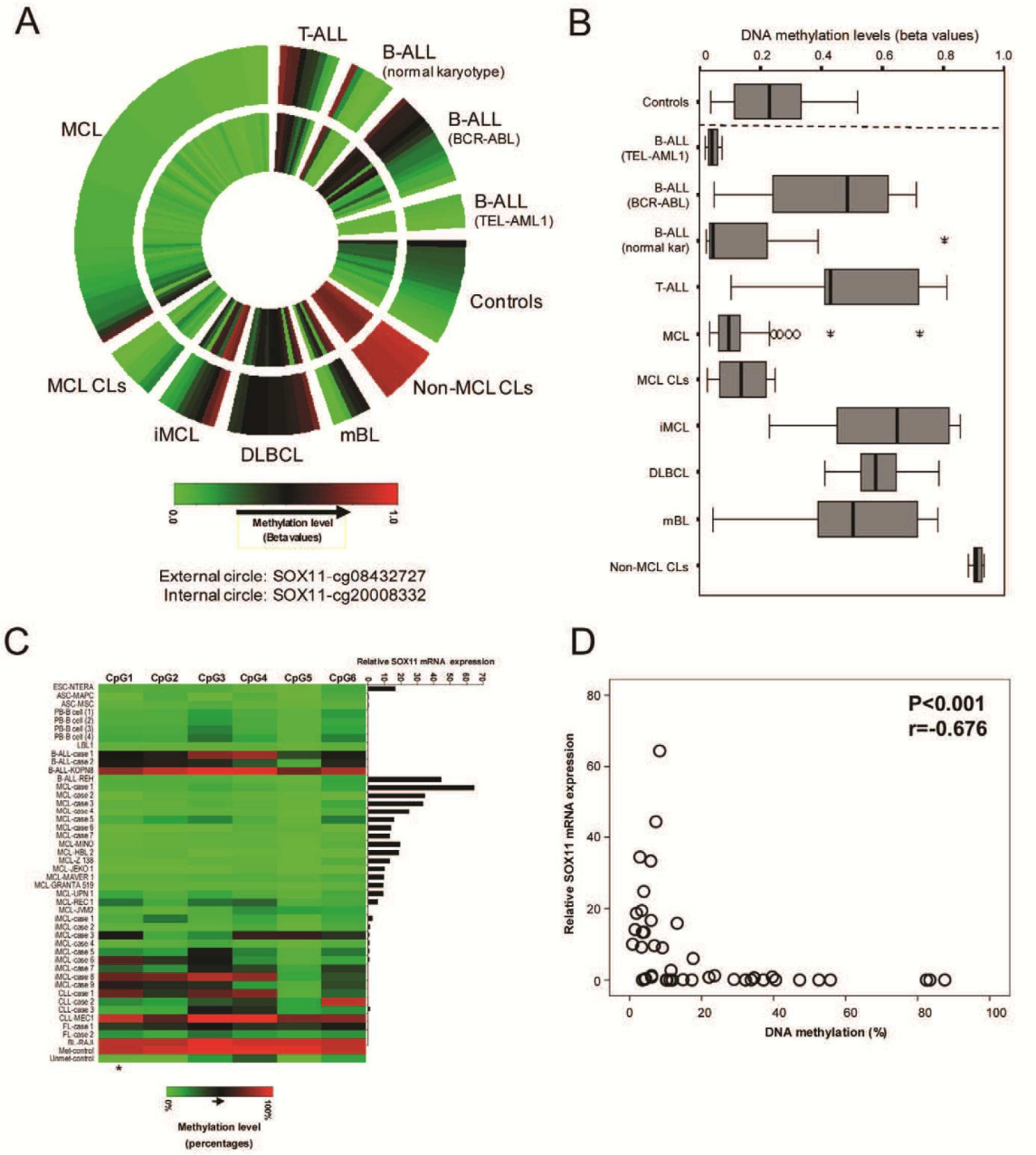

Figure 2. DNA methylation analyses of the promoter region of *SOX11*. (A) Circular heatmap of the two *SOX11*-specific CpGs measured with the 27k Illumina microarray. (B) Box-plot summarizing the data shown in panel 2A. (C) Heatmap of the six *SOX11*-specific CpGs quantified by bisulfite pyrosequencing and SOX11 gene expression analyzed by qRT-PCR. *This CpG is also analyzed by the Infinium array (cg20008332). (D) Scatter plot showing a negative correlation between DNA methylation levels and relative SOX11 mRNA expression (Rho Spearman coefficient = −0.675, p<0.001).
doi:10.1371/journal.pone.0021382.g002

after treatment with AZA, SAHA or both. For this study, we used two cell lines with silent SOX11 but different methylation status of *SOX11*, i.e. RAJI (promoter methylated) and JVM2 (promoter unmethylated).

SAHA treatments, which inhibit histone deacetylases, caused a significant dose-dependent increase in SOX11 mRNA and protein levels in JVM2 (62 fold SOX11 mRNA expression) (Figure 4A) and RAJI (105 fold SOX11 mRNA expression) (Figure 4B). AZA

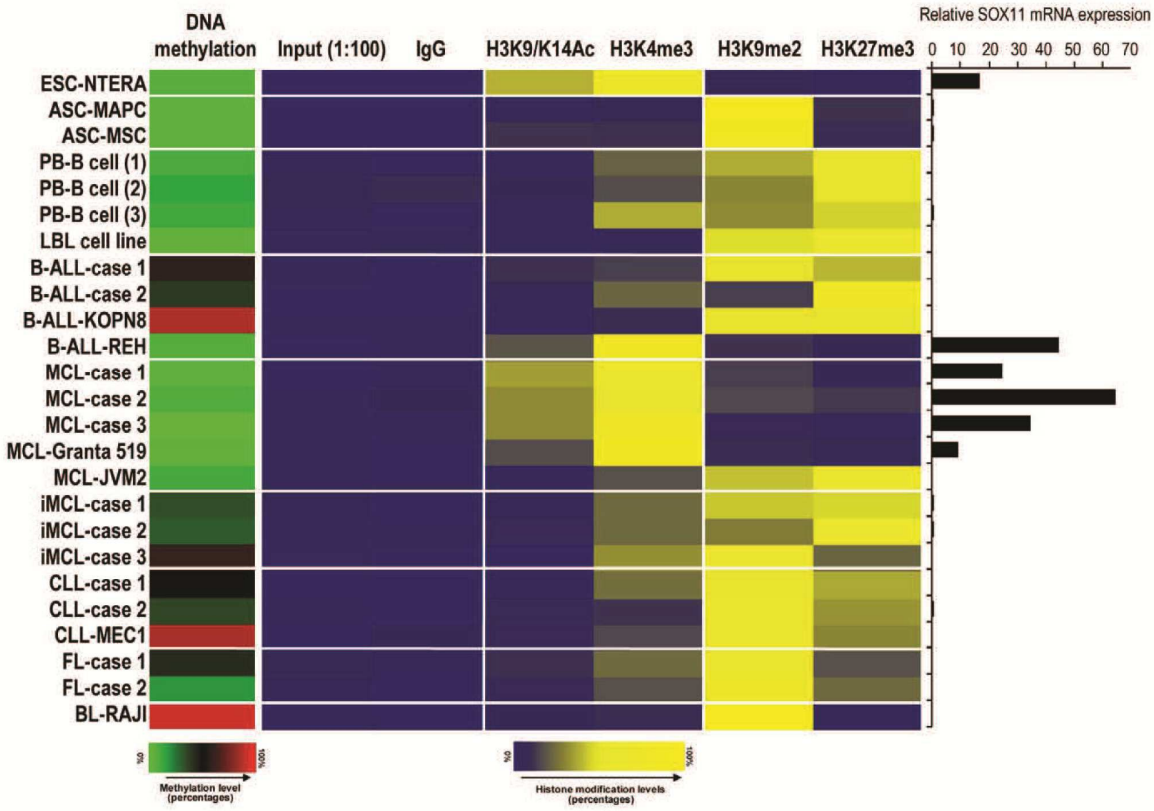

Figure 3. Enrichment of activating and inactivating chromatin marks in *SOX11* promoter and correlation with DNA methylation and gene expression. (Left) Heatmap showing the mean of the six *SOX11*-specific CpGs quantified by bisulfite-pyrosequencing. (Center) Heatmap representing the relative enrichment of H3K4me3 and H3K9/K14Ac as activating chromatin marks and H3K9me2 and H3K27me3 as inactivating chromatin marks in *SOX11* promoter. A rabbit IgG was used as a ChIP negative control. The values are relative to 1:100 diluted input samples. (Right) Relative SOX11 gene expression analyzed by qRT-PCR.
doi:10.1371/journal.pone.0021382.g003

alone, which inhibits DNA methyltransferases, although decreased DNA methylation levels in RAJI (Figure S2), had little influence on SOX11 gene expression in both cell lines. Only a slight increase in RAJI cells was observed (2.4 fold) (Figure 4B).

Histone modifications at the *SOX11* promoter were subsequently measured by quantitative-ChIP analyses after SAHA treatments. In both JVM2 and RAJI cell lines, an increase of H3 acetylation in the *SOX11* promoter was observed in the presence of SAHA (5.7 fold in JVM2 and 2.5 fold in RAJI). The activating H3K4me3 mark was also slightly induced by SAHA treatment (2.05 fold in JVM2 and in 1.3 fold in RAJI cells) (Figure 4C and 4D).

These functional analyses support our previous finding that histone modifications rather than DNA methylation play a predominant role in regulating SOX11 expression.

Discussion

Several studies have recently demonstrated that SOX11 is up-regulated in various aggressive lymphoid neoplasms [9,10,11, 12,13,14]. However, the molecular mechanisms leading to such deregulated expression remain unknown. Here, we have performed for the first time a thorough epigenetic characterization of *SOX11* in a wide range of lymphoid malignancies as well as in embryonic/adult stem cells and normal hematopoietic cells.

Our SOX11 expression analyses by microarrays and qRT-PCR extensively confirm and expand previous findings [9,10,11, 12,13,14]. In non-tumoral cells like ESCs (Figure 1A/1B) and the embryonic cell line NTERA-2 (Figure 1D), SOX11 is highly expressed. However, SOX11 loses its expression in adult progenitor cell types like in MAPCs and MSCs, and all normal hematopoietic cells studied (Figure 1). In contrast, lymphoid malignancies clearly show a differential SOX11 expression among different clinicopathological diseases. In particular, SOX11 is expressed in some subtypes of ALLs (TEL-AML1-positive or with E2A rearrangements), MCLs and part of the BL, but not in any of the other neoplasias analyzed, including the indolent variant of MCL.

As DNA methylation is the most widely studied epigenetic mechanism leading to deregulated gene expression in cancer [21,22], we initially analyzed the methylation status of *SOX11* promoter by microarrays [26] and bisulfite pyrosequencing [27]. As expected, our findings show that those samples expressing SOX11 are unmethylated. However, adult stem cells and normal hematopoietic cells, although silenced, are consistently unmethylated. In some lymphoid neoplasms without SOX11 expression, this gene acquires variable degrees of DNA methylation. These

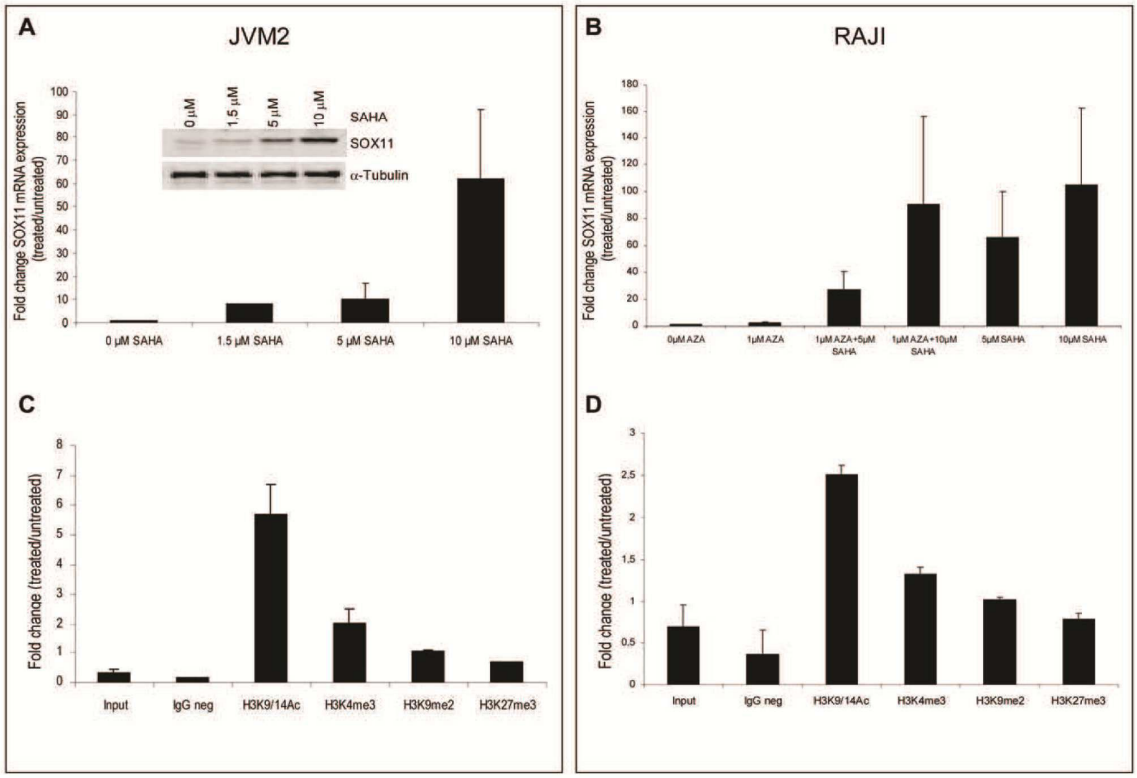

Figure 4. SOX11 gene re-expression and histone modification status analysis after treatments with AZA, SAHA or both in JVM2 and RAJI cell lines. (A) Analysis of relative SOX11 mRNA expression by qRT-PCR and Western blot analysis in JVM2 cells after being treated for 24 h with different concentrations of SAHA (0, 1.5, 5 and 10 µM). (B) Analysis of relative SOX11 gene expression by qRT-PCR in RAJI cells after being treated for 72 h with 1 µM AZA alone or in combination with 5 µM and 10 µM SAHA 24 h concluding the treatment with AZA. For treatment with SAHA alone, 5 µM or 10 µM of SAHA were added to the medium and cultured for 24 h. (C) Enrichment of H3K4me3, H3K9/K14Ac, H3K9me2 and H3K27me3 chromatin marks in the *SOX11* promoter of JVM2 cell line and (D) RAJI cell line treated with SAHA. Values are expressed as relative values of enrichment respect to untreated cells. In JVM2 and RAJI cell lines we observed changes in histone H3 levels after SAHA treatments. To avoid chromatin marks enrichment due to nucleosome increase, levels of H3K4me3, H3K9/K14Ac, H3K9me2 and H3K27me3 chromatin marks had been corrected by the total levels of histone H3 in each cell line.
doi:10.1371/journal.pone.0021382.g004

findings are in line with the DNA methylation of *SOX11* recently reported in CLL, FL and DLBCL [28,29]. In our series, although SOX11 was silenced in all cases showing methylation, a wide range of samples, from normal cells to lymphoid neoplasms (Figure 2D), were also silenced in spite of an unmethylated status of the *SOX11* promoter. Thus, DNA methylation does not seem to represent a mechanism leading to *de novo* repression in lymphoid neoplasms and in contrast to the conclusion of a recent publication [28], it might not be functionally relevant. The fact that *SOX11* is hypermethylated and silenced in some lymphomas can lead to assume that *SOX11* is a candidate tumor suppressor gene, as recently proposed by Gustavsson and coworkers. However, this assumption must also take into consideration the expression status of this gene in normal lymphoid cells (i.e. expressed in normal cells and repressed in tumor cells). As we here clearly show that *SOX11* is silenced by histone modifications in normal hematopoietic cells, hypermethylation in lymphomas does not modify SOX11 expression levels, and thus, does not seem to have a functional impact.

Combined epigenomic and transcriptomic studies have previously demonstrated that a large proportion of the genes becoming hypermethylated in solid tumors [30] and aggressive B-cell lymphomas [31] are already silenced in their normal cellular counterparts. This finding could be explained by a switch of epigenetic marks between normal cells and tumor samples [32]. As DNA methylation is a more stable repressing mark than histone modifications, it has been hypothesized that tumors reduce their epigenetic plasticity of hypermethylating genes silenced by histone marks in normal cells [32].

In order to gain further insights into SOX11 expression patterns observed in stem cells, normal hematopoietic cells and lymphoid neoplasms, we performed qPCR-ChIP experiments with antibodies against activating and silencing histone modifications. Our data demonstrate that SOX11 expression is associated with histone modifications in all the studied samples. In the embryonic cell line NTERA-2, SOX11 was expressed and its promoter was enriched for the activating marks H3K4me3 and H3K9/K14Ac. Interestingly, an B-ALL with TEL-ALM1 fusion (REH cell line) and all MCLs studied showed the same pattern of activation of *SOX11* as in embryonic stem cells, i.e. enrichment for H3K4me3 and H3K9/K14Ac. This finding is in line with studies proposing that haematological neoplasms acquire chromatin features similar to

stem cells [31,33]. In samples with SOX11 repression, including adult stem cells, normal hematopoietic cells and various lymphoid malignancies, we observed that the *SOX11* promoter was enriched for the silencing marks H3K9me2 and H3K27me3.

To study the causal relationship between SOX11 expression and epigenetic marks, we performed treatments with the AZA and/or SAHA, which inhibit DNA methylation and histone deacetylation enzymes, respectively. SAHA caused the upregulation of SOX11 expression in both JVM2 and RAJI cells, independent of the distinct promoter methylation status in these cells. However, treatment with AZA, although decreased the DNA methylation levels, it did not alter the pattern of histone modifications nor had any effect on the SOX11 gene expression levels in RAJI. Taken together, these findings show that SOX11 expression is associated with activating histone marks whereas SOX11 repression is associated with inactivating marks with or without the simultaneous presence of DNA methylation.

Our data show that the pathogenic effect of SOX11 in lymphoid neoplasias is most likely its aberrant expression associated with activating histone marks in some aggressive B-cell neoplasms. Theoretically, such upregulation could be explained either by a memory of the initial cell from which these neoplasms were originated or by its *de novo* expression. The first hypothesis postulates that SOX11 is expressed in a limited window during B-cell ontogenesis, and that MCLs and some ALLs may derive from such cell type. However, SOX11 is not expressed in any of the normal human hematopoietic cells analyzed, from stem cells to plasma cells (Figure 1A). Additionally, we have performed a more detailed bioinformatic analyses using different mouse hematopoietic cell types derived from the Immunological Genome Project [34]. Using this dataset (GEO accession number GSE15907), SOX11 was not expressed in any of the over 100 hematological cell types studied (Table S2). Therefore, this first hypothesis cannot be supported by experimental data and a *de novo* SOX11 expression caused by a switch from inactivating to activating histone modifications is the most likely explanation. Supporting this view is the fact that reprogramming hematopoietic cells to iPS by inducing expression of OCT4, SOX2, KLF4, and MYC [24], or only OCT4 and SOX2 [23] leads to a *de novo* expression of SOX11 (Figure 1C). Thus, it is likely to hypothesize that genetic or epigenetic changes affecting SOX11 regulators take place in lymphoid neoplasms and result in aberrant *de novo* SOX11 expression. In the case of TEL-AML1-positive B-ALLs it might be that such fusion protein induces SOX11 expression. A recent publication has characterized the transcriptome of cord blood cells after introducing the *TEL-AML1* fusion gene [35]. We extracted SOX11 expression from this study (ArrayExpress identifier E-MEXP-1403) and its expression did not change from wild-type cord blood cells to *TEL-AML1* transfected cells (Table S3). In the case of MCL, CCND1 expression derived from the t(11;14) translocation cannot lead to SOX11 expression, as indolent forms of MCL, that also contain the t(11;14) translocation, do not express SOX11 [18,19]. Therefore, the upstream mechanisms inducing an open chromatin conformation and subsequent oncogenic upregulation of SOX11 remain unknown.

In conclusion, our data provide a comprehensive characterization of the epigenetic mechanisms leading to SOX11 deregulation in lymphoid neoplasms. As SOX11 is not expressed in normal lymphoid cells, its DNA hypermethylation in some neoplasms without SOX11 expression is most likely functionally inert, and might be associated with reducing epigenetic plasticity in tumor cells [32]. We also show that *de novo* SOX11 expression is associated with aggressive lymphoid malignancies like MCL, some ALL subtypes and a fraction of BL cases, being this effect mediated by a switch between inactivating and activating histone modifications. Furthermore, as SOX11 is strongly expressed in ESCs, our data suggest that SOX11 expression could be associated with the acquisition of stem cell-like chromatin features, as previously proposed [31]. At the mechanistic level, additional studies are required to elucidate which is the functional role of the illegitimate SOX11 expression in lymphoid neoplasms, and which upstream transcription factors and histone modifying enzymes are involved in this phenomenon. At the clinical level, it seems that SOX11 expression confers the cells a more aggressive behaviour, is prognostically important in MCLs [14], and its silencing might represent a suitable strategy for therapeutic intervention.

Methods

Cell lines, patient samples and controls

A total of 27 cell lines and 173 primary tumors derived from lymphoid neoplasms were used for gene expression, DNA methylation, histone modification and/or protein analyses. The 27 cell lines included were one B-cell ALL (B-ALL) with *TEL-AML1* fusion (REH), one B-ALL with *BCR-ABL* fusion (KOPN8), one T-cell ALL (T-ALL) (JURKAT), one CLL (MEC1), nine MCL (JVM2, GRANTA519, MINO, JEKO1, Z138, HBL2, UPN1, MAVER1 and HBL2), five DLBCL (VAL, RL, RCK8, LY3 and LY10), two BL (RAJI and DAUDI), as well as seven Hodgkin lymphoma (L1236, L428, KM-H2, HDLM2, L591, L540 and UHO1).

The 173 primary cases studied included 29 B-ALLs (17 with *BCR-ABL* fusion, five with *TEL-AML1* fusion and seven with normal karyotype), nine T-ALLs, seven CLLs, 20 FL, 66 MCLs, 20 DLBCL and 12 BL. All these cases were diagnosed according to the WHO classification [36]. Additionally, we included 10 MCL lacking SOX11 expression. In a previous study we have shown that these MCLs carry the t(11;14), express CCND1, display simple karyotypes, and have an indolent clinical course (stable disease for more than two years without chemotherapy) [14]. These cases will be referred to as indolent MCL (iMCL).

We also studied three types of stem cells: NTERA-2, an embryonal carcinoma cell line widely used as a model of embryonic stem cell (ESC) and two adult stem cells, i.e. one adult mesenchymal stem cell (MCS) and one multipotent adult progenitor cell (MAPC) derived from the bone marrow of healthy individuals.

As normal controls, we used the following samples: two B-cell lines established form normal B-lymphocytes (LBL1 and LBL2), 10 samples of isolated normal CD19+ B cells (seven from peripheral blood and three from tonsils of healthy individuals; all these cells were separated by magnetic-activated cell sorting, Miltenyi Biotech) , one sample of tonsilar germinal center B-cells (CD19+, CD20high, CD38+, separated by subsequent magnetic (Miltenyi Biotech) and fluorescence-activated cell sorting (Becton Dickinson)), three normal lymph nodes, three spleen samples, two bone marrows and one peripheral blood PBLs.

Samples were obtained from the tumor banks of the following institutions: Department of Pathology of the Hospital Clínic (Barcelona, Spain), Institute of Pathology (Würzburg, Germany), Institute of Human Genetics/Pathology Department (Kiel, Germany), Department of Genetics (Pamplona, Spain) or Haematology Department (Cordoba, Spain). The study was approved by the Institutional Review Board of the respective institutions: Department of Pathology of the Hospital clinic, Barcelona, Spain (Hospital Clínic de Barcelona Ethics Institutional Review Board); Institute of Pathology, Wurzburg, Germany (Ethics Committee of the Medical Faculty of the University of

Table 1. Primers sequences (qRT-PCR, bisulfite pyrosequencing and qPCR-ChIP).

Name	Type	Sequence	Tm (°C)
SOX11_Forward	RT-PCR	CATGTAGACTAATGCAGCCATTGG	60
SOX11_Reverse	RT-PCR	CACGGAGCACGTGTCAATTG	60
SOX11 Probe	RT-PCR	TTTTAACCACGGATAATTG	60
SOX11_FP	RT-PCR	Biotin-TTGGGTAAGAGTTGGAAAATGTTGAA	55
SOX11_RP	RT-PCR	CCTAAACTTAACCCAAAAATCCATTTTAAAC	55
SOX11_seq	RT-PCR	CAAATAATCCACCATATACT	55
SOX11prom_Forward	qPCR-ChIP	GAGAGCTTGGAAGCGGAGA	60
SOX11prom_Forward	qPCR-ChIP	AGTCTGGGTCGCTCTCGTC	60

doi:10.1371/journal.pone.0021382.t001

Würzburg); Institute of Human Genetics/Pathology Department, Kiel, Germany (Ethics Commission of the Medical Faculty of the Christian-Albrechts-University Kiel); Department of Genetics, Pamplona, Spain (Research Ethics Committee at the University of Navarra); Haematology Department, Cordoba, Spain (Ethics Committee at the University Hospital Reina Sofia).

Written informed consent was obtained from all participants and the ethics committees approved this consent procedure in accordance with the principles of the Declaration of Helsinki.

Table S4 shows a summary of the cell lines, primary cases and controls used for different analyses.

DNA methylation microarrays

The Infinium Assay from Illumina (San Diego, CA) was used to quantify the DNA methylation status of two CpGs located 1077 (cg08432727) and 610 (cg20008332) base pairs upstream the transcriptional start site of *SOX11*. As this study focuses only on *SOX11*, the rest of the genes studied with the microarray were not considered for the present publication. Array experiments were performed according to the manufacturer's instructions [26].

Bisulfite pyrosequencing

Genomic DNA was bisulfite converted using the EpiTect Bisulfite Conversion Kit (Qiagen), according to manufacturer's instructions. Bisulfite pyrosequencing was performed according to standard protocols and evaluated with the analysis software Pyro Q-CpG 1.0.9 (Biotage). PCR and primer sequences are shown in Table 1.

SOX11 expression by microarrays and quantitative Real Time-Polymerase Chain Reaction (qRT-PCR)

Previously published stem cell, normal hematopoietic controls and different lymphoid neoplasia raw datasets from HG-U133A and HG-U133 Plus2 Affymetrix gene chips were downloaded from publicly available databases and processed using the R statistical software (http://www.R-project.org) in conjunction with the Bioconductor open source software. Arrays were normalized with the mas5 algorithm and three tags for SOX11 present in both HG-U133A and HG-U133 Plus2 arrays (i.e. 204913_s_at, 204914_s_at and 204915_s_at) were selected. As these three tags showed similar expression levels, they were averaged for further analyses. Table S2 contains a list of the 416 analyzed samples (including GEO identifiers or references) used to generate normalized gene expression intensities.

SOX11 mRNA expression was also investigated by qRT-PCR as described before [12] but with a newly designed primer set and TaqMan® MGB probe for SOX11 using Primer Express® Software Version 2.0 (Applied Biosystems) (Primer set and probe shown in Table 1).

Quantitative chromatin immunoprecipitation

Chromatin immunoprecipitation (ChIP) experiments were performed with the LowCell ChIP kit (Diagenode; Liege) according to manufacturer's instructions using the following antibodies: H3K9/14Ac, H3K4me3, H3K9me2, H3K27me3 (all four from Diagenode) and H3 (Abcam, ab1791). A rabbit IgG (Diagenode) was used as a negative control.

Immunoprecipitated DNA and 1:100 diluted input sample were analyzed in triplicate by quantitative real-time PCR analyses using SYBR-Green Master Mix in an ABI 7900 FAST sequence detection system. The primers for the *SOX11* gene promoter region are shown in Table 1.

Treatment with epigenetic drugs

Lymphoma cell lines were treated for 72 hours with 1 μM 5-aza-2′-deoxycytidine (AZA; Sigma-Aldrich, St. Louis, MO), with drug replacement every 24 hours. For suberoylanilide hydroxamic acid (SAHA; Selleck, Houston, TX) experiments, different concentrations of SAHA (1.5, 5 and 10 μM) were used and cultured during 24 hours. For treatment with both drugs, 10 μM of SAHA was added for the final 24 hours of the 72-hour AZA treatment period. Extension of treatment of cells with AZA (1 to 5 μM) for up to 96 h and higher doses of SAHA caused marked apoptotic effects in the cells.

Western Blot analysis

Protein extract preparation and Western blot were performed as previously described [37] using a polyclonal rabbit serum against a peptide corresponding to SOX11 specific residues 283-252 (QIKQEPDEEDEEP) generated in our lab (File S1 and Figure S3). A monoclonal antibody anti-α-Tubulin (Oncogene Research, Boston, MA) was used as a loading control.

Supporting Information

Figure S1 Scatter plot showing a correlation between DNA methylation percentages of the CpG site 1 quantified by bisulfite pyrosequencing and the values of the CpG analyzed by the Infinium array (cg20008332) (Rho Spearman coefficient = 0.902, p<0.001).
(TIF)

Figure S2 Analysis by bisulfite-pyrosequencing of the *SOX11* promoter de-methylation in RAJI cells after being

treated for 72 h with 1 μM AZA alone, in combination with 10 μM SAHA 24 h concluding the treatment with AZA or treated for 24 h with 10 μM of SAHA alone.
(TIF)

Figure S3 The specificity of the polyclonal antibody against SOX11 (1159) was verified by western blotting analysis. HEK293T cells were transfected with vectors encoding HA-SOX4, HA-SOX11 and with the empty vector pcDNA3.1 (CT). Twenty-four hours after transfection, cells were collected and protein extracts were subjected to immunoblotting with antibodies against SOX11 (1159) (left panels) and against HA (Sigma anti-HA; Saint Louis; Missouri) (middle panels), to detect SOX4 and SOX11. The expression levels of SOX11 protein in different MCL cell lines (JVM2, GRANTA519, Z138, JEKO1 and REC1) were detected by using the antibody against SOX11 (1159) (right panels). Differential expression of SOX11 protein in the MCL cell lines, already shown by qRT-PCR, was demonstrated by western blotting. The SOX11-1159 antibody specifically recognized the overexpressed exogenous SOX11 protein as well as endogenous SOX11 protein. The antibody can be used as an important tool for further exploration of the role of SOX11 in tumorigenesis. * Non-specific bands.
(TIF)

Table S1 Cases studied by Affymetrix gene expression arrays.
(XLS)

Table S2 SOX11 mouse-immunological genome project data.
(XLS)

Table S3 SOX11 TEL-AML1 transduced cells.
(XLS)

Table S4 Cases and analyses.
(XLS)

File S1 Supplemental Experimental Procedures.
(DOC)

Author Contributions

Conceived and designed the experiments: EC JIM-S VA. Performed the experiments: MCV CR JP IS IM-G AL JR SX-T AE JIM-S VA. Analyzed the data: BB SB LH PJ RS EC JIM-S VA. Contributed reagents/materials/analysis tools: XA MJC AR GO JR-G FP ME RS EC. Wrote the paper: JIM-S VA.

References

1. Lefebvre V, Dumitriu B, Penzo-Mendez A, Han Y, Pallavi B (2007) Control of cell fate and differentiation by Sry-related high-mobility-group box (Sox) transcription factors. Int J Biochem Cell Biol 39: 2195–2214.
2. Haslinger A, Schwarz TJ, Covic M, Chichung Lie D (2009) Expression of Sox11 in adult neurogenic niches suggests a stage-specific role in adult neurogenesis. Eur J Neurosci 29: 2103–2114.
3. Jankowski MP, Cornuet PK, McIlwrath S, Koerber HR, Albers KM (2006) SRY-box containing gene 11 (Sox11) transcription factor is required for neuron survival and neurite growth. Neuroscience 143: 501–514.
4. Jay P, Goze C, Marsollier C, Taviaux S, Hardelin JP, et al. (1995) The human SOX11 gene: cloning, chromosomal assignment and tissue expression. Genomics 29: 541–545.
5. Bergsland M, Werme M, Malewicz M, Perlmann T, Muhr J (2006) The establishment of neuronal properties is controlled by Sox4 and Sox11. Genes Dev 20: 3475–3486.
6. Brennan DJ, Ek S, Doyle E, Drew T, Foley M, et al. (2009) The transcription factor Sox11 is a prognostic factor for improved recurrence-free survival in epithelial ovarian cancer. Eur J Cancer 45: 1510–1517.
7. Lee CJ, Appleby VJ, Orme AT, Chan WI, Scotting PJ (2002) Differential expression of SOX4 and SOX11 in medulloblastoma. J Neurooncol 57: 201–214.
8. Weigle B, Ebner R, Temme A, Schwind S, Schmitz M, et al. (2005) Highly specific overexpression of the transcription factor SOX11 in human malignant gliomas. Oncol Rep 13: 139–144.
9. Chen YH, Gao J, Fan G, Peterson LC (2010) Nuclear expression of sox11 is highly associated with mantle cell lymphoma but is independent of t(11;14)(q13;q32) in non-mantle cell B-cell neoplasms. Mod Pathol 23: 105–112.
10. Dictor M, Ek S, Sundberg M, Warenholt J, Gyorgy C, et al. (2009) Strong lymphoid nuclear expression of SOX11 transcription factor defines lymphoblastic neoplasms, mantle cell lymphoma and Burkitt's lymphoma. Haematologica 94: 1563–1568.
11. Ek S, Dictor M, Jerkeman M, Jirstrom K, Borrebaeck CA (2008) Nuclear expression of the non B-cell lineage Sox11 transcription factor identifies mantle cell lymphoma. Blood 111: 800–805.
12. Mozos A, Royo C, Hartmann E, De Jong D, Baro C, et al. (2009) SOX11 expression is highly specific for mantle cell lymphoma and identifies the cyclin D1-negative subtype. Haematologica 94: 1555–1562.
13. Wang X, Asplund AC, Porwit A, Flygare J, Smith CI, et al. (2008) The subcellular Sox11 distribution pattern identifies subsets of mantle cell lymphoma: correlation to overall survival. Br J Haematol 143: 248–252.
14. Fernandez V, Salamero O, Espinet B, Sole F, Royo C, et al. (2010) Genomic and gene expression profiling defines indolent forms of mantle cell lymphoma. Cancer Res 70: 1408–1418.
15. Chaganti RS, Nanjangud G, Schmidt H, Teruya-Feldstein J (2000) Recurring chromosomal abnormalities in non-Hodgkin's lymphoma: biologic and clinical significance. Semin Hematol 37: 396–411.
16. Bea S, Salaverria I, Armengol L, Pinyol M, Fernandez V, et al. (2009) Uniparental disomies, homozygous deletions, amplifications, and target genes in mantle cell lymphoma revealed by integrative high-resolution whole-genome profiling. Blood 113: 3059–3069.
17. Hartmann EM, Campo E, Wright G, Lenz G, Salaverria I, et al. (2010) Pathway discovery in mantle cell lymphoma by integrated analysis of high-resolution gene expression and copy number profiling. Blood 116: 953–961.
18. Kawamata N, Ogawa S, Zimmermann M, Kato M, Sanada M, et al. (2008) Molecular allelokaryotyping of pediatric acute lymphoblastic leukemias by high-resolution single nucleotide polymorphism oligonucleotide genomic microarray. Blood 111: 776–784.
19. Salaverria I, Zettl A, Bea S, Hartmann EM, Dave SS, et al. (2008) Chromosomal alterations detected by comparative genomic hybridization in subgroups of gene expression-defined Burkitt's lymphoma. Haematologica 93: 1327–1334.
20. Scholtysik R, Kreuz M, Klapper W, Burkhardt B, Feller AC, et al. (2010) Detection of genomic aberrations in molecularly defined Burkitt lymphoma by array-based high resolution single nucleotide polymorphism analysis. Haematologica 95: 2047–55.
21. Esteller M (2008) Epigenetics in cancer. N Engl J Med 358: 1148–1159.
22. Jones PA, Baylin SB (2007) The epigenomics of cancer. Cell 128: 683–692.
23. Giorgetti A, Montserrat N, Aasen T, Gonzalez F, Rodriguez-Piza I, et al. (2009) Generation of induced pluripotent stem cells from human cord blood using OCT4 and SOX2. Cell Stem Cell 5: 353–357.
24. Loh YH, Hartung O, Li H, Guo C, Sahalie JM, et al. (2010) Reprogramming of T cells from human peripheral blood. Cell Stem Cell 7: 15–19.
25. Hummel M, Bentink S, Berger H, Klapper W, Wessendorf S, et al. (2006) A biologic definition of Burkitt's lymphoma from transcriptional and genomic profiling. N Engl J Med 354: 2419–2430.
26. Bibikova M, Le J, Barnes B, Saedinia-Melnyk B, Zhou L, et al. (2009) Genome-wide DNA methylation profiling using Infinium® assay. Epigenomics 1: 177–200.
27. Tost J, Gut IG (2007) DNA methylation analysis by pyrosequencing. Nat Protoc 2: 2265–2275.
28. Gustavsson E, Sernbo S, Andersson E, Brennan DJ, Dictor M, et al. (2010) SOX11 expression correlates to promoter methylation and regulates tumor growth in hematopoietic malignancies. Mol Cancer 9: 187.
29. Tong WG, Wierda WG, Lin E, Kuang SQ, Bekele BN, et al. (2010) Genome-wide DNA methylation profiling of chronic lymphocytic leukemia allows identification of epigenetically repressed molecular pathways with clinical impact. Epigenetics 5: 499–508.
30. Keshet I, Schlesinger Y, Farkash S, Rand E, Hecht M, et al. (2006) Evidence for an instructive mechanism of de novo methylation in cancer cells. Nat Genet 38: 149–153.
31. Martin-Subero JI, Kreuz M, Bibikova M, Bentink S, Ammerpohl O, et al. (2009) New insights into the biology and origin of mature aggressive B-cell lymphomas by combined epigenomic, genomic, and transcriptional profiling. Blood 113: 2488–2497.
32. Gal-Yam EN, Egger G, Iniguez L, Holster H, Einarsson S, et al. (2008) Frequent switching of Polycomb repressive marks and DNA hypermethylation in the PC3 prostate cancer cell line. Proc Natl Acad Sci U S A 105: 12979–12984.
33. Martin-Subero JI, Ammerpohl O, Bibikova M, Wickham-Garcia E, Agirre X, et al. (2009) A comprehensive microarray-based DNA methylation study of 367 hematological neoplasms. PLoS One 4: e6986.

34. Heng TS, Painter MW (2008) The Immunological Genome Project: networks of gene expression in immune cells. Nat Immunol 9: 1091–1094.
35. Hong D, Gupta R, Ancliff P, Atzberger A, Brown J, et al. (2008) Initiating and cancer-propagating cells in TEL-AML1-associated childhood leukemia. Science 319: 336–339.
36. Swerdlow SH, Campo E, Harris NL, Jaffe ES, Pileri SA, et al. (2008) World Health Organization Classification of Tumours of Haematopoietic and Lymphoid Tissues. Lyon: IARC Press. Fourth Edition. pp 1–439.
37. Amador V, Ge S, Santamaria PG, Guardavaccaro D, Pagano M (2007) APC/C(Cdc20) controls the ubiquitin-mediated degradation of p21 in prometaphase. Mol Cell 27: 462–473.

SUPPLEMENTAL EXPERIMENTAL PROCEDURES

Cell lines

Nine well characterized MCL cell lines (1), four B-cell neoplasia cell lines and one embryonal carcinoma cell line were used for gene expression, DNA methylation, histone modification and/or protein analyses. These included HBL2 (kindly provided by Dr M. Dreyling), UPN1 (kindly provided by A. Thurhan), MAVER1 (kindly provided by Dr A. Zamo), Z-138 (kindly provided by Dr E. Ortega-Paino), JEKO1 (CRL-3006, ATCC), JVM-2 (CRL-3002, ATCC), MINO (CRL-3000, ATCC), REC1 (ACC-584, DSMZ) and GRANTA (ACC-342, DSMZ). Other B-cell neoplasia cell lines included: one BL (RAJI, ACC-319, DSMZ), one CLL (MEC1, ACC-497, DSMZ), two B-ALLs (KOPN8, ACC-552, DSMZ; and REH, ACC-22, DSMZ) and the embryonic carcinoma cell line NTERA-2 (ACC-527, DMSZ). These cell lines were cultured in RPMI-1640 containing 10% fetal bovine serum (FBS; Sigma Chemical, St Louis, MO), 2 µM L-glutamine, 100 U/mL penicillin, and 100 µg/mL streptomycin (GIBCO, Grand Island, NY), except for GRANTA-519 that was cultured in DMEM containing 10% FBS, 2 µM L-glutamine, 100 U/mL penicillin, and 100 µg/mL streptomycin and MEC1 that was cultured in IMDM containing 10% FBS, 2 µM L-glutamine, 100 U/mL penicillin, and 100 µg/mL streptomycin. NTERA-2 was cultured in DMEM supplemented with 5% horse serum, 10% FCS, and 1% Pen/Strep (2).

For DNA methylation studies, cell line DNA was obtained from the following sources: L1236 (ACC-530), L-428 (ACC-197), KM-H2 (ACC-8), HDLM-2 (ACC-17), L591 (ACC-602), L540 (ACC-72), U-H01 (ACC-626) and RC-K8 (ACC-561) from the German Collection of Microorganisms and Cell Cultures (DMSZ, Braunschweig, Germany), JURKAT was kindly provided by Dr. M. Brüggemann, DAUDI by Dr. J. Hampe, LY3 by A. Rosenwald, RL by B. Caldwell and VAL and LY10 by R. Shaknovich.

Plasmids

SOX11 and *SOX4* were amplified by PCR using a cDNA library generated from Granta519 cells and JVM2, respectively (PCR primers are shown in Table 2) and Platinum *Pfx*® DNA polymerase (Invitrogen) following the manufacturer's instructions. The PCR products were inserted into pcDNA3.1 (Invitrogene). The cDNAs were sequenced.

Table 2. Primers used for cDNA cloning:

Name	5′ - sequence - 3′
cSOX11-HA F	CGGC**GGATCC***ATGTACCCATACGATGTTCCAGATTACGCT*GTGCAGCAGGCGGAGAGCTTC **BamH1** *HA-tag*
cSOX11-HA R	GCCG**CTCGAG**CGCCTTTCAATATGTGAACAC **XhoI**
cSOX4-HA F	CGGC**GGATCC***ATGTACCCATACGATGTTCCAGATTACGCT*GTGCAGCAAACCAACAATGCC **BamH1** *HA-tag*

Biochemistry

HA-SOX4 and HA-SOX11 constructs were transfected into HEK293T cells using the Lipofectamine 2000 (Invitrogene), according to manufacturer's instructions. Forty-eight hours later, cells were collected and lysed in lysis buffer (LB: 50 mM Tris-HCl pH 7.5, 150 µM NaCl, 1 µM EDTA, 50 µM NaF, 0.5% Triton X-100, plus protease inhibitors). Total protein extracts from MCL cell lines (JVM2, GRANTA 519, Z138, JEKO1 and REC1) were collected and lysed in LB. Immunoblotting analyses were performed as previously described (2).

Antibody

The rabbit policlonal antibody against SOX11 (SOX11-1159) antibody was generated by injecting rabbits with the peptide QIKQEPDEEDEEP as the antigen, corresponding to amino acids 232-254 of human SOX11. The antibody was then purified from serum using protein A-Sepharose and subsequently by two rounds of affinity chromatography using peptide chromatography (Antibody production facility, "Institut de Biotecnologia i Biomedicina (IBB), UAB, Barcelona). Details on the specificity of this antibody are provided in Figure S3.

REFERENCES

1. Salaverria I, Perez-Galan P, Colomer D, Campo E. (2006). Mantle cell lymphoma: from pathology and molecular pathogenesis to new therapeutic perspectives. *Haematologica* 91: 11-16.
2. Aranda P, Agirre X, Ballestar E, Andreu EJ, Román-Gómez J, Prieto I, Martín-Subero JI, Cigudosa JC, Siebert R, Esteller M, Prosper F. (2009). Epigenetic signatures associated with different levels of differentiation potential in human stem cells. *PLoS One* 4:e7809.
3. Amador V, Ge S, Santamaria PG, Guardavaccaro D, Pagano M. (2007). APC/C(Cdc20) controls the ubiquitin-mediated degradation of p21 in prometaphase. *Mol Cell* 27:462-473.

SUPPLEMENTAL FIGURES:

Fig. S1

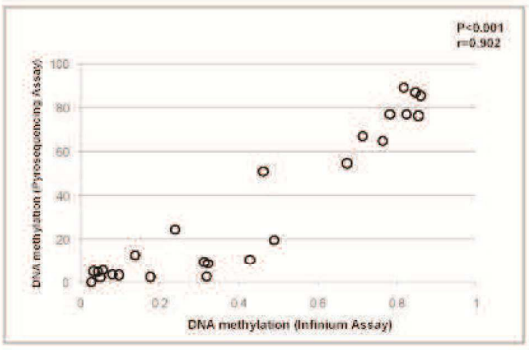

Vegliante MC., *et al.*, 2011

Figure S1. Scatter plot showing a correlation between DNA methylation percentages of the CpG site 1 quantified by bisulfite pyrosequencing and the values of the CpG analyzed by the Infinium array (cg20008332) (Rho Spearman coefficient=0.902, p<0.001).

Fig. S2

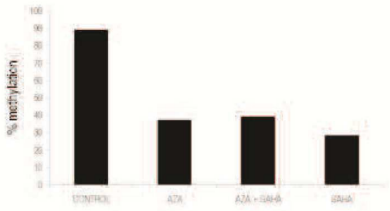

Vegliante MC., et al., 2011

Figure S2. Analysis by bisulfite-pyrosequencing of the *SOX11* promoter de-methylation in RAJI cells after being treated for 72h with 1 µM AZA alone, in combination with 10 µM SAHA 24h concluding the treatment with AZA or treated for 24h with 10 µM of SAHA alone.

Fig. S3

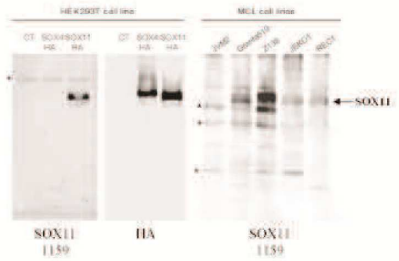

Vegliante MC., et al., 2011

Figure S3. The specificity of the polyclonal antibody against SOX11 (1159) was verified by western blotting analysis. HEK293T cells were transfected with vectors encoding HA-SOX4, HA-SOX11 and with the empty vector pcDNA3.1 (CT). Twenty-four hours after transfection, cells were collected and protein extracts were subjected to immunoblotting with antibodies against SOX11 (1159) (left panels) and against HA (Sigma anti-HA; Saint Louis; Missouri) (middle panels), to detect SOX4 and SOX11. The expression levels of SOX11 protein in different MCL cell lines (JVM2, GRANTA519, Z138, JEKO1 and REC1) were detected by using the antibody against SOX11 (1159) (right panels). Differential expression of SOX11 protein in the MCL cell lines, already shown by qRT-PCR, was demonstrated by western blotting. The SOX11-1159 antibody specifically recognized the overexpressed exogenous SOX11 protein as well as endogenous SOX11 protein. The antibody can be used as an important tool for further exploration of the role of SOX11 in tumorigenesis. * Non-specific bands.

Table S1. Cases studied by Affymetrix gene expression arrays.

SOX11expr-avg-forR-including SC	* log2 intensity values below 6 are considered not expressed			
Group	GEO record or reference	Average SOX11	log2(average SOX11)	log2(average SOX11
PMBCL	Lenz et al., Proc Natl Acad Sci U S A 2008; 105: 13520-5	6.054246992	2.597947533	6
PMBCL	Lenz et al., Proc Natl Acad Sci U S A 2008; 105: 13520-5	10.92423402	3.44946022	6
PMBCL	Lenz et al., Proc Natl Acad Sci U S A 2008; 105: 13520-5	13.03348203	3.704150661	6
PMBCL	Lenz et al., Proc Natl Acad Sci U S A 2008; 105: 13520-5	13.467144	3.751372023	6
PMBCL	Lenz et al., Proc Natl Acad Sci U S A 2008; 105: 13520-5	14.73876309	3.88154355	6
PMBCL	Lenz et al., Proc Natl Acad Sci U S A 2008; 105: 13520-5	20.35116599	4.347039549	6
PMBCL	Lenz et al., Proc Natl Acad Sci U S A 2008; 105: 13520-5	23.07129187	4.528026884	6
PMBCL	Lenz et al., Proc Natl Acad Sci U S A 2008; 105: 13520-5	24.14432439	4.593612189	6
PMBCL	Lenz et al., Proc Natl Acad Sci U S A 2008; 105: 13520-5	30.35578501	4.923899577	6
PMBCL	Lenz et al., Proc Natl Acad Sci U S A 2008; 105: 13520-5	31.9576212	4.998088119	6
PMBCL	Lenz et al., Proc Natl Acad Sci U S A 2008; 105: 13520-5	37.05536339	5.211610468	6
PMBCL	Lenz et al., Proc Natl Acad Sci U S A 2008; 105: 13520-5	40.15823116	5.32762382	6
PMBCL	Lenz et al., Proc Natl Acad Sci U S A 2008; 105: 13520-5	40.86677384	5.352856452	6
PMBCL	Lenz et al., Proc Natl Acad Sci U S A 2008; 105: 13520-5	42.95352886	5.424704756	6
PMBCL	Lenz et al., Proc Natl Acad Sci U S A 2008; 105: 13520-5	52.27125461	5.707945882	6
PMBCL	Lenz et al., Proc Natl Acad Sci U S A 2008; 105: 13520-5	60.56170486	5.920333914	6
PMBCL	Lenz et al., Proc Natl Acad Sci U S A 2008; 105: 13520-5	63.7938638	5.995345756	6
PMBCL	Lenz et al., Proc Natl Acad Sci U S A 2008; 105: 13520-5	64.81215934	6.018192596	6.018192596
PMBCL	Lenz et al., Proc Natl Acad Sci U S A 2008; 105: 13520-5	67.64463992	6.079903716	6.079903716
PMBCL	Lenz et al., Proc Natl Acad Sci U S A 2008; 105: 13520-5	108.7081572	6.764316391	6.764316391
DLBCL	Jares et al., unpublished data	7.655874084	2.936567102	6
DLBCL	Jares et al., unpublished data	8.634280999	3.110076045	6
DLBCL	Jares et al., unpublished data	10.44830851	3.385197496	6
DLBCL	Jares et al., unpublished data	10.58225325	3.403574944	6
DLBCL	Jares et al., unpublished data	11.69759397	3.548139913	6
DLBCL	Jares et al., unpublished data	12.03295769	3.588919394	6
DLBCL	Jares et al., unpublished data	13.47260177	3.75195658	6
DLBCL	Jares et al., unpublished data	13.48176925	3.752937933	6
DLBCL	Jares et al., unpublished data	14.48698045	3.856685017	6
DLBCL	Jares et al., unpublished data	14.56397543	3.864332307	6
DLBCL	Jares et al., unpublished data	15.61377217	3.964747219	6
DLBCL	Jares et al., unpublished data	16.61113231	4.054078514	6
DLBCL	Jares et al., unpublished data	18.73729491	4.227840782	6
DLBCL	Jares et al., unpublished data	18.94220792	4.243532597	6
DLBCL	Jares et al., unpublished data	19.21204484	4.263939176	6
DLBCL	Jares et al., unpublished data	22.39166332	4.484889795	6
DLBCL	Jares et al., unpublished data	23.30448547	4.542535755	6
DLBCL	Jares et al., unpublished data	23.3508317	4.545402031	6
DLBCL	Jares et al., unpublished data	24.37126027	4.607108952	6
DLBCL	Jares et al., unpublished data	25.61833372	4.679104737	6
DLBCL	Jares et al., unpublished data	26.72713877	4.740233495	6
DLBCL	Jares et al., unpublished data	28.77720936	4.84685479	6
DLBCL	Jares et al., unpublished data	29.275081	4.871601257	6
DLBCL	Jares et al., unpublished data	34.94582801	5.127048325	6
DLBCL	Jares et al., unpublished data	37.15068646	5.215316964	6
DLBCL	Jares et al., unpublished data	38.4281849	5.264092929	6
DLBCL	Jares et al., unpublished data	45.50115677	5.507831318	6
DLBCL	Jares et al., unpublished data	47.93902812	5.583128756	6
DLBCL	Jares et al., unpublished data	51.63509431	5.690280036	6
DLBCL	Jares et al., unpublished data	55.21223324	5.786916052	6
DLBCL	Jares et al., unpublished data	55.36258905	5.790839508	6
DLBCL	Jares et al., unpublished data	59.2546103	5.888855502	6
DLBCL	Jares et al., unpublished data	60.44931149	5.917654002	6
DLBCL	Jares et al., unpublished data	61.98836967	5.953925656	6
DLBCL	Jares et al., unpublished data	77.97473485	6.284934837	6.284934837
DLBCL	Jares et al., unpublished data	83.80929198	6.3890383	6.3890383
DLBCL	Jares et al., unpublished data	110.7964546	6.791767907	6.791767907
DLBCL	Jares et al., unpublished data	137.901285	7.10749209	7.10749209
DLBCL	Jares et al., unpublished data	148.7062887	7.216321849	7.216321849

FL	Dave et al., N Engl J Med 2004; 351: 2159-69	6.748872201	2.754646435	6
FL	Dave et al., N Engl J Med 2004; 351: 2159-69	7.037296037	2.815021204	6
FL	Dave et al., N Engl J Med 2004; 351: 2159-69	7.75792189	2.95567025	6
FL	Dave et al., N Engl J Med 2004; 351: 2159-69	8.321685692	3.056875799	6
FL	Dave et al., N Engl J Med 2004; 351: 2159-69	8.382863602	3.067443155	6
FL	Dave et al., N Engl J Med 2004; 351: 2159-69	11.91951556	3.575253697	6
FL	Dave et al., N Engl J Med 2004; 351: 2159-69	12.01144578	3.586337909	6
FL	Dave et al., N Engl J Med 2004; 351: 2159-69	12.70667436	3.667514587	6
FL	Dave et al., N Engl J Med 2004; 351: 2159-69	14.85990977	3.893353451	6
FL	Dave et al., N Engl J Med 2004; 351: 2159-69	18.03480798	4.172712157	6
FL	Dave et al., N Engl J Med 2004; 351: 2159-69	18.34973744	4.197687515	6
FL	Dave et al., N Engl J Med 2004; 351: 2159-69	18.60699391	4.217773092	6
FL	Dave et al., N Engl J Med 2004; 351: 2159-69	22.2131312	4.473340867	6
FL	Dave et al., N Engl J Med 2004; 351: 2159-69	25.59949056	4.678043195	6
FL	Dave et al., N Engl J Med 2004; 351: 2159-69	29.98763994	4.90629608	6
FL	Dave et al., N Engl J Med 2004; 351: 2159-69	30.8110629	4.945376547	6
FL	Dave et al., N Engl J Med 2004; 351: 2159-69	38.28793129	5.258817808	6
FL	Dave et al., N Engl J Med 2004; 351: 2159-69	41.48061602	5.374365414	6
FL	Dave et al., N Engl J Med 2004; 351: 2159-69	41.54196674	5.376497615	6
FL	Dave et al., N Engl J Med 2004; 351: 2159-69	46.52060823	5.539798054	6
FL	Dave et al., N Engl J Med 2004; 351: 2159-69	48.03813183	5.586108142	6
FL	Dave et al., N Engl J Med 2004; 351: 2159-69	48.43598928	5.598007503	6
FL	Dave et al., N Engl J Med 2004; 351: 2159-69	49.14544648	5.618985846	6
FL	Dave et al., N Engl J Med 2004; 351: 2159-69	51.65115781	5.690728784	6
FL	Dave et al., N Engl J Med 2004; 351: 2159-69	66.56941873	6.056787666	6.056787666
FL	Dave et al., N Engl J Med 2004; 351: 2159-69	76.48569691	6.257118079	6.257118079
FL	Dave et al., N Engl J Med 2004; 351: 2159-69	87.33112375	6.448423999	6.448423999
CLL	Fernandez et al., Cancer Res 2010; 70: 1408-18	5.516151065	2.463661967	6
CLL	Fernandez et al., Cancer Res 2010; 70: 1408-18	5.557205849	2.474359681	6
CLL	Fernandez et al., Cancer Res 2010; 70: 1408-18	7.111374303	2.830128394	6
CLL	Fernandez et al., Cancer Res 2010; 70: 1408-18	10.75225025	3.426566716	6
CLL	Fernandez et al., Cancer Res 2010; 70: 1408-18	16.00851803	4.000767853	6
CLL	Fernandez et al., Cancer Res 2010; 70: 1408-18	17.15194125	4.100299964	6
CLL	Fernandez et al., Cancer Res 2010; 70: 1408-18	19.38964297	4.277214334	6
CLL	Fernandez et al., Cancer Res 2010; 70: 1408-18	22.2064101	4.47290428	6
CLL	Fernandez et al., Cancer Res 2010; 70: 1408-18	28.22746724	4.819027781	6
CLL	Fernandez et al., Cancer Res 2010; 70: 1408-18	28.67777916	4.841861399	6
CLL	Fernandez et al., Cancer Res 2010; 70: 1408-18	29.48424975	4.881872579	6
CLL	Fernandez et al., Cancer Res 2010; 70: 1408-18	29.62834717	4.888906242	6
CLL	Fernandez et al., Cancer Res 2010; 70: 1408-18	29.63202683	4.889085405	6
CLL	Fernandez et al., Cancer Res 2010; 70: 1408-18	33.9937419	5.087197272	6
CLL	Fernandez et al., Cancer Res 2010; 70: 1408-18	38.76764968	5.276781368	6
CLL	Fernandez et al., Cancer Res 2010; 70: 1408-18	43.75680699	5.451435561	6
CLL	Fernandez et al., Cancer Res 2010; 70: 1408-18	44.41282607	5.47290447	6
CLL	Fernandez et al., Cancer Res 2010; 70: 1408-18	59.27030719	5.88923763	6
CLL	Fernandez et al., Cancer Res 2010; 70: 1408-18	102.2739913	6.676295498	6.676295498
BL	Dave et al. N Engl J Med 2006; 354: 2431-42	20.95641363	4.389319938	6
BL	Dave et al. N Engl J Med 2006; 354: 2431-42	21.47980082	4.42490871	6
BL	Dave et al. N Engl J Med 2006; 354: 2431-42	24.35990181	4.606436413	6
BL	Dave et al. N Engl J Med 2006; 354: 2431-42	34.13127256	5.0930223	6
BL	Dave et al. N Engl J Med 2006; 354: 2431-42	34.59622017	5.112542519	6
BL	Dave et al. N Engl J Med 2006; 354: 2431-42	35.22261338	5.13843005	6
BL	Dave et al. N Engl J Med 2006; 354: 2431-42	46.86009232	5.550287891	6
BL	Dave et al. N Engl J Med 2006; 354: 2431-42	66.6108139	6.057684505	6.057684505
BL	Dave et al. N Engl J Med 2006; 354: 2431-42	86.22567051	6.430045537	6.430045537
BL	Dave et al. N Engl J Med 2006; 354: 2431-42	209.0606419	7.707777673	7.707777673
BL	Dave et al. N Engl J Med 2006; 354: 2431-42	245.2966392	7.938383657	7.938383657
BL	Dave et al. N Engl J Med 2006; 354: 2431-42	419.6466747	8.713031339	8.713031339
BL	Dave et al. N Engl J Med 2006; 354: 2431-42	567.8175951	9.149283745	9.149283745
BL	Dave et al. N Engl J Med 2006; 354: 2431-42	587.837772	9.199274253	9.199274253
BL	Dave et al. N Engl J Med 2006; 354: 2431-42	600.0701329	9.228987315	9.228987315

BL	Dave et al. N Engl J Med 2006; 354: 2431-42	2005.980547	10.9700919	10.9700919
iMCL	Fernandez et al., Cancer Res 2010; 70: 1408-18	17.13278146	4.098687483	6
iMCL	Fernandez et al., Cancer Res 2010; 70: 1408-18	20.69562723	4.371254068	6
iMCL	Fernandez et al., Cancer Res 2010; 70: 1408-18	29.93969263	4.903987505	6
iMCL	Fernandez et al., Cancer Res 2010; 70: 1408-18	58.84706401	5.878898533	6
iMCL	Fernandez et al., Cancer Res 2010; 70: 1408-18	123.7076965	6.95079145	6.95079145
IMCL	Fernandez et al., Cancer Res 2010; 70: 1408-18	594.2986999	9.215044415	9.215044415
iMCL	Fernandez et al., Cancer Res 2010; 70: 1408-18	1289.557729	10.33266064	10.33266064
MCL	Fernandez et al., Cancer Res 2010; 70: 1408-18	768.7457754	9.586362767	9.586362767
MCL	Fernandez et al., Cancer Res 2010; 70: 1408-18	991.7683405	9.953859362	9.953859362
MCL	Fernandez et al., Cancer Res 2010; 70: 1408-18	1932.704501	10.91640536	10.91640536
MCL	Fernandez et al., Cancer Res 2010; 70: 1408-18	2394.303218	11.22539015	11.22539015
MCL	Fernandez et al., Cancer Res 2010; 70: 1408-18	3073.398402	11.58561908	11.58561908
MCL	Fernandez et al., Cancer Res 2010; 70: 1408-18	3474.80506	11.76271633	11.76271633
MCL	Fernandez et al., Cancer Res 2010; 70: 1408-18	3584.739947	11.80765275	11.80765275
MCL	Fernandez et al., Cancer Res 2010; 70: 1408-18	3831.001147	11.90350574	11.90350574
MCL	Fernandez et al., Cancer Res 2010; 70: 1408-18	4124.163403	12.00988578	12.00988578
MCL	Fernandez et al., Cancer Res 2010; 70: 1408-18	4654.649913	12.18445695	12.18445695
MCL	Fernandez et al., Cancer Res 2010; 70: 1408-18	5904.9668	12.52771323	12.52771323
MCL	Fernandez et al., Cancer Res 2010; 70: 1408-18	6153.340826	12.58715419	12.58715419
MCL	Fernandez et al., Cancer Res 2010; 70: 1408-18	6854.89839	12.74291957	12.74291957
MCL	Fernandez et al., Cancer Res 2010; 70: 1408-18	7762.945303	12.92238841	12.92238841
TEL-AML	GSE13425	30.33046279	4.922695606	6
TEL-AML	GSE13425	52.7112334	5.720038545	6
TEL-AML	GSE13425	122.8594052	6.940864494	6.940864494
TEL-AML	GSE13425	219.3834007	7.77731056	7.77731056
TEL-AML	GSE13425	353.710064	8.466423458	8.466423458
TEL-AML	GSE13425	402.6726834	8.653463796	8.653463796
TEL-AML	GSE13425	446.4658841	8.802406128	8.802406128
TEL-AML	GSE13425	591.6078944	9.208497494	9.208497494
TEL-AML	GSE13425	647.5575316	9.338864563	9.338864563
TEL-AML	GSE13425	687.4083928	9.425023656	9.425023656
TEL-AML	GSE13425	704.3825342	9.460215326	9.460215326
TEL-AML	GSE13425	762.1070889	9.573849925	9.573849925
TEL-AML	GSE13425	804.193056	9.651398069	9.651398069
TEL-AML	GSE13425	810.4895708	9.662649811	9.662649811
TEL-AML	GSE13425	875.8425508	9.774527731	9.774527731
TEL-AML	GSE13425	876.2045573	9.775123908	9.775123908
TEL-AML	GSE13425	952.0842313	9.894945405	9.894945405
TEL-AML	GSE13425	963.0612218	9.911483703	9.911483703
TEL-AML	GSE13425	970.2882987	9.922269664	9.922269664
TEL-AML	GSE13425	985.9849515	9.945421818	9.945421818
TEL-AML	GSE13425	1053.756608	10.04132596	10.04132596
TEL-AML	GSE13425	1075.247077	10.07045249	10.07045249
TEL-AML	GSE13425	1095.270384	10.09707135	10.09707135
TEL-AML	GSE13425	1097.764337	10.10035266	10.10035266
TEL-AML	GSE13425	1107.638221	10.11327103	10.11327103
TEL-AML	GSE13425	1133.53859	10.14661779	10.14661779
TEL-AML	GSE13425	1196.943807	10.22513971	10.22513971
TEL-AML	GSE13425	1281.497594	10.32361505	10.32361505
TEL-AML	GSE13425	1328.02133	10.3750626	10.3750626
TEL-AML	GSE13425	1351.626692	10.40048103	10.40048103
TEL-AML	GSE13425	1408.510201	10.4599543	10.4599543
TEL-AML	GSE13425	1572.251206	10.61861603	10.61861603
TEL-AML	GSE13425	1603.20877	10.64674659	10.64674659
TEL-AML	GSE13425	1605.524039	10.64882855	10.64882855
TEL-AML	GSE13425	1661.461321	10.69823699	10.69823699
TEL-AML	GSE13425	1692.503953	10.72494349	10.72494349
TEL-AML	GSE13425	1842.616339	10.84754	10.84754
TEL-AML	GSE13425	1844.988964	10.84939647	10.84939647
TEL-AML	GSE13425	1994.128383	10.96154258	10.96154258

TEL-AML	GSE13425	3088.960501	11.59290571	11.59290571
E2A-rearranged	GSE13425	29.31465434	4.87355014	6
E2A-rearranged	GSE13425	65.90873876	6.042397858	6.042397858
E2A-rearranged	GSE13425	219.787475	7.779965364	7.779965364
E2A-rearranged	GSE13425	263.538465	8.041869737	8.041869737
E2A-rearranged	GSE13425	415.016901	8.697026279	8.697026279
E2A-rearranged	GSE13425	872.3089378	9.768695362	9.768695362
E2A-rearranged	GSE13425	929.3531684	9.860083137	9.860083137
E2A-rearranged	GSE13425	945.3748655	9.884742698	9.884742698
E2A-rearranged	GSE13425	1038.256566	10.01994728	10.01994728
E2A-rearranged	GSE13425	1048.361527	10.0339206	10.0339206
E2A-rearranged	GSE13425	1235.968062	10.27142575	10.27142575
E2A-rearranged	GSE13425	1446.155342	10.49800682	10.49800682
E2A-rearranged	GSE13425	2137.814075	11.06192067	11.06192067
BCR-ABL	GSE13425	62.7442337	5.971410974	6
BCR-ABL	GSE13425	68.73001788	6.10286843	6.10286843
BCR-ABL	GSE13425	88.53989341	6.468255732	6.468255732
BCR-ABL	GSE13425	98.80750034	6.626548654	6.626548654
BCR-ABL	GSE13425	103.7684178	6.697223612	6.697223612
MLL-rearranged	GSE13425	39.05039503	5.287265237	6
MLL-rearranged	GSE13425	42.48268672	5.408803104	6
MLL-rearranged	GSE13425	108.5929445	6.762786561	6.762786561
MLL-rearranged	GSE13425	161.271006	7.333343278	7.333343278
hyperdiploid	GSE13425	10.88744534	3.444593571	6
hyperdiploid	GSE13425	18.9791467	4.246343225	6
hyperdiploid	GSE13425	31.90836607	4.995862829	6
hyperdiploid	GSE13425	33.90242593	5.083316606	6
hyperdiploid	GSE13425	36.09440311	5.173703241	6
hyperdiploid	GSE13425	37.89604456	5.243975368	6
hyperdiploid	GSE13425	39.86730685	5.317134245	6
hyperdiploid	GSE13425	42.14372988	5.397246099	6
hyperdiploid	GSE13425	43.32235131	5.437039642	6
hyperdiploid	GSE13425	47.18919707	5.560384719	6
hyperdiploid	GSE13425	47.99744004	5.584885556	6
hyperdiploid	GSE13425	51.37692918	5.683048757	6
hyperdiploid	GSE13425	55.16979686	5.785806763	6
hyperdiploid	GSE13425	58.88269146	5.879771712	6
hyperdiploid	GSE13425	62.49669965	5.9657081	6
hyperdiploid	GSE13425	63.82338032	5.996013116	6
hyperdiploid	GSE13425	64.08313285	6.001872774	6.001872774
hyperdiploid	GSE13425	66.57779578	6.056969202	6.056969202
hyperdiploid	GSE13425	67.41051332	6.074901706	6.074901706
hyperdiploid	GSE13425	72.18940171	6.173715142	6.173715142
hyperdiploid	GSE13425	72.68581814	6.183602	6.183602
hyperdiploid	GSE13425	78.63417769	6.297084599	6.297084599
hyperdiploid	GSE13425	86.51822556	6.434932172	6.434932172
hyperdiploid	GSE13425	86.64506389	6.437045657	6.437045657
hyperdiploid	GSE13425	86.78329301	6.439345425	6.439345425
hyperdiploid	GSE13425	88.7187195	6.471166638	6.471166638
hyperdiploid	GSE13425	93.72857816	6.550417092	6.550417092
hyperdiploid	GSE13425	96.7057627	6.595529957	6.595529957
hyperdiploid	GSE13425	97.19494117	6.602809321	6.602809321
hyperdiploid	GSE13425	101.0187854	6.658479791	6.658479791
hyperdiploid	GSE13425	103.6274698	6.695262676	6.695262676
hyperdiploid	GSE13425	104.4847888	6.707149116	6.707149116
hyperdiploid	GSE13425	108.2335763	6.758004312	6.758004312
hyperdiploid	GSE13425	111.3447159	6.798889283	6.798889283
hyperdiploid	GSE13425	111.6774893	6.803194603	6.803194603
hyperdiploid	GSE13425	117.3041246	6.874109931	6.874109931
hyperdiploid	GSE13425	130.4370257	7.027209639	7.027209639
hyperdiploid	GSE13425	133.6870175	7.06271556	7.06271556
hyperdiploid	GSE13425	135.8015144	7.085355758	7.085355758
hyperdiploid	GSE13425	137.8982819	7.107460672	7.107460672
hyperdiploid	GSE13425	170.4214894	7.412963454	7.412963454
hyperdiploid	GSE13425	230.2339849	7.846956996	7.846956996

hyperdiploid	GSE13425	373.0124445	8.543079952	8.543079952
hyperdiploid	GSE13425	478.5494711	8.902524264	8.902524264
pre-B	GSE13425	20.63628086	4.367111082	6
pre-B	GSE13425	25.48080116	4.671338734	6
pre-B	GSE13425	39.60983158	5.307786662	6
pre-B	GSE13425	39.68255575	5.31043304	6
pre-B	GSE13425	42.52318519	5.410177761	6
pre-B	GSE13425	59.07052115	5.884366435	6
pre-B	GSE13425	60.06243062	5.908390954	6
pre-B	GSE13425	62.1559308	5.957820152	6
pre-B	GSE13425	65.07123394	6.023948007	6.023948007
pre-B	GSE13425	65.59030861	6.035410758	6.035410758
pre-B	GSE13425	70.21460789	6.133699304	6.133699304
pre-B	GSE13425	75.77348596	6.243621216	6.243621216
pre-B	GSE13425	76.29595809	6.253534725	6.253534725
pre-B	GSE13425	95.22434543	6.573258561	6.573258561
pre-B	GSE13425	96.3408627	6.590075938	6.590075938
pre-B	GSE13425	98.58595839	6.623310273	6.623310273
pre-B	GSE13425	99.93050886	6.642853296	6.642853296
pre-B	GSE13425	100.2385944	6.647294279	6.647294279
pre-B	GSE13425	102.6422654	6.681481107	6.681481107
pre-B	GSE13425	103.9100674	6.699191627	6.699191627
pre-B	GSE13425	103.93466	6.699533032	6.699533032
pre-B	GSE13425	107.3953679	6.746787959	6.746787959
pre-B	GSE13425	109.1481787	6.770144247	6.770144247
pre-B	GSE13425	109.6152923	6.776305271	6.776305271
pre-B	GSE13425	113.2411754	6.823254819	6.823254819
pre-B	GSE13425	114.4326822	6.838355337	6.838355337
pre-B	GSE13425	120.0733842	6.907772584	6.907772584
pre-B	GSE13425	125.4486262	6.970952862	6.970952862
pre-B	GSE13425	126.2293787	6.979903913	6.979903913
pre-B	GSE13425	153.0155324	7.257534296	7.257534296
pre-B	GSE13425	188.0385858	7.554884925	7.554884925
pre-B	GSE13425	266.4688382	8.057823019	8.057823019
pre-B	GSE13425	291.6150318	8.187921278	8.187921278
pre-B	GSE13425	300.1169468	8.229380976	8.229380976
pre-B	GSE13425	380.0041417	8.569871332	8.569871332
pre-B	GSE13425	519.7623602	9.021708351	9.021708351
pre-B	GSE13425	902.3141064	9.81748593	9.81748593
pre-B	GSE13425	920.4814202	9.846244791	9.846244791
pre-B	GSE13425	927.7742931	9.857630062	9.857630062
pre-B	GSE13425	1084.283915	10.08252685	10.08252685
pre-B	GSE13425	1312.389138	10.35797984	10.35797984
pre-B	GSE13425	1355.637503	10.40475574	10.40475574
pre-B	GSE13425	1592.482437	10.63706175	10.63706175
pre-B	GSE13425	1650.40429	10.68860376	10.68860376
T-ALL	GSE13425	23.31936402	4.543456538	6
T-ALL	GSE13425	32.70791108	5.031567718	6
T-ALL	GSE13425	33.28521777	5.056809702	6
T-ALL	GSE13425	34.34991436	5.102234597	6
T-ALL	GSE13425	36.27689696	5.180979151	6
T-ALL	GSE13425	39.50516393	5.303969343	6
T-ALL	GSE13425	48.50632748	5.600101049	6
T-ALL	GSE13425	48.76116205	5.607660603	6
T-ALL	GSE13425	49.8606659	5.639830245	6
T-ALL	GSE13425	55.73259563	5.80044944	6
T-ALL	GSE13425	57.10656932	5.835584812	6
T-ALL	GSE13425	57.90162986	5.855532054	6
T-ALL	GSE13425	60.6056548	5.921380505	6
T-ALL	GSE13425	61.28321018	5.937419966	6
T-ALL	GSE13425	65.90761985	6.042373366	6.042373366

T-ALL	GSE13425	85.35038492	6.415325755	6.415325755
T-ALL	GSE13425	87.54285412	6.451917515	6.451917515
T-ALL	GSE13425	92.43824354	6.530417942	6.530417942
T-ALL	GSE13425	99.82844749	6.641379085	6.641379085
T-ALL	GSE13425	102.1498707	6.674543568	6.674543568
T-ALL	GSE13425	104.6515962	6.709450506	6.709450506
T-ALL	GSE13425	124.9562989	6.965279818	6.965279818
T-ALL	GSE13425	126.1808423	6.979349076	6.979349076
T-ALL	GSE13425	131.4654388	7.038539766	7.038539766
T-ALL	GSE13425	136.6801556	7.094659985	7.094659985
T-ALL	GSE13425	145.7229962	7.187084753	7.187084753
T-ALL	GSE13425	161.7527098	7.337646071	7.337646071
T-ALL	GSE13425	230.3313816	7.847567175	7.847567175
T-ALL	GSE13425	276.3258399	8.110226668	8.110226668
T-ALL	GSE13425	300.3035053	8.230277505	8.230277505
T-ALL	GSE13425	745.9134878	9.542864504	9.542864504
T-ALL	GSE13425	813.1836505	9.667437399	9.667437399
hESC	GSE18265	874.6658968	9.772588234	9.772588234
hESC	GSE9440	1042.986782	10.02650516	10.02650516
hESC	GSE22167	1573.077488	10.61937402	10.61937402
hESC	GSE18265	1589.826262	10.6346534	10.6346534
NTERA	Aranda et al., PLoS One 2009; 4: e7809	1593.389646	10.63788339	10.63788339
hESC	GSE18265	1866.57871	10.86618063	10.86618063
hESC	GSE22167	1960.390688	10.93692548	10.93692548
hESC	GSE9832	2361.627737	11.20556586	11.20556586
hESC	GSE18265	2508.565433	11.29264685	11.29264685
hESC	GSE18265	3737.06909	11.86769152	11.86769152
hESC	GSE16694	6066.552485	12.56666118	12.56666118
iPS	GSE18265	1471.070963	10.52265113	10.52265113
iPS	GSE22167	1581.004542	10.6266258	10.6266258
iPS	GSE18265	1749.148324	10.77243692	10.77243692
iPS	GSE18265	2309.449426	11.17333324	11.17333324
iPS	GSE18265	2328.895714	11.18543032	11.18543032
iPS	GSE22167	2372.193321	11.21200587	11.21200587
iPS	GSE22167	2589.205928	11.338294	11.338294
iPS	GSE18265	2815.34313	11.45909505	11.45909505
iPS	GSE22167	4082.639426	11.99528644	11.99528644
iPS	GSE16694	4336.630173	12.0823587	12.0823587
iPS	GSE22167	4473.283779	12.12711857	12.12711857
iPS	GSE16694	4630.244669	12.17687271	12.17687271
iPS	GSE16694	5100.266006	12.31635678	12.31635678
iPS	GSE22167	5276.71458	12.36542423	12.36542423
iPS	GSE16694	5441.09664	12.40968174	12.40968174
iPS	GSE22167	5521.576615	12.43086455	12.43086455
iPS	GSE18265	7374.643618	12.84835762	12.84835762
iPS	GSE18265	8748.016755	13.09474027	13.09474027
CB_CD133+_1	GSE16694	1.094782611	0.130644425	6
CB_CD133+_2	GSE16694	5.93699387	2.569732623	6
PB_CD34+_1	GSE22167	10.80681682	3.43386973	6
PBMCs_2	GSE22167	20.07144337	4.327072462	6
S_11976839 (leukocyte study)	GSE9196	22.08567043	4.465038722	6
S_21437514 (leukocyte study)	GSE9196	11.35646466	3.505441879	6
S_25014370 (leukocyte study)	GSE9196	23.50248348	4.554741307	6
S_27557812 (leukocyte study)	GSE9196	32.47634537	5.021317387	6
S_31212545 (leukocyte study)	GSE9196	35.9798633	5.1691178	6
S_3761772 (leukocyte study)	GSE9196	45.15848446	5.496925164	6
Flow sorted normal CMP cells, 1	GSE19599	24.59302833	4.620177491	6
Flow sorted normal CMP cells, 2	GSE19599	26.7013003	4.738838095	6
Flow sorted normal GMP cells, 1	GSE19599	13.35645464	3.739465202	6
Flow sorted normal GMP cells, 2	GSE19599	8.419269034	3.073694983	6
Flow sorted normal immature B-cells, 1	GSE19599	16.9213756	4.08077495	6
Flow sorted normal immature B-cells, 2	GSE19599	22.63879387	4.500725192	6
Flow sorted normal MEP cells, 1	GSE19599	6.39302224	2.676498113	6
Flow sorted normal MEP cells, 2	GSE19599	4.929592451	2.301468378	6
Flow sorted normal Myelocytes, 1	GSE19599	5.954637102	2.574013587	6

Flow sorted normal Myelocytes, 2	GSE19599	16.09595715	4.008626464	6
Flow sorted normal Pre-B cells, 1	GSE19599	22.06737304	4.463842992	6
Flow sorted normal Pre-B cells, 2	GSE19599	3.911367608	1.967673133	6
Flow sorted normal Pro-B cells, 1	GSE19599	15.75473461	3.977713547	6
Flow sorted normal Pro-B cells, 2	GSE19599	4.816840386	2.268087119	6
Flow sorted normal Pro-Myelocytes, 1	GSE19599	39.91786997	5.318962835	6
Flow sorted normal Pro-Myelocytes, 2	GSE19599	22.1183137	4.467169494	6
centroblast, tonsil#11	GSE15271	15.69565116	3.972292977	6
centroblast, tonsil#6	GSE15271	14.48232282	3.85622111	6
centroblast, tonsil#7	GSE15271	4.108387899	2.038572402	6
centroblast, tonsil#8	GSE15271	15.73115134	3.975552358	6
centrocyte, tonsil#11	GSE15271	10.467058	3.387784093	6
centrocyte, tonsil#6	GSE15271	17.16930703	4.101759907	6
centrocyte, tonsil#7	GSE15271	17.32220801	4.114550933	6
centrocyte, tonsil#8	GSE15271	21.12732553	4.401038245	6
normal B lymphocytes (NBL 001)	GDS2643	128.548525	7.006169246	7.006169246
normal B lymphocytes (NBL 002)	GDS2643	54.42845836	5.766289268	6
normal B lymphocytes (NBL 004)	GDS2643	68.91785186	6.106805829	6.106805829
normal B lymphocytes (NBL 005)	GDS2643	119.0499361	6.895423036	6.895423036
normal B lymphocytes (NBL 006)	GDS2643	69.17342412	6.112145967	6.112145967
normal B lymphocytes (NBL 531)	GDS2643	70.23163268	6.134049069	6.134049069
normal B lymphocytes (NBL 533)	GDS2643	23.88898432	4.578273611	6
normal B lymphocytes (NBL 534)	GDS2643	43.0810951	5.428983018	6
normal plasma cells (NPC 389)	GDS2643	83.45786165	6.382976051	6.382976051
normal plasma cells (NPC 545)	GDS2643	119.8321721	6.90487148	6.90487148
normal plasma cells (NPC 547)	GDS2643	169.2756868	7.403230963	7.403230963
normal plasma cells (NPC 625)	GDS2643	191.089829	7.578107181	7.578107181
normal plasma cells (NPC 642)	GDS2643	129.3770762	7.015438204	7.015438204

Table S2. SOX11 mouse-immunological genome project data (RMA).
Normalization: RMA (*Robust Multi-array* Average)

Case	Ref	Cell type	10399725-NM_009234-Sox11 (log2)	10605554-NM_008084-Gapdh (log2)
GSM538389	EA07068	AG#1.CEL	5.8966	12.36168
GSM538404	EA07068	AG#10.CEL	5.10625	12.24305
GSM538390	EA07068	AG#3.CEL	5.20199	12.54219
GSM538392	EA07068	AG#5.CEL	5.17068	12.13746
GSM538393	EA07068	AG#6.CEL	5.06805	12.14323
GSM538385	EA07068	AG#8.CEL	5.4011	11.78576
GSM538403	EA07068	AG#9.CEL	5.00493	12.34463
GSM538198	EA07068	B.Fo.PC#1.CEL	5.03154	12.06852
GSM538199	EA07068	B.Fo.PC#2.CEL	5.43417	12.01039
GSM538200	EA07068	B.Fo.PC#3.CEL	4.98837	12.10026
GSM476652	EA07068	B.FrE.BM#1.cel	5.62024	12.30189
GSM399438	EA07068	B.FrE.BM#2.cel	5.03466	12.26135
GSM399439	EA07068	B.FrE.BM#3.cel	4.82125	12.12495
GSM538204	EA07068	B.FRE.FL#1.CEL	4.74533	12.68672
GSM538205	EA07068	B.FRE.FL#2.CEL	5.00678	12.73425
GSM538206	EA07068	B.FRE.FL#3.CEL	5.00274	12.2467
GSM476653	EA07068	B.FrF.BM#1.cel	5.16155	11.83619
GSM399440	EA07068	B.FrF.BM#2.cel	5.02621	11.92485
GSM399441	EA07068	B.FrF.BM#3.cel	5.076	11.8587
GSM538207	EA07068	B.GC.SP#1.CEL	4.65794	13.12598
GSM538208	EA07068	B.GC.SP#2.CEL	4.95191	13.1559
GSM538209	EA07068	B.GC.SP#3.CEL	4.73381	13.15658
GSM538210	EA07068	B.MZ.Sp#1.CEL	5.00899	11.98974
GSM538211	EA07068	B.MZ.Sp#2.CEL	4.80925	12.16705
GSM538212	EA07068	B.MZ.Sp#3.CEL	4.63676	12.05728
GSM538213	EA07068	B.T1.Sp#1.CEL	5.0994	11.93655
GSM538214	EA07068	B.T1.Sp#2.CEL	4.97493	12.01937
GSM538215	EA07068	B.T1.Sp#3.CEL	4.71177	12.02839
GSM538216	EA07068	B.T2.Sp#1.CEL	4.91318	12.04738
GSM538217	EA07068	B.T2.Sp#2.CEL	4.64462	11.98191
GSM538218	EA07068	B.T2.Sp#3.CEL	4.87742	12.09277
GSM538219	EA07068	B.T3.Sp#1.CEL	5.12999	12.15447
GSM538220	EA07068	B.T3.Sp#2.CEL	4.91084	12.07795
GSM538221	EA07068	B.T3.Sp#3.CEL	4.68388	12.08042
GSM538222	EA07068	B1a.PC#1.CEL	4.83085	12.29748
GSM538223	EA07068	B1a.PC#2.CEL	4.69666	12.45018
GSM538224	EA07068	B1a.PC#3.CEL	4.61285	12.63553
GSM538225	EA07068	B1a.Sp#1.CEL	4.72771	12.32133
GSM538226	EA07068	B1a.Sp#2.CEL	4.82239	12.34165
GSM538227	EA07068	B1a.Sp#3.CEL	4.52152	12.21369
GSM538228	EA07068	B1b.PC#1.CEL	4.9147	12.08736
GSM538229	EA07068	B1b.PC#2.CEL	4.85563	12.30064
GSM538230	EA07068	B1b.PC#3.CEL	4.704	12.24845
GSM538201	EA07068	B6SPLFO#1.CEL	4.62478	11.92997
GSM538202	EA07068	B6SPLFO#2.CEL	4.80414	11.83896
GSM538203	EA07068	B6SPLFO#3.CEL	4.76002	11.81911
GSM399454	EA07068	CD150-CD48-.BM#1.CEL	4.55589	12.82708
GSM476654	EA07068	CD150-CD48-.BM#2.CEL	4.63491	12.525
GSM399455	EA07068	CD150-CD48-.BM#3.CEL	4.77105	12.69677
GSM403989	EA07068	CD19CONTROL#1.cel	4.81291	11.89034
GSM403988	EA07068	CD19CONTROL#2.cel	5.07237	11.94211
GSM403990	EA07068	CD19CONTROL#3.cel	4.7351	12.05162
GSM403991	EA07068	CD19CONTROL#4.cel	4.82157	12.03327
GSM403992	EA07068	CD19CONTROL#6.cel	4.89698	11.97051
GSM403993	EA07068	CD19CONTROL.CEL	4.51032	12.00977
GSM403987	EA07068	CD4+TESTDB.CEL	4.98754	12.22837
GSM403986	EA07068	CD4+TESTNA.CEL	5.11002	12.28747
GSM403995	EA07068	CD4CONTROL#1.cel	4.72689	12.07988
GSM403994	EA07068	CD4CONTROL#2.cel	4.87705	12.22511
GSM403997	EA07068	CD4CONTROL#3.cel	4.67932	12.22725
GSM403996	EA07068	CD4CONTROL#4.cel	4.82213	12.21735
GSM403998	EA07068	CD4CONTROL#5.cel	4.70723	12.18482
GSM403999	EA07068	CD4CONTROL.CEL	4.74872	12.20408
GSM404003	EA07068	CD4TESTCJ#2.CEL	5.06594	11.91198

GSM404004	EA07068	CD4TESTCJ#3.CEL	4.67949	12.10997
GSM404000	EA07068	CD4TESTJS#1.CEL	5.29777	12.24375
GSM404001	EA07068	CD4TESTJS#2.CEL	5.22445	12.16856
GSM404002	EA07068	CD4TESTJS#3.CEL	4.9947	12.25379
GSM538346	EA07068	CLP#5.CEL	4.86882	12.62961
GSM538234	EA07068	DC.103+11B-.LV#1.CEL	5.17254	12.42951
GSM538235	EA07068	DC.103+11B-.LV#2.CEL	5.12857	12.53461
GSM538239	EA07068	DC.103-11B+.LV#1.CEL	5.6317	12.97251
GSM538240	EA07068	DC.103-11B+.LV#2.CEL	5.23546	12.93495
GSM538241	EA07068	DC.103-11B+.LV#3.CEL	4.88069	12.82093
GSM538263	EA07068	DC.8-4-11B+.MLN#4.CEL	4.63934	12.65133
GSM538264	EA07068	DC.8-4-11B+.MLN#5.CEL	4.57721	12.34334
GSM538280	EA07068	DC.LC.SK#2.CEL	5.10668	12.65628
GSM538281	EA07068	DC.LC.SK#3.CEL	5.23851	12.53039
GSM538255	EA07068	DC1.LN#1.CEL	5.15705	12.23232
GSM538256	EA07068	DC1.LN#2.CEL	5.07443	11.95145
GSM538257	EA07068	DC1.LN#3.CEL	5.42889	12.06414
GSM538236	EA07068	DC1.LU#1.CEL	4.94753	12.49592
GSM538237	EA07068	DC1.LU#2.CEL	5.42917	12.41563
GSM538238	EA07068	DC1.LU#3.CEL	4.52881	12.27383
GSM538252	EA07068	DC1.MLN#1.CEL	5.34611	12.10342
GSM538253	EA07068	DC1.MLN#2.CEL	5.02538	12.07099
GSM538254	EA07068	DC1.MLN#3.CEL	4.85656	12.26146
GSM538258	EA07068	DC1.SP#5.CEL	4.95819	12.2716
GSM538259	EA07068	DC1.SP#6.CEL	4.92716	12.33468
GSM538260	EA07068	DC1.SP#8.CEL	5.12035	12.05255
GSM538261	EA07068	DC1.SP#9.CEL	5.05363	12.18045
GSM538245	EA07068	DC2.LN#1.CEL	5.40963	11.79865
GSM538246	EA07068	DC2.LN#2.CEL	5.15818	11.69169
GSM538247	EA07068	DC2.LN#3.CEL	5.58859	11.63367
GSM538231	EA07068	DC2.LU#1.CEL	4.76093	12.50436
GSM538232	EA07068	DC2.LU#2.CEL	5.24873	12.54429
GSM538233	EA07068	DC2.LU#3.CEL	5.09907	12.58714
GSM538242	EA07068	DC2.MLN#1.CEL	5.17237	12.07639
GSM538243	EA07068	DC2.MLN#2.CEL	5.29262	12.05169
GSM538244	EA07068	DC2.MLN#3.CEL	5.0713	12.01235
GSM538248	EA07068	DC2.SP#5.CEL	4.87438	12.21446
GSM538249	EA07068	DC2.SP#7.CEL	5.03064	12.0528
GSM538250	EA07068	DC2.SP#8.CEL	4.87076	12.20356
GSM538251	EA07068	DC2.SP#9.CEL	4.93911	12.23853
GSM538262	EA07068	DC3.MLN#3.CEL	4.99208	12.40443
GSM538265	EA07068	DC3.SP#1.CEL	5.30391	12.28591
GSM538266	EA07068	DC3.SP#2.CEL	5.13701	12.24299
GSM538267	EA07068	DC3.SP#3.CEL	5.50039	11.80352
GSM538271	EA07068	DC6.LN#1.CEL	5.85052	11.76329
GSM538272	EA07068	DC6.LN#2.CEL	5.07008	12.00272
GSM538273	EA07068	DC6.LN#3.CEL	5.28308	11.86632
GSM538268	EA07068	DC7.LN#1.CEL	4.84307	12.26051
GSM538269	EA07068	DC7.LN#2.CEL	4.97227	12.20062
GSM538270	EA07068	DC7.LN#3.CEL	4.97434	12.42112
GSM538274	EA07068	DC8.LN#1.CEL	4.76361	12.49289
GSM538275	EA07068	DC8.LN#2.CEL	5.44435	12.10858
GSM538276	EA07068	DC8.LN#3.CEL	4.95665	12.13122
GSM538277	EA07068	DC9.LN#1.CEL	5.00678	12.0118
GSM538278	EA07068	DC9.LN#2.CEL	5.10482	12.42222
GSM538279	EA07068	DC9.LN#3.CEL	5.11882	11.77073
GSM538353	EA07068	FRA#5.CEL	5.31371	12.08107
GSM476662	EA07068	immTgd.vg2.e17.Th#1.cel	4.88991	13.42961
GSM476660	EA07068	immTgd.vg2.e17.Th#2.cel	4.59537	13.35432
GSM476661	EA07068	immTgd.vg2.e17.Th#3.cel	4.57242	13.32032
GSM476658	EA07068	immTgd.vg2-.Th#1.cel	5.02493	12.79377
GSM476659	EA07068	immTgd.vg2-.Th#2.cel	4.77753	13.01608
GSM476655	EA07068	immTgd.vg2+.Th#1.cel	5.12998	12.71936
GSM476656	EA07068	immTgd.vg2+.Th#2.cel	4.83614	12.68943
GSM476657	EA07068	immTgd.vg2+.Th#3.cel	5.11146	12.89264

GSM399442	EA07068	LTHSC.BM#1.CEL	4.89619	12.5848
GSM399443	EA07068	LTHSC.BM#2.CEL	5.20216	12.69906
GSM476663	EA07068	LTHSC.BM#3.CEL	5.07666	12.3834
GSM476664	EA07068	matTgd.vg3.e17.Th#1.cel	4.89157	13.19272
GSM476666	EA07068	matTgd.vg3.e17.Th#3.cel	4.89847	13.28492
GSM476665	EA07068	matTgd.vg3.e17.Th.#2.cel	5.76557	13.16995
GSM538282	EA07068	MF.LU#1.CEL	5.13412	13.10359
GSM538283	EA07068	MF.LU#2.CEL	5.20987	13.14383
GSM538284	EA07068	MF.LU#3.CEL	4.91653	13.07512
GSM476667	EA07068	MLP1.BM#1.CEL	4.97735	12.78633
GSM399444	EA07068	MLP1.BM#2.CEL	5.18789	12.84951
GSM399445	EA07068	MLP1.BM#3.CEL	4.93626	13.03258
GSM399446	EA07068	MLP2.BM#1.CEL	4.77195	12.83103
GSM476668	EA07068	MLP2.BM#2.CEL	4.5545	13.00886
GSM399447	EA07068	MLP2.BM#3.CEL	5.08191	12.88471
GSM538288	EA07068	NK.49CI-.SP#1@N2.CEL	5.22214	11.7168
GSM538289	EA07068	NK.49CI-.SP#2.CEL	5.01634	11.74857
GSM538290	EA07068	NK.49CI-.SP#3.CEL	5.11676	11.74195
GSM538285	EA07068	NK.49CI+.SP#1@N2.CEL	5.24817	11.72271
GSM538286	EA07068	NK.49CI+.SP#2.CEL	5.01203	11.72884
GSM538287	EA07068	NK.49CI+.SP#3.CEL	5.65904	11.92605
GSM538291	EA07068	NK.B2M-.SP#1.CEL	4.90024	11.96577
GSM538292	EA07068	NK.B2M-.SP#2.CEL	5.1108	11.83997
GSM538293	EA07068	NK.B2M-.SP#3.CEL	4.9768	11.75462
GSM538294	EA07068	NK.DAP10-.SP#1.CEL	5.38995	11.50591
GSM538295	EA07068	NK.DAP10-.SP#2.CEL	4.7342	11.80706
GSM538296	EA07068	NK.DAP10-.SP#3.CEL	4.8548	11.61424
GSM538297	EA07068	NK.DAP12-.SP#1.CEL	5.1767	12.08038
GSM538298	EA07068	NK.DAP12-.SP#2.CEL	5.20697	11.9752
GSM538299	EA07068	NK.DAP12-.SP#3.CEL	5.16654	12.19233
GSM538306	EA07068	NK.H-.MCMV1.SP#1.CEL	4.72837	12.49162
GSM538307	EA07068	NK.H-.MCMV1.SP#2.CEL	5.37588	12.68716
GSM538308	EA07068	NK.H-.MCMV1.SP#3.CEL	4.86554	12.61802
GSM538300	EA07068	NK.H+.MCMV1.SP#1.CEL	4.78046	12.57261
GSM538301	EA07068	NK.H+.MCMV1.SP#2.CEL	4.98359	12.68278
GSM538302	EA07068	NK.H+.MCMV1.SP#3.CEL	5.26402	12.67672
GSM538303	EA07068	NK.H+.MCMV7.SP#1.CEL	5.52607	12.15107
GSM538304	EA07068	NK.H+.MCMV7.SP#2.CEL	5.82398	11.70558
GSM538305	EA07068	NK.H+.MCMV7.SP#3.CEL	5.39853	12.08352
GSM538309	EA07068	NK.H+MCMV1#1.CEL	5.06254	12.70375
GSM538310	EA07068	NK.H+MCMV1#2.CEL	4.99186	12.59365
GSM538311	EA07068	NK.H+MCMV1#3.CEL	5.42281	12.53096
GSM538312	EA07068	NK.MCMV7#1.CEL	5.35616	12.15244
GSM538313	EA07068	NK.MCMV7#2.CEL	4.81505	12.0628
GSM538314	EA07068	NK.MCMV7#3.CEL	5.08556	11.97782
GSM538315	EA07068	NK.SP#7.CEL	5.48679	11.88727
GSM538316	EA07068	NK.SP#8.CEL	5.46979	11.99181
GSM538317	EA07068	NK.SP#9.CEL	5.17359	11.92304
GSM538325	EA07068	NKT.4-.LV#1.CEL	4.93901	12.06978
GSM538326	EA07068	NKT.4-.LV#2.CEL	5.39912	11.94435
GSM538327	EA07068	NKT.4-.LV#3.CEL	5.25095	12.4133
GSM538328	EA07068	NKT.4-.LV#4.CEL	4.86318	12.3413
GSM538329	EA07068	NKT.4-.SP#1.CEL	5.49407	11.97653
GSM538330	EA07068	NKT.4-.SP#2.CEL	4.86401	12.26557
GSM538331	EA07068	NKT.4-.SP#3.CEL	5.08928	12.21788
GSM538318	EA07068	NKT.4+.LV#1.CEL	4.82976	12.47727
GSM538319	EA07068	NKT.4+.LV#2.CEL	4.83679	12.56394
GSM538320	EA07068	NKT.4+.LV#3.CEL	5.33753	12.39208
GSM538321	EA07068	NKT.4+.LV#4.CEL	5.08401	12.43207
GSM538322	EA07068	NKT.4+.SP#1.CEL	5.10311	12.60493
GSM538323	EA07068	NKT.4+.SP#2.CEL	5.46864	12.56772
GSM538324	EA07068	NKT.4+.SP#3.CEL	4.9328	12.49833
GSM538335	EA07068	NKT.44+NK1.1-.TH#1.CEL	5.15004	12.87207
GSM538336	EA07068	NKT.44+NK1.1-.TH#2.CEL	4.93525	12.88487
GSM538337	EA07068	NKT.44+NK1.1-.TH#3.CEL	4.64525	12.89211

GSM538332	EA07068	NKT.44+NK1.1+.TH#1.CEL	4.86191	12.39575
GSM538333	EA07068	NKT.44+NK1.1+.TH#2.CEL	5.22972	12.44516
GSM538334	EA07068	NKT.44+NK1.1+.TH#4.CEL	4.99637	12.60636
GSM538338	EA07068	NKT.44-NK1.1-.TH#1.CEL	4.90723	12.93258
GSM538339	EA07068	NKT.44-NK1.1-.TH#2.CEL	4.85957	12.97028
GSM476669	EA07068	preB.FrC.BM#1.cel	4.60431	12.94167
GSM399452	EA07068	preB.FrC.BM#2.cel	4.92567	12.9156
GSM399453	EA07068	preB.FrC.BM#3.cel	4.76832	12.85758
GSM399448	EA07068	preB.FrD.BM#1.cel	4.77594	11.91938
GSM399449	EA07068	preB.FrD.BM#2.cel	4.87603	12.21072
GSM476670	EA07068	preB.FrD.BM#3.cel	5.30271	12.03426
GSM538340	EA07068	PREB.FRD.FL#1.CEL	4.68706	12.68142
GSM538341	EA07068	PREB.FRD.FL#2.CEL	4.73802	12.4181
GSM538342	EA07068	PREB.FRD.FL#3.CEL	4.71663	12.26265
GSM399350	EA07068	preT.DN1.Th#1.cel	4.87982	12.55742
GSM399351	EA07068	preT.DN1.Th#2.cel	5.39342	12.64754
GSM399352	EA07068	preT.DN1.Th#3.cel	4.83592	12.53571
GSM399353	EA07068	preT.DN2.Th#1.cel	4.91805	12.96179
GSM399354	EA07068	preT.DN2.Th#2.cel	4.78138	12.83977
GSM399355	EA07068	preT.DN2.Th#3.cel	4.60316	12.78775
GSM399356	EA07068	preT.DN3.Th#1.cel	5.9654	12.84407
GSM399357	EA07068	preT.DN3.Th#2.cel	5.21373	12.99214
GSM399358	EA07068	preT.DN3.Th#3.cel	5.21815	13.08164
GSM399359	EA07068	preT.ETP.Th#1.cel	4.87248	12.73222
GSM399360	EA07068	preT.ETP.Th#3.cel	4.73613	12.83738
GSM399361	EA07068	preT.ETP.Th#4.cel	4.7183	12.8147
GSM538343	EA07068	proB.CLP.BM#1.CEL	4.80301	12.77971
GSM538344	EA07068	proB.CLP.BM#2.CEL	4.91131	12.84028
GSM538345	EA07068	PROB.CLP.BM#4.CEL	5.27371	12.20562
GSM538347	EA07068	PROB.CLP.BM#8.CEL	4.836	12.42684
GSM538348	EA07068	PROB.CLP.FL#1.CEL	4.88771	12.86049
GSM538349	EA07068	PROB.CLP.FL#2.CEL	4.72175	13.31363
GSM538350	EA07068	PROB.CLP.FL#3.CEL	4.84469	13.22362
GSM538351	EA07068	proB.FrA.BM#1.CEL	4.8178	12.7163
GSM538352	EA07068	PROB.FRA.BM#4.CEL	4.98872	12.5697
GSM538354	EA07068	PROB.FRA.BM#8.CEL	5.35386	12.07045
GSM538355	EA07068	PROB.FRA.FL#1.CEL	4.9947	12.84839
GSM538356	EA07068	PROB.FRA.FL#2.CEL	4.78516	13.09712
GSM538357	EA07068	PROB.FRA.FL#3.CEL	4.7458	13.0424
GSM399450	EA07068	proB.FrBC.BM#1.cel	4.69673	12.67838
GSM476671	EA07068	proB.FrBC.BM#2.cel	4.42573	12.89114
GSM399451	EA07068	proB.FrBC.BM#3.cel	4.93894	12.6898
GSM538418	EA07068	PROB.FRBC.BM#4.CEL	4.97779	12.51609
GSM538358	EA07068	PROB.FRBC.FL#1.CEL	4.97476	13.1691
GSM538359	EA07068	PROB.FRBC.FL#2.CEL	5.13327	13.11942
GSM538360	EA07068	PROB.FRBC.FL#3.CEL	4.98693	13.21272
GSM399362	EA07068	T.4+8int.Th#1.cel	5.45229	12.40065
GSM399363	EA07068	T.4+8int.Th#2.cel	5.09957	12.20771
GSM399364	EA07068	T.4+8int.Th#4.cel	5.13581	12.30953
GSM538361	EA07068	T.4FP3+25+.Sp#1.CEL	5.72473	12.37655
GSM399365	EA07068	T.4FP3+25+.Sp#2.cel	5.61701	12.61304
GSM399366	EA07068	T.4FP3+25+.Sp#3.cel	5.01016	12.32319
GSM399367	EA07068	T.4int8+.Th#1.cel	4.68746	12.70958
GSM399368	EA07068	T.4int8+.Th#2.cel	5.16443	12.38643
GSM399369	EA07068	T.4int8+.Th#3.cel	4.82669	12.67198
GSM538362	EA07068	T.4MEM.LN#1.CEL	4.9377	12.64738
GSM538363	EA07068	T.4MEM.LN#2.CEL	4.96708	12.63247
GSM538364	EA07068	T.4MEM.LN#3.CEL	5.4888	12.60145
GSM538365	EA07068	T.4Mem.Sp#1.CEL	4.74517	12.77595
GSM538366	EA07068	T.4Mem.Sp#4.CEL	4.8111	12.68739
GSM538367	EA07068	T.4Mem.Sp#5.CEL	4.78697	12.58257
GSM538368	EA07068	T.4MEM44H62L.LN#1.CEL	4.7654	12.70485
GSM538369	EA07068	T.4MEM44H62L.LN#2.CEL	5.58157	12.58642
GSM538370	EA07068	T.4MEM44H62L.LN#3.CEL	4.80056	12.67921
GSM538371	EA07068	T.4MEM44H62L.SP#1.CEL	5.09261	12.4258

GSM538372	EA07068	T.4MEM44H62L.SP#2.CEL	4.9537	12.59869
GSM538373	EA07068	T.4MEM44H62L.SP#3.CEL	4.85584	12.4961
GSM538374	EA07068	T.4Nve.LN#1.CEL	4.88505	12.192
GSM538375	EA07068	T.4Nve.LN#2.CEL	4.7968	12.1509
GSM538376	EA07068	T.4Nve.LN#3.CEL	4.90813	12.26092
GSM538377	EA07068	T.4Nve.MLN#1.CEL	5.55103	12.09203
GSM538378	EA07068	T.4Nve.MLN#2.CEL	5.14615	12.16998
GSM538379	EA07068	T.4Nve.MLN#3.CEL	5.17253	11.99176
GSM538380	EA07068	T.4NVE.PP#1.CEL	5.34582	11.73346
GSM538381	EA07068	T.4NVE.PP#2.CEL	5.90146	11.68481
GSM538382	EA07068	T.4Nve.Sp#1.CEL	5.45786	11.88056
GSM538383	EA07068	T.4Nve.Sp#2.CEL	5.27209	12.17939
GSM538384	EA07068	T.4Nve.Sp#3.CEL	5.42177	12.25367
GSM399370	EA07068	T.4SP24-.Th#1.cel	4.96841	12.64911
GSM399371	EA07068	T.4SP24-.Th#2.cel	5.17917	12.60029
GSM399372	EA07068	T.4SP24-.Th#3.cel	4.82729	12.48283
GSM399373	EA07068	T.4SP24int.Th#1.cel	4.66328	12.72214
GSM399374	EA07068	T.4SP24int.Th#2.cel	4.97094	12.83493
GSM399375	EA07068	T.4SP24int.Th#3.cel	5.01986	12.76247
GSM399376	EA07068	T.4SP69+.Th#1.cel	4.94871	12.70486
GSM399377	EA07068	T.4SP69+.Th#2.cel	5.01383	12.69267
GSM399378	EA07068	T.4SP69+.Th#3.cel	5.01711	12.80514
GSM538386	EA07068	T.8EFF.SP.OT1.D15.VSVOVA#4.CEL	5.30627	12.19036
GSM538405	EA07068	T.8EFF.SP.OT1.D45VSV.CEL	5.20453	12.31668
GSM538387	EA07068	T.8EFF.SP.OT1.D5.VSVOVA#1.CEL	5.01195	13.21664
GSM538388	EA07068	T.8EFF.SP.OT1.D5.VSVOVA#2.CEL	5.11026	13.24057
GSM538391	EA07068	T.8EFF.SP.OT1.D6.VSVOVA#4.CEL	5.18955	12.70768
GSM538394	EA07068	T.8EFF.SP.OT1.D8.VSVOVA#4.CEL	4.82502	12.20341
GSM538395	EA07068	T.8MEM.LN#1.CEL	5.21095	12.43585
GSM538396	EA07068	T.8MEM.LN#2.CEL	5.34824	12.24297
GSM538397	EA07068	T.8MEM.LN#3.CEL	5.57265	12.52641
GSM538398	EA07068	T.8Mem.Sp#1.CEL	5.06763	12.21383
GSM538399	EA07068	T.8Mem.Sp#3.CEL	5.06358	12.33659
GSM538400	EA07068	T.8Mem.Sp#4.CEL	4.90311	12.2392
GSM538401	EA07068	T.8MEM.SP.OT1.D106.VSVOVA#2.CEL	5.16069	12.18594
GSM538402	EA07068	T.8MEM.SP.OT1.D106.VSVOVA#3.CEL	5.34093	11.89483
GSM538406	EA07068	T.8Nve.LN#1.CEL	5.20423	12.31594
GSM538407	EA07068	T.8Nve.LN#2.CEL	4.85332	12.20915
GSM538408	EA07068	T.8Nve.LN#3.CEL	5.08377	12.29904
GSM538409	EA07068	T.8Nve.MLN#1.CEL	5.1513	12.12351
GSM538410	EA07068	T.8Nve.MLN#3.CEL	4.95215	12.30307
GSM538411	EA07068	T.8Nve.MLN#4.CEL	5.02487	12.24359
GSM538412	EA07068	T.8NVE.PP#1.CEL	5.24607	11.29322
GSM538413	EA07068	T.8NVE.PP#2.CEL	5.04978	11.88319
GSM538414	EA07068	T.8NVE.PP#4.CEL	5.59175	11.69581
GSM538415	EA07068	T.8Nve.Sp#1.CEL	5.61487	11.84524
GSM538416	EA07068	T.8Nve.Sp#2.CEL	5.5284	12.09838
GSM538417	EA07068	T.8Nve.Sp#3.CEL	4.96761	12.11763
GSM399379	EA07068	T.8SP24-.Th#1.cel	4.89913	12.57151
GSM399380	EA07068	T.8SP24-.Th#2.cel	4.99972	12.61421
GSM399381	EA07068	T.8SP24-.Th#3.cel	4.83843	12.59257
GSM399382	EA07068	T.8SP24int.Th#1.cel	4.84873	12.58457
GSM399383	EA07068	T.8SP24int.Th#2.cel	4.73645	12.60971
GSM399384	EA07068	T.8SP24int.Th#3.cel	4.99764	12.60653
GSM399385	EA07068	T.8SP69+.Th#1.cel	5.13662	12.4632
GSM399386	EA07068	T.8SP69+.Th#2.cel	4.99593	12.57886
GSM399387	EA07068	T.8SP69+.Th#3.cel	4.72508	12.86
GSM399388	EA07068	T.DN4.Th#1.cel	5.59959	13.06349
GSM399389	EA07068	T.DN4.Th#2.cel	5.1504	13.25454
GSM399390	EA07068	T.DN4.Th#3.cel	5.26275	13.10336
GSM399391	EA07068	T.DP.Th#1.cel	5.41203	12.32843
GSM399392	EA07068	T.DP.Th#2.cel	5.45738	12.17066
GSM399393	EA07068	T.DP.Th#3.cel	5.2142	12.26829
GSM399394	EA07068	T.DP69+.Th#1.cel	5.27507	12.8175
GSM399395	EA07068	T.DP69+.Th#2.cel	5.33518	12.91478

GSM399396	EA07068	T.DP69+.Th#3.cel	5.32751	12.6558
GSM399397	EA07068	T.DPbl.Th#1.cel	4.96268	12.96565
GSM399398	EA07068	T.DPbl.Th#2.cel	4.78613	13.13873
GSM399399	EA07068	T.DPbl.Th#3.cel	4.89651	13.11062
GSM399400	EA07068	T.DPsm.Th#1.cel	5.09641	12.3578
GSM399401	EA07068	T.DPsm.Th#2.cel	5.46079	12.21002
GSM399402	EA07068	T.DPsm.Th#3.cel	5.3305	12.38025
GSM399403	EA07068	T.ISP.Th#1.cel	4.99788	13.11335
GSM399404	EA07068	T.ISP.Th#2.cel	4.9976	13.16612
GSM399405	EA07068	T.ISP.Th#3.cel	4.954	13.06506
GSM476672	EA07068	TGD.SP#1.CEL	5.13286	12.29773
GSM476673	EA07068	TGD.SP#2.CEL	5.23567	12.07484
GSM476674	EA07068	TGD.SP#3.CEL	5.31358	12.22104
GSM476675	EA07068	TGD.TH#1.CEL	5.25073	13.00987
GSM476676	EA07068	TGD.TH#2.CEL	5.11259	13.01316
GSM476677	EA07068	TGD.TH#3.CEL	5.00653	13.03273
GSM476681	EA07068	Tgd.vg2-.act.Sp#1.cel	5.43303	11.85016
GSM476682	EA07068	Tgd.vg2-.act.Sp#2.cel	5.25494	12.20182
GSM476683	EA07068	Tgd.vg2-.act.Sp#3.cel	4.88006	12.28159
GSM476684	EA07068	Tgd.vg2-.Sp#1.cel	5.24284	11.93082
GSM476685	EA07068	Tgd.vg2-.Sp#2.cel	4.66718	12.26882
GSM476686	EA07068	Tgd.vg2-.Sp#3.cel	4.86257	12.29614
GSM476678	EA07068	Tgd.vg2+.act.Sp#1.cel	5.00856	12.13293
GSM476679	EA07068	Tgd.vg2+.act.Sp#2.cel	5.12041	12.13035
GSM476680	EA07068	Tgd.vg2+.act.Sp#3.cel	5.41798	12.30415

Table S3. SOX11 TEL-AML1 transduced cells.

	204913_s_at	204914_s_at	204915_s_at	Mean SOX11 (log2)		
HSC1.CEL	2.425	2.396	2.860	2.560	CD34+CD38-/lowCD19-	control
HSC2.CEL	4.360	4.998	7.357	5.572	CD34+CD38-/lowCD19-	control
HSC3.CEL	2.330	4.570	4.779	3.893	CD34+CD38-/lowCD19-	control
CD34pos_CD38low_neg_CD19pos_1.CEL	1.589	2.476	6.132	3.399	CD34+CD38-/lowCD19+	TEL-AML1 vector transduced
CD34pos_CD38low_neg_CD19pos_2.CEL	3.334	2.699	4.830	3.621	CD34+CD38-/lowCD19+	TEL-AML1 vector transduced
CD34pos_CD38low_neg_CD19pos_3.CEL	2.915	2.267	2.794	2.659	CD34+CD38-/lowCD19+	TEL-AML1 vector transduced
ProB1.CEL	3.175	3.952	6.928	4.685	CD34+CD38+CD19+	control vector transduced
ProB2.CEL	3.925	6.620	3.548	4.698	CD34+CD38+CD19+	control vector transduced
ProB3.CEL	6.270	3.524	4.299	4.698	CD34+CD38+CD19+	control vector transduced

Table S4. Cases and analyses.

Case	Type	Infinium	Pyrosequen	qRT-PCR	qChIP	Western blo
KM-H2	cHL cell line	YES	YES	-	-	-
L1236	cHL cell line	YES	-	-	-	-
L428	cHL cell line	YES	-	-	-	-
HDLM2	cHL cell line	YES	YES	-	-	-
L591	cHL cell line	-	YES	-	-	-
L540	cHL cell line	-	YES	-	-	-
UHO1	cHL cell line	-	YES	-	-	-
VAL-Rita	DLBCL cell line	YES	-	-	-	-
RL-Bill	DLBCL cell line	YES	-	-	-	-
LY10-Rita	DLBCL cell line	YES	YES	-	-	-
LY3	DLBCL cell line	-	YES	-	-	-
RCK8	DLBCL cell line	-	-	-	-	-
RAJI	BL cell line	YES	YES	YES	YES	YES
DAUDI	BL cell line	-	YES	-	-	-
JURKA	T-ALL cell line	YES	-	-	-	-
HBL2	MCL cell line	YES	YES	YES	-	-
JEKO1	MCL cell line	YES	YES	YES	-	YES
MAVER1	MCL cell line	-	YES	YES	-	-
MINO	MCL cell line	YES	YES	YES	-	-
REC1	MCL cell line	YES	YES	YES	-	YES
UPN1	MCL cell line	YES	YES	YES	-	-
Z-138	MCL cell line	YES	YES	YES	-	YES
GRANT519	MCL cell line	YES	YES	YES	YES	YES
JVM2	MCL cell line	YES	YES	YES	YES	YES
MEC1	CLL cell line	-	YES	YES	YES	-
KOPN8	B-ALL cell line	-	YES	YES	YES	-
REH	B-ALL cell line	-	YES	YES	YES	-
B-ALL-case1	B-ALL (BCR-ABL)	-	YES	YES	YES	-
B-ALL-case2	B-ALL (BCR-ABL)	-	YES	YES	YES	-
B-ALL-case3	B-ALL (BCR-ABL)	YES	-	-	-	-
B-ALL-case4	B-ALL (BCR-ABL)	YES	-	-	-	-
B-ALL-case5	B-ALL (BCR-ABL)	YES	-	-	-	-
B-ALL-case6	B-ALL (BCR-ABL)	YES	-	-	-	-
B-ALL-case7	B-ALL (BCR-ABL)	YES	-	-	-	-
B-ALL-case8	B-ALL (BCR-ABL)	YES	-	-	-	-
B-ALL-case9	B-ALL (BCR-ABL)	YES	-	-	-	-
B-ALL-case10	B-ALL (BCR-ABL)	YES	-	-	-	-
B-ALL-case11	B-ALL (BCR-ABL)	YES	-	-	-	-
B-ALL-case12	B-ALL (BCR-ABL)	YES	-	-	-	-
B-ALL-case13	B-ALL (BCR-ABL)	YES	-	-	-	-
B-ALL-case14	B-ALL (BCR-ABL)	YES	-	-	-	-
B-ALL-case15	B-ALL (BCR-ABL)	YES	-	-	-	-
B-ALL-case16	B-ALL (BCR-ABL)	YES	-	-	-	-
B-ALL-case17	B-ALL (BCR-ABL)	YES	-	-	-	-
B-ALL-case18	B-ALL (NORMAL KARYOTYPE)	YES	-	-	-	-
B-ALL-case19	B-ALL (NORMAL KARYOTYPE)	YES	-	-	-	-
B-ALL-case20	B-ALL (NORMAL KARYOTYPE)	YES	-	-	-	-
B-ALL-case21	B-ALL (NORMAL KARYOTYPE)	YES	-	-	-	-
B-ALL-case22	B-ALL (NORMAL KARYOTYPE)	YES	-	-	-	-
B-ALL-case23	B-ALL (NORMAL KARYOTYPE)	YES	-	-	-	-
B-ALL-case24	B-ALL (NORMAL KARYOTYPE)	YES	-	-	-	-
B-ALL-case25	B-ALL (TEL-AML1)	YES	-	-	-	-
B-ALL-case26	B-ALL (TEL-AML1)	YES	-	-	-	-
B-ALL-case27	B-ALL (TEL-AML1)	YES	-	-	-	-
B-ALL-case28	B-ALL (TEL-AML1)	YES	-	-	-	-
B-ALL-case29	B-ALL (TEL-AML1)	YES	-	-	-	-
T-ALL-case1	T-ALL (NORMAL KARYOTYPE)	YES	-	-	-	-
T-ALL-case2	T-ALL (NORMAL KARYOTYPE)	YES	-	-	-	-
T-ALL-case3	T-ALL (NORMAL KARYOTYPE)	YES	-	-	-	-
T-ALL-case4	T-ALL (NORMAL KARYOTYPE)	YES	-	-	-	-
T-ALL-case5	T-ALL (NORMAL KARYOTYPE)	YES	-	-	-	-
T-ALL-case6	T-ALL (NORMAL KARYOTYPE)	YES	-	-	-	-
T-ALL-case7	T-ALL (NORMAL KARYOTYPE)	YES	-	-	-	-

T-ALL-case8	T-ALL (NORMAL KARYOTYPE)	YES	-	-	-	-
T-ALL-case9	T-ALL (NORMAL KARYOTYPE)	YES	-	-	-	-
BL-case1	mBL	YES	-	-	-	-
BL-case2	mBL	YES	-	-	-	-
BL-case3	mBL	YES	-	-	-	-
BL-case4	mBL	YES	-	-	-	-
BL-case5	mBL	YES	YES	-	-	-
BL-case6	mBL	YES	-	-	-	-
BL-case7	mBL	-	YES	-	-	-
BL-case8	mBL	-	YES	-	-	-
BL-case9	mBL	-	YES	-	-	-
BL-case10	mBL	-	YES	-	-	-
BL-case11	mBL	-	YES	-	-	-
BL-case12	mBL	-	YES	-	-	-
DLBCL-case1	DLBCL-ABC	YES	-	-	-	-
DLBCL-case2	DLBCL-ABC	YES	-	-	-	-
DLBCL-case3	DLBCL-ABC	YES	-	-	-	-
DLBCL-case4	DLBCL-ABC	YES	-	-	-	-
DLBCL-case5	DLBCL-ABC	YES	-	-	-	-
DLBCL-case6	DLBCL-ABC	YES	-	-	-	-
DLBCL-case7	DLBCL-ABC	YES	-	-	-	-
DLBCL-case8	DLBCL-ABC	-	YES	-	-	-
DLBCL-case9	DLBCL-ABC	-	YES	-	-	-
DLBCL-case10	DLBCL-ABC	-	YES	-	-	-
DLBCL-case11	DLBCL-ABC	-	YES	-	-	-
DLBCL-case12	DLBCL-GCB	YES	-	-	-	-
DLBCL-case13	DLBCL-GCB	YES	-	-	-	-
DLBCL-case14	DLBCL-GCB	YES	-	-	-	-
DLBCL-case15	DLBCL-GCB	YES	-	-	-	-
DLBCL-case16	DLBCL-GCB	YES	-	-	-	-
DLBCL-case17	DLBCL-GCB	YES	-	-	-	-
DLBCL-case18	DLBCL-GCB	YES	-	-	-	-
DLBCL-case19	DLBCL-GCB	-	YES	-	-	-
DLBCL-case20	DLBCL-GCB	-	YES	-	-	-
cMCL-case1	cMCL	-	YES	YES	YES	-
cMCL-case2	cMCL	-	YES	YES	YES	-
cMCL-case3	cMCL	-	YES	YES	YES	-
cMCL-case4	cMCL	YES	YES	YES	-	-
cMCL-case5	cMCL	YES	YES	YES	-	-
cMCL-case6	cMCL	YES	YES	YES	-	-
cMCL-case7	cMCL	-	YES	YES	-	-
cMCL-case8	cMCL	-	YES	YES	-	-
cMCL-case9	cMCL	YES	YES	YES	-	
cMCL-case10	cMCL	YES	-	-	-	-
cMCL-case11	cMCL	YES	-	-	-	-
cMCL-case12	cMCL	YES	-	-	-	-
cMCL-case13	cMCL	YES	-	-	-	-
cMCL-case14	cMCL	YES	-	-	-	-
cMCL-case15	cMCL	YES	-	-	-	-
cMCL-case16	cMCL	YES	-	-	-	-
cMCL-case17	cMCL	YES	-	-	-	-
cMCL-case18	cMCL	YES	-	-	-	-
cMCL-case19	cMCL	YES	-	-	-	-
cMCL-case20	cMCL	YES	-	-	-	-
cMCL-case21	cMCL	YES	-	-	-	-
cMCL-case22	cMCL	YES	-	-	-	-
cMCL-case23	cMCL	YES	-	-	-	-
cMCL-case24	cMCL	YES	-	-	-	-
cMCL-case25	cMCL	YES	-	-	-	-
cMCL-case26	cMCL	YES	-	-	-	-
cMCL-case27	cMCL	YES	-	-	-	-
cMCL-case28	cMCL	YES	-	-	-	-
cMCL-case29	cMCL	YES	-	-	-	-
cMCL-case30	cMCL	YES	-	-	-	-
cMCL-case31	cMCL	YES	-	-	-	-

cMCL-case32	cMCL	YES	-	-	-	-
cMCL-case33	cMCL	YES	-	-	-	-
cMCL-case34	cMCL	YES	-	-	-	-
cMCL-case35	cMCL	YES	-	-	-	-
cMCL-case36	cMCL	YES	-	-	-	-
cMCL-case37	cMCL	YES	-	-	-	-
cMCL-case38	cMCL	YES	-	-	-	-
cMCL-case39	cMCL	YES	-	-	-	-
cMCL-case40	cMCL	YES	-	-	-	-
cMCL-case41	cMCL	YES	-	-	-	-
cMCL-case42	cMCL	YES	-	-	-	-
cMCL-case43	cMCL	YES	-	-	-	-
cMCL-case44	cMCL	YES	-	-	-	-
cMCL-case45	cMCL	YES	-	-	-	-
cMCL-case46	cMCL	YES	-	-	-	-
cMCL-case47	cMCL	YES	-	-	-	-
cMCL-case48	cMCL	YES	-	-	-	-
cMCL-case49	cMCL	YES	-	-	-	-
cMCL-case50	cMCL	YES	-	-	-	-
cMCL-case51	cMCL	YES	-	-	-	-
cMCL-case52	cMCL	YES	-	-	-	-
cMCL-case53	cMCL	YES	-	-	-	-
cMCL-case54	cMCL	YES	-	-	-	-
cMCL-case55	cMCL	YES	-	-	-	-
cMCL-case56	cMCL	YES	-	-	-	-
cMCL-case57	cMCL	YES	-	-	-	-
cMCL-case58	cMCL	YES	-	-	-	-
cMCL-case59	cMCL	YES	-	-	-	-
cMCL-case60	cMCL	YES	-	-	-	-
cMCL-case61	cMCL	YES	-	-	-	-
cMCL-case62	cMCL	YES	-	-	-	-
cMCL-case63	cMCL	YES	-	-	-	-
cMCL-case64	cMCL	YES	-	-	-	-
cMCL-case65	cMCL	YES	-	-	-	-
cMCL-case66	cMCL	YES	-	-	-	-
iMCL-case1	iMCL	YES	YES	YES	YES	-
iMCL-case2	iMCL	YES	YES	YES	YES	-
iMCL-case3	iMCL	YES	YES	YES	YES	-
iMCL-case4	iMCL	YES	YES	YES	-	-
iMCL-case5	iMCL	YES	YES	YES	-	-
iMCL-case6	iMCL	YES	YES	YES	-	-
iMCL-case7	iMCL	YES	YES	YES	-	-
iMCL-case8	iMCL	YES	YES	YES	-	-
iMCL-case9	iMCL	-	YES	YES	-	-
iMCL-case10	iMCL	YES	YES	-	-	-
B-CLL-case1	B-CLL	-	YES	YES	YES	-
B-CLL-case2	B-CLL	-	YES	YES	YES	-
B-CLL-case3	B-CLL	-	YES	YES	-	-
B-CLL-case4	B-CLL	-	YES	-	-	-
B-CLL-case5	B-CLL	-	YES	-	-	-
B-CLL-case6	B-CLL	-	YES	-	-	-
B-CLL-case7	B-CLL	-	YES	-	-	-
FL-case1	FL	-	YES	YES	YES	-
FL-case2	FL	-	YES	YES	YES	-
FL-case3	FL	-	YES	-	-	-
FL-case4	FL	-	YES	-	-	-
FL-case5	FL	-	YES	-	-	-
FL-case6	FL	-	YES	-	-	-
FL-case7	FL	-	YES	-	-	-
FL-case8	FL	-	YES	-	-	-
FL-case9	FL	-	YES	-	-	-
FL-case10	FL	-	YES	-	-	-
FL-case11	FL	-	YES	-	-	-
FL-case12	FL	-	YES	-	-	-
FL-case13	FL	-	YES	-	-	-

FL-case14	FL	-	YES	-	-	-
FL-case15	FL	-	YES	-	-	-
FL-case16	FL	-	YES	-	-	-
FL-case17	FL	-	YES	-	-	-
FL-case18	FL	-	YES	-	-	-
FL-case19	FL	-	YES	-	-	-
FL-case20	FL	-	YES	-	-	-
NTERA	Malignant pluripotent embryonal carcinom	-	YES	YES	YES	-
MAPC	Adult mesenchymal stem cell	-	YES	YES	YES	-
MSC	Multipotent adult progenitor cell	-	YES	YES	YES	-
PB-B cell (0)	Normal B-cell lymphocytes from periferal l	-	YES	YES	-	-
PB-B cell (1)	Normal B-cell lymphocytes from periferal l	-	YES	YES	YES	-
PB-B cell (2)	Normal B-cell lymphocytes from periferal l	-	YES	YES	YES	-
PB-B cell (3)	Normal B-cell lymphocytes from periferal l	-	YES	YES	YES	-
LBL-XX(1)	LBL cell line	YES	YES	YES	YES	-
LBL-XY(2)	LBL cell line	YES	-	-	-	-
BM3	Bone Marrow	YES	-	-	-	-
BM1	Bone Marrow	YES	-	-	-	-
lymph.pool	Peripheral Blood PBLs	YES	-	-	-	-
GC B-cells Ton1	Tonsilar GC B-cells	YES	-	-	-	-
GANGLI 1	lymph node Tissue	YES	-	-	-	-
GANGLI 2	lymph node Tissue	YES	-	-	-	-
GANGLI 3	lymph node Tissue	YES	-	-	-	-
MELSA 1	Spleen Tissue	YES	-	-	-	-
MELSA 2	Spleen Tissue	YES	-	-	-	-
MELSA 3	Spleen Tissue	YES	-	-	-	-
CA3B	Normal B-cell lymphocytes from periferal l	YES	-	-	-	-
CA10B	Normal B-cell lymphocytes from periferal l	YES	-	-	-	-
CA6B	Normal B-cell lymphocytes from periferal l	YES	-	-	-	-
A26 CD19+	Lymphocytes CD19+ from Tonsils	YES	-	-	-	-
A10 CD19+	Lymphocytes CD19+ from Tonsils	YES	-	-	-	-
A22 CD19+	Lymphocytes CD19+ from Tonsils	YES	-	-	-	-

3.2. Paper II

SOX11 regulates PAX5 expression and blocks terminal B-cell differentiation in aggressive mantle cell lymphoma.

Abstract

Mantle cell lymphoma (MCL) is one of the most aggressive lymphoid neoplasms whose pathogenesis is not fully understood. The neural transcription factor SOX11 is overexpressed in most MCL but is not detected in other mature B-cell lymphomas or normal lymphoid cells. The specific expression of SOX11 in MCL suggests that it may be an important element in the development of this tumor, but its potential function is not known. Here, we show that SOX11 promotes tumor growth in a MCL-xenotransplant mouse model. Using chromatin immunoprecipitation microarray analysis combined with gene expression profiling upon SOX11 knockdown, we identify target genes and transcriptional programs regulated by SOX11 including the block of mature B-cell differentiation, modulation of cell cycle, apoptosis, and stem cell development. PAX5 emerges as one of the major SOX11 direct targets. SOX11 silencing downregulates PAX5, induces BLIMP1 expression, and promotes the shift from a mature B-cell into the initial plasmacytic differentiation phenotype in both primary tumor cells and an *in vitro* model. Our results suggest that SOX11 contributes to tumor development by altering the terminal B-cell differentiation program of MCL and provide perspectives that may have clinical implications in the diagnosis and design of new therapeutic strategies.

Plenary Paper

SOX11 regulates PAX5 expression and blocks terminal B-cell differentiation in aggressive mantle cell lymphoma

Maria Carmela Vegliante,[1] Jara Palomero,[1] Patricia Pérez-Galán,[1] Gaël Roué,[1] Giancarlo Castellano,[1] Alba Navarro,[1] Guillem Clot,[1] Alexandra Moros,[1] Helena Suárez-Cisneros,[1] Sílvia Beà,[1] Luis Hernández,[1] Anna Enjuanes,[1] Pedro Jares,[1] Neus Villamor,[1] Dolors Colomer,[1] José Ignacio Martín-Subero,[2] Elias Campo,[1,2] and Virginia Amador[1]

[1]Hematopathology Unit, Pathology Department, Hospital Clínic, Institut d'Investigacions Biomèdiques August Pi i Sunyer; and [2]Department of Anatomic Pathology, Pharmacology and Microbiology, University of Barcelona, Barcelona, Spain

Key Points

- SOX11 silencing promotes the shift from a mature B cell into the initial plasmacytic differentiation phenotype in MCL.
- SOX11 promotes tumor growth of MCL cells in vivo, highlighting its implication in the aggressive behavior of conventional MCL.

Mantle cell lymphoma (MCL) is one of the most aggressive lymphoid neoplasms whose pathogenesis is not fully understood. The neural transcription factor SOX11 is overexpressed in most MCL but is not detected in other mature B-cell lymphomas or normal lymphoid cells. The specific expression of SOX11 in MCL suggests that it may be an important element in the development of this tumor, but its potential function is not known. Here, we show that SOX11 promotes tumor growth in a MCL-xenotransplant mouse model. Using chromatin immunoprecipitation microarray analysis combined with gene expression profiling upon SOX11 knockdown, we identify target genes and transcriptional programs regulated by SOX11 including the block of mature B-cell differentiation, modulation of cell cycle, apoptosis, and stem cell development. *PAX5* emerges as one of the major SOX11 direct targets. SOX11 silencing downregulates PAX5, induces BLIMP1 expression, and promotes the shift from a mature B cell into the initial plasmacytic differentiation phenotype in both primary tumor cells and an in vitro model. Our results suggest that SOX11 contributes to tumor development by altering the terminal B-cell differentiation program of MCL and provide perspectives that may have clinical implications in the diagnosis and design of new therapeutic strategies. (*Blood*. 2013;121(12):2175-2185)

Introduction

Mantle cell lymphoma (MCL) is one of the most aggressive lymphoid neoplasms.[1] This biological behavior has been attributed to the molecular mechanisms involved in its pathogenesis combining the deregulation of cell proliferation, disruption of the DNA-damage–response pathways, and the activation of cell-survival mechanisms.[2] Recent studies have identified a subgroup of patients with MCL that have an indolent clinical behavior and long survival even without chemotherapy. These tumors have very stable karyotypes and frequently carry hypermutated *IGHV*, indicating an origin in cells that have experienced the follicular germinal center microenvironment.[3-7] A gene expression profiling (GEP) study has shown that these indolent MCL differ from conventional MCL in a particular gene signature that lacks the expression of some transcription factors of the high-mobility group (HMG). One of the best discriminatory genes between these 2 subtypes of tumors is *SOX11* (SRY [sex-determining region-Y]-box11),[4,6] a neural transcription factor whose function in normal and neoplastic B-cell development is unknown.

SOX11 belongs to the *SOX* gene family encoding for transcription factors that play a critical role in the regulation of cell fate and differentiation in major developmental processes. In mice, Sox11 is important in organ development and neurogenesis.[8,9] SOX11 upregulation has been detected in various types of human solid tumors.[10,11] SOX4, the SOX family member with the highest homology to SOX11, is a prominent transcription factor in lymphocytes of both B- and T-cell lineage[12] and is crucial for B-cell lymphopoiesis.[13] In contrast, SOX11 has no known lymphopoietic function and it is not expressed in lymphoid progenitors or in mature normal B-cells. However, it is expressed in virtually all aggressive MCL and at lower levels in a subgroup of Burkitt and acute lymphoblastic lymphomas, but not in other lymphoid neoplasms.[14-16] These findings suggest that SOX11 plays a relevant role in the pathogenesis of these tumors. However, the function of SOX11 and its potential target genes in lymphoid cells remain unknown.

To identify direct target genes, transcriptional programs, and oncogenic pathways regulated by SOX11 in malignant lymphoid cells, we have used genome-wide promoter analysis and GEP after SOX11 silencing in MCL cell lines, followed by the validation in an in vivo murine model and in primary MCL tumors.

Submitted June 24, 2012; accepted December 10, 2012. Prepublished online as *Blood* First Edition paper, January 15, 2013; DOI 10.1182/blood-2012-06-438937.

M.C.V. and J.P. contributed equally to this study.

All microarray data are available in the Gene Expression Omnibus (accession numbers GSE34763 and GSE3502 for the gene expression array and the ChIP-chip array, respectively).

The online version of this article contains a data supplement.

There is an Inside *Blood* commentary on this article in this issue.

The publication costs of this article were defrayed in part by page charge payment. Therefore, and solely to indicate this fact, this article is hereby marked "advertisement" in accordance with 18 USC section 1734.

Materials and methods

Cell lines and patient samples

A total of 6 MCL cell lines, 5 SOX11 positive (Z138, GRANTA519, REC1, HBL2, and JEKO1) and 1 SOX11 negative (JVM2),[17] were used for chromatin immunoprecipitation (ChIP) microarray (ChIP-chip) and/or ChIP quantitative polymerase chain reaction (qPCR) experiments, gene expression analysis after SOX11 silencing, and western blot (WB) experiments. Human embryonic kidney 293 (HEK293) cells were used for luciferase assays.

Microarray GEP data previously generated in 38 primary MCL (16 SOX11-positive and 22 SOX11-negative) were used for gene set enrichment analysis (GSEA) (GSE36000).[7] Immunophenotypic surface markers were investigated in 6 of these primary MCL (3 SOX11 positive and 3 SOX11 negative) by flow cytometry.

Details on cell culture and primary tumor's information are provided in "supplemental Materials and methods."

ChIP

Z138, GRANTA519, and JVM2 cell lines were used for ChIP-chip and/or ChIP-qPCR analysis. Cells were crosslinked with 1% of formaldehyde for 10 minutes and chromatin sonicated using Branson Sonifer 250 followed by Biorupter sonicator from Diagenode. SOX11 antibody (sc-17347; Santa Cruz Biotechnology, Santa Cruz, CA) was used to immunoprecipitate protein-DNA complexes. Immunocomplexes were amplified in 2 steps using a GenomePlex Whole Genome Amplification WGA Kit (Sigma, St Louis, MO), following the manufacturer's instructions, and used for ChIP-chip analysis and/or ChIP-qPCR. We performed ChIP assays in triplicate from Z138-SOX11-positive cells and in a single experiment from JVM2 cell line as negative control (supplemental Materials and methods).

ChIP-qPCR

Primers for the qPCR analysis of the SOX11 ChIP-enriched genomic DNA regions were designed using Primer3 (http://frodo.wi.mit.edu/) (supplemental Table 1). Amplified SOX11-ChIP DNA and 1:100 diluted input samples were analyzed in triplicate by qPCR using Fast SYBR Green Master Mix in a StepOnePlus PCR detection system (Applied Biosystems, Foster City, CA).

Reporter plasmid constructs and luciferase assay

The SOX11-binding site from the regulatory region of *PAX5* gene (ChIP-peak region from 2435 bp to −1884 bp) was amplified by PCR using GRANTA519 genomic DNA and primers are listed in supplemental Table 1. Subsequently, the PCR fragment was cloned in front of a minimal promoter luciferase reporter vector pGL4.23[*luc2*/minP] (Promega, Leiden, The Netherlands). Constructs were sequenced using internal primers prior to use.

Lipofectamine 2000 system (Invitrogen, Life Technologies, Carlsbad, CA) was used for transient cotransfection experiments in HEK293 cells following the manufacturer's instructions. Cotransfected HEK293 cells were harvested and luciferase activity was measured 24 hours after transfection with Dual-Glo Luciferase Assay System (Promega) and a Modulus microplate luminometer (Turner BioSystems, Sunnyvale, CA). All assays were performed in triplicate on separated days.

Gene expression profiling

Total RNA of Z138 cells stably transduced with short hairpins targeting SOX11 and control short hairpin was extracted with the TRIzol reagent following the manufacturer's recommendations (Invitrogen). RNA integrity was examined with the Agilent 2100 Bioanalyser (Agilent Technologies, Palo Alto, CA) and hybridized to HG-U133plus2.0 GeneChips (Affymetrix) according to Affymetrix standard protocols. The analysis of the GEP is detailed in "supplemental Materials and methods."

GSEA

We performed GSEA[18] on 2 preranked lists of genes derived from in vitro SOX11 silencing microarray data and from our series of 38 purified primary MCL data. To generate these preranked lists, we analyzed the GEP of our in vitro cell line model as well as the GEP of 38 primary MCL according to their SOX11 expression levels. Details on GSEA are provided in "supplemental Materials and methods."

SOX11 silencing by lentiviral infection

SOX11 shRNA lentiviral particles (shRNASOX11.1, clone ID NM_003108.3-982s1c1; shRNASOX11.2, clone ID NM_003108.3-1235s1c1; and shRNASOX11.3, clone ID NM_003108.3-454s1c1) were purchased from Sigma-Aldrich. Control shRNA lentiviral particle (Clone ID sc-108080) was purchased from Santa Cruz Biotechnology.

SOX11 knockdown stable MCL cell lines were generated by lentiviral transduction of PLKO1-puro–shSOX11 and PLKO1-puro–scramble constructs in 3 MCL cell lines (Z138, GRANTA519, and JEKO1). Details on SOX11 silencing are provided in "supplemental Materials and methods."

WB analysis

Protein extract preparation and WB experiments were performed as previously described[19] using antibodies against hemagglutinin (Roche Applied Science, Indianapolis, IN; 12CA5), SOX11 (Atlas Antibodies, Stockholm, Sweden [HPA000536]; Santa Cruz Biotechnology [H-290 and C-20]), PAX5 (Santa Cruz Biotechnology; C-20), BLIMP1 (CNIO, Madrid, Spain; Ros 195G/G5), IRF4 (Santa Cruz Biotechnology; M-17), GAPDH (Santa Cruz Biotechnology; A-3), and α-tubulin (Oncogene, Uniondale, NY; CP06-100UG). Membranes were developed with chemiluminescence substrate Pierce ELC WB substrate (Thermo Fisher Scientific, South Logan, UT) and visualized on a LAS4000 device (Fujifilm, Tokyo, Japan). Protein quantification was done with Image Gauge software (Fujifilm).

qRT-PCR

qRT-PCR was performed as described before[19] using a designed primer set and TaqMan MGB probe for SOX11 using Primer Express Software Version 2.0 (Applied Biosystems) (primers used are shown in supplemental Table 1). Inventoried TaqMan Gene Expression Assays were used for *HSPD1* (Hs01941522_u1), *SUV39H2* (Hs00226595_m1), *SEPT2* (Hs00189358_m1), *MSI2* (Hs-00292670_m1), *PAX5* (Hs00277134_m1), *VPREB3* (Hs00429452_m1), *SPIB* (Hs0062150_m1), *EBF1* (Hs00365513_m1), *CD19* (Hs00174333_m1), *IKZF3* (Hs00232635_m1), *LEF1* (Hs01547250_m1), and *LCK* (Hs00178427_m1). Relative quantification of gene expression was analyzed with the $2^{-\Delta\Delta Ct}$ method using *GUS* (Hs00939627_m1) as the endogenous control.

Flow cytometry studies

For immunophenotype analysis, 500 000 cells of interest were collected in 1.5-mL tubes, washed once in phosphate-buffered saline 0.5% bovine serum albumin (BSA), and stained with 5 μL of antibody against CD20 (2H7), CD24 (ML5), immunoglobulin (Ig) M (G20-127), IgD (IA6-2), CD5 (UCHT2), CD19 (HIB19), CD38 (HIT2) (all from BD Pharmingen, San Diego, CA), and CD138 (B-A38; Beckman Coulter, Carlsbad, CA) for 30 minutes at 4°C in the dark. Cells were then washed 3 times in phosphate-buffered saline 0.5% BSA and acquired and analyzed using the Attune Acoustic Focusing Cytometer and Software (Applied Biosystems). For the analysis, 10 000 events were collected in the lymphocyte gate. Details on proliferation assay, cell-cycle analysis, and apoptosis assay are provided in "supplemental Materials and methods."

Xenograft mouse model and tumor phenotyping

CB17 severe combined immunodeficient (CB17-SCID) mice (Charles River Laboratory, Wilmington, MA) were housed in the animal care facility under

BLOOD, 21 MARCH 2013 • VOLUME 121, NUMBER 12

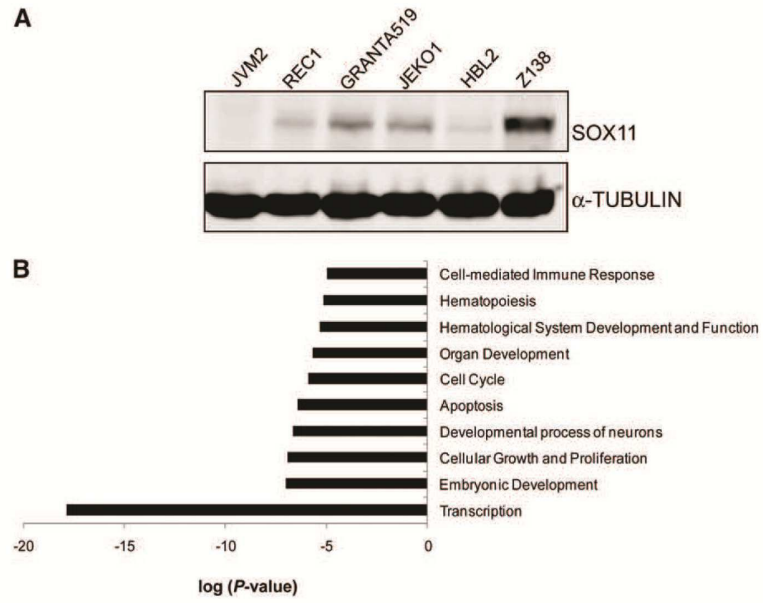

Figure 1. ChIP-chip screening of SOX11-bound target genes in MCL cell lines. (A) The expression levels of SOX11 protein in different MCL cell lines (JVM2, REC1, GRANTA519, JEKO1, HBL2, and Z138) were detected by WB using an anti-SOX11 antibody (H-290). α-Tubulin was used as a loading control. (B) IPA functional annotation tool related to the high-confidence SOX11-bound genes. The 10 most significant biological-process GO terms and their log *P* values are shown.

a 12/12-hour light/dark cycle at 22°C, and they received a standard diet and acidified water ad libitum. With the use of a protocol approved by the animal testing Ethical Committee of the University of Barcelona, mice were subcutaneously inoculated into their lower dorsum with 1×10^7 Z138shSOX11.1 (n = 8), shSOX11.3 (n = 6), shControl (n = 7), JEKOshSOX11.3 (n = 5), JEKOshControl (n = 5), GRANTA519shSOX11.3 (n = 5), and GRANTA519shControl (n = 5) in Matrigel basement membrane matrix (Becton Dickinson, San Jose, CA). The shortest and longest diameters of the tumor were measured with external calipers every 3 days, and tumor volume (in mm^3) was calculated with the use of the following standard formula: (the shortest diameter)^2 × (the longest diameter) × 0.5. Animals were sacrificed according to institutional guidelines, and tumor xenografts were paraffin embedded on silane-coated slides in a fully automated immunostainer (Bond Max; Vision Biosystems, Mount Waverley, Australia).

Immunohistochemical staining

Immunohistochemical studies were performed as previously described[16,20] using antibodies against human Ki67, kappa, lambda, and IgM (ready to use; Dako, Glostrup, Denmark), anti-phosphohistone H3 (Epitomics, Burlingame, CA; polyclonal), anti–caspase-3 cleaved (Cell Signaling Technology, Danvers, MA; 5A1E), SOX11 (Atlas Antibodies; HPA000536), cyclin D1 (Thermo Fisher Scientific; EPR2241IHC), PAX5 (Santa Cruz Biotechnology; sc-1974), and BLIMP1 (CNIO; Ros 195G/G5).

Necrotic areas were quantified using the digitalized images of the activated caspase-3 immunohistochemical staining acquired with an Olympus BX51 microscope at original magnification ×4 and analyzed with an Olympus Cell B Basic Imaging Software. Necrotic areas were delineated by cleaved caspase-3–positive staining and quantified as the sum of all necrotic areas (μm^2) divided by the total area of the core analyzed (μm^2).

Statistical analysis

Data are represented as mean ± standard deviation (SD) of 3 independent experiments. Statistical tests were performed using SPSS v16.0 software. Comparison between 2 groups of samples was evaluated by independent-sample *t* test, and results were considered statistically significant when $P < .05$.

Results

Genome-wide promoter analysis of SOX11 in MCL

We first investigated the direct target genes of SOX11 using ChIP and DNA microarrays (ChIP-chip). We used a MCL cell line with high SOX11 expression (Z138) and one negative for SOX11 (JVM2) (Figure 1A). ChIP was performed using a SOX11 specific antibody (supplemental Figure 1). ChIP-enriched DNA sequences were amplified and hybridized to a high-resolution DNA tiling array spanning promoter regions of the whole human genome. These experiments identified 5842 significant enriched peaks belonging to 1133 unique genes (SOX11-bound genes) that were consistently enriched in immunoprecipitated material across all 3 independent Z138 replicates after subtracting the corresponding nonspecific immunoprecipitated material in JVM2 (supplemental Table 2).

The promoter region of SOX11 was not identified in this analysis. We have reported that SOX11 expression is associated with active histone marks.[19] We have now observed a significant reduction in the enrichment of the activating histone mark H3K4me3 at the SOX11 promoter upon SOX11 silencing (supplemental Figure 2), suggesting that SOX11 may indirectly regulate its own expression by epigenetic mechanisms.

Gene ontology (GO) term enrichment analysis showed several biological processes overrepresented in the SOX11-bound genes, including transcription, embryonic and neuronal development, cell growth and proliferation, cell death and apoptosis, cell cycle, hematopoiesis, and hematological system development and function (Figure 1B).

Differential gene expression profiling after SOX11 silencing

To determine the transcriptional programs regulated by SOX11, we generated a MCL cellular model by silencing SOX11 expression (Figure 2A). We then compared the GEP of stably transduced shSOX11 and shControl Z138 cells (Figure 2B and

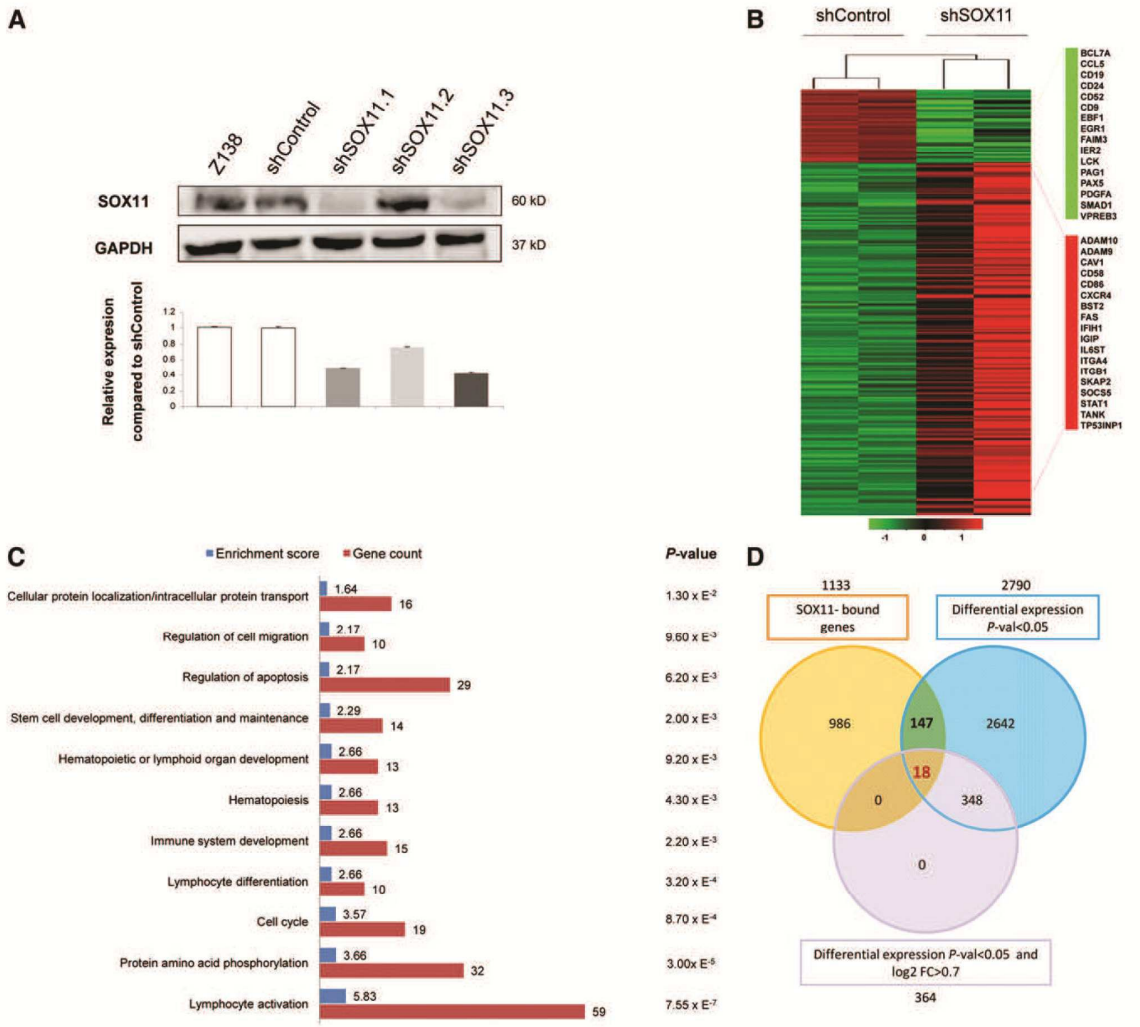

Figure 2. GEP upon SOX11 silencing. (A) SOX11 silencing in Z138 stably transduced with shSOX11.1, shSOX11.2, and shSOX11.3 was verified (upper panel) at the protein level by WB using GAPDH as a loading control and (lower panel) at the transcriptional level by qRT-PCR. A scramble shControl and untransduced cells (Z138) are also shown. Bar plot represents the mean ± SD of 3 independent experiments. (B) Heat map illustrating 366 significant differentially expressed genes (adjusted $P < .05$ and log2 FC > 0.7) in Z138 shSOX11.1 and shSOX11.3 compared with 2 Z138-shControl cells. Red indicates increased expression and green decreased expression relative to the median expression level according to the color scale shown. (C) DAVID functional annotation of the 366 differentially expressed genes. The 11 most significant ($P < .05$) biological process GO terms, their *P* value, enrichment score, and gene count are shown. (D) Venn diagram depicting the overlap of 1133 SOX11-bound genes (orange circle), 2790 significant differentially expressed genes ($P < .05$) upon SOX11 silencing (blue circle), and differentially expressed genes using more stringent statistical criteria ($P < .05$ and log2 FC > 0.7) (purple circle).

supplemental Table 3). The top annotated functions of the differentially expressed genes included lymphocyte activation and differentiation, phosphorylation, cell cycle, immune system development, and hematopoiesis (Figure 2C). A GSEA using the genes differentially expressed in primary SOX11-positive and SOX11-negative MCL confirmed that the GEP observed in our in vitro model was representative of that observed in these primary MCL (supplemental Table 4 and supplemental Figure 3).

Interestingly, among the significant differentially expressed genes between shSOX11 and shControl cells, we observed upregulation of key regulators of plasma cell differentiation and pronounced downregulation of B-cell genes. To further characterize the significance of these changes, we performed a GSEA using well-defined gene signatures related to the different steps of the mature B-cell and plasma cell differentiation programs (supplemental Table 4).[21-24] These analyses showed that the GEP of Z138shControl cells was enriched for gene signatures related to the mature B-cell program whereas Z138shSOX11 cells were enriched in gene signatures related to the plasma cell differentiation program (supplemental Table 5 and supplemental Figure 4). These findings indicate that SOX11 silencing triggers a shift from the mature B cell to a plasmacytic gene expression program in MCL cells.

SOX11 directly regulates the transcription of *PAX5*

To determine the direct targets transcriptionally regulated by SOX11, we overlaid the list of SOX11-bound genes and those with differential expression upon SOX11 knockdown and found 147

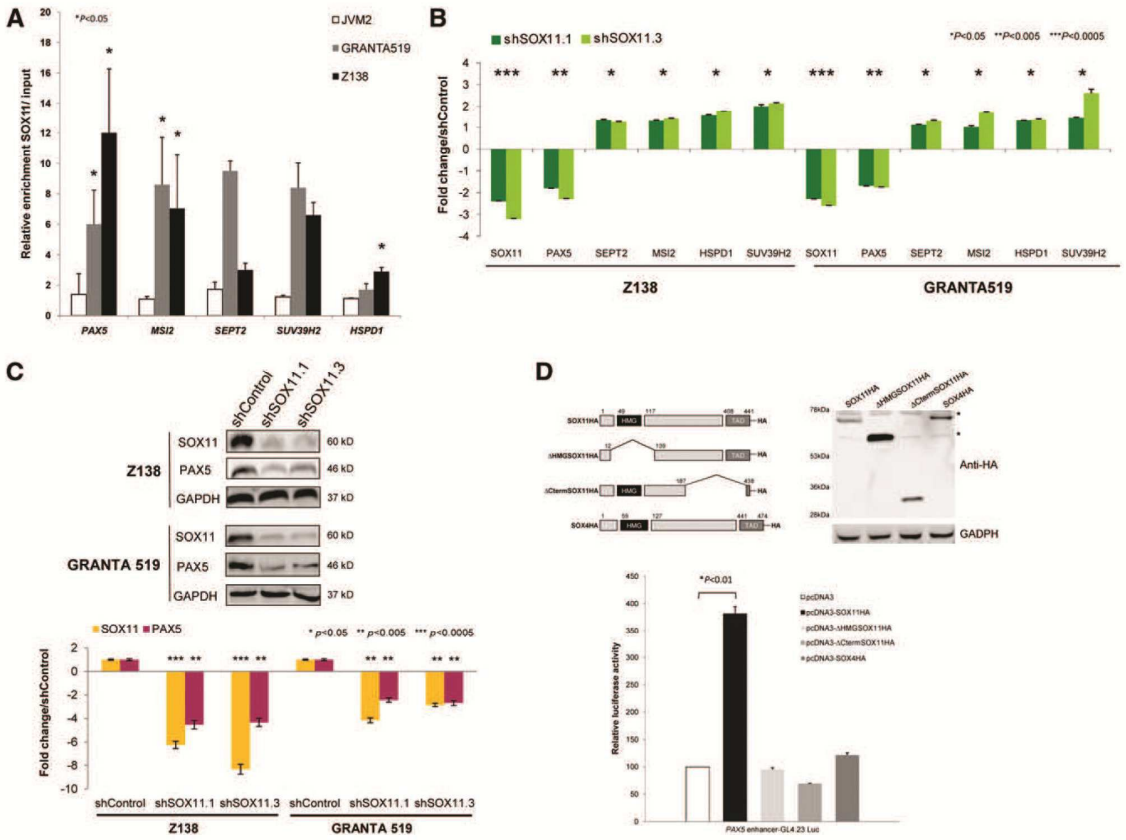

Figure 3. SOX11 directly regulates *PAX5* transcription. (A) Binding of SOX11 to regulatory regions of *PAX5*, *MSI2*, *SEPT2*, *SUV39H2*, and *HSPD1* was confirmed by ChIP-qPCR in different MCL cell lines. Results are shown as enrichment relative to input. (B) Levels of the indicated transcripts in Z138 and GRANTA519 quantified by qRT-PCR after SOX11 silencing. Fold-change differences compared with control cells are shown. (C) Upper panel: Levels of SOX11 and PAX5 in Z138 and GRANTA519 cell lines stably transduced with shControl, shSOX11.1, or shSOX11.3 determined by WB, using GAPDH as a loading control. Lower panel: Fold-change differences of SOX11 and PAX5 protein expression levels between control and silenced cells. SOX11 and PAX5 expression levels were corrected by quantification of GAPDH expression levels. (D) Luciferase assays in transient cotransfections of *PAX5* enhancer-GL4.23 Luc with SOX11 full-length, the truncated SOX11 proteins (SOX11ΔHMG and SOX11ΔCtermTAD), or SOX4 full-length expression vectors, in HEK293 cells. Upper panel: Schematic representation of the constructs and results of the WB experiment of SOX11 mutants are shown. *Nonspecific bands. Bottom panel: Results are shown as fold induction relative to luciferase activity in cotransfection with the empty vector (pcDNA3). Bar plot represents the mean ± SD of 3 independent experiments. The significance of difference was determined by paired *t* test. HA, hemagglutinin.

genes in common. From these 147 genes, 18 genes still overlapped using more stringent statistical criteria ($P < .05$ and log2 fold change > 0.7) (Figure 2D and supplemental Table 6).

Interestingly, among these 18 genes we identified PAX5, an essential transcription factor regulating B-cell identity in early B-cell development[25] and late B-cell differentiation,[26] as one of the highest-confident SOX11-bound genes (false discovery rate [FDR] < 0.1 and peak score ≥ 0.5). We also found genes that can contribute to SOX11 hematopoietic and B-cell activation functions (MSI2 and HSPD1, respectively).

We then verified the direct binding of SOX11 to the regulatory regions of the most significantly overlaid genes by ChIP-qPCR in Z138 and GRANTA519 MCL cell lines. As expected, no binding within these regulatory regions was detected in the SOX11-negative JVM2 (Figure 3A). Downregulation of PAX5 in stable SOX11-knockdown MCL cell lines was confirmed by qRT-PCR and WB (Figure 3B-C, respectively). Upregulation of MSI2, HSPD1, SUV39H2, and SEPT2 was also observed but to a much lesser extent than PAX5, prompting us to focus on the SOX11-PAX5 relationship.

To verify the transcriptional effect of SOX11 on the *PAX5* promoter, the amplified SOX11 ChIPed-*PAX5* fragment (supplemental Figure 5) was cloned in front of a minimal promoter luciferase reporter and tested in transient cotransfections with SOX11 expression vector. The induction in luciferase activity was detected in the coexpression with SOX11 but not with SOX4 or truncated SOX11 proteins lacking the HMG domain (ΔHMGSOX11) or the C-terminal TAD domain (ΔTADSOX11) (Figure 3D), both of which are required for its transcriptional activity.[27,28] These findings demonstrate the specificity of SOX11 in regulating the transcription of *PAX5*.

SOX11-knockdown MCL cell lines display early plasmacytic differentiation

PAX5 is the critical transcription factor that determines and maintains B-cell identity by activating the expression of B-cell–specific genes and simultaneously repressing genes that promote plasma cell differentiation.[25,26] The significant shift from a mature B cell to a plasmacytic gene expression program identified by GSEA in our SOX11-knockdown cells was highly suggestive of

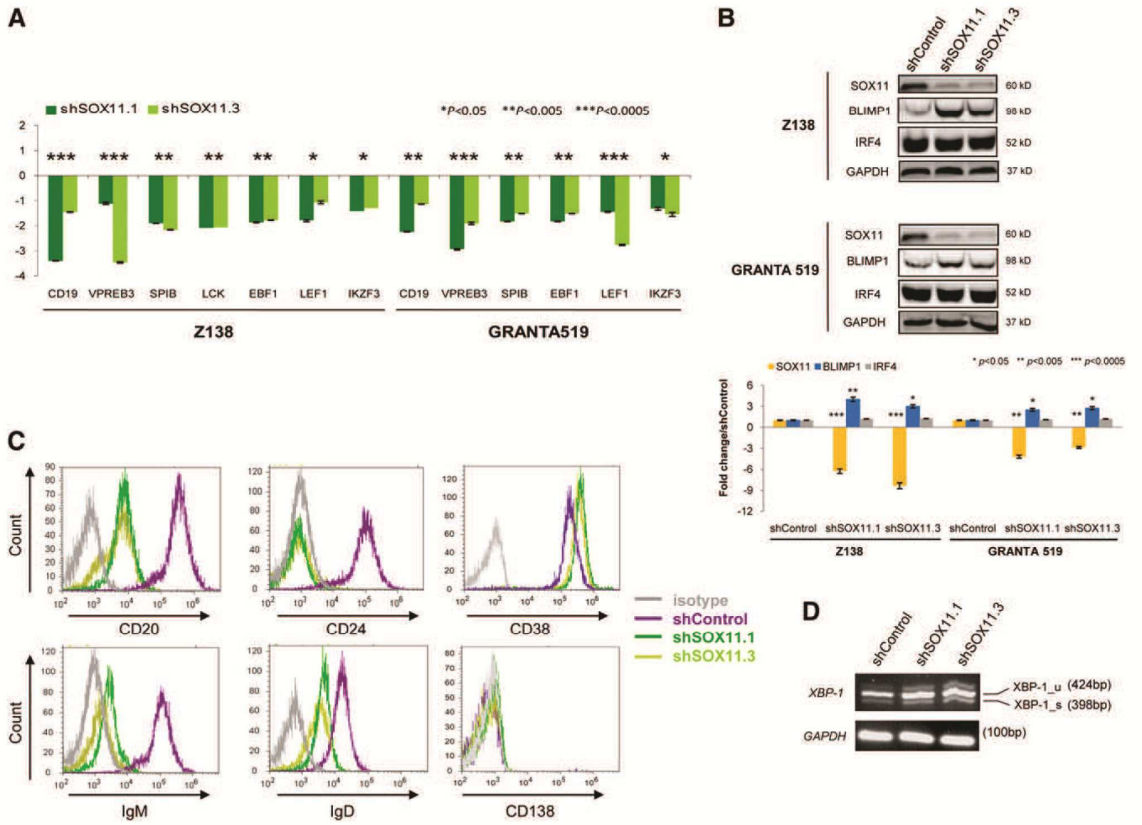

Figure 4. SOX11 activates B-cell–specific genes and represses plasma cell gene program. (A) Messenger RNA expression levels of the indicated genes were analyzed by qRT-PCR in Z138 and GRANTA519 stably transduced with shSOX11.1 or shSOX11.3. Figure shows the fold differences compared with the corresponding control cells (±SD; n = 3 technical replicates). *P* values are shown. The significance of difference was determined by independent-samples *t* test. (B) Upper panel: BLIMP1 and IRF4 expression levels in Z138 and GRANTA519 stably transduced with shControl, shSOX11.1, or shSOX11.3 assessed by WB, using GAPDH as a loading control. Lower panel: Fold-change differences of SOX11, BLIMP1, and IRF4 protein expression levels between control and silenced cells. SOX11, BLIMP1, and IRF4 expression levels were corrected by quantification of GAPDH expression levels. (C) Histograms showing the expression of B-cell and plasma cell surface markers (CD20, CD24, CD38, and CD138) and surface IgM and IgD measured by flow cytometry in shControl, shSOX11.1, and shSOX11.3 Z138 cell lines. Isotype control is shown in gray. (D) XBP1 mRNA expression levels by RT-PCR in Z138shControl, shSOX11.1, or shSOX11.3. GADPH was used for the loading control.

a major effect of the direct modulation of PAX5 by SOX11 in these tumor cells. These observations prompted us to further investigate the expression of genes regulated by PAX5 in SOX11-knockdown cells. As expected, several B-cell genes were downregulated (CD19, VPREB3, SPIB, LCK, EBF1, LEF1, and IKZF3) in SOX11 knockdown cells compared with control cells (Figure 4A).

The transcription factors BLIMP1, XBP1, and IRF4 are critical regulators promoting plasma cell differentiation whereas PAX5 inhibits plasma cell development by repressing BLIMP1 and XBP1 expression.[26,29] We next examined the modulation of these transcription factors in SOX11-knockdown MCL cells. IRF4 was already expressed in control cells and SOX11 silencing did not modify its expression levels. On the contrary, SOX11 knockdown resulted in a marked increase of BLIMP1 protein levels compared with control cells (Figure 4B and supplemental Figure 6C). Consistent with BLIMP1 function as a repressor of the B-cell program during plasma cell differentiation,[30] we found decreased or undetectable expression of B-cell surface markers CD20, CD24, IgD, and IgM in SOX11-silenced cells compared with control cells. The plasma cell marker CD38 was already expressed in control cells and only marginally upregulated in SOX11 knockdown whereas expression of CD138 was undetected in both control and silenced cell lines (Figure 4C).

Full plasma cell differentiation includes synthesis and secretion of immunoglobulins, and this secretory program is controlled by the activated splicing form of XBP1. SOX11 knockdown slightly increased the levels of XBP1(u) but the levels of the spliced form of XBP1(s) did not change (Figure 4D).

Altogether, these findings indicate that SOX11 silencing in MCL cell lines promotes the initial steps into plasmacytic differentiation with downregulation of mature B-cell markers and increasing levels of BLIMP1. However, the absence of XBP1 splicing and CD138 expression indicates that the full plasma cell program is not completed.[31,32]

SOX11 promotes tumor growth of MCL in vivo

To investigate the potential tumorigenic ability of SOX11 in vivo, we studied the effect of SOX11 downregulation in a MCL-xenotransplant model by inoculating CB17-SCID mice with stably transduced Z138shSOX11 and shControl cell lines. Tumor

BLOOD, 21 MARCH 2013 • VOLUME 121, NUMBER 12

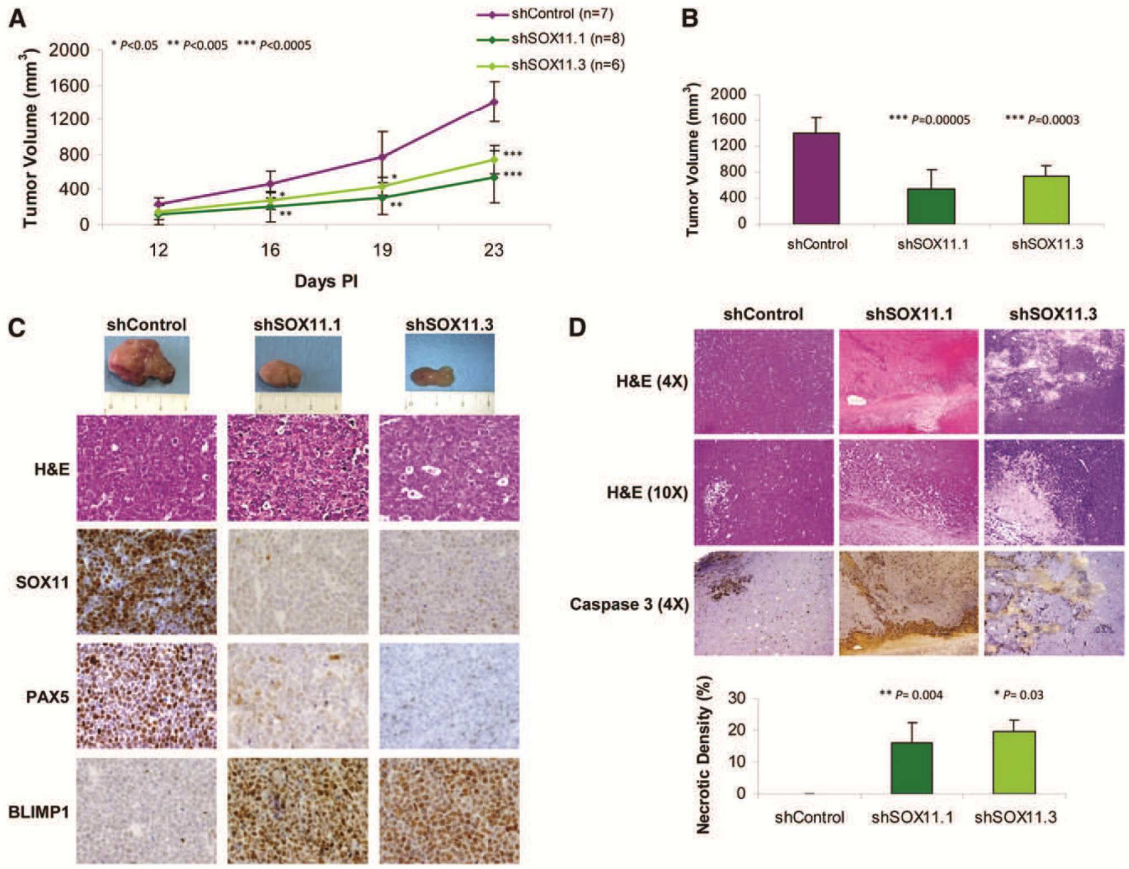

Figure 5. SOX11 silencing inhibits the growth of MCL tumors in SCID mice. (A) Z138 stably transduced with shSOX11.1, shSOX11.3, and shControl (10^7cells/mouse) were subcutaneously inoculated into the right flank of CB17-SCID mice. Tumor growth was measured using a caliper at the indicated days PI. Bar plot represents the mean ± SD. (B) Tumor volume (mm^3) of Z138shSOX11.1 (n = 8), Z138shSOX11.3 (n = 6), and Z138shControl (n = 7) cells at day 23 PI into the lower dorsum of CB17-SCID mice. (C) Macroscopic appearance (upper panel) and consecutive histological sections from representative shSOX11 and shControl tumors stained with hematoxylin and eosin (H&E) and specific antibodies anti-human SOX11, PAX5, and BLIMP1 (×40). (D) Histologic sections of representative shSOX11 and shControl tumors (upper panels, H&E ×4 and ×10). shSOX11 tumors show extensive necrotic areas that are minimal in shControl tumors. Necrotic areas are highlighted by the immunostaining for activated caspase-3 (×4). Lower panel: Density (percentage of necrotic areas vs total area of the histologic section) of necrotic areas in control and SOX11-silenced tumors delineated by the presence of activated caspase-3–positive areas. Bar plot represents the mean percentage ± SD. *P* values are shown. The significance of difference was determined by independent-samples *t* test.

growth was followed up, and at 23 days postinoculation (PI) tumor size in control mice reached 8.8% of the body weight. SOX11 silencing reduced tumor growth compared with SOX11-positive control tumors, and significant differences in tumor size were already achieved at day 16 PI (Figure 5A). Tumors isolated from mice bearing shSOX11.1- and shSOX11.3-silenced cells showed 73.1% and 54.9% reduction in tumor burden, respectively, compared with SOX11-positive tumors (Figure 5B). We also observed a similar significant reduction in tumor growth and size, at day 23 PI, of the tumors derived from JEKO1shSOX11 and GRANTA519shSOX11 compared with their SOX11-positive tumor counterparts, JEKO1shControl and GRANTA519shControl (supplemental Figure 6A-B).

Concordant with the in vitro results, the in vivo SOX11-silenced tumors showed SOX11 and PAX5 downregulation and BLIMP1 upregulation compared with SOX11-positive tumors (Figure 5C and supplemental Figure 6D). The Ki-67 proliferation index and phosphohistone H3 were similar in control and silenced tumors (supplemental Figure 7A). We did not observe significant changes in cell density, proliferation, cycle phases, or viability after SOX11 silencing in cell lines in culture (supplemental Figure 7B-E). However, in vivo SOX11-silenced tumors had large necrotic areas with high levels of activated cleaved caspase-3 that were minimal or not observed in SOX11-positive tumors (Figure 5D and supplemental Figure 6D). These results suggest that SOX11 sustains the B-cell differentiation program and tumor cell survival in vivo and support the implication of SOX11 expression in the aggressive behavior of these tumors.

SOX11 expression and B-cell differentiation program in primary tumors

We next investigated whether SOX11 modulation of the mature B-cell and early plasmacytic differentiation programs observed in vitro also occurred in primary cells from SOX11-positive and SOX11-negative MCL tumors.

We first investigated whether the expression of the SOX11-bound genes was modulated in MCL. GSEA analysis showed

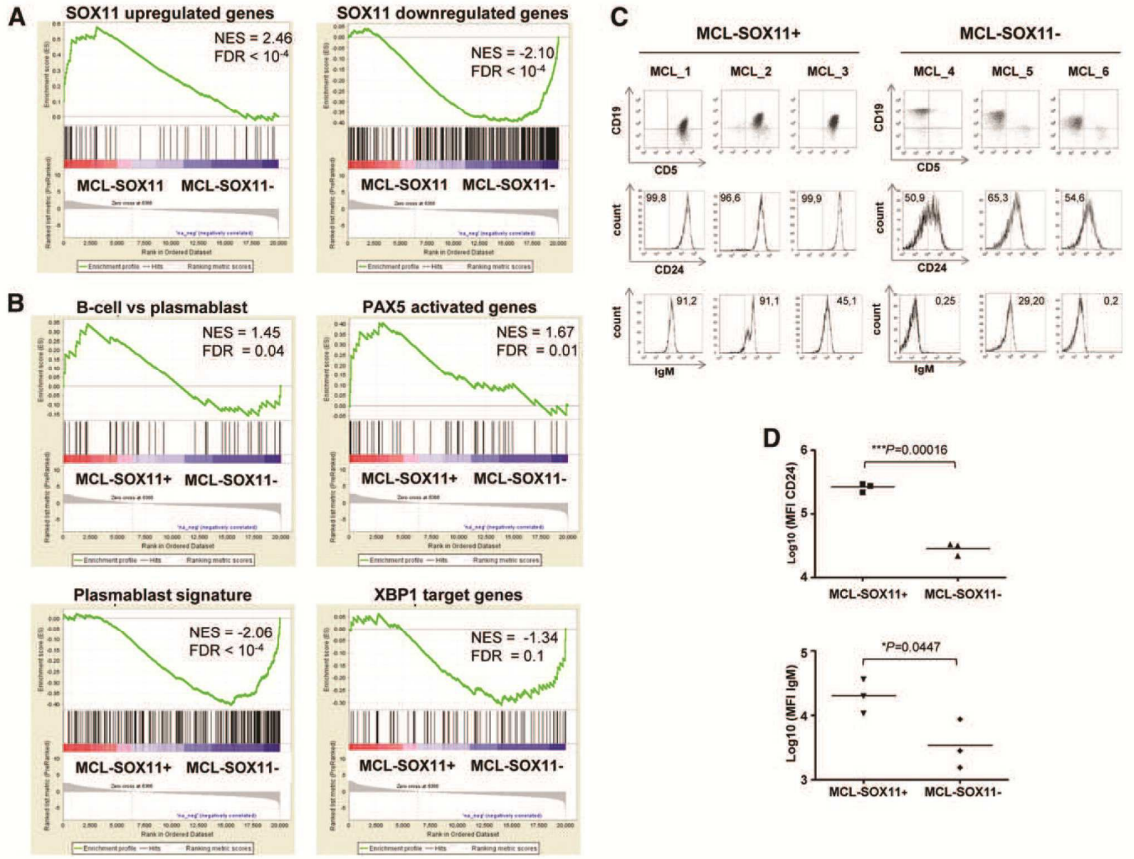

Figure 6. MCL SOX11-negative primary tumors lose B-cell identity and gain in a plasmablast gene signature. (A-B) GSEA analysis on preranked lists. (A) Using our customized gene sets described in "supplemental Materials and methods," SOX11 upregulated and downregulated genes and primary MCL-SOX11$^+$ tumors are enriched for SOX11-upregulated genes whereas primary MCL-SOX11$^-$ tumors are enriched in SOX11-downregulated genes. (B) MCL-SOX11$^+$ tumors are enriched in B-cell vs plasmablast and PAX5 activated genes gene sets whereas MCL-SOX11$^-$ tumors are enriched in plasmablast signature and XBP1 target genes. NES and FDR are shown. Statistical significance is considered when FDR < 0.1. (C) Analysis of CD24 and surface IgM expression in CD19+ CD5+ cells (MCL-SOX11$^+$) or CD19+ CD5$^-$ cells (MCL-SOX11$^-$). Numbers inside the histograms indicate the percentage of positive cells above the isotype control. (D) Mean fluorescence intensity (MFI) of surface CD24 and IgM expression in primary MCL tumors.

a statistically significant enrichment of SOX11 high-confident bound genes identified by ChIP-chip (supplemental Table 2) in both Z138shControl and primary SOX11-positive MCL (supplemental Figure 8), indicating that in these models SOX11 significantly activates the expression of its target genes.

We then defined 2 gene sets related to SOX11 transcriptional program extracted from our in vitro microarray data: SOX11-upregulated genes (genes downregulated upon SOX11 silencing) and SOX11-downregulated genes (upregulated upon knockdown) (supplemental Table 4). Notably, we found that SOX11-positive primary MCL had a GEP significantly enriched in SOX11-upregulated genes (normalized enrichment score [NES] = 2.46, FDR $< 10^{-4}$). Conversely, SOX11-negative primary MCL presented an enrichment in SOX11-downregulated genes (NES = −2.10, FDR $< 10^{-4}$) (Figure 6A).

These results suggest that the SOX11 transcriptional program derived from our knockdown experiments is also observed in primary tumors, prompting us to evaluate whether the modulation of B-cell and plasmacytic differentiation programs also occurs in these primary tumors.

We thus performed a GSEA with gene signatures of the different steps of the mature B-cell and plasma cell differentiation programs used in our previous analysis (supplemental Table 4). In line with the in vitro observations, this analysis revealed that SOX11-positive MCL were significantly enriched in B-cell vs plasmablast and PAX5 activated genes gene sets (NES = 1.45, FDR = 0.04 and NES = 1.67, FDR = 0.01, respectively) whereas SOX11-negative MCL showed statistical significance in the plasmablast signature[23] and XBP1 target genes (NES = −2.06, FDR $< 10^{-4}$ and NES = −1.34, FDR = 0.1, respectively) (Figure 6B).

We then studied the same panel of surface B-cell markers in the primary MCL cohort by flow cytometry. Concordant with the in vitro studies, SOX11-positive tumors had stronger expression of the mature B-cell marker CD24 and brighter IgM than SOX11-negative MCL (Figure 6C-D).

SOX11-silenced tumors in xenografted experiments showed increased apoptotic cells. We performed a GSEA using gene signatures related to apoptotic pathways and observed that SOX11-knockdown MCL cell lines were enriched in several apoptotic gene signatures (Fas, apoptosis, and caspase pathways). The

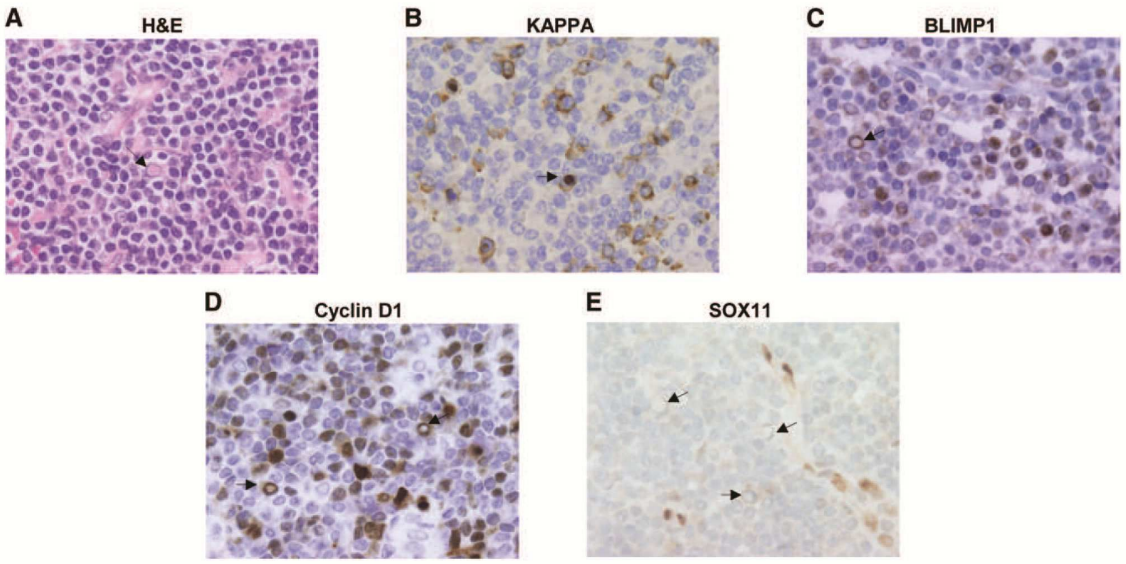

Figure 7. Plasma cells in MCL tumors are SOX11 negative. (A) MCL with focal plasmacytic differentiation. Some cells show Dutcher bodies corresponding to the accumulation of restricted immunoglobulins (arrow) (H&E; ×60). (B-C) Tumor cells expressing restricted kappa light chain and BLIMP1 (×60). (D) Tumor cells expressing cyclin D1 (×60). (E) SOX11 expression is negative in the tumor cells but positive in internal controls such as endothelial and histiocytic cells (×60). Arrows point to tumor cells with Dutcher bodies.

caspase-pathway gene signature was also significantly enriched in SOX11-negative primary MCL (supplemental Figure 9). These results suggest that SOX11 may regulate cell survival by controlling the expression of apoptotic genes in MCL cells.

Primary MCL have a monotonous cell morphology lacking the modulation toward plasmacytic differentiation observed in other types of B-cell lymphomas.[1] Intriguingly, some rare cases of MCL may show plasmacytic differentiation.[33] We postulated that this differentiation would occur in SOX11-negative MCL. In a review of our files, we found 2 MCL with plasmacytic differentiation expressing IgM, kappa, and BLIMP1 (Figure 7A-C). All tumor cells, including the cells with plasmacytic differentiation, expressed strong cyclin D1 but were SOX11 negative (Figure 7D-E). These results reinforce the idea that SOX11-negative MCL may modulate the mature B-cell and early plasma cell differentiation programs in primary tumors whereas the strong expression of SOX11 in conventional MCL may block the cells in a mature B-cell stage, preventing their further progress into differentiation.

Discussion

In this study, we have used a ChIP-chip approach to reveal the first human genome-wide promoter analysis of SOX11 and identified 1133 unique genes as putative targets of this transcription factor in MCL. Using GEP, we have also identified 366 genes whose expression was modulated by silencing SOX11 in MCL cell lines. GO analyses identified that genes regulated by SOX11 in these lymphoid cells were involved in lymphocyte activation and differentiation, phosphorylation, cell cycle, immune system development, hematopoiesis, and lymphoid organ development as the top annotated functions, but also in stem cell development, apoptosis, and cell migration.

The role of different members of the *SOX* gene family, including *SOX11*, as direct regulators of an expression program of early neural lineage development has been recently recognized in a murine model.[34] Our ChIP-chip study confirmed SOX11 binding to regulatory regions of similar genes involved in neuronal development (*BTG2, MEIS1,* and *NR2E1),* but these genes were not expressed in our lymphoid model, indicating the tissue-specific regulation of the SOX11-bound genes. In our study, the main target genes modulated by SOX11 were involved in immune system development and hematopoiesis, and *PAX5*, *MSI2*, and *HSPD1* were among the most significant genes directly regulated by SOX11.

The significant shift from a mature B cell to a plasmacytic gene expression program identified by GSEA in our SOX11 knockdown cells was highly suggestive of a major effect of the direct modulation of PAX5 by SOX11 in these tumor cells. We have demonstrated here that PAX5 is a direct target gene regulated by SOX11 and the constitutional expression of SOX11 in these tumors maintains the downstream PAX5 program. Thus, several B-cell–specific genes directly activated by PAX5 were downregulated in SOX11-knockdown MCL cell lines whereas BLIMP1 was upregulated upon SOX11 repression. The slight upregulation of XBP1(u) variant and the surface phenotype of Z138shSOX11 cells confirmed that SOX11 downregulation is able to initiate the terminal B-cell differentiation process but is not sufficient to drive the full plasma cell program.

SOX11 is constitutively overexpressed in the vast majority of MCL.[14-16] However, recent studies have identified a subset of SOX11-negative MCL[4] that differ from conventional SOX11-positive tumors in their frequent hypermutated *IGHV*, leukemic, nonnodal presentation and more indolent clinical behavior.[3-5,7] The significant reduction on tumor growth of the SOX11-silenced cells in the xenograft experiments is consistent with the indolent clinical course of the nonnodal SOX11-negative primary MCL and highlights the implication of SOX11 expression in the aggressive behavior of conventional MCL. Some studies have identified

SOX11-negative MCL with aggressive behavior but virtually all these cases have *TP53* alterations.[6,7,35] In our study, we confirmed that the gene signatures modulated upon SOX11 silencing in vitro were also enriched in primary MCL, indicating that our cell line model closely reflects the in vivo situation. Similarly, primary SOX11-positive MCL showed a GEP characteristic of mature B cells whereas negative tumors exhibited a relative shift to genes distinctive of early plasmacytic differentiation steps. However, the downregulation of SOX11 in both the in vitro model and primary tumors is not sufficient to trigger a mature plasma cell program. These results, together with our finding that the uncommon plasmacytic differentiation in MCL appears to occur in SOX11-negative tumors, reinforce the idea that these tumors may modulate the mature B-cell and plasmacytic differentiation programs. Conversely, SOX11 overexpression in aggressive MCL may block the cells in a mature B-cell stage, preventing their further differentiation. The resistance of MCL to new treatments with proteasome inhibitors has been linked to the development of plasmacytic differentiation, suggesting that the findings in our study may also have implications in the design of new therapeutic strategies.[36]

The significance of blocking plasma cell differentiation program as a relevant oncogenic mechanism in lymphoid neoplasias has been previously observed. The impairment of terminal B-cell differentiation caused by SOX11 overexpression in MCL may parallel the forced expression of *PAX5* by the t(9;14)(p13;q32) translocation identified in some B-cell lymphomas,[37-39] and the inactivating mutations of *PRDM1* in diffuse large B-cell lymphomas.[40-42]

In summary, our study reveals the global transcriptional network and direct target genes regulated by SOX11 in MCL that may contribute to the development and aggressive behavior of this tumor. Our findings provide an improved understanding of the molecular mechanisms contributing to the pathogenesis of MCL and may have clinical implications in the diagnosis of patients and selection of therapeutic strategies more adapted to the molecular diversity of this tumor.

Acknowledgments

This work was supported by grants from the Ministerio de Economía y Competitividad (MINECO) (BFU2009-09235 and RYC-2006-002110) (V.A.), (RYC-2009-05134) (P.P.-G.), (SAF08/3630) (E.C.), and the Instituto de Salud Carlos III RTICC (2006RET2039) (E.C.), (PS09/00060) (G.R.), Fondo Europeo de Desarrollo Regional, Unión Europea, Una manera de hacer Europa.

Authorship

Contribution: M.C.V. performed the ChIP experiments; J.P. performed all in vitro experiments; P.P.-G. performed experiments with the MCL primary cases; G.R. performed the in vivo study supervising; A.M. and J.P. performed in vivo experiments; A.N. generated microarray data from MCL primary tumors; G.C. performed statistical analysis; S.B. provided information of the MCL patients; A.E. and H.S.-C. helped with the ChIP-chip experiments; P.J., G.C., and J.I.M.-S. helped with microarray data; L.H. and D.C. helped with the discussion; N.V. performed fold-change analysis; E.C. performed immunohistochemistry experiments, identified morphologically MCL tumors with PC differentiation, analyzed data, and supervised experiments; V.A. designed, performed, and supervised experiments, analyzed data, and wrote the manuscript; and all authors discussed the results and commented on the manuscript.

Conflict-of-interest disclosure: The authors declare no competing financial interests.

Correspondence: Virginia Amador, Centre Esther Koplowitz (CEK), C/Rosselló 153, Barcelona 08036, Spain; e-mail: vamador@clinic.ub.es.

References

1. Swerdlow S, Campo E, Harris N, et al, eds. WHO Classification of Tumours of Haematopoietic and Lymphoid Tissues. Lyon, France: International Agency for Research on Cancer; 2008.
2. Jares P, Colomer D, Campo E. Genetic and molecular pathogenesis of mantle cell lymphoma: perspectives for new targeted therapeutics. *Nat Rev Cancer.* 2007;7(10):750-762.
3. Orchard J, Garand R, Davis Z, et al. A subset of t(11;14) lymphoma with mantle cell features displays mutated IgVH genes and includes patients with good prognosis, nonnodal disease. *Blood.* 2003;101(12):4975-4981.
4. Fernàndez V, Salamero O, Espinet B, et al. Genomic and gene expression profiling defines indolent forms of mantle cell lymphoma. *Cancer Res.* 2010;70(4):1408-1418.
5. Ondrejka SL, Lai R, Smith SD, et al. Indolent mantle cell leukemia: a clinicopathological variant characterized by isolated lymphocytosis, interstitial bone marrow involvement, kappa light chain restriction, and good prognosis. *Haematologica.* 2011;96(8):1121-1127.
6. Royo C, Navarro A, Clot G, et al. Non-nodal type of mantle cell lymphoma is a specific biological and clinical subgroup of the disease. *Leukemia.* 2012;26(8):1895-1898.
7. Navarro A, Clot G, Royo C, et al. Molecular subsets of mantle cell lymphoma defined by the IGHV mutational status and SOX11 expression have distinct biologic and clinical features. *Cancer Res.* 2012;72(20):5307-5316.
8. Sock E, Rettig SD, Enderich J, et al. Gene targeting reveals a widespread role for the high-mobility-group transcription factor Sox11 in tissue remodeling. *Mol Cell Biol.* 2004;24(15):6635-6644.
9. Haslinger A, Schwarz TJ, Covic M, et al. Expression of Sox11 in adult neurogenic niches suggests a stage-specific role in adult neurogenesis. *Eur J Neurosci.* 2009;29(11):2103-2114.
10. Weigle B, Ebner R, Temme A, et al. Highly specific overexpression of the transcription factor SOX11 in human malignant gliomas. *Oncol Rep.* 2005;13(1):139-144.
11. de Bont JM, Kros JM, Passier MM, et al. Differential expression and prognostic significance of SOX genes in pediatric medulloblastoma and ependymoma identified by microarray analysis. *Neuro-oncol.* 2008;10(5):648-660.
12. van de Wetering M, Oosterwegel M, van Norren K, et al. Sox-4, an Sry-like HMG box protein, is a transcriptional activator in lymphocytes. *EMBO J.* 1993;12(10):3847-3854.
13. Smith E, Sigvardsson M. The roles of transcription factors in B lymphocyte commitment, development, and transformation. *J Leukoc Biol.* 2004;75(6):973-981.
14. Dictor M, Ek S, Sundberg M, et al. Strong lymphoid nuclear expression of SOX11 transcription factor defines lymphoblastic neoplasms, mantle cell lymphoma and Burkitt's lymphoma. *Haematologica.* 2009;94(11):1563-1568.
15. Ek S, Dictor M, Jerkeman M, et al. Nuclear expression of the non B-cell lineage Sox11 transcription factor identifies mantle cell lymphoma. *Blood.* 2008;111(2):800-805.
16. Mozos A, Royo C, Hartmann E, et al. SOX11 expression is highly specific for mantle cell lymphoma and identifies the cyclin D1-negative subtype. *Haematologica.* 2009;94(11):1555-1562.
17. Salaverria I, Perez-Galan P, Colomer D, et al. Mantle cell lymphoma: from pathology and molecular pathogenesis to new therapeutic perspectives. *Haematologica.* 2006;91(1):11-16.
18. Subramanian A, Tamayo P, Mootha VK, et al. Gene set enrichment analysis: a knowledge-based approach for interpreting genome-wide expression profiles. *Proc Natl Acad Sci USA.* 2005;102(43):15545-15550.
19. Vegliante MC, Royo C, Palomero J, et al. Epigenetic activation of SOX11 in lymphoid neoplasms by histone modifications. *PLoS ONE.* 2011;6(6):e21382.
20. Roué G, Pérez-Galán P, Mozos A, et al. The Hsp90 inhibitor IPI-504 overcomes bortezomib resistance in mantle cell lymphoma in vitro and in vivo by down-regulation of the prosurvival ER chaperone BiP/Grp78. *Blood.* 2011;117(4):1270-1279.

21. Tarte K, Zhan F, De Vos J, et al. Gene expression profiling of plasma cells and plasmablasts: toward a better understanding of the late stages of B-cell differentiation. *Blood.* 2003;102(2):592-600.
22. Shaffer AL, Wright G, Yang L, et al. A library of gene expression signatures to illuminate normal and pathological lymphoid biology. *Immunol Rev.* 2006;210:67-85.
23. Jourdan M, Caraux A, Caron G, et al. Characterization of a transitional preplasmablast population in the process of human B cell to plasma cell differentiation. *J Immunol.* 2011; 187(8):3931-3941.
24. McManus S, Ebert A, Salvagiotto G, et al. The transcription factor Pax5 regulates its target genes by recruiting chromatin-modifying proteins in committed B cells. *EMBO J.* 2011;30(12): 2388-2404.
25. Cobaleda C, Jochum W, Busslinger M. Conversion of mature B cells into T cells by dedifferentiation to uncommitted progenitors. *Nature.* 2007;449(7161):473-477.
26. Nera KP, Kohonen P, Narvi E, et al. Loss of Pax5 promotes plasma cell differentiation. *Immunity.* 2006;24(3):283-293.
27. Dy P, Penzo-Méndez A, Wang H, et al. The three SoxC proteins—Sox4, Sox11 and Sox12—exhibit overlapping expression patterns and molecular properties. *Nucleic Acids Res.* 2008;36(9): 3101-3117.
28. Wiebe MS, Nowling TK, Rizzino A. Identification of novel domains within Sox-2 and Sox-11 involved in autoinhibition of DNA binding and partnership specificity. *J Biol Chem.* 2003; 278(20):17901-17911.
29. Tarlinton D, Radbruch A, Hiepe F, et al. Plasma cell differentiation and survival. *Curr Opin Immunol.* 2008;20(2):162-169.
30. Shaffer AL, Lin KI, Kuo TC, et al. Blimp-1 orchestrates plasma cell differentiation by extinguishing the mature B cell gene expression program. *Immunity.* 2002;17(1):51-62.
31. Kallies A, Hasbold J, Fairfax K, et al. Initiation of plasma-cell differentiation is independent of the transcription factor Blimp-1. *Immunity.* 2007; 26(5):555-566.
32. Nutt SL, Tarlinton DM. Germinal center B and follicular helper T cells: siblings, cousins or just good friends? *Nat Immunol.* 2011;12(6):472-477.
33. Visco C, Hoeller S, Malik JT, et al. Molecular characteristics of mantle cell lymphoma presenting with clonal plasma cell component. *Am J Surg Pathol.* 2011;35(2):177-189.
34. Bergsland M, Ramsköld D, Zaouter C, et al. Sequentially acting Sox transcription factors in neural lineage development. *Genes Dev.* 2011; 25(23):2453-2464.
35. Nygren L, Baumgartner Wennerholm S, Klimkowska M, et al. Prognostic role of SOX11 in a population-based cohort of mantle cell lymphoma. *Blood.* 2012;119(18):4215-4223.
36. Pérez-Galán P, Mora-Jensen H, Weniger MA, et al. Bortezomib resistance in mantle cell lymphoma is associated with plasmacytic differentiation. *Blood.* 2011;117(2):542-552.
37. Busslinger M, Klix N, Pfeffer P, et al. Deregulation of PAX-5 by translocation of the Emu enhancer of the IgH locus adjacent to two alternative PAX-5 promoters in a diffuse large-cell lymphoma. *Proc Natl Acad Sci USA.* 1996;93(12): 6129-6134.
38. Iida S, Rao PH, Nallasivam P, et al. The t(9;14) (p13;q32) chromosomal translocation associated with lymphoplasmacytoid lymphoma involves the PAX-5 gene. *Blood.* 1996;88(11):4110-4117.
39. Morrison AM, Jäger U, Chott A, et al. Deregulated PAX-5 transcription from a translocated IgH promoter in marginal zone lymphoma. *Blood.* 1998;92(10):3865-3878.
40. Mandelbaum J, Bhagat G, Tang H, et al. BLIMP1 is a tumor suppressor gene frequently disrupted in activated B cell-like diffuse large B cell lymphoma. *Cancer Cell.* 2010;18(6):568-579.
41. Tam W, Gomez M, Chadburn A, et al. Mutational analysis of PRDM1 indicates a tumor-suppressor role in diffuse large B-cell lymphomas. *Blood.* 2006;107(10):4090-4100.
42. Pasqualucci L, Compagno M, Houldsworth J, et al. Inactivation of the PRDM1/BLIMP1 gene in diffuse large B cell lymphoma. *J Exp Med.* 2006; 203(2):311-317.

SUPPLEMENTAL INFORMATION

SOX11 REGULATES PAX5 EXPRESSION AND BLOCKS TERMINAL B-CELL DIFFERENTIATION IN AGGRESSIVE MANTLE CELL LYMPHOMA

Vegliante et al.

I. SUPPLEMENTAL MATERIALS AND METHODS

Cell lines and primary tumors

MCL cell lines Z138 (CRL-3001, ATCC), JEKO1 (CRL-3006, ATCC), REC1 (ACC-584, DSMZ), HBL2 (kindly provided by Prof. M. Dreyling) and JVM2 (CRL-3002, ATCC) were cultured in RPMI 1640 medium, supplemented with 10% fetal bovine serum (FBS; Sigma Chemical, Co. St Louis, Mo), 2µM L-glutamine, 100U/mL penicillin, and 100µg/mL streptomycin (GIBCO, Grand Island, NY). All these cell lines carry the t(11;14) translocation and express high levels of cyclin D1. GRANTA519 (ACC-342, DSMZ) and human embryonic kidney 293 cells (HEK293) (CRL-1573; ATCC) were cultured in DMEM medium, supplemented with 10% FBS, 2 µM L-glutamine, 100 U/mL penicillin, and 100 µg/mL streptomycin.

The tumor samples of the 38 primary MCL used in the GEP and the six used for flow cytometry analysis were highly purified leukemic MCL cells (>95% as determined by flow cytometry). All cases had the t(11;14) and/or overexpressed cyclin D1. These cases were diagnosed according to previous defined criteria[1,2] and their SOX11 expression levels were quantified by qRT-PCR.[3] The study was approved by the Institutional Review Board of the Hospital Clínic, Barcelona, Spain.

Written informed consent was obtained from all participants and the Ethics Committees approved this consent procedure in accordance with the principles of the Declaration of Helsinki.

Immunoprecipitation (IP)

Protein extracts were obtained from Z138 and JVM2 cells or from HEK293 cells transiently transfected with pcDNA3-SOX11HA or pcDNA3-SOX4HA expression plasmids using Triton buffer as previously described.[4] 5mg of protein extracts were used for IP using specific antibodies against SOX11 (rabbit H-290 (sc-20096); goat C-20 (sc-17347), Santa Cruz Biotechnology). IP was performed overnight (O/N) at 4ºC with slow rotation. Lysates were then rotated with Dynabeads Protein G (Invitrogen) for 2h at 4ºC, after which the supernatant was separated from the beads, washed three times with triton buffer and SOX11 protein eluted with Laemmli buffer 1h at room temperature (RT). Immunoprecipitated proteins were analyzed by WB using the HA antibody (12CA5, Roche Applied Science, Indianapolis, IN) for IP experiments done in the HEK293 cell; and the antibody (HPA000536, Atlas Antibodies, Stockholm, Sweden) that detects SOX11 and SOX4 proteins for IPs done in the MCL cell lines.

Chromatin Immunoprecipitation

Z138, GRANTA519 and JVM2 cell lines ($5x10^7$ cells) were fixed with 1% formaldehyde in culture medium for 10min at RT followed by quenching with 0.125M glycine for 5min. Cells were washed twice with ice-cold PBS and nuclei were isolated by incubation with ChIP buffer (25mM HEPES pH 8.0, 1.5mM $MgCl_2$, 10mM KCl, 0.1% Nonidet-P40, and 1mM DTT) for 10min at 4°C. Nuclei were resuspended in 1mL of lysis buffer (50mM HEPES, 140mM NaCl, 1mM EDTA, 1% Triton X-100, 0.1% SDS and 0.1% Na-deoxycholate) and sonicated on ice with a Branson Sonifier 250 (20 X 20 seconds, duty 20%, output control 7, hold on ice 1min between pulses) followed by sonication using Bioruptor™ sonicator from Diagenode (20 cycles of [40 seconds "ON"/ 20 seconds "OFF"]). Sonicated fragments ranged in size from 200-1000bp. After a spinning step to reduce debris, 10µg of anti-SOX11 antibody (goat C-20; sc-17347;

Santa Cruz Biotechnology, Santa Cruz, CA) were used to immunoprecipitate protein-DNA complexes O/N at 4°C and collected using DNA-saturated Protein G Sepharose™ 4 Fast Flow (GE Healthcare, Little Chalfont, United Kingdom) for 2h. After incubation, the immunocomplexes were washed sequentially with low-salt wash buffer (0.1% SDS, 1% Triton X-100, 2mM EDTA, 20mM Tris-HCl, at pH 8.0 and 150mM NaCl), high-salt wash buffer (0.1% SDS, 1% Triton X-100, 2mM EDTA, 20mM Tris-HCl, at pH 8.0, and 500mM NaCl), LiCl wash buffer (0.25M LiCl, 1% NP-40, 1% Na-deoxycholate, 1mM EDTA and 10mM Tris-HCl, at pH 8.0) and TE buffer (10mM Tris-HCl, at pH 8.0, and 1mM EDTA). Immunocomplexes were eluted in ChIP elution buffer (1%SDS and 0.1M $NaHCO_3$), crosslinking was reverted by addition of 5M NaCl and incubation at 65°C for at least 4h, and DNA was precipitated with ethanol O/N at -20°C. Samples were then treated with Proteinase K solution (1M Tris-HCl at pH 6.5, 0.5M EDTA and proteinase K 10mg/mL) at 45°C for 2h and DNA purified using QIAquick® PCR Purification Kit (QIAGEN, Hilden, Germany). 10ng purified DNA (SOX11-ChIP and Input from Z138, GRANTA519 and JVM2 cells) were amplified in two steps using a GenomePlex® Whole Genome Amplification WGA Kit (Sigma), following the manufacturer's instructions and used for ChIP-chip analysis and/or ChIP-qPCR. We performed ChIP assays in triplicate from Z138 cell line expressing SOX11 and in a single experiment from JVM2 cell line as negative control.

ChIP-chip analysis

Amplified immunoprecipitated and input DNA (9.5µg) from Z138 and JVM2 cell lines were quality controlled, quantified, and sent to NimbleGen System for probe labeling and hybridization to NimbleGen Human ChIP-chip 2.1M Deluxe Promoter array (Roche NimbleGen, Iceland)

(http://www.nimblegen.com/products/chip/index.html). Raw data were analyzed for peaks (significant regions of SOX11 enrichment) using NimbleScan v2.4 software and data were visualized in SignalMap v1.9 software. Nimblegen software detects peaks using default parameters, by searching for four probes using a 500bp sliding window.

Genomic fragments that overlapped across three independent replicates in Z138 SOX11 ChIP-chip experiments and were not present in the JVM2 SOX11 ChIP-chip experiment were considered SOX11-bound regions. This analysis yielded high confidence genes bound by SOX11 (FDR<0.1 and Peak Score>0.5), which were used to perform GO analysis using Ingenuity Pathway analysis (IPA, Ingenuity® Systems) and DAVID (The Databse for Annotation, Visualization and Integrated Discovery) Bioinformatic Resources (http://david.abcc.ncifcrf.gov/).

Vector constructs

The expression plasmids pcDNA$_3$-SOX11HA and pcDNA$_3$-SOX4HA were generated as previously described.[4] Deletion mutants of SOX11 protein lacking HMG domain (ΔHMGSOX11HA) or C-terminal TAD motif (ΔCtermSOX11HA) were generated by PCR using the QuikChange Kit (Stratagene, La Jolla, CA) reagents and following the manufacturer's instructions with some modifications. pcDNA$_3$-SOX11HA was used as a DNA template and the PCR primers were modified on the 5'-end with a phosphate group: for pcDNA3-ΔHMGSOX11HA, 5'-TCCCGGGGCAGGTTGCTCT-3' (Forward primer) and 5'-GAAAAAGCCCAAAATGGACC-3' (Reverse primer) and for pcDNA3-ΔCtermSOX11HA were 5'-GGTCCATTTTGGGCTTTTTC-3' (Forward primer) and 5'-AACTTCTCCGACCTGGTGTT-3' (Reverse primer). PCR products were treated with DpnI (Stratagene) to degrade the vector template, and purified using QIAquick®

PCR Purification Kit (QIAGEN), following manufacturer's instructions. Cleaned PCR fragments were religated with T4 ligase (Promega, Leiden, The Netherlands), following the manufacturer's instructions. All expression plasmids were sequenced prior to use. Expression plasmids were transiently transfected in HEK293 cell line using Lipofectamine 2000 system (Invitrogen, Carlsbad, CA), following the manufacturer's instructions. The efficiency of expression was assayed by WB experiments using mouse monoclonal anti-HA antibody (12CA5).

SOX11 silencing by lentiviral infection

For lentiviral infections, $1.5x10^6$ exponentially growing MCL target cells (Z138, GRANTA519 and JEKO1), cultured in their corresponding mediums with 10% of FBS and without antibiotics, were mixed with $1x10^5$ infectious units (IFU) of the lentiviral particles and plated on 6 well plates at $0.5x10^6$ cells/mL. Cells were spined for 150min at 2500rpm and 32ºC. After centrifugation, 6mL of complete medium were added to the cells and incubated at 37ºC and 5%CO_2. Infected MCL cells were resuspended in new complete medium with puromycin selection at a final concentration of 0.25mg/mL. The efficiency of the knockdown was assayed by qRT-PCR and WB experiments.

Gene expression profiling analysis

The hybridized arrays were scanned. The analysis of the scanned images and the determination of the signal value for each probe set of the array were obtained with GeneChip® Command Console® Software (AGCC) (Affymetrix). Raw data were imported to R Statistical Package (http://www.r-project.org/) for analysis and data were normalized using the Robust Multichip Analysis (RMA) algorithm of the BioConductor affy Package and genes with *P*-val>0.05 were excluded. Differential gene expression

between Z138shSOX11.1 and shSOX11.3 and Z138shControl.1 and shControl.2 was determined using moderated t-statistics with empirical Bayes shrinkage of the standard errors implemented in the BioConductor limma Package.[5] The FDR controlling method of Benjamini and Hochberg was used to adjust the *P*-val for each gene based on a significance level of 0.05 and log2 FC>0.7. The signatures in these two independent SOX11 silenced MCL cell lines were highly similar (r2= 0.95 taking all the genes covered in the array, and r2=0.99, within the differentially expressed genes).

Gene Set Enrichment Analysis (GSEA)

We performed GSEA on two pre-ranked lists of genes derived from *in vitro* SOX11 silencing microarray data and from our series of 38 purified primary MCL dataset. To generate these pre-ranked lists we analyzed the GEP of our *in vitro* cell line model as well as the GEP of 38 primary MCL according to their SOX11 expression levels.

The top 26,000 genes selected with a greatest InterQuartile Range (IQR) were first ranked with respect to the phenotype, shControl vs shSOX11 and SOX11-positive vs -negative primary tumors, by using *t*-statistic value. With this approach, the final position in the ranked gene lists depended only on the strength of the gene in discriminating between phenotypes. We used 1,000 permutations and a weighted statistic to assess statistical significance.

The query gene sets included gene signatures related to B-cell and plasma cell differentiation programs and apoptotic pathways. The well-defined gene signatures related to the different steps of the mature B-cell and plasma cell differentiation programs, and signatures of genes modulated by PAX5, IRF4, BLIMP1, and XBP1

were obtained from different publications (Table S4 and Table S5), whereas the apoptotic signatures (KEGG_Apoptosis, Biocarta_Fas pathway and caspase 3 pathway) were downloaded from the MSigDB, Molecular Signature Database of Broad Institute.

Additionally, we customized two gene sets derived from our knockdown experiments, SOX11 upregulated and downregulated genes. For this purpose, we considered genes regulated by SOX11 knockdown with log2 FC>0.7 and FDR *P*-val<0.05 for components of SOX11 gene expression signature (Table S3). We also customized two more gene sets derived from microarray data from our series of 38 purified primary MCL, MCL-SOX11+ and MCL-SOX11- genes (Table S4). To generate these gene sets we considered differentially expressed genes between SOX11-positive and negative MCL-primary tumors with log2 FC>0.7 and FDR *P*-val<0.05.

Furthermore, GSEA was also performed on microarray data of MCL patients and SOX11 knockdown experiments dataset to test the enrichment of high confidence SOX11 target genes (PS>0.5 and FDR<0.1, Table S2) among phenotypes. Difference of classes and *t*-Test were used as metric method for ranking genes from SOX11 silencing and MCL patient's dataset respectively and a weighted statistic to assess statistical significance.

XBP-1 splicing

XBP-1 mRNA spliced and unspliced forms were detected by RT-PCR using the protocol and primers previously described.[6] PCR products representing spliced [*XBP1(s)*, 398 base pairs) and unspliced (*XBP1(u)*, 424 base pairs)] were detected on agarose gel.

Cell density assay

Cells of interest were cultured at 0.2 x10^6 cells/mL in complete RPMI or DMEM medium and every 24h cell density was measured in a TC10 System Sample Slide Dual Chamber using the BIO-RAD TC10 Automated Cell Counter (Bio-rad, Hercules, CA).

Proliferation assay

Cells of interest were resuspended in PBS-0.1% BSA at a final concentration of 1x10^6 cells/mL and incubated with serial doubling concentrations of CFSE FITC (CellTrace CFSE Cell Proliferation Kit, Invitrogen) (2.5, 5, 10µM) at 37ºC for 10min. The staining was quenched by adding 5 volumes of ice-cold RPMI to the cells on ice for 5min. Cells were then washed three times in fresh RPMI, and cultured for five days at 37ºC under a 5%CO_2 atmosphere at a cell density of 0.2 x10^6 cells/mL. Every 24h, 500,000 cells were collected and analyzed using the Attune Accoustic Focusing Cytometer and Software (Applied Biosystems, Foster City, CA). For the analysis, 10,000 events were collected in the lymphocyte gate.

Cell cycle

Cells of interest at a final concentration of 1x10^6 cells/mL were stained with DyeCycle Violet (Invitrogen) for 30min at 37ºC in the dark and acquired and analyzed using the Attune Acoustic Focusing Cytometer and Software (Applied Biosystems). For the analysis, 10,000 events were collected in the lymphocyte gate, and cell cycle was analyzed every 24h.

Apoptosis assay

Cells were cultured at 0.2 x10^6 cells/mL in complete RPMI or DMEM medium for five days, and every 24h cell viability was analyzed. Cells of interest were resuspended in annexinV-binding buffer at a final concentration of 1x10^6 cells/mL and stained with annexin-V-FITC (eBioscience, San Diego, CA) for 15min at 4ºC in the dark. After washing the cells twice with annexinV-binding buffer, Propidium Iodide (PI) was added to the cell suspension, and cells were acquired and analyzed using the Attune Acoustic Focusing Cytometer and Software (Applied Biosystems). For the analysis, 10.000 events were collected in the lymphocyte gate.

Quantitative chromatin immunoprecipitation of histone marks

Chromatin immunoprecipitation (ChIP) experiments were performed as previously described [4] using LowCell ChIP kit (Diagenode; Liege, Belgium) according to manufacturer's instructions with the following antibodies: H3K9/14Ac, H3K4me3 (Diagenode). A rabbit IgG (Diagenode) was used as a negative control.

Immunoprecipitated DNA and 1:100 diluted input samples were analyzed in triplicate by quantitative real-time PCR analyses using Fast SYBR ®Green Master Mix in a StepOnePlus PCR detection system (Applied Biosystems). The primers for the *SOX11* gene promoter region are: SOX11prom_Forward: 5'-GAGAGCTTGGAAGCGGAGA-3' and SOX11prom_Reverse: 5'-AGTCTGGGTCGCTCTCGTC-3'.

II. SUPPLEMENTAL FIGURES

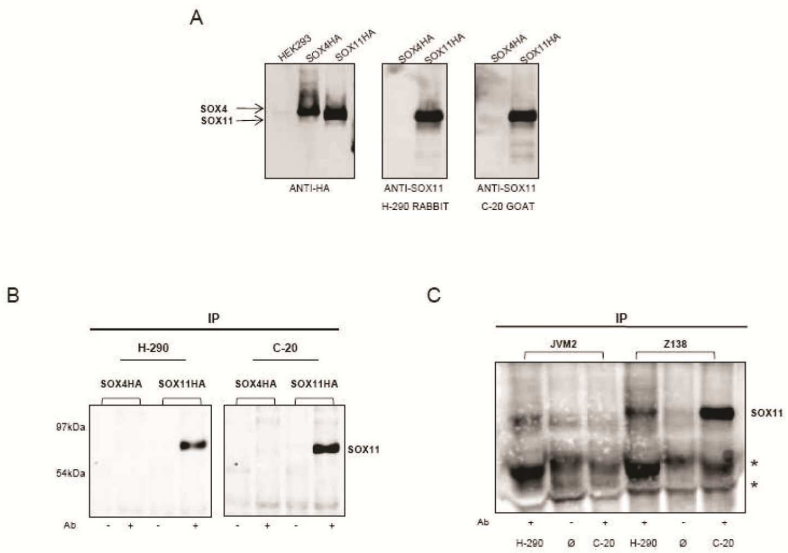

Figure S1. SOX11 antibody for Chromatin Immunoprecipitation (ChIP).

(A) The specificity of different polyclonal antibodies against SOX11 was tested by WB analysis in HEK293 cells transfected with vectors encoding for SOX4HA, SOX11HA proteins and with the empty vector pcDNA3.1 as a control (HEK293). 24h after transfection, cells were collected and protein extracts were subjected to immunoblotting with the indicated antibodies: (left panels) against Hemagglutinin epitope tagged (HA) (mouse monoclonal anti-HA, 12CA5) to detect SOX4HA and SOX11HA proteins and (right panel) against SOX11 (the polyclonal rabbit H-290 and the polyclonal goat C-20 anti-SOX11 antibodies).

(B) Immunoprecipitation (IP) of SOX11 protein was performed using HEK293 cells expressing SOX4HA or SOX11HA proteins and two different antibodies (H-290 and C-20 anti-SOX11 antibodies) (+). Control rabbit IgG was used as a negative control (-).

The efficiency and specificity of these antibodies to immunoprecipitate SOX11 were tested by WB using the anti-HA antibody.

(C) The efficiency of the indicated SOX11 antibodies H-290 and C-20 (+) to IP SOX11 in MCL cell lines was tested by IP-WB experiments in Z138 and JVM2 cell lines. Control rabbit IgG was used as a negative control (Ø) (-). The presence of immunoprecipitated SOX11 was determined by WB using the rabbit polyclonal anti-SOX11 antibody (HPA000536), that detects SOX4 and SOX11 proteins. * Non-specific bands.

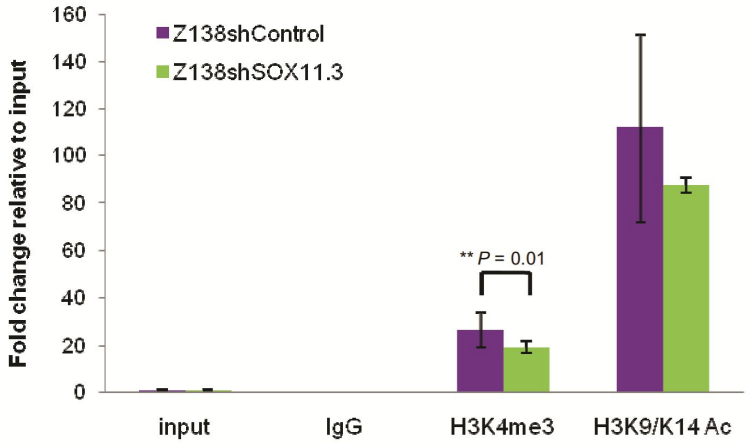

Figure S2. Enrichment of activating chromatin marks in *SOX11* promoter after SOX11-silencing in MCL Z138 cell line. Enrichment of H3K4me3 and H3K9/K14Ac active chromatin marks in *SOX11* promoter in Z138shControl and Z138shSOX11.3 MCL cell lines. A rabbit IgG was used as a ChIP negative control. The values are relative to 1:100 diluted input samples.

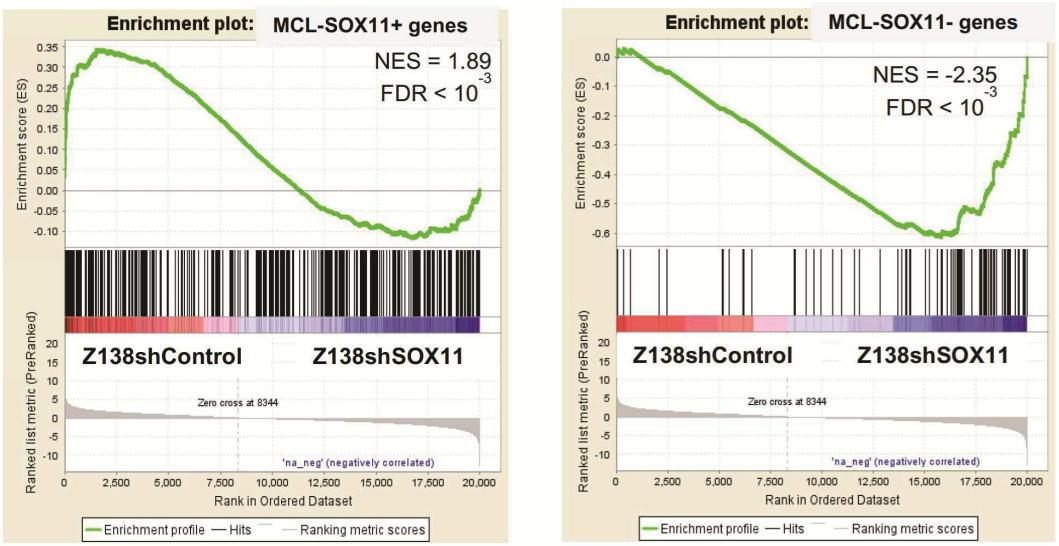

Figure S3. Z138shControl and Z138shSOX11 *in vitro* model cell lines show a significant enrichment in the clinical MCL GE markers. We generated two gene sets derived from the microarray expression data of SOX11-positive and negative MCL primary tumors (MCL-SOX11+ and MCL-SOX11- genes) (Table S4) and performed a GSEA on the *in vitro* pre-ranked list showing that (Left) Z138shControl had a GEP significantly enriched in SOX11-positive primary MCL genes whereas (Right) Z138shSOX11 presented a GEP enriched in SOX11-negative primary MCL genes. NES and FDR *P*-values are shown. Statistical significance is considered when FDR<0.05.

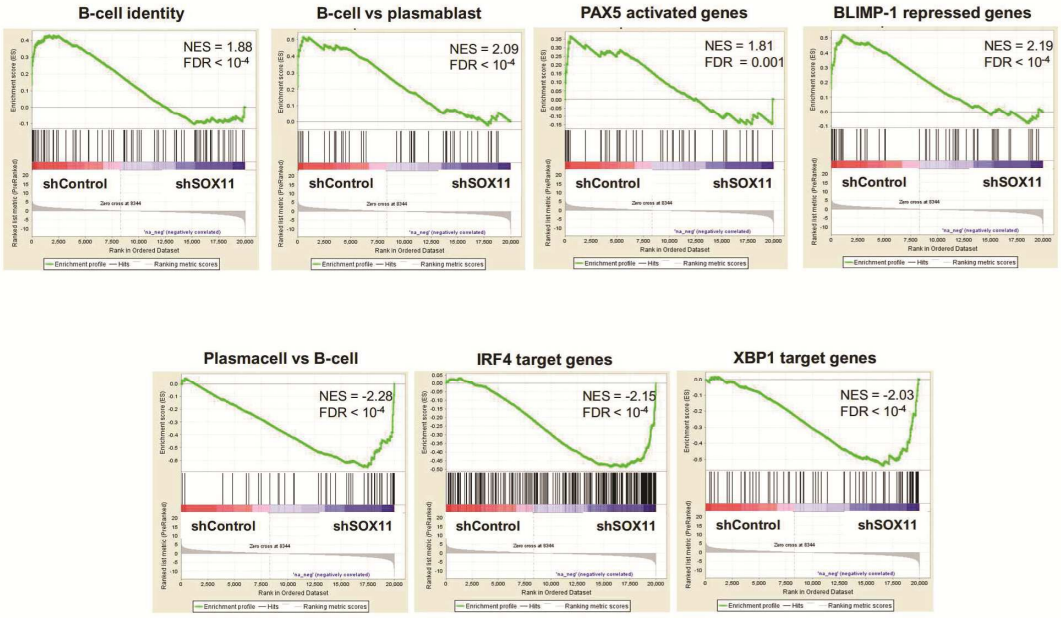

Figure S4. Shift from a mature B-cell to a plasmacytic gene expression program in SOX11-knockdown MCL cells. GSEA on the *in vitro* pre-ranked list showing that Z138shControl cells were significantly enriched in gene signatures related to the B-cell program (B-cell identity, B-cell vs plasmablast, PAX5 activated genes and BLIMP1 repressed genes) whereas gene signatures related to the plasma cell program (Plasmacell vs B-cell, IRF4 target genes and XBP1 target genes) were significantly enriched in shSOX11 cells. NES and FDR *P*-values are shown. Statistical significance is considered when FDR<0.05.

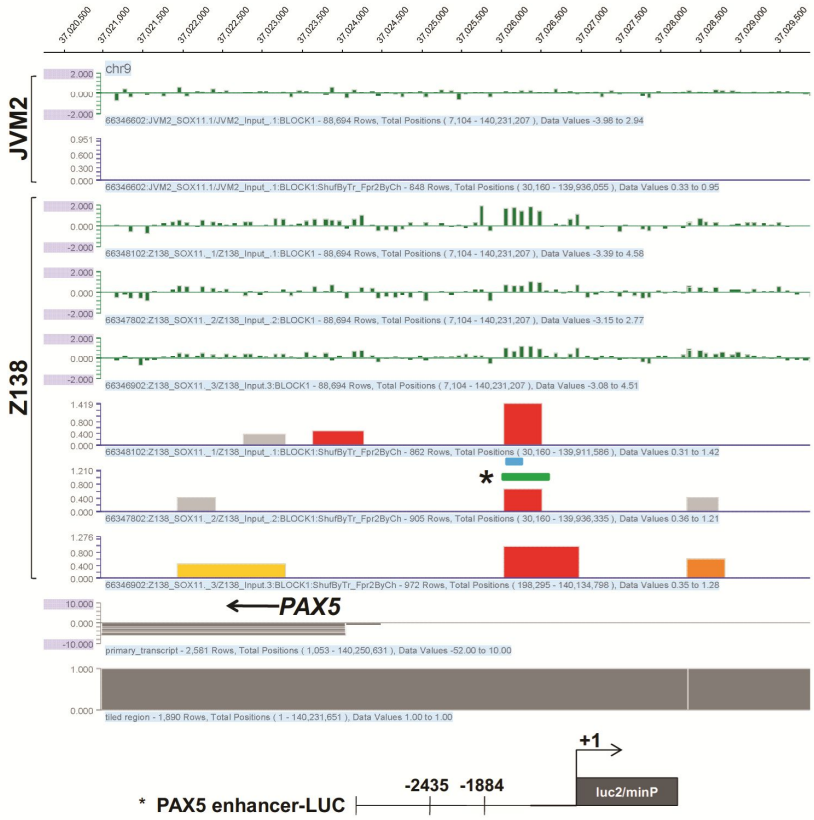

Figure S5. SignalMap representation of SOX11 binding at the *PAX5* promoter-enhancer site. SOX11 binding site at the promoter of *PAX5* by triplicates in Z138 MCL cell line. Green bars represent fluorescent intensity of probe around *PAX5* promoter region expressed as log2 ratio and red bars show high confidence peaks using Nimblescan peak finding algorithm. Position of gene transcripts and the region tiled on the array (from 5kb upstream to 1kb downstream of the TSS) are indicated at the bottom panels, in grey. The blue bar below the red peak indicates the SOX11 binding region validated by ChIP-qPCR, and the green asterisked bar identifies high confidence peaks within sequences of *PAX5* cloned at the luciferase reporter construct. The scale at the top of the panel indicates the base pair position on chromosome 9. No peaks at the promoter-enhancer site of *PAX5* in JVM2 MCL cell line were observed.

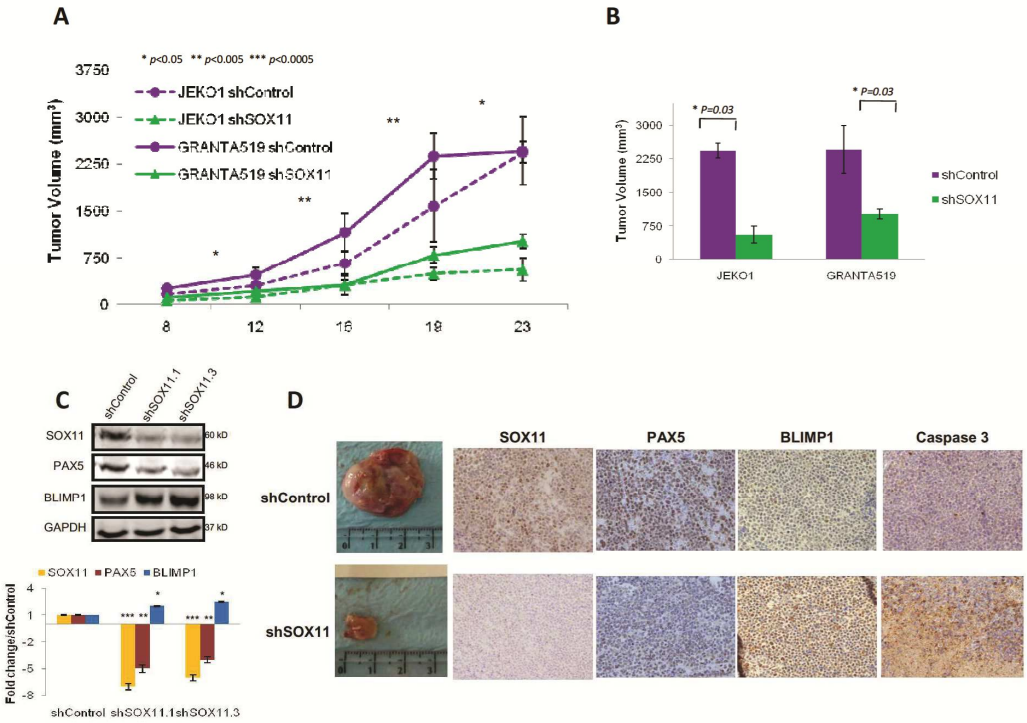

Figure S6. SOX11 inhibits the growth of MCL cell lines-derived tumors in SCID mice.

(A) JEKO1 and GRANTA519 stably transduced with shSOX11.3 and shControl (10^7cells/mouse) were subcutaneously inoculated into the right flank of CB17-SCID mice. Tumor growth was measured using a caliper at the indicated days Post Inoculation (PI).

(B) Tumor volume (mm^3) of JEKO1shSOX11.3 (n=5), GRANTA519shSOX11.3 (n=5), JEKO1shControl (n=5) and GRANTA519shControl (n=5) cells at day 23 PI into the lower dorsum of CB17-SCID mice.

(C) (Upper panel) SOX11, PAX5 and BLIMP1 expression levels in JEKO1 stably transduced with shControl, shSOX11.1 or shSOX11.3 assessed by WB, using GAPDH

as a loading control. (Lower panel) Fold differences compared to control cells are shown of SOX11, PAX5 and BLIMP1 protein expression levels. Protein quantification was done with Image Gauge software, and SOX11, PAX5 and BLIMP1 expression levels were corrected by quantification of GAPDH expression levels.

(D) Macroscopic appearance and consecutive histological sections from representative shSOX11 and shControl derived tumors stained with specific antibodies anti-human SOX11, PAX5, BLIMP1 and activated caspase-3 (x20). shSOX11 tumors show extensive necrotic areas that are minimal in shControl tumors. Necrotic areas are highlighted by the immunostaining for activated caspase-3 (x20).

Bar plot represents the mean percentage ±SD. *P*-val are shown. The significance of difference was determined by independent samples *t*-test.

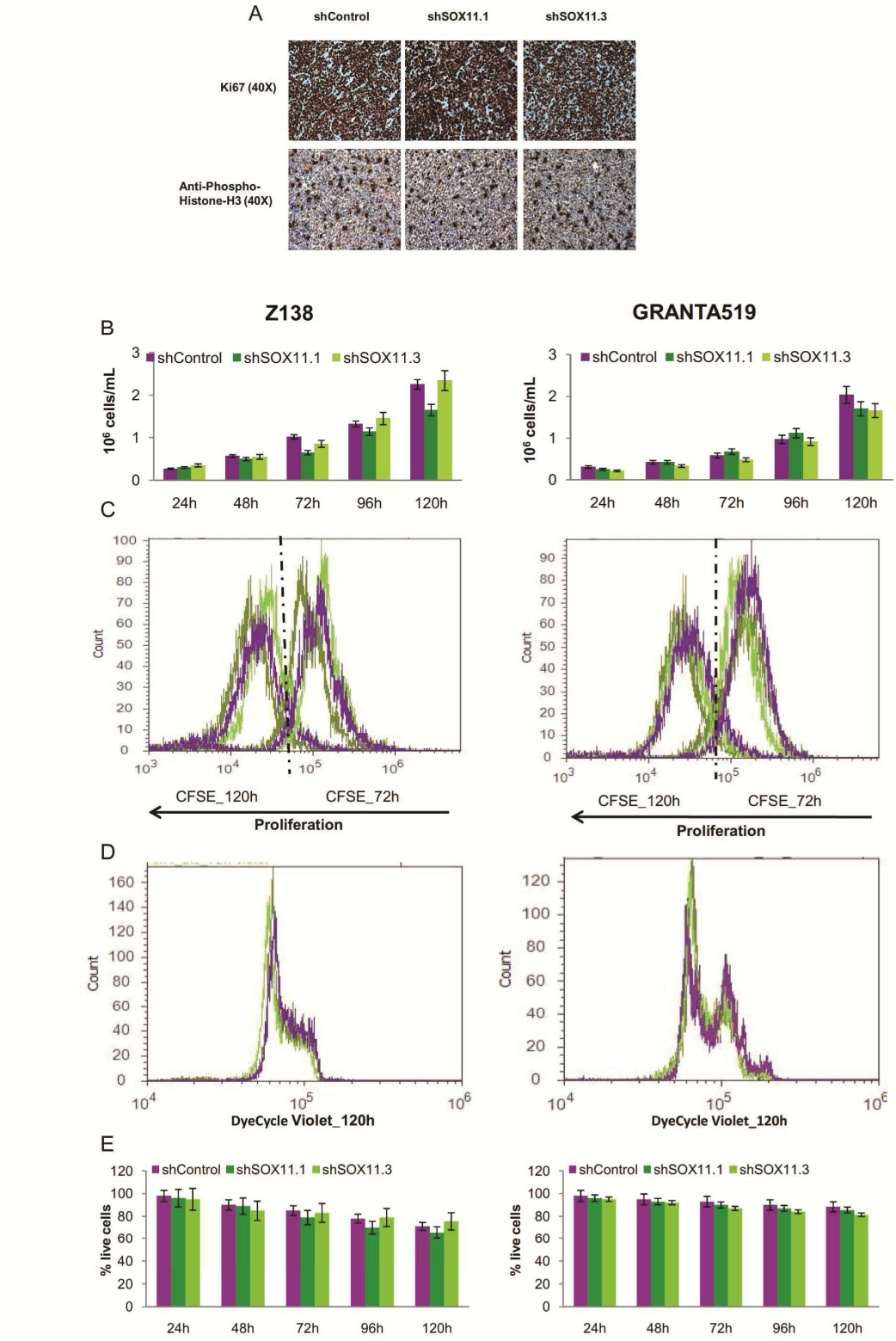
A
shControl
shSOX11.1
shSOX11.3
Ki67 (40X)
Anti-Phospho-Histone-H3 (40X)
Z138
GRANTA519
B
shControl shSOX11.1 shSOX11.3
10⁶ cells/mL
24h 48h 72h 96h 120h
C
Count
CFSE_120h
CFSE_72h
Proliferation
D
Count
DyeCycle Violet_120h
E
% live cells

Figure S7. SOX11 knockdown has no effect on cell proliferation, cell cycle and cell viability in MCL.

(A) Consecutive histological sections from representative shSOX11 and shControl tumors stained with human specific antibodies anti-Ki67 and phospho-histone-H3 (x40). No differences in proliferation index were observed.

(B) Cell density of Z138 and GRANTA519 growing cells stably transduced with shSOX11.1, shSOX11.3 or shControl every 24h at the indicated time points.

(C-E) Flow cytometry analysis on growing Z138 and GRANTA519 cells stably transduced with shSOX11.1, shSOX11.3 or shControl (C) stained with doubling concentrations of CFSE measuring cell proliferation at 72 and 120h (D) stained with DyeCycle Violet measuring cell cycle at 120h, and (E) stained with annexin-V analyzing cell viability at the indicated time points.

No differences in cell proliferation, cell cycle phases or cell viability were seen between the samples.

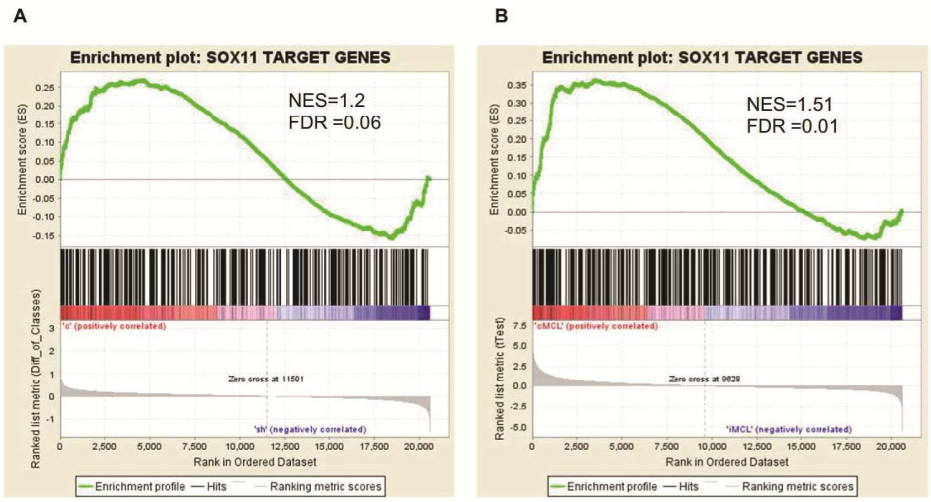

Figure S8. SOX11-bound high confidence genes are significantly enriched in the SOX11-positive MCL primary cases and Z138shControl MCL cell lines microarray data. GSEA on the primary tumors and MCL cell line dataset was performed using the SOX11 high confidence target genes derived from ChIP-chip as a gene signature. Enrichment of SOX11-bound genes was shown in both Z138shControl (A) and SOX11 positive MCL primary cases (B). NES and FDR *P*-values are shown. Statistical significance is considered when FDR<0.1.

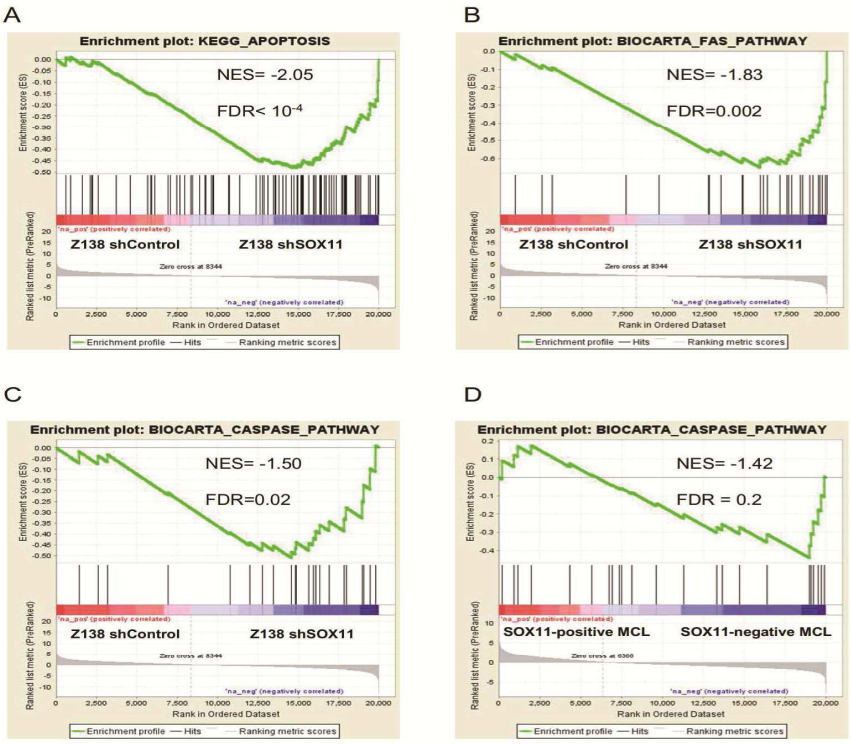

Figure S9. SOX11 regulates the expression of pro-apoptotic genes in MCL cell lines and primary cases. GSEA analysis performed on pre-ranked lists derived from the microarray expression data of SOX11-positive and negative MCL primary tumors and of SOX11-modulated Z138 cell lines. Graphs show a significant enrichment of (A – C) Fas, apoptosis and caspase pathway on Z138shSOX11cell lines and of (D) caspase pathway on SOX11-negative MCL tumors. Gene sets were downloaded from the MSigDB (Molecular Signature Database of Broad Institute). NES and FDR *P*-values are shown. Statistical significance is considered when FDR≤0.2.

III. SUPPLEMENTAL TABLES

Table S1. Oligonucleotides used for ChIP-qPCR, luciferase assay and qRT-PCR experiments.

Gene	Primer sequence	Annealing temperature	Expected size	Experiment
PAX5	Forward 5'-TAATCCTCTGCCCTTCATGG-3'	63.9 °C	247bp	ChIP-qPCR
	Reverse 5'-TGTTGCCTTAGGGAATTTCG-3'	63.7 °C		
MSI2	Forward 5'-CAAAAACAAAACAGAATAACAACAGA-3'	61.9 °C	232bp	ChIP-qPCR
	Reverse 5'-GACAAAATCCAGAAGGGAATG-3'	62.2 °C		
SEPT-2	Forward 5'-AGCAGGGGGTAGGGTATAGG-3'	62.9 °C	123bp	ChIP-qPCR
	Reverse 5'- GGTTTGTCTGGGCCAGTAGG-3'	65.6 °C		
SUV39H2	Forward 5'-GTCAGTGAAATCTTTTTCTGCAT-3'	61.1 °C	129bp	ChIP-qPCR
	Reverse 5'-GCAAAGGAAATGCTCTTTGAA-3'	63.1 °C		
HSPD1	Forward 5'-CGCGGTGAAAGATTAACTCG-3'	64.5 °C	130bp	ChIP-qPCR
	Reverse 5'-AGCCACTAGCGCAAGCTAAA-3'	63.9 °C		
PAX5	Forward 5'-CCGCTCGAGTAATCCTCTGCCCTTCATGG-3´	76.1 °C	552bp	Luciferase assay
	Reverse 5'-CCCAAGCTTTGTTTCCATTTAGAGGGCTTG-3'	72.3 °C		
SOX11	Forward 5'-CATGTAGACTAATGCAGCCATTGG-3´	62.9 °C	87bp	qRT-PCR
	Reverse 5'-CACGGAGCACGTGTCAATTG-3´	63.7 °C		

Table S2. SOX11-bound genes

	Z138.1		Z138.2		Z138.3	
Gene Name	**PEAK_SCORE**	**PEAK_FDR**	**PEAK_SCORE**	**PEAK_FDR**	**PEAK_SCORE**	**PEAK_FDR**
AANAT	0.542484	0.01588	0.526241	0.12084	0.576247	0.06777
ABCA1	0.647087	0.00232	0.508007	0.14672	0.448938	0.13502
ABCC12	0.46583	0.05078	0.501408	0.14672	0.428169	0.16693
ABCG2	0.649976	0.00462	0.524316	0.14672	0.848306	0.00287
ABT1	0.547067	0.023	0.38951	0.1565	0.640747	0.00764
ACAA2	0.367901	0.13555	0.49685	0.08005	0.761159	0.00471
ACOT1	0.460775	0.05942	0.551733	0.09619	0.767168	0.00471
ACPT	0.632137	0.003	0.678784	0.06407	0.389119	0.18703
ACSS2	0.38131	0.09315	0.588507	0.08274	0.645064	0.05558
ACTG1	0.876321	0	0.837202	0.004	0.912391	0.00153
ACVRL1	0.529323	0.03147	0.415837	0.19063	0.698189	0.01824
ADAMTS10	0.800707	0.00034	0.460603	0.07182	0.753918	0.01005
ADAMTS13	0.60534	0.00462	0.508007	0.14672	0.496195	0.13433
ADAR	0.974867	0	0.647538	0.03938	0.96131	0.0004
ADCK2	0.40754	0.13719	0.482054	0.17949	0.539108	0.08735
ADORA1	0.445048	0.0798	0.527624	0.12084	0.562718	0.06777
AFG3L2	0.519389	0.01404	0.49685	0.14672	0.50744	0.10837
AGMAT	0.466241	0.05942	0.671521	0.02999	0.562718	0.06777
AHNAK	0.503453	0.03147	0.490274	0.17949	0.599322	0.05287
AHR	1,051,025	0	0.964108	0.00094	0.609426	0.04211
AK1	0.480097	0.02176	0.677343	0.02999	0.803363	0.00384
ALK	0.452757	0.0798	0.463763	0.03644	0.567579	0.06777
ALOX12B	0.438161	0.06849	0.717602	0.04075	0.768329	0.02547
AMIGO2	0.396992	0.17587	0.513681	0.14672	0.505585	0.13433
AMZ2	0.47989	0.04302	0.526241	0.10562	0.888381	0.16
ANK1	0.512111	0.03147	0.5123	0.08005	0.449553	0.19866
ANKRD15	0.521845	0.023	0.459626	0.14849	0.496195	0.13433
ANKRD20A1	0.480097	0.04302	0.60477	0.0636	0.614336	0.04211

ANKRD20A3	0.375728	0.17587	0.628961	0.04899	0.590708	0.02929
ANKRD53	0.517436	0.01404	0.707849	0.02218	0.591228	0.05287
ANP32A	0.759332	0.00044	0.503218	0.14672	0.586613	0.05287
ANXA2	0.569499	0.00292	0.455292	0.12597	0.7274	0.0012
AOF2	0.487434	0.04302	0.503641	0.14672	0.586165	0.02929
AP1M2	0.358211	0.13555	0.53333	0.12084	0.437759	0.16693
AP4B1	0.38147	0.12426	0.479658	0.17949	0.515825	0.10837
APBB2	0.515498	0.02176	0.574251	0.04939	1,017,968	0.00047
APBB3	0.690571	0.00159	0.507962	0.14672	0.959727	0.0004
APCDD1	0.584313	0.00292	0.733445	0.01098	0.599701	0.04211
APEX1	1,193,827	0	0.59971	0.0636	1,348,356	0
APOA2	0.339084	0.14501	0.575589	0.07797	0.515825	0.10837
APOB	0.883953	0	0.707849	0.02218	0.80407	0.00384
AQP3	0.375728	0.12426	0.653152	0.03938	0.519823	0.10837
ARHGAP17	0.708871	0.00062	0.549161	0.09619	0.547104	0.08735
ARHGAP9	0.529323	0.03147	0.684908	0.02999	0.577812	0.06777
ARHGEF18	0.463567	0.05942	0.484845	0.17949	0.462079	0.19866
ARHGEF2	1,207,988	0	0.647538	0.01536	1,219,222	0
ARHGEF5	0.772182	0.00044	0.843594	0.004	0.632866	0.03233
ARID3B	1,202,276	0	0.575106	0.07797	1,032,439	0.00069
ARID5B	0.857061	0	0.514658	0.14672	0.357267	0.10793
ARL16	0.47989	0.04302	0.502321	0.14672	0.528226	0.10837
ARL3	0.942767	0	0.49015	0.17949	0.762171	0.00693
ARNTL2	0.81604	0.00049	0.464759	0.07182	0.553736	0.09489
ARPC2	0.668355	0.00232	0.488172	0.10098	0.733122	0.01005
ARPM1	0.835632	0	0.481594	0.17949	0.445738	0.08849
ATF3	0.720554	0.00087	0.503641	0.14672	0.679951	0.01824
ATG4C	0.99606	0	0.671521	0.02999	0.726844	0.0012
ATP12A	0.39629	0.17587	0.443214	0.15876	0.544573	0.08735
ATP1A2	0.339084	0.15404	0.575589	0.07797	0.539271	0.08735
ATP1B1	0.529819	0.023	0.359743	0.19837	0.539271	0.08735

ATP2B4	0.656976	0.00232	0.647538	0.03938	0.750291	0.00693
ATP5G2	0.419048	0.09315	0.415837	0.19063	0.457434	0.19866
ATP5J2	0.750732	0.11016	0.482054	0.17949	0.468789	0.10845
ATP6V1G1	1,043,689	0	0.677343	0.02999	1,086,903	0
ATP6V1G2	0.612715	0.00745	0.438199	0.16507	0.545821	0.08735
ATXN2L	0.668364	0.00134	0.573037	0.07797	0.523317	0.10837
AUTS2	0.536237	0.023	0.506157	0.14672	0.468789	0.16574
AVPR1B	0.656976	0.00232	0.791435	0.00608	0.586165	0.05287
AXIN2	0.667673	0.00159	0.526241	0.12084	0.600257	0.05287
AZI1	0.438161	0.0798	0.621922	0.04899	0.576247	0.06777
B3GALNT2	1,229,180	0	0.671521	0.02999	0.89097	0.00153
B3GALT3	0.642794	0.003	0.529753	0.06249	0.633417	0.03233
B3GNT4	0.352882	0.15404	0.660447	0.06484	0.505585	0.12085
B4GALNT1	0.463158	0.06849	0.807213	0.00608	0.457434	0.14113
BAG5	0.649274	0.00232	0.575722	0.07797	0.627683	0.03233
BAT4	0.700246	0.00159	0.413854	0.19063	0.498359	0.08288
BAT5	0.547067	0.00206	0.511232	0.08005	0.640747	0.03233
BCL2	1,038,779	0	0.615148	0.06839	1,199,403	0
BCL6	0.66422	0.00232	0.650152	0.03938	0.656877	0.01041
BCORL1	0.723885	0.00087	0.568632	0.09619	0.404421	0.10578
BIN2	0.595489	0.0242	0.587064	0.07797	0.74634	0.01005
BLOC1S1	0.485213	0.05942	0.415837	0.1824	0.650038	0.03233
BLVRA	0.664934	0.00232	0.578465	0.00957	0.468789	0.01215
BMF	0.527314	0.00932	0.575106	0.03811	0.703936	0.00474
BNC2	0.626213	0.003	0.556389	0.09619	0.543451	0.08735
BRAF	1,308,419	0	0.819492	0.00481	0.867261	0.00193
BRD2	1,466,141	0	0.657298	0.01536	1,281,494	0
BRI3	0.42899	0.10476	0.506157	0.14672	0.609426	0.0666
BRP44	1,080,831	0	0.695504	0.02218	0.844077	0.00196
BRUNOL4	0.389542	0.12426	0.567829	0.03811	0.55357	0.06777
BSG	0.842849	0	0.727268	0.01656	0.632319	0.04211

BTG2	0.720554	0.00087	0.74347	0.01098	0.914417	0.00149
BYSL	0.56895	0.01588	0.438199	0.16507	0.640747	0.03233
BZRAP1	0.938915	0	0.598001	0.0292	0.81635	0.00384
C10orf77	0.621369	0.00462	0.514658	0.01263	0.476357	0.16574
C12orf22	0.749875	0.00087	0.73383	0.01656	0.650038	0.03233
C12orf24	0.419048	0.09315	0.562603	0.09456	0.409283	0.17011
C12orf30	0.77193	0	0.366915	0.19837	0.770416	0.00079
C12orf47	0.86015	0	0.758291	0.01098	0.818566	0.00384
C12orf5	0.396992	0.17587	0.366915	0.19837	0.505585	0.13433
C12orf52	0.948371	0	0.587064	0.07797	0.866717	0
C12orf62	0.705764	0.00159	0.48922	0.17949	0.577812	0.06777
C13orf18	1,034,758	0	1,108,035	0	1,018,114	0.00057
C14orf132	0.376998	0.17587	0.383815	0.11173	0.46495	0.16574
C14orf159	0.397942	0.13719	0.479768	0.10098	0.418455	0.16693
C14orf166B	0.607386	0.00462	0.671675	0.06407	0.581188	0.05287
C15orf20	0.421851	0.10476	0.575106	0.07797	0.492755	0.13433
C15orf23	0.569499	0.00292	0.503218	0.14672	0.539684	0.05038
C15orf27	0.421851	0.10476	0.527181	0.12084	0.469291	0.16574
C15orf38	0.548407	0.01588	0.527181	0.12084	0.868188	0.00193
C16orf47	0.364562	0.17587	0.573037	0.08746	0.451956	0.19866
C17orf49	0.938915	0	0.478401	0.17949	0.86437	0.00196
C17orf81	0.500755	0.03147	0.406641	0.19063	0.504216	0.13433
C18orf21	0.865649	0	0.544169	0.04939	0.55357	0.06777
C18orf4	1,514,886	0	1,372,253	0	1,568,450	0
C19orf18	1,137,846	0	0.775753	0.00771	1,240,317	0
C19orf2	0.442496	0.0798	0.557572	0.09619	0.583679	0.06777
C19orf37	0.674279	0.00159	0.53333	0.06249	0.705279	0.01824
C1orf115	0.529819	0.00932	0.671521	0.01102	0.586165	0.05287
C1orf131	0.466241	0.05942	0.407709	0.19063	0.656504	0.0234
C1orf14	0.360277	0.13555	0.527624	0.12084	0.445485	0.19866
C1orf174	0.61459	0.00462	0.503641	0.08005	0.468932	0.10845

C1orf38	0.402663	0.10286	0.695504	0.02218	0.703397	0.01325
C1orf66	0.953675	0	0.527624	0.12084	0.703397	0.01325
C20orf18	0.782689	0	0.635588	0.03938	0.529874	0.05038
C20orf91	0.461586	0.04302	0.635588	0.00642	0.437722	0.19866
C21orf124	0.53275	0.01588	0.414706	0.12725	0.421054	0.15516
C2orf10	0.409637	0.09315	0.414946	0.19063	0.614877	0.04211
C2orf31	0.409637	0.13719	0.536989	0.12084	0.709473	0.01325
C3orf60	0.407103	0.13719	0.577913	0.07797	0.492658	0.13433
C6orf21	0.547067	0.00206	0.511232	0.08005	0.640747	0.03233
C6orf32	0.634598	0.00462	0.486887	0.17949	0.640747	0.0152
C6orf47	0.700246	0.00159	0.413854	0.19063	0.498359	0.08288
C7orf24	0.471889	0.05942	0.506157	0.14672	0.656305	0.0234
C7orf34	0.471889	0.05942	0.602567	0.0636	0.656305	0.0234
C8orf33	0.405421	0.13719	0.609882	0.0636	0.662499	0.0234
C9orf100	0.396602	0.13719	0.508007	0.14672	0.56708	0.06777
C9orf66	0.313107	0.18102	0.483816	0.10098	0.448938	0.13502
C9orf76	1,419,417	0	0.846679	0.004	1,228,672	0
CABIN1	0.747756	0.00034	0.536373	0.09619	0.664005	0.01824
CABP1	0.573434	0.18827	0.464759	0.12597	0.577812	0.06777
CACNA1S	0.508626	0.03147	0.503641	0.14672	0.445485	0.19866
CACNB4	0.452757	0.0798	0.585806	0.03811	0.567579	0.06777
CALB1	0.384084	0.17587	0.5123	0.14672	0.70982	0.01325
CALCA	0.356612	0.15726	0.612842	0.0636	0.575349	0.01664
CALM2	0.883953	0	0.488172	0.17949	0.591228	0.0129
CAMK2D	1,008,584	0	0.649153	0.04899	0.751357	0.01005
CANT1	0.396431	0.13719	0.574081	0.07797	0.456195	0.19866
CASC1	0.926316	0	0.587064	0.07797	0.625963	0.04211
CBWD1	1,034,872	0	0.805484	0.00608	0.779734	0.00471
CBWD2	1,034,872	0	0.805484	0.00608	0.614877	0.00796
CBWD3	1,001,941	0	0.556389	0.09619	0.779734	0.00471
CBWD5	0.709709	0	0.725725	0.01656	0.779734	0

CBX4	0.459025	0.01721	0.478401	0.05974	0.792339	0.00101
CCBL1	1,127,184	0	0.628961	0.04899	1,275,929	0
CCDC47	0.709403	0.00087	0.478401	0.17949	0.648278	0.03233
CCDC50	1,114,176	0	0.577913	0.07797	0.844556	0.00196
CCDC63	0.485213	0.03375	0.48922	0.17949	0.529661	0.10837
CCDC97	1,432,844	0	0.921206	0.00121	1,215,998	0
CCM2	0.750732	0.00672	0.433849	0.16507	0.562547	0.06777
CCNA1	0.462338	0.0798	0.664821	0	0.56825	0.06777
CCR6	0.415771	0.13719	0.511232	0.14672	0.569553	0.06777
CD109	0.56895	0.00477	0.632953	0.01902	0.593284	0.02929
CD1D	0.805325	0.00034	0.479658	0.17949	0.609611	0.04211
CD300E	0.52162	0.023	0.526241	0.03306	0.528226	0.10837
CD302	0.668355	0.00064	0.536989	0.06249	0.52028	0.06541
CD37	0.695351	0.00134	0.630299	0.06839	0.462079	0.19866
CD46	0.529819	0.023	0.623555	0.04899	0.797184	0.00384
CD86	0.814206	0	0.481594	0.17949	0.516118	0.06541
CDC37L1	0.960194	0	0.508007	0.14672	0.779734	0.00471
CDC42SE1	0.868903	0	0.527624	0.06249	0.867523	0
CDC6	1,105,834	0	0.478401	0.17949	0.696298	0.01824
CDCP1	0.514235	0.01404	0.481594	0.17949	0.539578	0.08735
CDH6	0.474768	0.05942	0.507962	0.14672	0.538383	0.08735
CDH7	0.71416	0.00134	0.851743	0.00257	0.853421	0
CDK5RAP2	0.563592	0.00292	0.435435	0.15876	0.543451	0.08735
CDK6	0.85798	0	0.506157	0.14672	0.679745	0.01824
CDKN1B	1,323,308	0	1,027,362	0	1,227,850	0
CENPF	0.76294	0.00044	0.551606	0.09619	0.562718	0.03751
CENTA2	0.375566	0.12426	0.526241	0.12084	0.624267	0.04211
CEP68	0.862394	0	0.488172	0.10098	0.591228	0.05287
CHD3	0.688538	0.00134	0.574081	0.03811	0.528226	0.00544
CHD9	0.607604	0.003	0.477531	0.17949	0.761189	0.00693
CHIT1	0.529819	0.0031	0.551606	0.02276	0.586165	0.05287

CHRM2	0.450439	0.02839	0.506157	0.08005	0.492229	0.08288
CITED1	0.85163	0	0.420293	0.19063	0.808843	0.00384
CLDN7	0.375566	0.12426	0.454481	0.12597	0.456195	0.19866
CLEC4C	0.485213	0.05942	0.587064	0.07797	0.674114	0.05558
CLIC1	1,028,487	0	0.77902	0.00771	0.972986	0.0004
CLK2	0.635783	0.003	0.599572	0.0636	0.492378	0.08288
CLNS1A	0.713225	0.00087	0.563815	0.09619	0.527403	0.10837
CLYBL	0.726532	0.00134	0.517083	0.08005	0.544573	0.09489
CMPK	0.699361	0.00134	0.503641	0.14672	0.679951	0.01824
CMTM1	0.364562	0.17587	0.405901	0.12725	0.689827	0.00711
CNOT6L	0.739628	0	0.524316	0.14672	0.557458	0.08735
CNTN2	0.551012	0.01588	0.575589	0	0.445485	0.13502
CNTNAP2	0.579136	0.00292	0.482054	0.10098	0.468789	0.16574
CNTNAP3	0.60534	0.00462	0.725725	0.01656	0.590708	0.05287
COG1	0.563349	0.011	0.430561	0.15876	0.792339	0.00471
COL18A1	0.430298	0.0798	0.658651	0.03938	0.467838	0.16574
COL1A2	0.536237	0.0031	0.62667	0.00965	0.421911	0.07991
COL23A1	0.496348	0.04302	0.55634	0.09619	0.444751	0.19866
COL27A1	1,064,563	0	0.991824	0	0.850619	0.00196
COL5A3	1,032,490	0	1,042,418	0	1,191,678	0
COPZ1	0.595489	0.011	0.562603	0.09456	0.553736	0.08735
COQ10A	0.573434	0.18827	0.415837	0.1824	0.409283	0.17011
COX4I1	0.364562	0.17587	0.405901	0.19063	0.451956	0.19866
CPNE2	0.445576	0.00805	0.358148	0.14041	0.49953	0.08288
CR1L	0.61459	0.00462	0.695504	0.02218	0.468932	0.10845
CREB3	0.730582	0.00062	0.459626	0.12597	0.685221	0.01824
CREB3L3	0.358211	0.13555	0.581815	0.08746	0.486399	0.16574
CRH	0.426759	0.06808	0.683067	0.02999	0.591517	0.05287
CRIP2	0.607386	0.00462	0.359826	0.14041	0.65093	0.01041
CRK	0.438161	0.06849	0.478401	0.17949	0.384165	0.18703
CROP	0.52162	0.00932	0.406641	0.1824	0.504216	0.13433

CS	0.330827	0.18102	0.48922	0.10098	0.577812	0.06777
CSNK2B	0.700246	0.00159	0.413854	0.19063	0.498359	0.08288
CSPG4LYP1	0.491299	0.04302	0.428276	0.1565	0.592043	0.06777
CTHRC1	0.405421	0.13719	0.536696	0.03091	0.520535	0.03168
CTNNA1	0.668991	0.01019	0.435396	0.16507	0.514975	0.10837
CUEDC1	0.47989	0.05078	0.526241	0.10562	0.792339	0.0269
CUTA	0.80966	0	0.681642	0.02999	0.735672	0.01005
CX36	0.485129	0.02176	0.69492	0.02218	0.539684	0.08735
CXCR4	0.754594	0	0.366129	0.19837	0.709473	0.00474
CYB5D1	0.417296	0.10476	0.526241	0.12084	0.720309	0.01325
CYB5R3	0.413233	0.0798	0.559694	0.07797	0.641109	0.0234
CYFIP1	0.400759	0.13719	0.599069	0.0292	0.469291	0.10845
DARC	0.317892	0.18102	0.695504	0.02218	0.468932	0.10845
DAXX	1,181,666	0	0.77902	0.00771	1,044,180	0.00069
DBNDD2	0.602069	0.03147	0.423725	0.16507	0.437722	0.19866
DCXR	0.605079	0.00462	0.526241	0.12084	0.576247	0.06777
DDX23	0.793985	0.00044	0.758291	0.01098	0.987095	0.0004
DDX42	0.709403	0.00087	0.478401	0.17949	0.648278	0.03233
DDX54	0.948371	0	0.587064	0.07797	0.866717	0
DEFB1	0.490773	0.04302	0.414719	0.19063	0.520535	0.10837
DEK	0.56895	0	0.511232	0.14672	0.68821	0.00711
DENND2A	0.922328	0	0.506157	0.08005	0.867261	0.00193
DEPDC2	0.917533	0	0.707463	0.02218	0.70982	0.00474
DFNB31	0.396602	0.06393	0.435435	0.15876	0.590708	0.05287
DHH	0.441103	0.10476	0.48922	0.17949	0.625963	0.04211
DHX32	0.707075	0.00134	0.49015	0.17949	0.500174	0.08288
DIDO1	0.822827	0	0.541427	0.09619	0.829368	0.00196
DIRC2	0.578514	0.0242	0.529753	0.12084	0.516118	0.06541
DKFZP434A0131	0.750732	0	0.650773	0.06484	0.679745	0.01824
DKFZP434B0335	0.729283	0.00087	0.433849	0.15876	0.515668	0.03168
DKFZp779O175	0.653208	0.00232	0.436361	0.09521	0.729599	0.01325

DLEU1	0.968709	0	0.590952	0.01477	0.899729	0
DLEU2	0.968709	0	0.590952	0.01477	0.899729	0
DLEU8	0.638467	0	0.517083	0.14672	0.852374	0.00196
DLG4	0.438161	0.0798	0.550161	0.09619	0.504216	0.04471
DLL3	1,264,274	0	0.872722	0.00257	0.753918	0.01005
DMTF1	0.600586	0.00745	0.433849	0.15876	0.44535	0.19866
DNAJC6	0.572205	0.011	0.695504	0.00658	0.609611	0.04211
DNAJC7	0.375566	0.1193	0.406641	0.1824	0.456195	0.19866
DNM1L	0.551378	0.03321	0.48922	0.13676	0.457434	0.13502
DOCK8	0.563592	0.011	0.532198	0.12084	0.448938	0.13502
DOK2	0.384084	0.17587	0.5123	0.04338	0.449553	0.06293
DPEP2	0.324055	0.15404	0.429778	0.16507	0.475743	0.13266
DPF2	0.943974	0	0.441246	0.16507	0.527403	0.06541
DPP6	0.579136	0.011	0.602567	0.0636	0.515668	0.06541
DPYS	0.469435	0.05942	0.46351	0.14849	0.449553	0.13502
DPYSL2	0.426759	0.01602	0.414719	0.08664	0.591517	0.05287
DRD1IP	0.385678	0.17587	0.637195	0.00965	0.523992	0.10837
DRG1	0.491944	0.0031	0.489732	0.14672	0.526625	0.01517
DSC2	0.649237	0.003	0.449531	0.07182	0.55357	0.03751
DSCR1L1	0.634598	0.00462	0.438199	0.07139	0.593284	0.05287
DTX2	0.557687	0.01588	0.578465	0.07797	0.656305	0.0234
DULLARD	0.500755	0.03147	0.406641	0.19063	0.504216	0.13433
DUOX2	0.674962	0.00159	0.623032	0.00965	0.7274	0.01005
DYDC1	0.407104	0.09315	0.68621	0.02999	0.619264	0.04211
DYNLT1	0.459537	0.04765	0.657298	0.03938	0.52209	0.06541
E2F7	0.970426	0	0.48922	0.17949	0.529661	0.10837
ECRG4	0.517436	0.03147	0.51258	0.14672	0.591228	0.05287
EDEM3	0.572205	0.011	0.479658	0.17949	0.703397	0.00474
EDNRA	0.470672	0.02839	0.499349	0.02037	0.484747	0.16574
EEF1G	0.482476	0.04302	0.367705	0.19837	0.407539	0.10578
EFCBP1	0.490773	0.02176	0.658672	0.03938	0.496874	0.08288

EFNA4	0.445048	0.0798	0.503641	0.12138	0.398592	0.17011
EGLN1	0.656976	0.00232	0.479658	0.17949	0.539271	0.08735
EHD1	0.776156	0.00478	0.539301	0.10562	0.767132	0.02547
EIF2AK2	0.474317	0.05942	0.561398	0.09619	0.472982	0.16574
EIF3S6IP	0.413233	0.06849	0.466412	0.13676	0.526625	0.09489
EIF3S9	0.707833	0.12782	0.506157	0.14672	0.585987	0.05287
ELAVL1	0.969277	0	0.387876	0.1565	0.535039	0.02786
EN1	0.431197	0.10476	0.488172	0.17949	0.472982	0.16574
EN2	0.450439	0.0798	0.482054	0.10098	0.609426	0.04211
ENAH	0.551012	0.01588	0.719487	0.04075	0.562718	0.08618
ENPP7	0.312972	0.17381	0.598001	0.08274	0.456195	0.19866
ENTPD6	0.421448	0.0798	0.470806	0.10098	0.414684	0.10931
EP400NL	0.683709	0.01019	0.587064	0.08746	0.818566	0.02105
EPHA1	0.386091	0.12426	0.457951	0.07182	0.562547	0.06777
EPN1	0.842849	0	0.387876	0.1565	0.778238	0.00693
ERN1	0.584214	0.00745	0.478401	0.17949	0.528226	0.10837
ESPL1	0.463158	0.0798	0.587064	0.07797	0.674114	0.0234
EZH2	0.579136	0.011	0.457951	0.14849	0.515668	0.10837
F11R	0.402663	0.13719	0.527624	0.12084	0.656504	0.00413
FAM102A	0.500971	0.03147	0.508007	0.14672	0.519823	0.10837
FAM107B	0.792782	0	0.514658	0.14672	0.809806	0.00384
FAM112A	0.501724	0.00932	0.494346	0.12138	0.437722	0.13502
FAM35A	0.664222	0	0.637195	0.04899	0.476357	0.16574
FAM54B	0.38147	0.17587	0.623555	0.04899	0.679951	0.01824
FAM70B	0.484355	0.05942	0.467837	0.07182	0.615604	0.04211
FAM96A	0.696055	0.00134	0.742845	0.01098	0.703936	0.00474
FANCD2	0.321397	0.17381	0.433434	0.16507	0.398818	0.17011
FBXL10	0.661654	0.003	0.48922	0.10098	0.674114	0.01041
FBXL2	0.407103	0.09315	0.577913	0.07797	0.469198	0.10845
FBXO17	0.632137	0.01225	0.509088	0.14672	0.583679	0.06777
FBXO21	0.529323	0.00324	0.635986	0.04899	0.553736	0.08735

FBXO31	0.546844	0.00292	0.405901	0.19063	0.451956	0.08849
FGF20	0.725491	0.00087	0.756253	0.01098	0.662499	0.0234
FGFR1	0.405421	0.13719	0.658672	0.03938	0.473213	0.10845
FKBP14	0.729283	0	0.530259	0.06249	0.562547	0.06777
FLAD1	0.847711	0	0.599572	0.08274	0.468932	0.10845
FLII	0.417296	0.08279	0.502321	0.14672	0.480206	0.13266
FLJ10081	0.323398	0.18102	0.414946	0.1824	0.496631	0.13433
FLJ10154	1,122,822	0	0.566329	0.09619	0.686635	0.01824
FLJ10986	0.487434	0.04302	0.431692	0.15876	0.468932	0.10845
FLJ14154	0.425323	0.0798	0.596914	0.0636	0.808763	0.00384
FLJ14768	0.653208	0.00232	0.824237	0.00481	0.437759	0.16693
FLJ14803	1,008,126	0	0.698978	0.02218	1,054,776	0
FLJ14834	0.484355	0.05942	0.566329	0.09619	0.449864	0.08849
FLJ20366	0.469435	0.05942	0.634277	0.04899	0.591517	0.05287
FLJ20433	0.417476	0.10476	0.628961	0.00965	0.519823	0.06541
FLJ20489	0.904261	0	0.587064	0.07797	0.650038	0.03233
FLJ21767	0.686384	0	0.506157	0.08005	0.656305	0.00413
FLJ21908	0.529323	0.03147	0.538142	0.12084	0.625963	0.04211
FLJ25415	0.797714	0.00049	0.488172	0.17949	0.638526	0.03233
FLJ25801	0.403433	0.17587	0.574251	0.09619	0.508984	0.08288
FLJ30707	0.484355	0.03375	0.467837	0.07182	0.615604	0.04211
FLJ32679	0.548407	0.01588	0.503218	0.14672	0.492755	0.13433
FLJ35784	0.463567	0.05942	0.436361	0.15876	0.462079	0.19866
FLJ36749	0.376998	0.17587	0.503757	0.14672	0.604435	0.04211
FLJ39005	0.463567	0.05768	0.53333	0.10562	0.413439	0.17011
FLJ39739	1,229,180	0	0.695504	0.00658	0.844077	0.00196
FLJ41131	0.568923	0.011	0.53333	0.12084	0.729599	0.01325
FLJ41841	0.459537	0.04765	0.77902	0.00771	0.450896	0.19866
FLJ42562	1,142,672	0	0.561398	0.09619	0.969614	0.0004
FLJ43692	0.750732	0.00062	0.698978	0	0.750063	0.00693
FLJ45079	0.459025	0.01721	0.574081	0.01477	0.456195	0.19866

FLJ45187	1,499,857	0	0.857763	4	1,262,345	0
FLJ45983	0.471384	0.05942	0.833255	0.00481	0.523992	0.10837
FLJ46385	0.674279	0.00842	0.557572	0.02081	0.851198	0.02068
FLJ90231	0.419544	0.10476	0.612842	0.08274	0.599322	0.05287
FLVCR	0.635783	0.003	0.503641	0.14672	0.539271	0.08735
FN3K	0.375566	0.1193	0.430561	0.16507	0.408175	0.17011
FN3KRP	0.584214	0.00745	0.574081	0.07797	0.456195	0.19866
FNDC3A	0.6825	0.00232	0.615575	0.0636	0.947083	0.00103
FOXA3	0.674279	0.00159	0.484845	0.17949	0.486399	0.16574
FOXC1	0.459537	0.04765	0.584265	0.07797	1,067,911	0
FOXD1	0.517929	0.00699	0.628906	0.04899	0.538383	0.01517
FOXJ1	0.563349	0.011	0.358801	0.10812	0.600257	0.05287
FOXK2	0.417296	0.01602	0.502321	0.14672	0.528226	0.06541
FRMD3	0.375728	0.12426	0.411244	0.12725	0.826991	0.00287
FUT5	0.568923	0.0242	0.460603	0.14849	0.389119	0.18703
FZD7	0.409637	0.13719	0.488172	0.17949	0.685824	0.01824
GAB1	0.784454	0.00062	0.574251	0.09619	0.63017	0.02429
GABRA2	0.515498	0.04302	0.773991	0.01098	1,090,680	0
GAD1	0.495876	0.04302	0.561398	0.09619	0.80407	0.00384
GALR1	0.454466	0.0798	0.591488	0.0636	0.668898	0.00711
GAPDH	0.595489	0.011	0.611525	0.01089	0.529661	0.03168
GATA3	0.471384	0.05942	0.833255	0.00481	0.523992	0.10837
GBA	0.868903	0	0.767452	0.00771	0.937863	0.00103
GCAT	0.491944	0.023	0.466412	0.17949	0.480832	0.08288
GHRHR	0.514788	0.03147	0.433849	0.15876	0.515668	0.10837
GLDC	0.93932	0	0.459626	0.14849	0.56708	0.03751
GLT25D2	0.699361	0.00134	0.551606	0.09619	0.867523	0.00193
GLT8D3	0.551378	0.023	0.513681	0.14672	0.457434	0.19866
GNA12	0.42899	0.10476	0.506157	0.08005	0.515668	0.10837
GNB2L1	0.539509	0.023	0.580528	0.07797	0.725647	0.01005
GNG12	0.445048	0.04765	0.575589	0.07797	0.562718	0.06777

GNG4	0.508626	0.01404	0.551606	0.04939	1,008,203	0.00057
GNPTG	0.688618	0.00087	0.501408	0.14672	0.49953	0.13433
GOLGA8E	0.506222	0.03147	0.646994	0.06484	0.445826	0.19866
GOLGA8F	0.548407	0.01588	0.503218	0.14672	0.422362	0.16693
GOLPH3	0.561089	0.01588	0.507962	0.12138	0.585199	0.05287
GP6	0.316068	0.17381	0.509088	0.08005	0.559359	0.08735
GPC5	0.418306	0.13719	0.541706	0.12084	0.520895	0.10837
GPR132	0.397942	0.13719	0.59971	0.0636	0.55794	0.06777
GPR148	0.517436	0.03147	0.781075	0.00771	0.449333	0.19866
GPR81	0.463158	0.0798	0.48922	0.10098	0.505585	0.13433
GPSM3	0.547067	0.023	0.413854	0.19063	0.68821	0.01824
GRB10	0.386091	0.1193	0.62667	0.00965	0.515668	0.06541
GRP	0.497748	0.04302	0.686126	0.02218	0.576636	0.05287
H19	0.419544	0.06808	0.661869	0.01536	0.527403	0.03168
H1F0	0.590333	0.14267	0.466412	0.17949	0.480832	0.08288
H3F3A	1,250,373	0	0.767452	0.00771	1,289,562	0
H6PD	0.339084	0.15404	0.479658	0.13676	0.468932	0.16574
HAVCR1	0.431607	0.10476	0.580528	0.07797	0.468159	0.16574
HCN3	0.635783	0.003	0.599572	0.0636	0.492378	0.08288
HELZ	0.605079	0.00462	0.478401	0.17949	0.696298	0.01824
HES7	0.688538	0.00134	0.645842	0.03938	0.648278	0.0152
HGS	0.47989	0.04302	0.621922	0.04899	0.528226	0.10837
HHAT	0.61459	0.00462	0.719487	0.01656	0.422038	0.16693
HIC2	0.688722	0.00062	0.443091	0.14849	0.549522	0.08618
HIP1	0.622035	0.00462	0.650773	0.03938	0.492229	0.13433
HIP1R	0.904261	0	0.48922	0.17949	0.842642	0.00287
HIPK1	0.593397	0.00745	0.479658	0.17949	0.633058	0.03233
HIPK3	1,006,906	0	0.637356	0.04899	0.671241	0.0234
HIST1H2AM	1,247,314	0	0.584265	0.01477	1,328,956	0
HIST1H3E	0.56895	0.01588	0.681642	0.01102	0.498359	0.13433
HIST1H3J	1,247,314	0	0.584265	0.01477	1,328,956	0

HIST3H2A	0.635783	0.003	0.695504	0.02218	0.445485	0.19866
HIST3H2BB	0.635783	0.003	0.695504	0.02218	0.445485	0.19866
HIVEP3	0.826518	0	0.599572	0.0636	0.609611	0.02429
HK1	0.449957	0.04765	0.539165	0.12084	0.690717	0.0501
HLRC1	0.589994	0.16499	0.484845	0.17949	0.437759	0.15516
HMG20B	0.526781	0.00932	0.557572	0.09619	0.559359	0.05038
HMGCR	0.798473	0.00049	0.411208	0.19063	0.538383	0.08735
HMGN4	0.634598	0.01637	0.438199	0.15876	0.498359	0.13433
HMX1	0.511089	0.011	0.489475	0.14672	0.593733	0.05287
HMX2	0.535663	0.023	0.68621	0.02999	0.785988	0.00471
HNF4A	0.38131	0.13719	0.423725	0.15876	0.506836	0.10837
HNRPD	1,299,952	0	0.699088	0.00451	1,066,442	0.00069
HNRPK	1,419,417	0	0.846679	4	1,228,672	0
HNRPL	1,137,846	0	0.872722	0.00257	0.559359	0.08735
HNRPU	0.61459	0.00462	0.479658	0.17949	0.633058	0.03233
HOOK3	0.917533	0	0.414719	0.19063	0.496874	0.13433
HOXA4	0.579136	0.011	0.62667	0.01902	0.773503	0.00101
HOXA7	0.40754	0.13719	0.530259	0.12084	0.539108	0.08735
HOXB13	0.667673	0.00159	0.526241	0.03091	0.81635	0.00384
HOXB4	0.47989	0.02176	0.741522	0.01098	0.624267	0.04211
HOXB7	0.396431	0.13719	0.358801	0.10812	0.576247	0.0108
HS2ST1	0.784132	0.00049	0.527624	0.06249	0.586165	0.02929
HSPC049	0.42899	0.10476	0.530259	0.10562	0.539108	0.08735
HSPC159	0.538996	0.00932	0.561398	0.09619	0.567579	0.01664
HSPD1	1,013,313	0	0.707849	0.02218	0.969614	0.0004
HSPE1	1,013,313	0	0.707849	0.02218	0.969614	0.0004
ID1	0.541862	0.011	0.470806	0.17949	0.552912	0.06777
IFITM1	0.755179	0.00044	0.637356	0.04899	0.719186	0.01325
IFT20	0.375566	0.17587	0.406641	0.19063	0.504216	0.08288
IFT80	1,071,323	0	0.698311	0.02218	0.985316	0.00047
IGF2BP1	1,356,211	0	0.645842	0.03938	0.984422	0

IL17RD	0.535662	0.023	0.553833	0.09619	0.469198	0.10845
IL4I1	0.948205	0	0.581815	0.03811	0.583679	0.06777
ILDR1	0.685647	0	0.481594	0.05974	0.633417	0.03233
ILF2	0.99606	0	0.863384	0.00257	0.726844	0.01005
IMPA2	0.649237	0.003	0.733445	0.01098	0.738094	0.00693
IMPACT	0.411183	0.09315	0.591488	0.0636	0.80729	0.00287
ING4	0.617544	0.00745	0.587064	0.07797	0.505585	0.13433
INOC1	0.316389	0.17381	0.838696	4	0.703936	0.01325
INTS5	0.461498	0.05768	0.441246	0.16507	0.479458	0.13266
IPF1	0.330242	0.18102	0.369345	0.10812	0.449864	0.13502
IQWD1	1,080,831	0	0.695504	0.02218	0.844077	0.00196
IRAK4	0.529323	0.03147	0.48922	0.17949	0.433359	0.10931
IRF2	0.403433	0.04197	0.474381	0.07182	0.557458	0.02378
IRF2BP2	1,631,843	0	1,199,144	0	1,875,726	0
IRF5	0.536237	0.00932	0.602567	0.0292	0.609426	0.04211
IRF8	0.506337	0.023	0.549161	0.09619	0.880125	0.00193
ITGB2	0.471278	0.05078	0.658651	0.03938	0.725149	0.03171
ITGB8	0.42899	0.10476	0.674875	0.02999	0.726624	0.01005
IXL	0.379282	0.17587	0.436361	0.16507	0.656639	0.03233
JUNB	0.695351	0.00134	0.53333	0.12084	0.729599	0.01325
KAZALD1	0.599943	0.00249	0.857763	0.004	0.666899	0.0234
KCNA6	0.419048	0.09315	0.635986	0.04899	0.505585	0.00526
KCNH1	0.61459	0.00462	0.479658	0.17949	0.726844	0.0012
KCNH6	0.667673	0.00159	0.980722	0	1,152,494	0
KCNN4	0.758564	0	0.557572	0.09456	0.729599	0
KCNS3	0.452757	0.0798	0.488172	0.17949	0.449333	0.13502
KDELC1	0.726532	0.00134	0.664821	0.06484	0.520895	0.10837
KIAA0195	0.625944	0.003	0.526241	0.12084	0.456195	0.19866
KIAA0703	0.384816	0.09315	0.644667	0.06484	0.404382	0.10578
KIAA0907	0.656976	0.00064	0.479658	0.17949	0.726844	0.01005
KIAA1212	0.819274	0	0.634623	0.04899	0.80407	0.00384

KIAA1383	0.339084	0.07974	0.719487	0.01656	0.492378	0.13433
KIAA1430	1,053,410	0	0.449414	0.09521	0.848306	0.00287
KIAA1545	0.330827	0.18102	0.391376	0.11173	0.457434	0.19866
KIAA1683	0.421425	0.08279	0.606057	0.08274	0.535039	0.10968
KIAA1688	0.426759	0.10476	0.439115	0.16507	0.496874	0.13433
KIAA1729	0.918932	0	0.749023	0.01656	0.872544	0.00196
KIAA1754L	0.646795	0.003	0.585806	0.07797	0.52028	0.10837
KIAA1772	0.411183	0.13719	0.544169	0.09619	0.369047	0.18703
KIAA1794	1,138,999	0	0.69492	0.02218	1,220,156	0
KIAA1822	0.439831	0.0798	0.671675	0.02999	0.418455	0.16693
KLF10	0.554787	0.01588	0.487905	0.17949	0.520535	0.10837
KLF4	0.500971	0.03147	0.508007	0.08005	0.519823	0.03168
KLHDC5	0.639599	0.00193	0.660447	0.03938	0.794491	0.00471
KRT18	0.683709	0.00232	0.660447	0.03938	0.987095	0.00478
LA16c-360B4.1	0.506337	0.023	0.62079	0.04899	0.475743	0.16574
LBR	0.572205	0.011	0.527624	0.12084	0.679951	0.01824
LBX1	0.449957	0.0798	0.710718	0.02218	0.619264	0.02429
LDLRAP1	0.38147	0.17587	0.551606	0.04939	0.609611	0.04211
LECT1	0.528387	0.03147	0.714067	0	0.544573	0.00789
LEMD3	0.419048	0.13719	0.513681	0.14672	0.529661	0.00544
LEO1	0.801518	0.00034	0.503218	0.14672	0.7274	0.01005
LGR5	0.419048	0.13719	0.48922	0.17949	0.722265	0.01325
LHX2	0.354854	0.06096	0.532198	0.06249	0.519823	0.10837
LILRA5	0.400353	0.13719	0.557572	0.09619	0.705279	0.00711
LIM2	0.316068	0.17381	0.412119	0.19063	0.486399	0.16574
LIME1	0.521793	0.00477	0.588507	0.0636	0.506836	0.03168
LIMS3	0.388077	0.17587	0.732258	0.01656	0.449333	0.19866
LIN9	0.360277	0.11338	0.479658	0.17949	0.726844	0.01005
LITAF	0.830392	0	0.501408	0.14672	0.594679	0.05287
LMAN2	0.453187	0.0798	0.459585	0.07182	0.468159	0.16574
LMO3	0.705764	0.00159	0.415837	0.19063	0.529661	0.10837

LOC126860	0.741747	0.00062	0.719487	0.01656	0.562718	0.06777
LOC129138	0.413233	0.06849	0.466412	0.13676	0.526625	0.09489
LOC136263	1,008,126	0	0.698978	0.02218	1,054,776	0
LOC138046	0.490773	0.04302	0.561091	0.04939	0.567856	0.03751
LOC144363	0.926316	0	0.587064	0.07797	0.625963	0.04211
LOC146439	0.729125	0.11842	0.549161	0.09456	0.523317	0.10837
LOC148696	0.360277	0.15726	0.407709	0.19063	0.633058	0.03233
LOC152586	0.627563	0.00249	0.674121	0.03938	0.436272	0.0386
LOC161527	0.632777	0.003	0.599069	0.08274	0.469291	0.13266
LOC201895	0.963758	0	0.798958	0.00771	1,017,968	0.00047
LOC283340	0.449957	0.0798	0.514658	0.08005	0.476357	0.10845
LOC283392	0.595489	0.011	0.73383	0.01656	0.625963	0.02429
LOC285148	0.409637	0.13719	0.51258	0.12138	0.54393	0.08735
LOC285989	0.600586	0.00745	0.482054	0.17949	0.468789	0.10845
LOC286334	0.396602	0.13719	0.556389	0.09619	0.543451	0.01517
LOC338799	1,124,812	0	0.464759	0.12597	1,107,472	0
LOC339123	0.445576	0.05942	0.525284	0.06249	0.523317	0.06541
LOC339229	0.500755	0.01404	0.550161	0.09456	0.648278	0.03233
LOC375133	0.629689	0	0.489732	0.14672	0.480832	0.13433
LOC388152	0.632777	0.003	0.599069	0.08274	0.680471	0.01824
LOC388558	0.463567	0.05942	0.484845	0.13676	0.413439	0.17011
LOC389199	0.537911	0.03147	0.574251	0.09619	0.508984	0.13433
LOC390811	0.47989	0.04302	0.478401	0.17949	0.528226	0.10837
LOC392331	0.480097	0.04302	0.60477	0.0636	0.614336	0.04211
LOC400713	0.568923	0.00063	0.775753	0.00771	0.559359	0.08735
LOC400948	0.452757	0.0798	0.414946	0.19063	0.472982	0.16574
LOC402670	0.364641	0.13555	0.433849	0.16507	0.468789	0.13266
LOC402682	0.40754	0.13719	0.457951	0.14849	0.375032	0.18703
LOC405753	0.485129	0.04302	0.910585	0.00121	0.492755	0.08288
LOC440093	0.507268	0.05078	0.415837	0.1824	0.457434	0.14113
LOC440330	0.445576	0.05942	0.525284	0.06249	0.523317	0.06541

LOC440345	0.607604	0.003	0.549161	0.09456	0.547104	0.08735
LOC441426	0.375728	0.12426	0.628961	0.04899	0.590708	0.02929
LOC441548	0.449957	0.0798	0.661703	0.03938	0.666899	0.0234
LOC442578	0.750732	0	0.650773	0.06484	0.679745	0.01824
LOC442582	0.750732	0	0.650773	0.06484	0.679745	0.01824
LOC51136	0.52162	0.023	0.430561	0.09521	0.480206	0.13266
LOC541473	0.450439	0.0798	0.674875	0.02999	0.539108	0.08735
LOC641702	0.421425	0.10476	0.654541	0.01536	0.535039	0.10837
LOC642423	0.611684	0.00462	0.383404	0.1565	0.680471	0.01824
LOC642431	0.405856	0.13719	0.883318	0.00608	0.715385	0.00711
LOC642432	0.611684	0.00462	0.383404	0.1565	0.680471	0.01824
LOC642491	0.590833	0.011	0.535576	0.12084	0.498359	0.13433
LOC642586	0.448577	0.0798	0.722715	0.03938	0.567375	0.05038
LOC642620	0.579136	0.011	0.62667	0.04899	0.468789	0.10845
LOC642693	0.696673	0.00087	0.414706	0.19063	0.514622	0.06541
LOC642781	0.431607	0.06808	0.55634	0.04939	0.655423	0.00413
LOC643305	582	0.00086	0.353104	0.10812	0.57595	0.05287
LOC643647	0.776154	0.11842	0.561398	0.09619	0.496631	0.08288
LOC643664	0.396431	0.06393	0.358801	0.04737	0.528226	0.10837
LOC643749	0.612715	0.00077	0.486887	0.17949	0.593284	0.00679
LOC644241	0.503302	0.01084	0.486887	0.17949	0.617015	0.00796
LOC644349	0.445576	0.00805	0.358148	0.14041	0.49953	0.08288
LOC644368	0.517929	0.00699	0.628906	0.04899	0.538383	0.01517
LOC644558	0.480097	0.04302	0.60477	0.0636	0.614336	0.04211
LOC644605	0.99606	0	0.863384	0.00257	0.937863	0.00103
LOC644912	0.536237	0.023	0.506157	0.14672	0.468789	0.16574
LOC645052	1,229,180	0	0.695504	0.00658	0.844077	0.00196
LOC645215	0.965227	0	0.771286	0.03047	0.609426	0.0666
LOC645248	0.686384	0	0.530259	0.12084	0.656305	0.0234
LOC645370	0.388446	0.17587	0.55634	0.09619	0.655423	0.0234
LOC645444	0.403433	0.12426	0.574251	0.02276	0.533221	0.06541

LOC645562	1,419,417	0	0.846679	0.004	1,228,672	0
LOC645580	0.445048	0.0798	0.503641	0.14672	0.703397	0.01325
LOC645722	0.52162	0.023	0.885042	0.00103	0.672288	0.0234
LOC645856	0.667961	0.00159	0.919251	0.00121	0.897876	0.00153
LOC646073	0.409637	0.13719	0.536989	0.12084	0.709473	0.01325
LOC646098	0.632137	0.003	0.678784	0.06407	0.389119	0.18703
LOC646365	0.364562	0.17587	0.405901	0.19063	0.451956	0.19866
LOC646471	0.38147	0.17587	0.623555	0.04899	0.679951	0.01824
LOC646484	0.627563	0.00249	0.674121	0.03938	0.436272	0.0386
LOC646590	0.356054	0.15726	0.503757	0.14672	0.441703	0.19866
LOC646765	0.607386	0.00462	0.671675	0.06407	0.581188	0.05287
LOC647135	0.99606	0	0.863384	0.00257	0.937863	0.00103
LOC647219	0.508626	0.03147	0.503641	0.14672	0.445485	0.19866
LOC647251	0.48172	0.04302	0.791617	0.00608	0.627683	0.03233
LOC649897	0.544553	0.02747	0.407803	0.1824	0.395208	0.17011
LOC653033	0.547067	0.023	0.632953	0.04899	0.68821	0.01824
LOC653091	0.611684	0.00462	0.383404	0.1565	0.680471	0.01824
LOC653148	0.548407	0.01588	0.527181	0.12084	0.868188	0.00193
LOC653168	0.405856	0.09315	0.829784	0.01098	0.616711	0.02929
LOC653178	0.448577	0.0798	0.722715	0.03938	0.567375	0.05038
LOC653277	0.548407	0.01588	0.503218	0.14672	0.422362	0.16693
LOC653301	1,499,857	0	0.857763	0.004	1,262,345	0
LOC653344	0.464037	0.03375	0.527181	0.03306	0.445826	0.19866
LOC653361	0.579136	0.011	0.602567	0.0636	0.679745	0.01824
LOC653392	0.622035	0.00462	0.650773	0.03938	0.492229	0.13433
LOC653456	0.653208	0.00232	0.436361	0.09521	0.729599	0.01325
LOC653550	0.425323	0.0798	0.525284	0.06249	0.49953	0.13433
LOC653648	0.417476	0.06808	0.508007	0.14672	0.732478	0.01005
LOC653688	0.674279	0	0.53333	0.12084	0.778238	0.00693
LOC653709	0.379282	0.12426	0.557572	0.09456	0.656639	0.03233
LOC653748	0.579136	0.011	0.602567	0.0636	0.44535	0.19866

LOC653749	0.506222	0.03147	0.646994	0.06484	0.445826	0.19866
LOC653759	0.474317	0.05942	0.536989	0.12084	0.425684	0.16693
LOC653840	0.579136	0.011	0.602567	0.0636	0.679745	0.01824
LOC91664	0.33714	0.15404	0.509088	0.12138	0.413439	0.17011
LRIG1	0.535662	0.00932	0.650152	0.03938	0.609957	0.02429
LRRC45	0.396431	0.13719	0.358801	0.19837	0.480206	0.16574
LRRFIP1	0.668355	0.00232	0.561398	0.09619	0.567579	0.06777
LTA	0.437654	0.10476	0.55992	0.04939	0.474627	0.10845
LUZP5	0.343192	0.14501	0.482054	0.17949	0.609426	0.04211
LYSMD1	0.466241	0.03375	0.551606	0.09456	0.468932	0.16574
MAFK	0.40754	0.13719	0.530259	0.12084	0.539108	0.05038
MAGEF1	0.385676	0.17587	0.505674	0.08005	0.445738	0.19866
MANEAL	0.445048	0.0798	0.359743	0.19837	0.515825	0.10837
MAP1LC3A	0.481655	0.01404	0.706209	0.01656	0.737216	0.00693
MAP1LC3C	0.423855	0.10476	0.503641	0.12138	0.375145	0.18703
MAP3K12	0.551378	0.00932	0.415837	0.19063	0.698189	0.01824
MAP3K8	0.642796	0.003	0.465643	0.14849	0.762171	0.00693
MAP4	0.535662	0.00932	0.529753	0.12084	0.797637	0.00384
MAPBPIP	0.551012	0.01588	0.503641	0.14672	0.726844	0.0012
MAPK1	0.747756	0.00034	0.652976	0.02999	1,007,457	0
MAPKAPK5	0.86015	0	0.758291	0.01098	0.818566	0.00384
MAPT	0.375566	0.1193	0.454481	0.03644	0.456195	0.08849
MARCH4	0.495876	0.04302	0.585806	0.07797	0.54393	0.08735
MARCKS	1,794,381	0	1,046,808	0	0.854329	0.00196
MARS	0.529323	0.03147	0.684908	0.02999	0.601887	0.05287
MATN2	0.384084	0.17587	0.536696	0.12084	0.496874	0.13433
MATR3	0.820054	0	0.55634	0.09619	1,053,359	0
MAZ	0.749378	0.00049	0.573037	0.07797	0.737402	0.01005
MBD3	0.653208	0.00232	0.509088	0.14672	1,094,398	0
MCC	0.517929	0.03147	0.653094	0.03938	0.538383	0.08735
MCM10	0.471384	0.05942	0.661703	0.03938	0.666899	0.0234

MED11	0.605079	0.01637	0.430561	0.16507	0.384165	0.18703
MED12L	0.449956	0.0798	0.553833	0.09456	0.516118	0.10968
MEF2C	0.388446	0.17587	0.55634	0.09619	0.655423	0.0234
MEIS1	0.668355	0.00232	0.707849	0.02218	0.567579	0.03751
MEIS2	0.864795	0	0.43133	0.09521	0.891652	0.00153
METTL5	0.776154	0.11842	0.561398	0.09619	0.496631	0.08288
MGC12760	0.551012	0.18827	0.431692	0.16507	0.492378	0.13433
MGC14289	0.493338	0.04302	0.482054	0.10098	0.585987	0.05287
MGC16186	0.407104	0.09315	0.68621	0.02999	0.619264	0.04211
MGC16597	0.500755	0.01404	0.550161	0.09456	0.648278	0.03233
MGC16824	0.58735	0.00462	0.62079	0.04899	0.475743	0.16574
MGC23270	0.544553	0.02747	0.407803	0.12725	0.743921	0.02547
MGC24125	0.874106	0	0.574251	0.09619	0.581696	0.06777
MGC24381	0.688618	0.00087	0.477531	0.17949	0.475743	0.16574
MGC26694	0.379282	0.17587	0.484845	0.17949	0.729599	0.01325
MGC3265	0.690571	0	0.435396	0.04947	0.468159	0.10845
MGC39633	0.690571	0.00159	0.507962	0.14672	0.608607	0.04211
MGC4093	0.379282	0.17587	0.509088	0.14672	0.559359	0.08735
MICAL-L2	0.386091	0.17587	0.650773	0.03938	0.773503	0.00471
MIF4GD	0.500755	0.03147	0.478401	0.17949	0.624267	0.04211
MIXL1	0.529819	0.023	0.719487	0.01656	0.586165	0.02929
MKL1	0.3542	0.17587	0.41977	0.15876	0.480832	0.13433
MLLT11	0.868903	0	0.527624	0.06249	0.867523	0
MLLT6	0.834591	0	0.406641	0.19063	0.81635	0.00384
MLSTD2	0.818111	0	0.539301	0.12084	0.599322	0.05287
MMP17	0.441103	0.08279	0.538142	0.12084	0.48151	0.16574
MOBKL2A	0.632137	0.003	0.53333	0.06249	0.729599	0.01325
MORC2	0.787111	0	0.489732	0.14672	0.961663	0.00047
MOSC2	0.466241	0.05942	0.599572	0.0636	0.773737	0.00471
MOSPD3	0.364641	0.13555	0.433849	0.16507	0.375032	0.18703
MPPE1	1,168,626	0	0.638807	0.06484	0.599701	0.02429

MPPED2	0.67127	0.00159	0.686383	0.02999	0.719186	0.01325
MPZ	0.572205	0.011	0.479658	0.17949	0.539271	0.05038
MPZL1	0.784132	0.00049	0.479658	0.17949	0.492378	0.08288
MRPL12	0.542484	0.01588	0.645842	0.03938	0.648278	0.0152
MRPL17	0.398567	0.06393	0.490274	0.17949	0.647268	0.03233
MRPL24	0.720554	0.00087	0.479658	0.17949	0.914417	0
MRPS18B	1,203,548	0	0.876397	0.00257	0.996717	0.00047
MSH5	1,028,487	0	0.77902	0.00771	0.972986	0.0004
MSI2	0.813727	0	0.502321	0.04162	1,032,442	0.00057
MSRB3	0.573434	0.01588	0.440298	0.15876	0.529661	0.06541
MTA1	0.397942	0.13719	0.551733	0.09619	0.511445	0.06541
MTERFD1	1,173,588	0	0.561091	0.09619	0.567856	0.06777
MTG1	0.535663	0.023	0.563673	0.09619	0.619264	0.04211
MTRF1L	0.459537	0.0798	0.511232	0.14672	0.569553	0.06777
MUTYH	0.678169	0.00159	0.503641	0.12138	0.797184	0.02105
MVP	0.749378	0.00049	0.573037	0.07797	0.737402	0.01005
MX1	0.409807	0.10476	0.536678	0.06249	0.538014	0.05038
MX2	0.368827	0.17587	0.4391	0.15876	0.421054	0.10931
MXRA7	0.563349	0.011	0.669762	0.02999	0.576247	0.06777
MYBPH	0.76294	0.00044	0.431692	0.09521	0.89097	0.00153
MYCBP2	1,122,822	0	0.812559	0.00608	0.639281	0.00764
MYCL1	0.317892	0.17381	0.671521	0.06407	0.609611	0.0666
MYL2	0.419048	0.13719	0.611525	0.0636	0.698189	0.01824
MYL6	0.639599	0.01637	0.635986	0.04899	0.698189	0.0501
MYLPF	0.344309	0.11338	0.429778	0.15876	0.618466	0.02429
MYNN	0.835632	0	0.481594	0.17949	0.445738	0.08849
MYO10	0.539509	0.00932	0.55634	0.09619	0.538383	0.05038
MYO5B	0.389542	0.17587	0.473191	0.05121	0.55357	0.06777
MYO9B	0.547852	0.01588	0.654541	0.03938	0.680959	0.0234
NAG8	0.471889	0.05942	0.578465	0.07797	0.562547	0.06777
NAGK	0.733035	0	0.414946	0.19063	0.709473	0.01325

NALP1	0.605079	0.01637	0.621922	0.04899	0.576247	0.03751
NANOS2	0.463567	0.05942	0.727268	0.01656	0.559359	0.05038
NBPF11	0.699361	0.00134	0.599572	0.0636	0.586165	0.05287
NCF1	0.686384	0.13158	0.554362	0.09619	0.843821	0.16978
NCLN	0.758564	0.00044	0.824237	0.00481	0.705279	0.01824
NCOA7	0.590833	0.011	0.511232	0.14672	0.498359	0.12085
NCOR2	0.441103	0.10476	0.611525	0.0636	0.529661	0.10837
NDRG4	0.405069	0.10476	0.501408	0.14672	0.451956	0.19866
NEK5	0.616451	0.00745	0.590952	0.03811	0.639281	0.01053
NEUROD1	0.582116	0.011	0.488172	0.17949	0.638526	0.03233
NFATC3	0.52659	0.00111	0.69242	0.02218	0.856337	0.00196
NFE2L2	0.474317	0.05942	0.585806	0.07797	0.472982	0.16574
NFKBIE	0.612715	0.00745	0.632953	0.04899	0.640747	0.03233
NIP	0.358574	0.15726	0.718883	0.01656	0.539684	0.08735
NIPSNAP1	0.3542	0.17587	0.489732	0.12138	0.480832	0.08288
NLN	0.949536	0	0.725661	0.01656	0.538383	0.08735
NME1	1,043,239	0	0.669762	0.01102	0.696298	0.01824
NME1-NME2	1,043,239	0	0.669762	0.01102	0.696298	0.01824
NMI	0.819274	0.00034	0.488172	0.13676	0.662175	0.0234
NOL1	0.661654	0.01225	0.635986	0.04899	0.577812	0.06777
NOP5/NOP58	0.344957	0.15404	0.488172	0.17949	0.496631	0.13433
NOS1	0.595489	0.00292	1,027,362	0	0.74634	0.0012
NOVA2	0.589994	0.00745	0.727268	0.01656	0.729599	0.00175
NOX5	0.400759	0.13719	0.623032	0.04899	0.680471	0.01824
NPAS4	0.629316	0.00114	0.514787	0.14672	0.647268	0.0152
NPHS2	0.678169	0	0.767452	0.00351	0.867523	0
NPR1	0.720554	0	0.647538	0.01536	0.726844	0
NPR3	0.388446	0.17587	0.55634	0.04939	0.397936	0.07315
NPY5R	0.470672	0.0099	0.549284	0.06249	0.557458	0.01517
NR2F2	0.379666	0.17587	0.43133	0.15876	0.469291	0.10845
NRN1	0.56895	0.01588	0.413854	0.19063	0.617015	0.02429

NRXN2	0.629316	0.003	0.759924	0.01098	0.575349	0.06777
NTE	0.379282	0.17587	0.412119	0.19063	0.972798	0.00103
NTNG2	0.459223	0.05942	0.60477	0.0636	0.496195	0.00526
NTRK2	0.417476	0.06808	0.508007	0.14672	0.732478	0.01005
NTSR2	0.819274	0.00034	0.488172	0.10098	0.52028	0.06541
NUMA1	0.67127	0.00159	0.490274	0.10098	0.743159	0.01005
NUMBL	0.547852	0.01588	0.606057	0.0636	0.632319	0.04211
NXPH1	0.42899	0.04164	0.650773	0.03938	0.632866	0.03233
NXPH2	0.862394	0	1,025,161	0	0.969614	0
NY-SAR-48	0.632137	0.003	0.509088	0.14672	0.753918	0.01005
OAS3	0.595489	0.011	0.562603	0.09619	0.529661	0.10837
ODF2L	0.38147	0.1193	0.431692	0.16507	0.562718	0.06777
OGT	0.915502	0	0.568632	0.09619	0.642316	0.0152
OLFML2B	0.445048	0.0798	0.551606	0.09619	0.562718	0.06777
ONECUT2	0.627596	0.00193	0.49685	0.04162	0.784225	0
OR2A20P	0.772182	0.00044	0.843594	0.004	0.632866	0.03233
ORC6L	0.627857	0.00232	0.549161	0.09619	0.761189	0.00693
OSBPL1A	0.735802	0.00087	0.638807	0.01536	0.761159	0.00471
OSGEP	1,193,827	0	0.59971	0.0636	1,348,356	0
OSM	0.432911	0.03375	0.513053	0.12084	0.549522	0.06777
OTOA	0.384816	0.13719	0.573037	0.01477	0.547104	0.08735
OXT	0.421448	0.0798	0.447266	0.12597	0.598988	0.00796
P2RX7	0.749875	0.00726	0.660447	0.06484	0.48151	0.13266
PAF1	0.379282	0.17587	0.436361	0.16507	0.656639	0.03233
PALM2	0.751456	0.00044	0.435435	0.15876	0.637965	0.03233
PANK2	0.561931	0.00745	0.517886	0.10562	0.437722	0.19866
PAPSS2	0.514237	0.03147	0.58818	0.07797	0.785988	0.00471
PARD6A	0.364562	0.17587	0.596914	0.0636	0.49953	0.13433
PARVB	0.550978	0.00249	0.466412	0.17949	0.732696	0.00693
PAX5	1,398,543	0	0.628961	0.04899	0.945133	0
PCDH8	0.946693	0	0.615575	0.0636	0.686635	0.01824

PCDHA6	0.366866	0.13555	0.507962	0.12138	0.514975	0.10837
PCDHB15	0.388446	0.12426	0.55634	0.09619	0.468159	0.16574
PCDHB3	0.561089	0.02747	0.628906	0.06839	0.632015	0.06151
PCDHGA9	0.668991	0.00232	0.55634	0.04939	0.561791	0.03751
PCF11	0.482476	0.01084	0.73541	0.01656	0.623295	0.04211
PCNA	0.903103	0	0.753289	0.00771	1,221,014	0
PDAP1	0.664934	0.00232	0.674875	0.02999	0.656305	0.0234
PDCD1	0.431197	0.06808	0.463763	0.07182	0.449333	0.13502
PDE4D	0.431607	0.10476	0.55634	0.04939	0.655423	0.00413
PDXP	0.373878	0.13719	0.583014	0.0636	0.480832	0.12085
PELP1	0.667673	0.00159	0.502321	0.08005	0.480206	0.10845
PEO1	0.514237	0.03147	0.58818	0.03811	0.452539	0.13502
PERP	0.590833	0.011	0.705987	0.02218	0.854329	0.00196
PFKL	0.53275	0.02747	0.512284	0.12138	0.678365	0.0501
PFKM	0.793985	0.00044	0.48922	0.17949	0.457434	0.19866
PFN1	0.730268	0.00062	0.430561	0.15876	0.696298	0.00711
PFTK1	0.643485	0.003	0.433849	0.15876	0.609426	0.04211
PHF19	0.730582	0.00062	0.749915	0.01098	0.56708	0.06777
PHF23	0.709403	0	0.406641	0.19063	0.504216	0.13433
PIGN	0.476107	0.05942	0.473191	0.17949	0.668898	0.01824
PIK3R5	0.438161	0.0798	0.574081	0.07797	0.504216	0.13433
PIM2	0.830339	0	0.815863	0.00608	0.832632	0.00287
PKD1L2	0.405069	0.10476	0.501408	0.14672	0.428169	0.10931
PKD1L3	0.324055	0.14501	0.477531	0.17949	0.451956	0.19866
PLAUR	0.400353	0.09315	0.53333	0.03091	0.632319	0.0666
PLB1	0.366517	0.15726	0.439355	0.16507	0.685824	0.01824
PLCD3	0.563349	0.011	0.454481	0.12597	0.672288	0.0234
PLD1	0.36425	0.15726	0.577913	0.07797	0.539578	0.08735
PLEK2	0.376998	0.17587	0.59971	0.0636	0.441703	0.19866
PLEKHA8	0.729283	0	0.530259	0.06249	0.562547	0.06777
PLEKHG5	0.423855	0.10476	0.407709	0.19063	0.539271	0.08735

PLEKHG6	0.419048	0.09315	0.684908	0.01102	0.529661	0.10837
PLEKHO1	1,080,831	0	0.503641	0.14672	0.797184	0.00384
PLEKHQ1	0.569499	0.011	0.670957	0.02999	0.657007	0.0234
PLK1	0.506337	0.023	0.501408	0.14672	0.570892	0.06777
PLXDC2	0.55709	0.01588	0.465643	0.12597	0.738353	0.0012
PLXNA4A	0.386091	0.17587	0.530259	0.12084	0.609426	0.04211
PNKP	0.358211	0.06096	0.484845	0.17949	0.607999	0.02929
POFUT1	0.622138	0.00232	0.447266	0.12597	0.368608	0.18303
POLA2	0.776156	0.00049	0.637356	0.04899	0.647268	0.03233
POLDIP3	0.3542	0.17587	0.559694	0.07797	0.549522	0.06777
POP5	0.749875	0.00087	0.587064	0.07797	0.625963	0.04211
PPAPDC2	0.438349	0.0798	0.508007	0.14672	0.472566	0.16574
PPCDC	0.358574	0.15726	0.479255	0.17949	0.657007	0.0234
PPL	0.344309	0.13555	0.549161	0.09456	0.404382	0.17011
PPP1R10	1,203,548	0	0.876397	0.00257	0.996717	0.00047
PPP1R14A	0.484638	0.04302	0.606057	0.0636	0.437759	0.15516
PPP2CA	0.62583	0.00462	0.483774	0.10098	0.772463	0.00471
PPT2	0.547067	0.023	0.632953	0.04899	0.68821	0.01824
PRDM13	0.437654	0.10476	0.705987	0.02218	0.569553	0.06777
PRDM8	0.403433	0.17587	0.674121	0.03938	0.557458	0.08735
PRIC285	0.461586	0.04302	0.470806	0.17949	1,036,710	0
PRKAG1	0.573434	0.01588	0.587064	0.07797	0.48151	0.16574
PRKCG	0.800707	0.00034	0.727268	0	0.656639	0.00764
PRKCH	0.397942	0.09315	0.935548	0.00159	0.488198	0.08288
PRLR	0.431607	0.06808	0.459585	0.12597	0.585199	0.05287
PRO1073	0.755179	0	0.539301	0.06249	0.623295	0.04211
ProSAPiP1	0.38131	0.10286	0.659128	0.02999	0.57595	0.07582
PROX1	0.529819	0.00932	0.647538	0.03938	0.562718	0.0108
PRR5	0.373878	0.13719	0.699617	0.04075	0.549522	0.06777
PRR6	0.646808	0.00232	0.598001	0.08274	0.504216	0.12085
PRR8	0.493338	0.01084	0.554362	0.09619	0.750063	0.00079

PRRT1	0.547067	0.023	0.632953	0.04899	0.68821	0.01824
PRRT2	0.749378	0.00049	0.573037	0.07797	0.737402	0.01005
PRUNE	0.61459	0.00462	0.503641	0.14672	0.726844	0.01005
PSEN1	0.733052	0.00062	0.479768	0.17949	0.55794	0.03751
PSMA8	0.519389	0.03147	0.473191	0.10098	0.576636	0.05287
PSMD3	0.584214	0.00745	0.621922	0.04899	0.504216	0.08288
PTDSS1	1,173,588	0	0.561091	0.09619	0.567856	0.06777
PTGER2	0.418887	0.04164	0.575722	0.07797	0.697426	0.01325
PTGER4	0.820054	0.00034	0.628906	0.04899	0.983135	0
PTK2	0.618801	0	0.536696	0.12084	0.520535	0.10837
PTPRN	0.409637	0.10286	0.488172	0.13676	0.402035	0.17011
PTPRN2	0.386091	0.17587	0.530259	0.12084	0.44535	0.19866
PTPRO	0.705764	0.00159	0.611525	0.01089	0.650038	0.03233
PTPRU	0.99606	0	0.623555	0.04899	1,219,222	0
PUM1	1,186,795	0	0.599572	0.0636	1,008,203	0.00057
PURB	0.707833	0	0.506157	0.08005	0.632866	0.03233
PUS7L	0.529323	0.03147	0.48922	0.17949	0.433359	0.10931
PXMP4	0.401379	0.10476	0.564967	0.07797	0.483798	0.13433
RAB30	1,048,860	0	0.588328	0.07797	0.695213	0.00257
RAB34	1,105,834	0	0.526241	0.12084	1,176,504	0
RAB3IL1	0.398567	0.13719	0.514787	0.14672	0.479458	0.10845
RAB5C	0.563349	0.00292	0.550161	0.09619	0.576247	0.06777
RAB6B	0.492809	0.04302	0.553833	0.09619	0.563038	0.06777
RAD52	0.551378	0.03321	0.709369	0.05409	0.48151	0.16574
RAFTLIN	0.642794	0.00114	0.361195	0.19837	0.539578	0.05038
RAI16	0.405421	0.10286	0.658672	0.06484	0.638838	0.06151
RANBP9	0.765894	0.00062	0.657298	0.03938	0.68821	0.01824
RASA1	0.453187	0.0798	0.532151	0.12084	0.983135	0.00047
RASA3	0.440322	0.10476	0.418591	0.08664	0.56825	0.01664
RASA4	0.42899	0.10476	0.62667	0.06839	0.656305	0.05558
RASAL2	0.529819	0.0031	0.551606	0.09619	0.703397	0.01325

RASGEF1A	0.49281	0.01084	0.58818	0.07797	0.428721	0.16693
RASGRP4	0.547852	0.01588	0.509088	0.08005	0.486399	0.16574
RASSF2	0.582116	0.00086	0.447266	0.14849	0.368608	0.18703
RAX	0.389542	0.17587	0.686126	0.02218	0.438243	0.19866
RBM4	0.650293	0.00232	0.416732	0.1824	0.719186	0.01325
RBMX	0.638722	0.003	0.815863	0.00608	1,094,317	0
RBMY1A1	0.427216	0.10476	0.856551	0.00351	0.592043	0.06777
RBMY1B	0.320412	0.10341	0.749482	0.02999	0.468701	0.06293
RBMY1D	0.384495	0.12426	0.776249	0.00658	0.419364	0.14277
RBMY1E	0.427216	0.10476	0.66918	0.01089	0.592043	0.06777
RBMY1F	0.427216	0.10476	0.856551	0.00351	0.592043	0.06777
RBP7	0.402663	0.10286	0.551606	0.09456	0.656504	0.0234
RCSD1	0.551012	0.01588	0.479658	0.17949	0.515825	0.02786
RDH8	1,032,490	0	1,042,418	0	1,191,678	0
RELB	0.695351	0.00134	0.484845	0.10098	0.632319	0.04211
REXO1L2P	0.405421	0.10286	0.536696	0.12084	0.473213	0.16574
REXO4	0.60534	0.00462	0.508007	0.14672	0.496195	0.13433
RFP2	0.572419	0.01588	0.517083	0.14672	0.449864	0.13502
RFX3	1,022,815	0	0.822488	0.00481	0.850619	0.00196
RGS14	0.453187	0.0798	0.459585	0.07182	0.468159	0.16574
RHEBL1	0.374937	0.11338	0.538142	0.12084	0.866717	0.00196
RHOA	0.471382	0.05942	0.601992	0.0292	0.516118	0.10837
RILP	0.354701	0.11338	0.526241	0.03091	0.456195	0.13502
RINT1	0.85798	0	0.506157	0.14672	0.632866	0.03233
RIPK5	0.551012	0.01588	0.407709	0.19063	0.703397	0.01325
RND1	0.793985	0.00044	0.48922	0.17949	0.577812	0.03751
RNF121	0.37759	0.12426	0.539301	0.12084	0.551376	0.08735
RNF138	0.735802	0.00087	0.615148	0.04899	0.576636	0.05287
RNF168	1,221,308	0	0.457514	0.07182	0.844556	0.00196
RNF170	0.917533	0	0.414719	0.19063	0.496874	0.13433
RNF175	0.560324	0.00206	0.524316	0.04338	0.581696	0.01664

RNF41	0.463158	0.0798	0.48922	0.17949	0.698189	0.01824
RNH1	0.587362	0.02024	0.514787	0.14672	0.599322	0.05287
RNPEP	0.423855	0.10476	0.455675	0.14849	0.703397	0.04366
ROBO1	0.771353	0.00044	0.409355	0.19063	0.609957	0.04211
RORC	0.423855	0.10476	0.719487	0.01656	0.375145	0.18303
RP11-138L21.1	0.60534	0.00462	0.725725	0.01656	0.590708	0.05287
RP11-139H14.4	0.990725	0	0.787936	0.00771	0.686635	0.01824
RP5-1119A7.4	0.413233	0.0798	0.443091	0.14849	0.480832	0.13433
RP5-1153D9.3	0.602069	0.01225	0.447266	0.14849	0.506836	0.10968
RPA1	0.500755	0.03147	0.598001	0.0636	0.696298	0.00711
RPIP8	0.605079	0.15642	0.789362	0.02982	0.432185	0.15516
RPL10	1,149,700	0	0.568632	0.04939	0.856422	0.00196
RPL18A	0.547852	0.02747	0.484845	0.17949	0.607999	0.05287
RPL22	0.593397	0.00745	0.647538	0.03938	0.492378	0.13433
RPL23A	1,105,834	0	0.574081	0.07797	1,176,504	0
RPL26	0.667673	0.00159	0.645842	0.03938	0.456195	0.19866
RPL3	0.983889	0	0.513053	0.12084	0.824283	0.00196
RPL35	0.626213	0.003	0.628961	0.04899	0.661593	0.01041
RPL36	0.990348	0	1,018,175	0	0.997118	0
RPL36AL	0.733052	0.00062	0.59971	0.0636	0.720673	0.01005
RPL4	0.90698	0	0.479255	0.17949	0.445826	0.13502
RPS13	0.776156	0.00049	0.612842	0.0636	0.743159	0.01005
RPS3A	0.627596	0.00462	0.425872	0.15876	0.605933	0.05287
RPS6KA1	0.529819	0.023	0.527624	0.12084	0.609611	0.0666
RRM2	0.905513	0	0.488172	0.17949	0.898666	0.00153
RTF1	0.506222	0.03147	0.479255	0.17949	0.821259	0.00287
RUSC2	0.375728	0.17587	0.628961	0.04899	0.637965	0.0152
RUTBC1	0.459025	0.05942	0.478401	0.10098	0.456195	0.19866
S100A6	0.445048	0.0798	0.671521	0.02999	0.445485	0.19866
S100PBP	0.890096	0	0.407709	0.19063	0.539271	0.08735
SALL1	0.384816	0.09315	0.69242	0.02218	0.903912	0.00153

SALL3	0.584313	0.00292	0.733445	0.01098	0.599701	0.04211
SAMM50	0.413233	0.06849	0.699617	0.0031	0.435038	0.19866
SCAND2	0.569499	0.011	0.575106	0.07797	0.469291	0.16574
SCARB2	1,008,584	0	0.449414	0.07139	0.557458	0.08735
SCD	1,114,180	0	0.808748	0.00608	1,357,616	0
SCNN1B	0.567097	0.00249	0.716297	0	0.784976	0.00471
SCRIB	0.384084	0.17587	0.609882	0.0292	0.615177	0.02429
SDHC	0.572205	0.011	0.479658	0.17949	0.539271	0.05038
SDSL	0.330827	0.17381	0.562603	0.09619	0.529661	0.10968
SEC22L1	0.551012	0.01588	0.647538	0.06484	0.609611	0.0666
SECTM1	0.47989	0.04302	0.550161	0.09619	0.696298	0.01824
SELT	0.942764	0	0.842789	0.004	0.727257	0.01005
SEMA4D	0.626213	0.00114	0.532198	0.12084	0.496195	0.13433
SENP1	0.793985	0.00044	0.48922	0.17949	0.457434	0.19866
SEPT2	0.905513	0	0.829892	0	0.685824	0.00711
SEPT9	0.563349	0.011	0.621922	0.04899	0.456195	0.19866
SEPT15	0.784132	0.00049	0.527624	0.06249	0.586165	0.02929
SERF1A	1,100,598	0	0.677283	0.02999	0.983135	0.00047
SERF1B	1,100,598	0	0.677283	0.02999	0.983135	0.00047
SERPINB6	0.503302	0.04302	0.486887	0.17949	0.664478	0.0234
SERPINE1	0.643485	0.01225	0.940005	0.00159	0.773503	0.00471
SETD1B	1,124,812	0	0.464759	0.12597	1,107,472	0
SETMAR	1,371,294	0	0.77055	0.00771	1,149,535	0
SFRP2	0.806867	0	0.674121	0	0.824069	0.00384
SFRS10	1,264,161	0	0.481594	0.17949	1,079,155	0
SFRS3	1,925,677	0	1,046,808	0	1,542,539	0
SFRS8	0.551378	0.023	0.513681	0.04162	0.698189	0.01824
SGCA	0.563349	0.00292	0.598001	0.00632	0.624267	0.00796
SGTB	0.949536	0	0.725661	0.01656	0.538383	0.08735
SH2D4A	0.640139	0.003	0.658672	0.01536	0.496874	0.08288
SH3BGRL2	0.678364	0.00232	0.705987	0.00658	0.68821	0.01824

SH3BP1	0.373878	0.13719	0.606335	0.04899	0.366348	0.18303
SH3BP5	0.792779	0.00049	0.601992	0.0636	0.469198	0.16574
SIAH1	0.405069	0.10476	0.382025	0.1565	0.523317	0.06541
SIGLEC8	0.442496	0.06849	0.678784	0.01102	0.413439	0.17011
SKP1A	0.841634	0	0.870793	0.00257	0.725647	0.01005
SLC1A1	0.60534	0.00193	0.60477	0.0636	0.56708	0.03751
SLC23A2	0.421448	0.0798	0.588507	0.0292	0.506836	0.10837
SLC24A4	0.314165	0.18102	0.551733	0.09619	0.488198	0.13433
SLC25A6	0.510978	0.03147	0.494463	0.17949	0.616711	0.05287
SLC27A2	0.485129	0.04302	0.575106	0.03811	0.703936	0.01325
SLC30A10	0.847711	0	0.74347	0.01098	0.609611	0.02429
SLC34A2	0.403433	0.12426	0.574251	0.02276	0.533221	0.06541
SLC35A2	0.404524	0.13719	0.39557	0.11173	0.737474	0.01005
SLC35B2	0.590833	0.011	0.852053	0	0.806866	0
SLC35F5	0.452757	0.0798	0.51258	0.14672	0.449333	0.19866
SLC38A1	1,036,592	0	0.684908	0.02999	1,107,472	0
SLC38A2	0.639599	0.00462	0.562603	0.09619	0.987095	0.0004
SLC39A1	0.678169	0.00159	0.431692	0.07139	0.679951	0.00711
SLC43A3	0.37759	0.12426	0.46576	0.07182	0.455485	0.13502
SLC4A8	0.595489	0.011	0.562603	0.09619	0.529661	0.10968
SLC5A11	0.364562	0.17587	0.501408	0.14672	0.451956	0.13502
SLC5A5	0.442496	0.0798	0.703026	0.02218	0.705279	0.01824
SLC8A3	0.858718	0	0.791617	0.00608	0.534693	0.08735
SLCO5A1	0.469435	0.05942	0.683067	0.02999	0.473213	0.16574
SLITRK5	0.770564	0.00062	0.640198	0.01902	0.639281	0.03233
SMAD9	0.704516	0	0.418591	0.19063	0.757666	0.00693
SMARCA2	1,315,048	0	0.508007	0.14672	0.874248	0.00193
SMARCC2	0.639599	0.00462	0.635986	0.06839	0.601887	0.05287
SMC4L1	1,071,323	0	0.698311	0.02218	0.985316	0.00047
SMC5L1	0.93932	0	0.508007	0.14672	1,063,274	0
SMYD4	0.500755	0.03147	0.598001	0.0636	0.696298	0.00711

SNAPAP	0.423855	0.08279	0.527624	0.10562	0.375145	0.18303
SNAPC1	0.963439	0	0.479768	0.13676	0.604435	0.04211
SNRP70	0.674279	0	0.53333	0.12084	0.778238	0.00693
SNX1	0.696055	0.00134	0.742845	0.01098	0.703936	0.00474
SNX25	1,053,410	0	0.449414	0.09521	0.848306	0.00287
SORT1	0.678169	0.00159	0.479658	0.17949	0.492378	0.13433
SOX5	0.705764	0.00159	0.782752	0.00771	0.674114	0.0234
SP8	0.471889	0.05942	0.506157	0.14672	0.609426	0.00796
SPAG9	0.95978	0	0.645842	0.03938	0.672288	0.0234
SPCS2	0.860065	0	0.588328	0.07797	0.791105	0.00471
SPDYC	0.440521	0.0798	0.416732	0.19063	0.455485	0.13502
SPEN	0.445048	0.0798	0.503641	0.14672	0.703397	0.01325
SPTBN1	0.689915	0.00159	0.610215	0.0636	0.378386	0.18303
SQLE	0.789505	0.00049	0.487905	0.17949	0.662499	0.00413
SRGAP1	0.441103	0.06808	0.440298	0.07139	0.457434	0.19866
SRGAP3	0.407103	0.09315	0.601992	0.0292	0.375358	0.13007
SRM	0.445048	0.0798	0.503641	0.14672	0.492378	0.08288
SSTR2	0.47989	0.04302	0.478401	0.17949	0.528226	0.10837
ST8SIA3	0.454466	0.0798	0.591488	0.0636	0.576636	0.05287
ST8SIA4	0.755312	0.00062	0.653094	0.01536	0.491567	0.13433
STAT5B	0.918051	0	0.645842	0.03938	0.744319	0.01005
STC2	0.517929	0.01404	0.604717	0.0292	0.608607	0.00842
STIM2	0.448259	0.06808	0.449414	0.15876	0.678645	0.0234
STIP1	0.629316	0.003	0.563815	0.09619	0.815078	0.00384
STK11IP	0.452757	0.0798	0.781075	0.00771	0.591228	0.05287
STK24	0.616451	0.00249	0.517083	0.14672	0.781343	0.00101
STX3A	0.461498	0.05942	0.588328	0.07797	0.719186	0.01325
SULT2B1	0.379282	0.17587	0.53333	0.12084	0.510719	0.13433
SUMO2	1,001,510	0	0.598001	0.0636	0.696298	0.00711
SUMO3	0.471278	0.04302	0.414706	0.19063	0.514622	0.06541
SUV39H2	0.835635	0	0.58818	0.07797	0.54781	0.05038

SUV420H1	0.398567	0.13719	0.490274	0.17949	0.575349	0.06777
SVEP1	0.375728	0.17587	0.483816	0.17949	0.590708	0.05287
SVOP	0.441103	0.04164	0.538142	0.06249	0.457434	0.19866
SYNE2	0.418887	0.08279	0.503757	0.14672	0.511445	0.10837
SYNGAP1	0.80966	0	0.681642	0.02999	0.735672	0.01005
SYNJ2	0.656481	0.003	0.754675	0.01098	0.617015	0.04211
SYT2	0.487434	0.04302	0.527624	0.12084	0.562718	0.03751
SYTL3	0.459537	0.0798	0.657298	0.03938	0.52209	0.06541
TANC1	0.646795	0.003	0.659032	0.03938	0.969614	0.0004
TARBP2	0.551378	0.00932	0.415837	0.19063	0.698189	0.01824
TARSL1	0.699361	0.00134	0.791435	0.00608	0.726844	0.01005
TAS2R38	0.557687	0.01588	0.409746	0.19063	0.468789	0.16574
TBC1D10B	0.344309	0.11338	0.429778	0.15876	0.618466	0.02429
TBCA	0.431607	0.10476	0.507962	0.14672	0.421343	0.16693
TBRG4	0.42899	0.10476	0.433849	0.15876	0.632866	0.03233
TBX3	0.551378	0.023	0.611525	0.0636	0.625963	0.04211
TBXAS1	0.943778	0	0.457951	0.12597	0.937579	0
TCTA	0.471382	0.05942	0.601992	0.0292	0.516118	0.10837
TDRD5	0.529819	0.023	0.719487	0.01656	0.562718	0.06777
TDRD7	0.459223	0.05942	0.58058	0.07797	0.56708	0.06777
TEX2	0.438161	0.0099	0.526241	0.12084	0.552237	0.08735
TFAP2C	0.361241	0.17587	0.77683	0.00608	0.598988	0.04211
TFDP1	0.528387	0.01404	0.443214	0.09521	0.520895	0.03168
TFRC	0.749926	0.00062	0.481594	0.17949	0.469198	0.10845
TGIF	0.908931	0	0.449531	0.12597	0.899552	0.00149
THEM5	0.508626	0.0422	0.887367	0.01128	0.492378	0.13433
THRAP2	0.72782	0	0.562603	0.04939	0.601887	0.02929
TIA1	1,164,231	0	0.683441	0.02999	1,182,456	0
TJP2	0.480097	0.04302	0.508007	0.14672	0.685221	0.01824
TK1	0.584214	0.02024	0.621922	0.04899	0.744319	0.03171
TLE2	0.484638	0.05078	0.509088	0.14672	0.607999	0.07582

TLN1	0.730582	0.00062	0.459626	0.12597	0.685221	0.01824
TLX3	0.647411	0.003	0.628906	0.01902	0.491567	0.13433
TMCC2	0.805325	0.00188	0.551606	0.09456	0.515825	0.10837
TMED1	0.379282	0.12426	0.557572	0.09456	0.656639	0.03233
TMEM1	0.471278	0.04302	0.487889	0.17949	0.467838	0.01215
TMEM129	0.470672	0.0798	0.449414	0.16507	0.508984	0.13433
TMEM138	0.461498	0.05942	0.661869	0.06484	0.455485	0.14113
TMEM20	0.514237	0.03147	0.539165	0.12084	0.523992	0.10837
TMEM63A	0.635783	0.01225	1,031,264	0	1,078,543	0
TMEM8	0.58735	0.00462	0.596914	0.0636	0.570892	0.08618
TNFAIP3	0.503302	0.01084	0.486887	0.17949	0.617015	0.00796
TNFAIP8	0.776893	0.00044	0.507962	0.14672	0.538383	0.08735
TNFRSF13B	0.500755	0.0422	0.574081	0.07797	0.648278	0.03233
TNFSF12	0.542484	0.00111	0.885042	0.00103	0.672288	0.01041
TNFSF12-TNFSF13	0.542484	0.00111	0.885042	0.00103	0.672288	0.01041
TNFSF14	0.442496	0.06849	0.509088	0.14672	0.486399	0.16574
TNFSF7	0.484638	0.04302	0.412119	0.1824	0.437759	0.15516
TOE1	0.678169	0.00159	0.575589	0.07797	0.797184	0.02105
TOM1L1	0.584214	0.00249	0.598001	0.01089	0.504216	0.13433
TOMM40L	0.339084	0.14501	0.575589	0.07797	0.515825	0.10837
TOR3A	0.911289	0	0.455675	0.12597	0.468932	0.10845
TPD52	0.682815	0.00159	0.585486	0.07797	0.638838	0.03233
TPM1	0.632777	0.003	0.43133	0.09521	0.539684	0.08735
TPM3	0.466241	0.05942	0.479658	0.10098	0.422038	0.15516
TPM4	0.442496	0.04765	0.581815	0.08746	0.437759	0.16693
TRADD	0.58735	0.00462	0.573037	0.07797	0.808763	0.00384
TRAF5	0.529819	0.023	0.503641	0.14672	0.375145	0.18703
TRFP	0.56895	0.01588	0.438199	0.16507	0.640747	0.03233
TRHDE	0.595489	0.011	0.73383	0.01656	0.625963	0.02429
TRIM41	0.733732	0.00087	0.507962	0.08005	0.538383	0.00789

TRIM52	0.388446	0.17587	0.532151	0.12084	0.514975	0.10837
TRIM72	0.384816	0.13719	0.549161	0.04939	0.523317	0.10837
TRPV5	0.42899	0.10476	0.602567	0.0636	0.468789	0.16574
TSC22D1	0.330242	0.18102	0.541706	0.12084	0.449864	0.13502
TSFM	0.573434	0.01588	0.660447	0.03938	0.794491	0.00471
TSGA14	1,244,070	0	0.482054	0.17949	0.984458	0.00047
TSHZ1	0.389542	0.17587	0.567829	0.07797	0.461309	0.06538
TSHZ3	0.484638	0.04302	0.53333	0.06249	0.559359	0.08735
TSPAN16	0.50571	0.0422	0.509088	0.12138	0.583679	0.08618
TSPY1	0.448577	0.0798	0.883318	0.00608	0.814059	0.00471
TSPY2	0.448577	0.0798	0.883318	0.00608	0.814059	0.00471
TSSC1	0.538996	0.023	0.488172	0.17949	0.449333	0.19866
TTC15	0.538996	0.023	0.488172	0.17949	0.449333	0.19866
TTC26	0.514788	0.03147	0.530259	0.12084	0.539108	0.05038
TUBA4	0.388077	0.17587	0.439355	0.16507	0.449333	0.19866
TUBB6	0.454466	0.02839	0.52051	0.06249	0.80729	0
TUG1	0.787111	0	0.489732	0.14672	0.961663	0.00047
TUSC4	0.36425	0.13555	0.481594	0.13676	0.633417	0.06151
TXLNA	0.423855	0.10476	0.479658	0.17949	0.468932	0.16574
UBC	0.86015	0	0.538142	0.03091	0.553736	0.08735
UBE2D3	0.762041	0.00087	0.574251	0.04939	0.508984	0.08288
UBE2N	0.81604	0.00049	0.709369	0.02218	0.698189	0.01824
UBE2O	0.542484	0.01588	0.574081	0.03811	0.576247	0.06777
UBE3C	0.900879	0	0.433849	0.15876	0.492229	0.03586
UBQLN4	0.61459	0.00462	0.503641	0.14672	0.726844	0.0012
UBR2	0.919073	0	0.511232	0.14672	0.87806	0
UEV3	0.587362	0.00745	0.416732	0.19063	0.647268	0.03233
UGDH	1,120,649	0	0.87386	0.004	0.605933	0.05287
ULK1	0.529323	0.03147	0.587064	0.07797	0.722265	0.01325
UNC13D	0.438161	0.04765	0.526241	0.06249	0.648278	0.03233
UPB1	0.452589	0.04302	0.606335	0.06839	0.618212	0.03233

UQCR	0.674279	0.00159	0.484845	0.17949	0.632319	0.04211
UQCRFS1	0.379282	0.04197	0.436361	0.15876	0.535039	0.03168
VAMP4	0.826518	0	0.623555	0.04899	0.750291	0.00693
VAPA	0.973855	0	0.662467	0.02999	0.645832	0.00413
VCL	0.664222	0.01019	0.465643	0.12597	0.666899	0.0234
VIL2	0.634598	0.00193	0.486887	0.17949	0.949255	0.00103
VIPR1	0.407103	0.13719	0.457514	0.07182	0.563038	0.06777
VPS13B	0.960209	0	0.487905	0.17949	0.567856	0.03751
VPS35	0.627857	0.00232	0.549161	0.09619	0.761189	0.00693
WDR45L	0.375566	0.17587	0.502321	0.14672	0.624267	0.04211
WISP2	0.361241	0.17587	0.494346	0	0.483798	0.13433
WNT10B	1,411,529	0	0.611525	0.01089	0.577812	0.01664
XRRA1	0.860065	0	0.588328	0.07797	0.791105	0.00471
YARS	0.890096	0	0.407709	0.19063	0.656504	0.0234
YTHDF1	0.461586	0.04302	0.494346	0.04162	0.46076	0.16574
ZAP70	0.431197	0.10476	0.488172	0.17949	0.496631	0.08288
ZBTB7A	0.463567	0.05768	0.509088	0.12138	0.802558	0.0269
ZBTB9	0.503302	0.04302	0.754675	0.01098	0.593284	0.05287
ZC3H11A	0.360277	0.13555	0.503641	0.14672	0.468932	0.13266
ZCCHC11	0.487434	0.04302	0.359743	0.19837	0.609611	0.04211
ZDHHC17	0.926316	0	0.415837	0.19063	0.674114	0.0234
ZFP30	0.653208	0.00232	0.509088	0.14672	0.656639	0.03233
ZHX2	1,130,913	0	0.609882	0.0636	1,183,033	0
ZIC2	0.528387	0	0.590952	0.00987	0.591927	0.05287
ZNF160	0.611066	0.00462	0.557572	0.09456	0.656639	0.03233
ZNF217	0.903103	0	0.517886	0.06249	1,082,786	0
ZNF238	0.868903	0	0.479658	0.17949	0.82063	0.00287
ZNF271	0.757443	0	0.425872	0.09521	0.830356	0.00196
ZNF414	0.442496	0.06849	0.509088	0.12138	0.535039	0.10968
ZNF447	0.400353	0.13719	0.581815	0.07797	0.583679	0.06777
ZNF471	0.50571	0.00324	0.606057	0.0636	0.875518	0.00196

ZNF498	0.493338	0.04302	0.530259	0.12084	0.398471	0.14277
ZNF555	0.484638	0.04302	0.630299	0.04899	0.535039	0.10837
ZNF566	1,053,562	0	0.75151	0.01098	0.875518	0.00196
ZNF568	0.653208	0.00232	0.436361	0.09521	0.729599	0.01325
ZNF569	0.421425	0.10476	0.509088	0.12138	0.705279	0.01824
ZNF573	0.632137	3	0.654541	0.03938	0.437759	0.16693
ZNF579	0.484638	0.04302	0.606057	0.0636	0.535039	0.06541
ZNF584	0.463567	0.05768	0.53333	0.10562	0.413439	0.17011
ZNF585B	0.568923	0.011	0.460603	0.14849	0.607999	0.05287
ZNF586	0.716422	0.00087	0.703026	0.02218	0.486399	0.16574
ZNF594	0.688538	0	0.478401	0.05974	0.696298	0.00711
ZNF606	0.653208	0.00232	0.581815	0.07797	0.656639	0.03233
ZNF608	1,294,821	0	0.725661	0.01656	1,006,543	0.00057
ZNF613	0.50571	0.01404	0.557572	0.09456	0.632319	0.02429
ZNF616	0.86392	0	0.606057	0.0636	0.802558	0.00471
ZNF670	0.720554	0.00087	0.599572	0.0292	0.703397	0.01325
ZNF691	0.529819	0.023	0.407709	0.08664	0.445485	0.19866
ZNF695	0.487434	0.04302	0.503641	0.14672	0.539271	0.08735
ZNF71	0.653208	0.00232	0.53333	0.06249	0.486399	0.10845
ZNF74	0.432911	0.05942	0.466412	0.17949	0.549522	0.06777
ZWILCH	0.90698	0	0.479255	0.17949	0.445826	0.13502

Table S3. Differentially Expressed Genes upon SOX11 silencing

Probe ID	Genes	logFC	adj.P.Val
216379_x_at	*CD24*	3,16302549	1,2728E-06
220068_at	*VPREB3*	1,67165209	0,00398443
201218_at	*CTBP2*	1,6395099	0,00014354
204915_s_at	*SOX11*	1,60850026	1,2377E-05
213371_at	*LDB3*	1,31967267	0,00024434
209789_at	*CORO2B*	1,30688531	3,1934E-05
225955_at	*METRNL*	1,28392765	0,00406165
205122_at	*TMEFF1*	1,20951192	0,00027447
205347_s_at	*TMSB15A*	1,18129656	0,00512965
206398_s_at	*CD19*	1,15036079	0,0149571
201005_at	*CD9*	1,11724892	0,00172783
225626_at	*PAG1*	1,10783574	0,0225821
1559618_at	*LOC100129447*	1,07874864	0,02033525
223500_at	*CPLX1*	1,06917592	0,00032997
227404_s_at	*EGR1*	1,05689475	0,0005994
210279_at	*GPR18*	1,05452031	0,00088345
232555_at	*CREB5*	1,03991546	0,02869173
205463_s_at	*PDGFA*	1,01291252	0,00247188
208713_at	*HNRNPUL1*	0,99582873	0,00093409
242136_x_at	*MGC70870*	0,98937117	0,00014893
206413_s_at	*TCL1B*	0,98734438	0,00541798
227336_at	*DTX1*	0,98495664	0,00072383
213436_at	*CNR1*	0,96882971	0,00080841
200644_at	*MARCKSL1*	0,89860517	0,0007729
202391_at	*BASP1*	0,87634604	0,02403768
221601_s_at	*FAIM3*	0,86299061	0,00235042
210993_s_at	*SMAD1*	0,86147304	0,00075225
226043_at	*GPSM1*	0,84500907	0,0041213
221539_at	*EIF4EBP1*	0,84284172	0,00070922
224990_at	*C4orf34*	0,84062846	0,00208088
205003_at	*DOCK4*	0,83842339	0,00347517
229487_at	*EBF1*	0,83713658	0,00047624
238480_at	*TTC39C*	0,83551438	0,00123218
206864_s_at	*HRK*	0,82272501	0,0012655
230381_at	*C1orf186*	0,81897284	0,01350178
203921_at	*CHST2*	0,81419213	0,01264445
201998_at	*ST6GAL1*	0,81096359	0,02344304
203865_s_at	*ADARB1*	0,80782815	0,01532905

1554114_s_at	*SSH2*	0,79945425	0,0052339
236918_s_at	*LRRC34*	0,79920875	0,00237934
212886_at	*CCDC69*	0,79138729	0,0227912
206140_at	*LHX2*	0,78528562	0,00068178
240633_at	*DOK7*	0,78474764	0,0014842
38340_at	*HIP1R*	0,78222454	0,0008279
1405_i_at	*CCL5*	0,77775195	0,00069417
221969_at	*PAX5*	0,77654829	0,02954662
214788_x_at	*DDN*	0,77488848	0,00155887
243313_at	*SYNPO2L*	0,77105517	0,00133474
204891_s_at	*LCK*	0,75468935	0,02108237
218974_at	*SOBP*	0,74759485	0,01510782
212737_at	*GM2A*	0,74215325	0,0069208
219745_at	*TMEM180*	0,74187555	0,00075683
211200_s_at	*EFCAB2*	0,74145775	0,00061389
204661_at	*CD52*	0,74089777	0,04640271
226548_at	*SBK1*	0,73915586	0,00221509
203119_at	*CCDC86*	0,73726628	0,04512642
37462_i_at	*SF3A2*	0,73697707	0,00250911
219232_s_at	*EGLN3*	0,73558733	0,00108642
203795_s_at	*BCL7A*	0,72888963	0,0009641
228762_at	*LFNG*	0,71205164	0,01114564
1569003_at	*VMP1*	0,71013962	0,01115874
202081_at	*IER2*	0,70587581	0,00136741
227617_at	*TMEM201*	0,70498252	0,00218308
235252_at	*KSR1*	0,70014684	0,02462122
216521_s_at	*BRCC3*	-0,70122229	0,01785683
210465_s_at	*SNAPC3*	-0,70162284	0,0068293
222061_at	*CD58*	-0,70194891	0,00169607
1552931_a_at	*PDE8A*	-0,70247917	0,02423954
201297_s_at	*MOB1A*	-0,7025069	0,02821483
1559096_x_at	*FBXO9*	-0,70291241	0,02148627
210840_s_at	*IQGAP1*	-0,70384051	0,01084815
201940_at	*CPD*	-0,70448031	0,00078786
201663_s_at	*SMC4*	-0,70528294	0,00179436
224314_s_at	*EGLN1*	-0,70531364	0,00119392
227609_at	*EPSTI1*	-0,70856678	0,00165747
220773_s_at	*GPHN*	-0,70962154	0,00427793
210568_s_at	*RECQL*	-0,70969347	0,04419921
207992_s_at	*AMPD3*	-0,70994001	0,00207243

221618_s_at	*TAF9B*	-0,71008681	0,02343905
204369_at	*PIK3CA*	-0,71257313	0,01480554
1557984_s_at	*RPAP3*	-0,71364713	0,04410941
200607_s_at	*RAD21*	-0,71364819	0,01056123
202113_s_at	*SNX2*	-0,71413215	0,00095461
203141_s_at	*AP3B1*	-0,71473019	0,04182951
1552812_a_at	*SENP1*	-0,71504193	0,01690368
209255_at	*KLHDC10*	-0,71568967	0,00486467
219499_at	*SEC61A2*	-0,71644328	0,00252194
211559_s_at	*CCNG2*	-0,71839764	0,0432253
210685_s_at	*UBE4B*	-0,71849445	0,00875966
213295_at	*CYLD*	-0,71935494	0,00105014
220220_at	*LRRC37A4P*	-0,72035629	0,02335904
1554441_a_at	*WAPAL*	-0,72048499	0,0091386
202842_s_at	*DNAJB9*	-0,72059955	0,00254491
1555797_a_at	*ARPC5*	-0,72117983	0,02504153
228032_s_at	*DENND1B*	-0,72262315	0,00168274
209508_x_at	*CFLAR*	-0,72358068	0,00116174
212482_at	*RMND5A*	-0,72455389	0,04773357
218640_s_at	*PLEKHF2*	-0,72597274	0,00245196
201681_s_at	*DLG5*	-0,72624231	0,01229776
222587_s_at	*GALNT7*	-0,72710931	0,00481315
238959_at	*LARP4*	-0,72829839	0,04401406
214729_at	*TWISTNB*	-0,72885752	0,03238764
219757_s_at	*C14orf101*	-0,73023477	0,00752213
200712_s_at	*MAPRE1*	-0,73137348	0,00738864
218446_s_at	*FAM18B1*	-0,73286114	0,0177656
210379_s_at	*TLK1*	-0,733489	0,03459952
210057_at	*SMG1*	-0,7349655	0,04493178
227835_at	*LOC389831*	-0,73535686	0,00340739
221638_s_at	*STX16*	-0,73569938	0,00715225
217894_at	*KCTD3*	-0,73580997	0,01055896
205446_s_at	*ATF2*	-0,73879766	0,00776474
238851_at	*ANKRD13A*	-0,73926005	0,00583413
219869_s_at	*SLC39A8*	-0,7408313	0,03199364
217920_at	*MAN1A2*	-0,74166664	0,01961137
228149_at	*C7orf60*	-0,74181648	0,0006982
226962_at	*ZBTB41*	-0,74385474	0,01272519
212022_s_at	*MKI67*	-0,74440574	0,00093421
222239_s_at	*INTS6*	-0,74451474	0,02106016

207164_s_at	*ZNF238*	-0,74458011	0,01165471
225246_at	*STIM2*	-0,74476408	0,0299112
1555858_at	*LOC440944*	-0,74505446	0,00773658
204128_s_at	*RFC3*	-0,74597934	0,04316096
203526_s_at	*APC*	-0,747953	0,04536741
207108_s_at	*NIPBL*	-0,75087405	0,01178125
212335_at	*GNS*	-0,75102723	0,02737561
1553219_a_at	*AMMECR1*	-0,75175538	0,01816338
207583_at	*ABCD2*	-0,75194371	0,02646719
211919_s_at	*CXCR4*	-0,75221698	0,00192983
215794_x_at	*GLUD2*	-0,75223179	0,04611787
201399_s_at	*TRAM1*	-0,75266962	0,01421525
201635_s_at	*FXR1*	-0,75352652	0,00349256
221830_at	*RAP2A*	-0,75402716	0,01827237
218782_s_at	*ATAD2*	-0,7544177	0,00232437
219262_at	*SUV39H2*	-0,75445835	0,04410101
232682_at	*MREG*	-0,75505817	0,00488514
216899_s_at	*SKAP2*	-0,75584061	0,00698143
212217_at	*PREPL*	-0,75597875	0,02123871
219209_at	*IFIH1*	-0,75793732	0,00067869
1552625_a_at	*TRNT1*	-0,75795132	0,03042563
202722_s_at	*GFPT1*	-0,75936905	0,00323192
224150_s_at	*CEP70*	-0,7606234	0,00073363
214578_s_at	*ROCK1*	-0,76185851	0,04204407
1565269_s_at	*ATF1*	-0,76276895	0,02741839
201514_s_at	*G3BP1*	-0,76670906	0,02252281
204732_s_at	*TRIM23*	-0,77013509	0,01400664
207620_s_at	*CASK*	-0,77390561	0,00345212
207616_s_at	*TANK*	-0,77505235	0,00935904
202381_at	*ADAM9*	-0,77604061	0,00072091
230226_s_at	*KDM5A*	-0,77679971	0,00780749
210895_s_at	*CD86*	-0,7774205	0,01439107
200950_at	*ARPC1A*	-0,77780931	0,00050008
218035_s_at	*RBM47*	-0,77811785	0,00060648
200008_s_at	*GDI2*	-0,77814524	0,02304105
226977_at	*IGIP*	-0,7784966	0,00068097
201300_s_at	*PRNP*	-0,77850412	0,00051007
212902_at	*SEC24A*	-0,77975646	0,00820039
201946_s_at	*CCT2*	-0,78007117	0,00078863
231975_s_at	*MIER3*	-0,78087874	0,01261663

229115_at	*DYNC1H1*	-0,78164039	0,02682036
227372_s_at	*BAIAP2L1*	-0,78221758	0,00414609
212289_at	*ANKRD12*	-0,78402065	0,00104743
232635_at	*CEP128*	-0,78496968	0,0144737
244038_at	*WDR89*	-0,78512681	0,03223115
201745_at	*TWF1*	-0,78513792	0,00876502
213501_at	*ACOX1*	-0,7867717	0,00114537
221703_at	*BRIP1*	-0,78712642	0,03904937
223352_s_at	*C17orf80*	-0,78736027	0,01781858
231918_s_at	*GFM2*	-0,78765874	0,00351532
212800_at	*STX6*	-0,7904494	0,00060407
212761_at	*TCF7L2*	-0,79068009	0,00230409
206369_s_at	*PIK3CG*	-0,79097257	0,01228021
235003_at	*UHMK1*	-0,7919374	0,01217526
212398_at	*RDX*	-0,79223141	0,00862845
203065_s_at	*CAV1*	-0,79486817	0,00061137
242900_at	*ALG10B*	-0,79767578	0,03986646
223530_at	*TDRKH*	-0,79842749	0,00047241
1552531_a_at	*NLRP11*	-0,80211324	0,00987631
242163_at	*THRAP3*	-0,80274703	0,01859601
217800_s_at	*NDFIP1*	-0,80414345	0,00256138
202932_at	*YES1*	-0,80492521	0,0033075
210007_s_at	*GPD2*	-0,80515875	0,0040925
202514_at	*DLG1*	-0,80540798	0,0189998
228367_at	*ALPK2*	-0,80563302	0,01057868
235067_at	*MKLN1*	-0,80625881	0,01617976
205809_s_at	*WASL*	-0,80683009	0,03919778
202654_x_at	*MARCH7*	-0,80686767	0,03791064
202278_s_at	*SPTLC1*	-0,80801358	0,02098948
216733_s_at	*GATM*	-0,80819928	0,03978667
200806_s_at	*HSPD1*	-0,80853066	0,00064342
214697_s_at	*PTBP3*	-0,81096496	0,01898405
200722_s_at	*CAPRIN1*	-0,81144082	0,03276273
233750_s_at	*TRMT1L*	-0,81182959	0,03734289
210538_s_at	*BIRC3*	-0,81345764	0,00407017
225238_at	*MSI2*	-0,81453184	0,0056854
211968_s_at	*HSP90AA1*	-0,81494121	0,00038149
217301_x_at	*RBBP4*	-0,81595747	0,00801843
228485_s_at	*SLC44A1*	-0,81769256	0,01354891
202874_s_at	*ATP6V1C1*	-0,82067832	0,00159101

234299_s_at	*NIN*	-0,82102032	0,0219534
212177_at	*PNISR*	-0,8237975	0,03402623
238644_at	*MYSM1*	-0,82408667	0,02623082
200778_s_at	*SEPT2*	-0,8245523	0,01284693
204147_s_at	*TFDP1*	-0,82617258	0,0082757
202784_s_at	*NNT*	-0,82801217	0,0011719
217094_s_at	*ITCH*	-0,82801743	0,04120048
1555037_a_at	*IDH1*	-0,82902631	0,00034058
214693_x_at	*NBPF10*	-0,83055668	0,02746084
224600_at	*CGGBP1*	-0,83061487	0,0223016
1554806_a_at	*FBXO8*	-0,83074806	0,00230486
212008_at	*UBXN4*	-0,83136253	0,02456603
233878_s_at	*XRN2*	-0,83334194	0,00895479
224663_s_at	*CFL2*	-0,83456413	0,00059003
1556551_s_at	*SLC39A6*	-0,83504924	0,02402523
224943_at	*BTBD7*	-0,83509337	0,01840564
212409_s_at	*TOR1AIP1*	-0,83675853	0,00054213
1556009_at	*PEX13*	-0,83706368	0,00033258
205543_at	*HSPA4L*	-0,83709277	0,00136143
211220_s_at	*HSF2*	-0,83745324	0,01518297
202058_s_at	*KPNA1*	-0,83789575	0,01512829
235103_at	*MAN2A1*	-0,83848284	0,00953402
221397_at	*TAS2R10*	-0,83868789	0,00242705
201951_at	*ALCAM*	-0,84051729	0,0012154
226897_s_at	*ZC3H7A*	-0,84158468	0,01357232
216976_s_at	*RYK*	-0,84170129	0,00059706
201641_at	*BST2*	-0,84416568	0,00565762
212595_s_at	*DAZAP2*	-0,84501036	0,00208772
222626_at	*RBM26*	-0,84563483	0,02888497
222518_at	*ARFGEF2*	-0,84653045	0,01058963
202236_s_at	*SLC16A1*	-0,84665774	0,01906774
208195_at	*TTN*	-0,84669693	0,00221043
216607_s_at	*CYP51A1*	-0,8474255	0,00249906
234975_at	*GSPT1*	-0,84861912	0,03905378
206288_at	*PGGT1B*	-0,84874582	0,0126315
243835_at	*ZDHHC21*	-0,85048647	0,03368738
218850_s_at	*LIMD1*	-0,85067085	0,00790921
205841_at	*JAK2*	-0,85188762	0,01353532
209006_s_at	*C1orf63*	-0,85448547	0,03991871
1552921_a_at	*FIGNL1*	-0,85662037	0,01516677

213016_at	*BBX*	-0,85861721	0,00503128
220285_at	*FAM108B1*	-0,85864292	0,00075237
1554277_s_at	*FANCM*	-0,85921465	0,03636956
212195_at	*IL6ST*	-0,86116139	0,00304701
1553856_s_at	*P2RY10*	-0,8626859	0,00194131
211804_s_at	*CDK2*	-0,86370863	0,00160318
222600_s_at	*UBA6*	-0,86481514	0,0050873
201831_s_at	*USO1*	-0,86746173	0,00602849
210716_s_at	*CLIP1*	-0,86814646	0,01150823
213424_at	*KIAA0895*	-0,86948217	0,00058266
233899_x_at	*ZBTB10*	-0,87129231	0,03542684
235484_at	*PTAR1*	-0,87415767	0,02557713
217881_s_at	*CDC27*	-0,87417301	0,00713169
208983_s_at	*PECAM1*	-0,87718877	0,00135395
215711_s_at	*WEE1*	-0,8788158	0,03889418
201294_s_at	*WSB1*	-0,87903951	0,02763725
219683_at	*FZD3*	-0,88190613	0,01891366
212105_s_at	*DHX9*	-0,88483946	0,01040812
209647_s_at	*SOCS5*	-0,88529833	0,00064245
202558_s_at	*HSPA13*	-0,88884462	0,02331597
212634_at	*UFL1*	-0,89011481	0,02614654
222747_s_at	*SCML1*	-0,89095859	0,00081286
219740_at	*VASH2*	-0,89172087	0,00115422
219239_s_at	*ZNF654*	-0,89425057	0,00165783
209055_s_at	*CDC5L*	-0,89427262	0,03776556
230036_at	*SAMD9L*	-0,89520461	0,0251652
210041_s_at	*PGM3*	-0,89602183	0,00633748
200641_s_at	*YWHAZ*	-0,90442396	0,00412612
201627_s_at	*INSIG1*	-0,90936634	0,0007143
203294_s_at	*LMAN1*	-0,91047534	0,02880088
228561_at	*CDC37L1*	-0,91394831	0,00298337
206383_s_at	*G3BP2*	-0,9173126	0,01414367
201971_s_at	*ATP6V1A*	-0,91784584	0,02510232
241366_at	*RBAK*	-0,92105347	0,03846773
AFFX-HUMISGF3A/M97935_MB_at	*STAT1*	-0,92377385	0,03006173
209512_at	*HSDL2*	-0,92619278	0,00639139
210432_s_at	*SCN3A*	-0,93242311	0,0012325
207983_s_at	*STAG2*	-0,94116823	0,01509963
214831_at	*MED28*	-0,94122825	0,02185035
1552660_a_at	*C5orf22*	-0,94164142	0,0172509

225386_s_at	*HNRPLL*	-0,94180343	0,00498336
212720_at	*PAPOLA*	-0,94606048	0,01933817
202382_s_at	*GNPDA1*	-0,94863343	0,00079866
206235_at	*LIG4*	-0,94887533	0,00931348
203017_s_at	*SSX2IP*	-0,95176164	0,00023555
225144_at	*BMPR2*	-0,95265321	0,00018255
224829_at	*CPEB4*	-0,95420725	0,00081121
211801_x_at	*MFN1*	-0,95474509	0,02258846
1553112_s_at	*CDK8*	-0,95533386	0,00177201
208925_at	*CLDND1*	-0,95580731	0,02413023
206667_s_at	*SCAMP1*	-0,95646947	0,03762502
211814_s_at	*CCNE2*	-0,95705094	0,04509819
201059_at	*CTTN*	-0,95935961	0,00037416
214545_s_at	*PROSC*	-0,96315727	0,00100648
201718_s_at	*EPB41L2*	-0,97200243	0,01048445
216226_at	*TAF4B*	-0,9726958	0,00082378
209392_at	*ENPP2*	-0,97819401	0,0014586
204290_s_at	*ALDH6A1*	-0,97940547	0,00016441
203158_s_at	*GLS*	-0,98292215	0,0039666
1555814_a_at	*RHOA*	-0,98760009	0,00027992
203319_s_at	*ZNF148*	-0,98805919	0,00348401
238542_at	*ULBP2*	-0,98918682	0,02526012
203810_at	*DNAJB4*	-0,98942998	0,00095307
232278_s_at	*DEPDC1*	-0,98993717	0,00260915
210284_s_at	*TAB2*	-0,9985977	0,01615238
232591_s_at	*TMEM30A*	-1,0039724	0,01005283
238490_at	*KIAA2026*	-1,00990881	0,00324407
202990_at	*PYGL*	-1,01022804	0,00024405
236621_at	*RPS27*	-1,01778265	0,00552782
1555154_a_at	*QKI*	-1,02234657	0,00566466
220477_s_at	*TMEM230*	-1,02234947	0,00094251
238468_at	*TNRC6B*	-1,02263594	0,00066416
206544_x_at	*SMARCA2*	-1,02783765	0,00014737
1560346_at	*HBS1L*	-1,03025751	0,00011433
208744_x_at	*HSPH1*	-1,03092314	0,00021481
1552760_at	*HDAC9*	-1,04114933	0,00275976
202062_s_at	*SEL1L*	-1,04132904	0,00256019
211450_s_at	*MSH6*	-1,04986983	0,01136767
241820_at	*RIF1*	-1,05044659	0,01711909
201988_s_at	*CREBL2*	-1,05874403	0,00089022

235341_at	*DNAJC3*	-1,06357276	0,0064213
216266_s_at	*ARFGEF1*	-1,06820483	0,00227049
200604_s_at	*PRKAR1A*	-1,06963139	0,0005874
209896_s_at	*PTPN11*	-1,07783791	0,0105007
1554411_at	*CTNNB1*	-1,08390066	0,00936307
206098_at	*ZBTB6*	-1,08449452	0,02423008
201742_x_at	*SRSF1*	-1,08602691	0,00570245
213470_s_at	*HNRNPH1*	-1,08725119	0,01026734
231955_s_at	*HIBADH*	-1,0953941	0,0052507
211536_x_at	*MAP3K7*	-1,10775555	0,00201342
212092_at	*PEG10*	-1,12395359	0,02273757
202213_s_at	*CUL4B*	-1,12473589	0,00703666
201646_at	*SCARB2*	-1,12625059	0,00391948
1554260_a_at	*FRYL*	-1,12864281	0,01839908
1554614_a_at	*PTBP2*	-1,13144999	0,04440203
232383_at	*TFEC*	-1,13385263	0,04645388
225912_at	*TP53INP1*	-1,15025128	9,5069E-05
223585_x_at	*KBTBD2*	-1,1511125	0,0368141
209754_s_at	*TMPO*	-1,15227638	0,01072848
205884_at	*ITGA4*	-1,15886395	0,01146328
208852_s_at	*CANX*	-1,17438201	0,00210825
1555106_a_at	*CTDSPL2*	-1,20467906	0,02584418
1554433_a_at	*ZNF146*	-1,20683428	0,02086655
204344_s_at	*SEC23A*	-1,23454384	0,02163057
218036_x_at	*NMD3*	-1,23888561	0,01822097
1553725_s_at	*ZNF644*	-1,24839378	0,01326509
206624_at	*USP9Y*	-1,26775389	0,00178565
223701_s_at	*USP47*	-1,28958393	0,01028621
214786_at	*MAP3K1*	-1,29022283	0,04440117
221428_s_at	*TBL1XR1*	-1,29640573	0,01533065
1552619_a_at	*ANLN*	-1,29690351	0,01065663
226099_at	*ELL2*	-1,30776806	8,5906E-05
1555167_s_at	*NAMPT*	-1,31177112	0,0003207
224851_at	*CDK6*	-1,31193221	0,01345065
215739_s_at	*TUBGCP3*	-1,32100283	0,02701033
211090_s_at	*PRPF4B*	-1,32701419	0,01214507
1557100_s_at	*HECTD1*	-1,34265677	0,03311674
223341_s_at	*SCOC*	-1,35488392	0,0005524
203768_s_at	*STS*	-1,3746243	3,4533E-05
218858_at	*DEPTOR*	-1,38223083	0,00017143

1553530_a_at	*ITGB1*	-1,42064396	0,00870341
214895_s_at	*ADAM10*	-1,4466992	0,00692505
211080_s_at	*NEK2*	-1,44781192	0,00206671
203357_s_at	*CAPN7*	-1,4587103	0,00148031
227337_at	*ANKRD37*	-1,54008722	0,01102987
215719_x_at	*FAS*	-1,74294792	2,1487E-05
221695_s_at	*MAP3K2*	-1,77617303	0,0077154
204427_s_at	*TMED2*	-2,06232427	0,00366088

Table S4. Significantly enriched gene signatures by GSEA analysis

MCL-SOX11+ genes							Enriched in Z138 shControl cell line			
SOX11	ZNF167	TUBB2B	DFNA5	CD24	CSNK1E	TSPAN14	KCNK9	HS3ST3B1	GAL3ST4	PHC2
ABL1	CTBP2	ZNF711	HOMER3	CDKN1C	MARCKSL1	TCL6	FADS3	ZSCAN2	SYT17	TMEFF1
DBN1	HRK	PODXL	FMNL2	CD9	JAG1	CKB	EHD1	GLUL	ZBED3	TM6SF1
PROX1	YWHAG	GPSM1	H2AFY	CNR1	PTPLAD1	TTYH3	PHC1	SERPINE2	BCR	UBE2E3
MBP	GTF2IRD1	SBK1	EGLN3	MCM7	RCC2	FLJ12334	PXDN	KHDRBS3	CENPO	MDK
SPIN1	RTN4	FARP1	SMARCA4	RGS12	PLXNB1	BDH2	RP9	TIAM1	ZNF496	DACT1
PTP4A3	PDIA5	DTNBP1	GRIP1	UCHL1	STMN1	FNBP1L	LCK	NUDT11	PHYHD1	APITD1
HES6	ZNF219	DDAH1	AMOTL1	FBXO15	MYBL2	PLXND1	KIAA1274	JAKMIP2	FBLN2	CCDC69
KCNMB4	GPC2	KCTD15	SETMAR	ARHGEF5	CARHSP1	LATS2	ZNF618	PELI2	LOC283454	CHML
RAB43	KHDRBS1	MSI2	NAV1	LDOC1L	UBE2R2	CAMSAP1	RIMS3	CAMK2N1	TACC3	CREM
APBB2	HS2ST1	PGM2L1	FADS1	MGC39372	GAS2	JUP	FGF9	CDCA7	GDF11	SATB1
DOCK6	PHGDH	MAP4K4	IGF1R	COL27A1	PDE9A	MYO6	MARK1	TJP2	PHLDB2	LTBP1
FAM125B	TCL1A	SEMA4C	HIP1	ARHGEF4	MYH10	SLFN13	PLCG1	CDK2AP1	CHI3L2	CTPS2
FCGBP	AGPAT4	MCF2L	ACVR2B	PFN2	LOC286434	FZD2	CABLES1	DLL1	TMPO	SSBP3
CDC14B	GTF2IRD2	ZBED4	SEPHS1	DNMT3A	LOC389906	AACS	EPS8L2	CYB561	HDGFRP3	KIAA1407
SUSD1	TRIM36	PTPRG	LAPTM4B	GRAMD3	PAK1	H1FX	ZNF135	AXIN2	VANGL2	CYP2R1
PARD3	DTX3	LRP6	TXNRD1	KIF26B	CIB2	IL17RB	FAM84B	ZNF22	CHL1	CRY1
LOC643529	P2RX1	CASP6	PKD2	TUBB	WWC3	CMTM3	MAP1B	FOSL2	SPTA1	FUT4
CPXM1	MIOX	ITGB8	HMGB3	SMARCA1	MIB2	MYB	DCHS1	MAGEH1	OGFRL1	FZD6
FGFR1	KIF21A	PLXNA1	PCTP	MYADM	GPR133	RAPGEF3	KIAA1958	CTTNBP2NL	SVIL	FHL1
BAIAP3	FAM69B	NSUN7	B3GALNT1	SERPINF1	GABARAPL1	CACNB3	RBMS1	CACHD1	RNF130	LDLRAD3
ATP11A	CLDN23	ARSD	SMAD2	SETD4	ZNF542	CRIM1	BTBD3	GNAS	PSD3	TNFRSF21
TMEM44	GSTP1	LUZP1	ODZ4	MEST	MYO10	MLF1IP	CECR2	NTAN1	THAP9	MBOAT2
E2F3	ZNF608	ABCA9	NBEA	LGALS3BP	UBE2F	ABCA6	TFDP2	RCN1	RUFY3	ZNF275
ZNF184	STK17A	HMG20B	PRICKLE1	MAGED1	BIK	SOCS6	CELSR1	LMO7	ULK2	SCAMP5
SRGAP3	LRRN1	AZI2	VEZT	DIP2C	SCCPDH	RRBP1	PTPRS	PNMA2	DLG5	SPATA7
PON2	N4BP2	PLCXD2	CASD1	CNN3	PLA2G2D	BAZ2B	NFE2L3	LIG4	MSR1	SMAD5
YES1	SH3BP4	TTC7B	CHMP1B	DEGS2	TIA1	RNGTT	OLFM4	WDR41	TRO	SSX2IP
SLC7A11	PACS2									

MCL-SOX11- genes							Enriched in Z138 shSOX11 cell line			
DEGS1	SLAMF1	PCSK7	SLC25A28	POU6F1	CD200	FBXW7	SYNJ2	KLF3	SLC25A37	CD82
TNFRSF1B	STAT5B	DVL1	MLLT10	MAP3K5	GPR65	SNAP23	WNT16	IDE	TFR2	ZMYM6
HVCN1	ATM	KIAA1731	PPP2R1B	EED	MXD1	MDFIC	CD48	STAMBPL1	MEF2C	DENND1B
NPAT	RHOQ	FARP2	ZNF318	POLK	MAPK14	SETDB2	PBX3	BTLA	ACAT1	DUS2L
PCYT1A	ADD3	P4HA1	PHTF2	GLS	ZBTB32	ANKRD13C	PPA1	LOC401320	PTPN22	BAG2
IFNGR1	SLC30A5	CAPN2	ACSL4	REV3L	PDE8A	CLN8	ITSN2	USP45	FAS	TMED5
PELI1	PPP3CC	AMPD3	GNRH1	PCMTD1	TMEM38B	MYC	VPS54	BLOC1S2		

B-cell vs Plasmablast							Enriched in Z138 shControl cell line and SOX11-positive MCL primary tumors				
A20	ADAM8	ALOX5AP	CBLB	CCR7	CD19	CD22	CD24	CD72	CD74	c-IAP2	COL1A1
CR1	D6S49E	DDR1	EGR1	FCGRT	FGR	GPR18	GS3686	HHEX	HLA-DOB	HLA-DQA1	HRY
HSPB1	IFITM1	IFITM2	IGFBP4	IGHD	IGKV1D-8	IGLL1	IL4R	IL8	ITGAX	JUP	KIAA0239
LGALS9	LYZ	MLP	MTAP44	MX1	MX2	MYL5	NELL2	NFKB2	PLCB2	PTGDS	PTPRK
RBMS1	RELB	RI58	RPLP0	S100A8	SATB1	SERPINB6	SKAP55	SORL1	SPIB	STAF50	SYPL
TCL1A	TGIF	TLR1									

B-cell identity							Enriched in Z138 shControl cell line				
ADAM28	ADK	AIM2	AKAP2	ARMC3	BANK1	BEND5	BIRC3	BLK	C1QTNF7	CACNA1A	CCR6
CD19	CD200	CD22	CD24	CD37	CD40	CD72	CD79A	CD79B	CNTNAP2	CORO2B	CR2
CXCR5	EBF1	EZR	FADS3	FCER2	FCRL1	FCRL2	FCRLA	GYLTL1B	HIP1R	HLA-DOB	HLA-DQA1
HRK	HVCN1	ID3	IFT57	IGHG1	IL4R	KCNG1	KIAA0040	KIAA0125	LARGE	LCN6	MAP4K2
METTL8	MGC87042	MS4A1	MTSS1	NT5E	OSBPL10	P2RX5	P2RY10	PAWR	PAX5	PCDH9	PDLIM1
PFTK1	PKHD1L1	PLA2G4C	POU2AF1	PPAPDC1B	QRSL1	RASGRP3	RP9	SCN3A	SEMA4B	STAG3	STAP1
SWAP70	SYCP3	SYT17	TNFRSF13C	TPD52	VPREB3	ZCCHC7	ZNF777	ZNF821			

PAX5 activated genes							Enriched in Z138 shControl cell line and SOX11-positive MCL primary tumors				
ALDH1B1	ALPL	ARNTL	ATP1B1	BACH2	BCAR3	BCL2L1	BFSP2	BLNK	BST1	BTG2	CCND3
CD19	CD55	CD79A	CD97	CPLX2	CRIP1	DKK3	E2F2	EBF1	EPHA2	FCRLA	ID3
IFI30	IKZF3	IRF4	IRF8	LEF1	MYH10	NEDD9	OASL1	OTUB2	PDE2A	PLEKHA2	PRKD2
RAPGEF5	SDC4	SIT1	SMARCA4	TCF7L2	TNFRSF19	TPST1	UCHL1	VPREB3			

BLIMP1 repressed genes							Enriched in Z138 shControl cell line				
AICDA	ALOX5	ARHGDIB	ATP2A3	BCL6	BLNK	BTK	CD180	CD19	CD22	CD24	CD27
CD37	CD52	CD53	CD74	CD79A	CD86	CIITA	CR2	CXCR5	DEK	EBF1	FCER1G
FCER2	FCRLA	GCET2	GPR18	HLA-DMB	HLA-DPA1	HLA-DPB1	HLA-DQA1	HLA-DRA	HLA-DRB1	IL16	INPP5D
IRF8	LRMP	LYN	MS4A1	MYBL1	MYO1E	NR1H2	PAG1	PAX5	PCDHGA8	PLEK	POU2AF1
POU2F2	RGS13	RHOH	SP110	SP140	SPIB	ST6GAL1	STAP1	STAT6	SYK	TANK	TLR10
TRAF5	VNN2	VPREB3	ZFP36L1								

Plasmacell vs B-cell							Enriched in Z138 shSOX11 cell line				
AARS	AGA	AQP3	ARF4	ARP	BCMA	C8FW	CANX	CASP10	CAV1	CCR2	CD162
CD27	CD38	CD43	CITED2	CXCR3	DCN	DDOST	DRIL1	DUSP7	ELL2	FABGL	FGL2
FKBP2	FUT8	GAS6	GGCX	GP36B	HAGH	HDLBP	HEXB	HSPA5	HU-K4	ICAM2	IGH
IGL	IL15RA	IL6R	IRF4	ITGA6	ITM1	KDELR1	KDELR2	KIAA0057	KIAA0102	KIAA0103	LGALS3
MAN1A1	NEU1	NOT56L	NUCB2	ORP150	P4HB	P5	P63	PDIR	PDK1	PDRX4	PDXK
PI12	PLOD	PM5	PPIB	PRG1	PRKCI	PYCR1	PYGB	RNASE4	RPN1	RPN2	SEC61B
SEL1L	SLC7A1	SSR1	TM9SF2	TMP21	TRA1	TRAM	UGTREL1	YIF1A			

XBP1 target genes							Enriched in Z138 shSOX11 cell line and SOX11-negative MCL primary tumors				
ACSS1	ALDH1A1	ARF3	ATF6B	ATP2A2	BMP6	CD81	CDKN3	COPE	COX15	CST3	DAD1
DDOST	DEGS1	DNAJB9	DNAJC10	DNAJC3	EDEM1	ERGIC1	FKBP14	FNBP1	FTL	FTSJ1	GLRX
GPR89B	HERPUD1	HM13	HSP90B1	HSPA5	ISG20	ITGAM	ITGB5	LIPA	LMAN1	MANF	MCFD2
MGAT2	MGC29506	MOGS	OS9	PDIA3	PDIA4	PDIA5	PLOD1	PPIB	PPP2CB	PRDX4	RABAC1
RBM7	RHOQ	RNASE4	RPN1	SEC23B	SEC24C	SEC61A1	SEC61G	SLC1A4	SLC30A5	SLC33A1	SLC3A2
SLPI	SPCS3	SPOP	SRP54	SRP9	SRPR	SSR1	SSR3	SSR4	ST6GALNA	SYVN1	TMED10
TRAM1	TXNDC5	UAP1	USO1								

IRF4 target genes							Enriched in Z138 shSOX11 cell line			
ABHD10	ACP1	ACSS2	ADAM9	AGPAT2	AHCY	ALDH1L2	ALDOC	AMPD1	ANKRD37	ANKZF1
APOBEC3B	APOBEC3D	APOBEC3H	ASB13	ATF3	ATF4	ATP5D	ATP6V1E2	ATRX	AURKA	AVPI1
AXIN1	B3GNT1	BCKDHA	BCL2	BCL2L2	BHLHB8	BMI1	BMP6	BNIP2	BSPRY	C11orf24
C12orf57	C14orf93	C16orf14	C17orf39	C1orf2	C20orf133	C22orf9	C5orf32	C9orf100	CALCOCO2	CANX
CASP3	CAV1	CCDC134	CCDC52	CCDC74B	CCL3	CCNC	CCPG1	CD38	CD97	CDK6
CDKN1B	CDT1	CEBPZ	CENPF	CFLAR	CHRAC1	CMTM8	CNOT6	CTH	CTR9	CYCS
CYP51A1	DDHD2	DDIT3	DDR2	DENND2C	DEPDC1	DIXDC1	DKFZp547E087	DNAJB5	DNAJB9	DNAJC10
DUSP5	E2F5	EIF2C2	EIF2S2	EIF3S6	EIF4A2	ELL2	ELN	EML2	ENO1	F12
FADS1	FAM100B	FBXO16	FDFT1	FHL1	FKBP11	FLJ25006	FLJ35767	FRG2	FRMD6	FYN
FZD2	FZD7	GAA	GARS	GART	GFOD1	GFPT1	GLDC	GLS	GNG10	GNG7
GNPDA1	GOLGA7	GPT2	GRB14	GRPEL2	GRSF1	GTF2IRD1	GTF3C2	HADHA	HDAC5	HIG2
HIVEP2	HK2	HMBS	HMGB1	HMGCR	HMGCS1	HMMR	HSP90AA1	HSP90B1	HSPB1	HVCN1
IDH1	IDI1	IFI16	IFNAR1	INSIG1	IRF4	ISG20	ITGA4	ITGB7	ITPKA	ITPR2
JUP	KIAA0241	KIAA0323	KLF2	KLK1	KRAS	KTN1	LDHA	LDLR	LDLRAP1	LOC157562
LOC389458	LOC442013	LOC55565	LOC728315	LOC92312	LONP1	MALAT1	MAN2A1	MARS	MDC1	ME2
MICB	MKI67	MLSTD2	MMAB	MMD	MNAT1	MOCOS	MPP1	MPZL1	MTHFD1L	MVK
MXI1	MYB	MYC	NAPSA	NAPSB	NDRG1	NFIL3	NP	NR4A1	NUP205	OSBPL8
P18SRP	P4HA1	PABPC4	PAICS	PAIP2	PALM2-AKAP2	PAM	PBEF1	PCYT1B	PDCD10	PDIA4
PDK1	PELI3	PFKFB4	PGK1	PHKA1	PIM2	PIP5K1B	PLEKHA4	PMS2L3	PPP1R2	PPP2R5C
PRDM1	PRPF40A	PRPF4B	PRR7	PTPN22	PTPN6	RAB30	RAB33A	RAD21	RIN2	RNF122
ROCK1	RPP30	SAMD8	SAV1	SC4MOL	SC5DL	SCC-112	SCD	SCYE1	SEC61A2	SERF1A
SERPINH1	SETBP1	SIRT3	SKP2	SLAMF7	SLC12A4	SLC25A37	SLC2A1	SLC31A1	SLC37A4	SLC38A2
SLC3A2	SMOC2	SNRK	SNX9	SORT1	SP3	SPATS2	SPFH1	SQLE	SREBF2	SRPK1
SSR1	ST3GAL1	ST6GAL1	STAG2	STK38L	STRBP	STS	STX18	SUB1	SUMO1	TAF9B
TAGLN2	TBC1D14	TBC1D8	TCEA1	TCERG1	TCF20	TCOF1	TDG	TERT	TIMP2	TLOC1
TM9SF4	TMEFF1	TMEM38A	TMTC4	TNFAIP3	TNFRSF12A	TNFRSF17	TNFRSF8	TNNT1	TPR	TRAM1
TUBGCP3	TUFT1	TXNDC5	UAP1	UBE2B	UBE2H	UBE2J1	UCK2	UNG	USP9X	VDAC1
VEGFA	WHSC1	WWC3	XPOT	YARS	YES1	ZC3H10	ZFP36	ZNF37A		

Plasmablast signature							Enriched in SOX11-negative MCL primary tumors			
ABLIM1	ADRBK2	AICDA	AKAP13	AKNA	ALOX5	AMIGO2	AMPD3	AMSH-LP	ANKH	ANXA4
AP1G2	APBB1IP	ARHGAP17	ARHGAP25	ARHGAP9	ARHGEF3	ARPC5	ATP2A3	BACH2	BANK1	BCL11A
BCL2	BHLHB2	BIN1	BIRC3	BIRC4BP	BLR1	BMF	BMP2K	BRDG1	BTBD15	CAPG
CARD11	CAT	CCDC6	CCNG2	CCR1	CCR6	CD19	CD1C	CD22	CD24	CD40
CD44	CD47	CD52	CD69	CD74	CD83	CDC2L6	CENTB1	CENTD1	CKIP-1	CTSS
CYBASC3	CYBB	CYSLTR1	DAAM1	DEK	DOCK10	DOK3	DTNB	DTX3L	EBF	ELF4
ELK3	ELL3	EMILIN2	FADS3	FAIM3	FAM26B	FCRH3	FCRL2	FCRL4	FCRL5	FCRLM1
FGD2	FOXP1	GBP1	GBP2	GCA	GGA2	GPR114	GPR18	GPR92	GRB2	GRN
GSN	GZMB	HCK	HHEX	HIP1R	HLA-DMA	HLA-DMB	HLA-DOA	HLA-DOB	HLA-DPB1	HLADQA2
HLA-DQB1	HLA-DRA	HLA-E	IBRDC2	ICAM3	IDH2	IFITM1	IFITM2	IFITM3	IFNGR1	IGHM
IL10RA	IL16	IL4R	ILK	INPP5A	INPP5D	IRF8	ITGB2	ITPR1	IVNS1ABP	JAK3
JAM3	JMJD2C	KMO	LACTB	LBH	LCHN	LILRB1	LMO2	LPXN	LTB	LY86
LYN	LYSMD2	MAG	MAP3K5	MAPRE2	MARCH-I	MARCKSL1	MCOLN2	MKNK2	MNDA	MPEG1
MS4A1	MS4A7	MTSS1	MX1	MX2	NAPSB	NCF4	NFKBIZ	NOD27	NOD3	NSF
NSUN6	NYREN18	OIP106	PARP12	PARP14	PARP9	PAX5	PBXIP1	PCSK7	PDCD1LG1	PDE7A
PEA15	PFKFB3	PHF11	PHF16	PIK3AP1	PIK3CD	PIP5K3	PKIG	PLAC8	PLEKHF2	PLSCR1
PLXNC1	POU2F2	PREX1	PRKX	PSCD4	PTGS1	PTK2	PTPN1	PTPN18	PTPN6	QSCN6L1
RAB31	RAB7L1	RABEP2	RABGAP1	RALGPS2	RASSF2	RBMS1	RFX5	RGL1	RHOH	RNASET2
RUNX3	S100A4	SAT	SCAP2	SEMA4D	SERPINB1	SERPINB9	SERTAD2	SESN3	SGPP1	SH3BGRL
SIDT2	SIGLEC10	SLAMF1	SLC2A3	SLC41A1	SLC7A7	SLIC1	SNN	SNX2	SOCS3	SOX5
SP110	SP140	SPIB	STAT3	STAT6	STX7	SUV420H1	SYK	SYPL1	TBC1D10C	TBC1D5
TCF4	TFEB	TGFBR2	TICAM2	TLR10	TMEM71	TMEM77	TMEPAI	TOB2	TPP1	TRAF5
TRAFD1	TRIM22	TRIM34	TRIM38	TSPAN3	TSPAN33	UBE1L	UCP2	UGCG	UNC119	UNC84B
URP2	UVRAG	VNN2	VPS13C	VRK2	WDFY4	YPEL5	ZBED2	ZBTB4	ZC3H12D	ZFP36L1
ZNF238	ZNF447									

SOX11-upregulated genes							Enriched in SOX11-positive MCL primary tumors			
ADARB1	AFF3	APOBEC3C	BASP1	C1orf186	CCDC69	CCDC86	CCL5	CD19	CD24	CD52
CD69	CD9	CDV3	CHST2	CNR1	CORO2B	CPLX1	CREB5	CTBP2	DDN	DMD
DOCK4	DOK7	DTX1	EFCAB2	EGLN3	EGR1	EIF4EBP1	FADS1	FAIM3	FOXO1	GPR18
GPSM1	HNRNPUL1	HRK	IKZF2	LCK	LDB3	LFNG	LHX2	LOC100129447	LRRC34	MARCKSL1
METRNL	MGC70870	PAG1	PAX5	PDGFA	SBK1	SF3A2	SLAIN2	SMAD1	SOBP	SOX11
SSH2	ST6GAL1	SYNPO2L	TCL1B	TMEFF1	TMEM180	TMSB15A	TTC39C	VMP1	VPREB3	

SOX11-downregulated genes							Enriched in SOX11-negative MCL primary tumors			
ABCD2	ACOX1	ADAM10	ADAM9	AKIRIN1	ALCAM	ALDH6A1	ALG10B	ALPK2	AMMECR1	AMPD3
ANKRD12	ANKRD13A	ANKRD37	ANLN	AP3B1	APC	ARFGEF1	ARFGEF2	ARHGAP5	ARPC1A	ARPC5
ASPM	ATF1	ATF2	ATL2	ATP13A3	ATP6V1A	ATRX	B3GNT2	BAIAP2L1	BBX	BCLAF1
BDP1	BIRC3	BMPR2	BST2	BTBD7	C12orf35	C14orf101	C14orf145	C16orf72	C17orf80	C1GALT1
C1orf63	C20orf30	C5orf22	C5orf24	C5orf53	C7orf60	CALU	CANX	CAPN7	CASK	CAV1
CCNE2	CCT2	CD86	CDC27	CDC37L1	CDC42SE2	CDC5L	CDK2	CDK6	CDK8	CEP290
CEP350	CEP70	CFL2	CFLAR	CGGBP1	CLDND1	CLIP1	CPEB4	CPNE3	CREBL2	CTDSPL2
CTNNB1	CTTN	CUL4B	CXCR4	CYLD	CYP51A1	DAZAP2	DBT	DCAF16	DCUN1D1	DENND1B
DEPDC1	DEPTOR	DHX9	DLG1	DLG5	DNAJB4	DNAJB9	DNAJC3	DYNC1H1	EEA1	EFHC1
EIF4A2	ELL2	ENPP2	ENPP4	EPB41L2	EPSTI1	ERLIN1	ESCO1	EXOC5	EXOC6	FAM108B1
FAM18B1	FAM98A	FANCB	FANCM	FAS	FBXO8	FGFR1OP2	FIGNL1	FRYL	FXR1	FZD3
G3BP2	GALNT7	GATM	GDI2	GFM2	GLS	GLUD2	GNPDA1	GNS	GOLIM4	GPATCH2
GPD2	GPHN	GSPT1	HAUS6	HDAC9	HEATR1	HECTD1	HERC4	HIBADH	HNRNPH1	HNRPLL
HSDL2	HSF2	HSP90AA1	HSPA13	HSPA4L	HSPD1	HSPH1	IDH1	IFIH1	IFNGR1	IKZF3
IL6ST	INSIG1	INTS6	IQGAP1	ITCH	ITGA4	ITGB1	JAK2	KBTBD2	KCTD3	KDM5A
KIAA0776	KIAA0895	KIAA2026	KLHDC10	KPNA1	LIG4	LIMD1	LMAN1	LOC389831	LOC440944	LOC642236
LRCH3	LRRC37A4	LSM11	LTN1	MAN1A1	MAN2A1	MAP3K1	MAP3K2	MAP3K7	MAPKAPK2	MAPRE1
MBNL1	MED28	MFN1	MIER3	MKI67	MLL	MPHOSPH9	MREG	MSH6	MSI2	MST4
MYSM1	NAMPT	NDFIP1	NEDD1	NEK2	NFX1	NIN	NLRP11	NMD3	NNT	NUPL1
OLFML2A	OXR1	P2RY10	PAPOLA	PECAM1	PEG10	PEX13	PGGT1B	PGM3	PHF3	PICALM
PIK3AP1	PIK3CA	PIK3CG	PLEKHF2	PLXNC1	PREPL	PRKAB2	PRKAR1A	PRNP	PROSC	PRPF4B
PSME4	PTAR1	PTBP2	PTPN11	PYGL	QKI	RAB8B	RAD21	RANBP2	RAP2A	RBAK
RBBP4	RBM26	RBM39	RBM47	RDX	RECQL	RFC3	RFX7	RHOA	RIF1	RIOK3
RNF146	RNGTT	ROCK1	ROD1	RPAP3	RPS27	RSRC1	RYK	SAMD9L	SCARB2	SCML1
SCN3A	SCOC	SEC23A	SEC24A	SEC61A2	SEL1L	SELPLG	SENP1	SEPT2	SGPP1	SKAP2
SLC39A6	SLC39A8	SLC44A1	SLFN13	SMARCA2	SMCHD1	SMG1	SNX2	SOCS5	SPTLC1	SRSF1
SS18	SSR1	SSX2IP	STAG2	STIM2	STS	STX16	STX6	SUV39H2	TAB2	TAF4B
TANK	TAS2R10	TBL1XR1	TCF7L2	TDRKH	TFAM	THRAP3	TLK1	TMED2	TMEM30A	TMPO
TNKS2	TNRC6B	TOR1AIP1	TP53INP1	TPR	TRAM1	TRIM23	TRMT1L	TTN	TUBGCP3	TWF1
TWISTNB	UBA6	UBE4B	UBXN4	ULBP2	UQCRC2	USO1	USP47	USP9Y	VASH2	WAPAL
WASL	WDR89	WEE1	WSB1	XRN2	YES1	YWHAZ	ZBTB10	ZBTB41	ZBTB6	ZC3H7A
ZMYM6	ZNF146	ZNF148	ZNF238	ZNF644	ZNF654	ZNF655	ZNF678	ZNF800		

Table S5. B-cell differentiation gene signatures in Z138shControl and Z138shSOX11 cell lines.

	Enrichment in			
	Z138shControl		**Z138shSOX11**	
Gene signature	NES	FDR	NES	FDR
B-cell vs plasmablast [1]	2.09	$<10^{-4}$		
B-cell identity [2]	1.88	$<10^{-4}$		
PAX5 activated genes [3]	1.81	0.001		
BLIMP-1 repressed genes [2]	2.19	$<10^{-4}$		
Plasma cell vs B-cell [1]			-2.28	$<10^{-4}$
IRF4 target genes [2]			-2.15	$<10^{-4}$
XBP1 target genes [2]			-2.03	$<10^{-4}$

GSEA was used to test for significant enrichment of defined gene signatures related to different steps of the mature B-cell and plasma cell differentiation programs. NES and FDR *P*-val are shown. Significance is considered when FDR<0.05. Gene signatures of B-cell differentiation (**1**) were extracted from data of [7] and (**3**) of [8] or downloaded (**2**) from http://lymphochip.nhi.gov/signauredb/index.html.[9]

Table S6. SOX11-bound genes that overlap with differential expression data upon SOX11 silencing

Statistical criteria	ChIP-chip expression array	**FDR<0.1 and peak score>0.5** ***P*-val<0.05**	**FDR<0.1 and peak score>0.5** ***P*-val<0.05 and logFC>0.7**
		147 overlapping genes	**18 overlapping genes**
		CDK6	*PAX5*
		SCARB2	*MSI2*
		SMARCA2	*HSPD1*
		RHOA	*SUV39H2*
		CDC37L1	*SEPT2*
		TFDP1	*EGLN1*
		MSI2	*SENP1*
		HSPD1	*ZNF238*
		CD86	*STIM2*
		SUV39H2	*CXCR4*
		CXCR4	*CD86*
		STIM2	*TFDP1*
		ZNF238	*CDC37L1*
		SENP1	*RHOA*
		EGLN1	*SMARCA2*
		ZC3H11A	*SCARB2*
		OGT	*CDK6*
		LIN9	*LHX2*
		RANBP9	
		EDEM3	
		SELT	
		RFX3	
		CNOT6L	
		ZNF217	
		MYCBP2	
		ONECUT2	
		SPAG9	
		CCDC47	
		SMAD9	
		ZNF160	
		STIP1	
		VAPA	
		PURB	
		TUG1	
		CD46	
		CD1D	
		MAPK1	
		PSEN1	
		CDC6	
		NFATC3	
		PXMP4	

ZWILCH
MPZL1
SLC38A2
HIPK1
TFRC
DNM1L
PIGN
MGC24125
CLYBL
GAB1
PPP1R10
HOOK3
FAM54B
CDK5RAP2
DNAJC7
ODF2L
SUV420H1
FLII
HMGCR
SQLE
DDX42
AHNAK
PRUNE
LRRFIP1
CD37
UBR2
ARID5B
GOLPH3
BRP44
SLC35F5
PRDM8
MKL1
IRF2BP2
MX1
PCF11
TPD52
TDRD7
IGF2BP1
ATXN2L
MAP1LC3A
SVEP1
CANT1
ARHGEF18
GNB2L1
CDC42SE1
YARS

SSTR2
H6PD
MCM10
ZNF579
CRH
PPP2CA
CEP68
RNF41
PTGER4
NTRK2
MYCL1
RHEBL1
CHD9
GNA12
DLG4
ATP12A
UBQLN4
NIPSNAP1
DENND2A
COL1A2
ULK1
MTG1
HOXA4
ALK
GLDC
CPNE2
IRF5
FGFR1
NOX5
MYO9B
AUTS2
NCOR2
CMTM1
PRIC285
ENAH
ARHGAP17
AP1M2
MLLT6
PLAUR
KCNN4
EP400NL
PRR5
DPEP2
PRLR
MTA1
LMO3

IRF8
ZHX2
GPSM3
DNAJC6
FLJ39739
CABP1
MLLT11
MAP3K12
FOXC1
ZNF606
PAX5
LHX2
SEPT2
SEPT9

IV. SUPPLEMENTAL REFERENCES:

1. Swerdlow S, Campo E, Harris N et al. (Eds.):WHO Classification of Tumours of Haematopoietic and Lymphoid Tissues. AIRC: Lyon; 2008.

2. Fernandez V, Salamero O, Espinet B et al. Genomic and gene expression profiling defines indolent forms of mantle cell lymphoma. *Cancer Res.* 2010;**70**(4):1408-1418.

3. Royo C, Navarro A, Clot G et al. Non-nodal type of mantle cell lymphoma is a specific biological and clinical subgroup of the disease. *Leukemia* 2012; **26**(8):1895-1898.

4. Vegliante MC, Royo C, Palomero J et al. Epigenetic activation of SOX11 in lymphoid neoplasms by histone modifications. *PLoS.One.* 2011;**6**(6):e21382.

5. Smyth GK. Linear models and empirical bayes methods for assessing differential expression in microarray experiments. *Stat.Appl.Genet.Mol.Biol*. 2004;3:Article3.

6. Brennan SK, Meade B, Wang Q et al. Mantle cell lymphoma activation enhances bortezomib sensitivity. *Blood* 2010;**116**(20):4185-4191.

7. Tarte K, Zhan F, De VJ, Klein B, Shaughnessy J, Jr. Gene expression profiling of plasma cells and plasmablasts: toward a better understanding of the late stages of B-cell differentiation. *Blood* 2003;**102**(2):592-600.

8. McManus S, Ebert A, Salvagiotto G et al. The transcription factor Pax5 regulates its target genes by recruiting chromatin-modifying proteins in committed B cells. *EMBO J.* 2011;**30**(12):2388-2404.

9. Shaffer AL, Wright G, Yang L et al. A library of gene expression signatures to illuminate normal and pathological lymphoid biology. *Immunol.Rev.* 2006;**210**:67-85.

4. DISCUSSION

4.1. Paper I

SOX11 expression is activated by histone modification marks in MCL

In this study, we sought to enhance our understanding of the biology of MCL through the characterization of SOX11 function, a transcription factor highly expressed in most aggressive MCL and absent in a small subset of MCL patients with indolent clinical behavior (Fernandez et al., 2010; Royo et al., 2012).

Our first objective, reached in paper I, was to study the molecular mechanisms leading to the aberrant expression of SOX11 in MCL. To achieve this goal, we performed a comprehensive SOX11 gene expression and epigenetics study in stem cells, normal hematopoietic cells and different lymphoid neoplasms. MCLs harbor high number of genetic aberrations but none involving the SOX11 genomic region at chromosome 2p25 (Royo et al., 2011), suggesting that epigenetic changes, like DNA methylation and histone modifications, are the most likely mechanisms responsible for its expression in this lymphoid neoplasm.

Although the role of SOX11 in hematopoiesis remains unknown, its expression has been observed in several aggressive B-cell lymphomas; it is highly expressed in MCL, in a particular subtype of ALL and in some BL. Conversely, patients with indolent variant of MCL, and other mature B-cell neoplasias such as CLL, FL or DLBCL do not express SOX11 (Ek et al., 2008; Dictor et al., 2009).

In paper I, we first gathered SOX11 expression data via microarray and qRT-PCR in a broad range of lymphoid malignancies as well as in embryonic/adult stem cells and normal hematopoietic cells.

Interestingly, high SOX11 expression level was detected in non-tumoral cells like ESCs and in the embryonic cell line NTERA-2. However, SOX11 lost its expression in adult progenitor cell type like in MAPCs and MSCs, and all normal hematopoietic cells studied. In contrast, lymphoid malignancies clearly showed a differential SOX11 expression pattern among different clinicopathological diseases. In particular, SOX11 was expressed in some subtypes of ALLs (TEL-AML1-positive or with E2A

rearrangements), MCLs and part of BLs, but not in any of the other neoplasias analyzed, including the indolent variant of MCL.

As DNA methylation is the most extensively studied epigenetic mechanism leading to deregulated gene expression in cancer (Esteller, 2008; Jones and Baylin, 2007), we initially analyzed the methylation pattern of SOX11 promoter by microarrays (Bibikova et al., 2009) and bisulfite pyrosequencing (Tost and Gut, 2007). As expected, our findings showed that those samples expressing SOX11 were unmethylated.

Intriguingly, we observed that adult stem cells and normal hematopoietic cells, lacking SOX11 expression, were consistently unmethylated. In some lymphoid neoplasms without SOX11 expression, this gene acquires variable degrees of DNA methylation. These findings were in line with the DNA methylation of SOX11 recently reported in CLL, FL and DLBCL (Gustavsson et al., 2010; Tong et al., 2010).

In our series, although SOX11 was silenced in all cases showing promoter methylation, a wide range of samples, from normal cells to some lymphoid neoplasms, were also silenced independently of DNA methylation status of SOX11 promoter.

Thus, *de novo* repression in lymphoid neoplasms is unlikely to be caused by DNA methylation, that it might not be functionally relevant.

Previous studies combining epigenomic and transcriptomic analysis have demonstrated that a large proportion of the genes becoming hypermethylated in solid tumors (Keshet et al., 2006) and aggressive B-cell lymphomas (Martin-Subero et al., 2009b) are already silenced in their normal cellular counterparts. This finding could be explained by a switch of epigenetic marks between normal cells and tumor samples (Gal-Yam et al., 2008). As DNA methylation is considered to be a very stable epigenetic modification rather than histone marks, it has been hypothesized that tumors reduce their epigenetic plasticity of hypermethylating genes silenced by histone marks in normal cells (Gal-Yam et al., 2008).

In order to gain further insights into SOX11 expression patterns observed in stem cells, normal hematopoietic cells and lymphoid neoplasms, we performed ChIP followed by qPCR experiments with antibodies against activating and silencing histone marks.

We observed that SOX11 expression is associated with histone active marks in all the analyzed samples. In the embryonic cell line NTERA2, SOX11 was found expressed and its promoter displayed enrichment for the activating marks H3K4me3 and

H3K9/K14Ac. Interestingly, a B-ALL subtype with TEL-ALM1 fusion (REH cell line) and all cMCLs studied showed the same pattern of activation of SOX11 as in embryonic stem cells, i.e. enrichment for H3K4me3 and H3K9/K14Ac. This finding is in line with studies proposing that haematological neoplasms acquire chromatin features similar to stem cells (Martin-Subero et al., 2009a; Martin-Subero et al., 2009b).

In samples with SOX11 repression, including adult stem cells, normal hematopoietic cells and various lymphoid malignancies, we observed that SOX11 promoter was enriched for the silencing marks H3K9me2 and H3K27me3.

Furthermore, to study the causal relationship between SOX11 expression and epigenetic marks, we performed treatments with AZA (5-azacytidine) and/or SAHA (suberoylanilide hydroxamic acid), which inhibit DNA methylation and histone deacetylation enzymes, respectively. SAHA caused upregulation of SOX11 expression in both JVM2 and RAJI cells, independent of the distinct promoter methylation status in these cell lines. However, treatment with AZA, although decreased the DNA methylation levels, did neither alter the pattern of histone modifications nor had any effect on the SOX11 gene expression levels in RAJI.

Overall, these findings show that SOX11 expression is associated with activating histone marks whereas SOX11 repression is associated with inactivating marks with or without the simultaneous presence of DNA methylation.

Our data show that the pathogenic effect of SOX11 in lymphoid neoplasias is most likely due to its aberrant expression associated with activating histone marks in some aggressive B-cell neoplasms. Theoretically, such upregulation could be explained either by a memory of the initial cell from which these neoplasms were originated or by its *de novo* expression. The first hypothesis postulates that SOX11 is expressed in a limited window during B-cell ontogenesis, and that MCLs and some ALLs may derive from such cell type. However, SOX11 is not expressed in any of the normal human hematopoietic cells analyzed, from stem cells to plasma cells.

Additionally, we have performed a more detailed bioinformatic analysis using different mouse hematopoietic cell types derived from the Immunological Genome Project (Heng and Painter, 2008). Using this dataset, SOX11 was not expressed in any of the over 100 hematological cell types studied. Therefore, this first hypothesis cannot be supported by experimental data and a *de novo* SOX11 expression caused by a switch from

inactivating to activating histone modifications is the most likely explanation. Supporting this view is the fact that reprogramminghematopoietic cells to iPS by inducing expression of OCT4, SOX2, KLF4, and MYC (Loh et al., 2010), or only OCT4 and SOX2 (Giorgetti et al., 2009) leads to a*de novo* expression of SOX11. Thus, it is likely to hypothesize that genetic or epigenetic changes affecting SOX11 regulators take place in lymphoid neoplasms and result in aberrant *de novo* SOX11 expression (Figure 1).

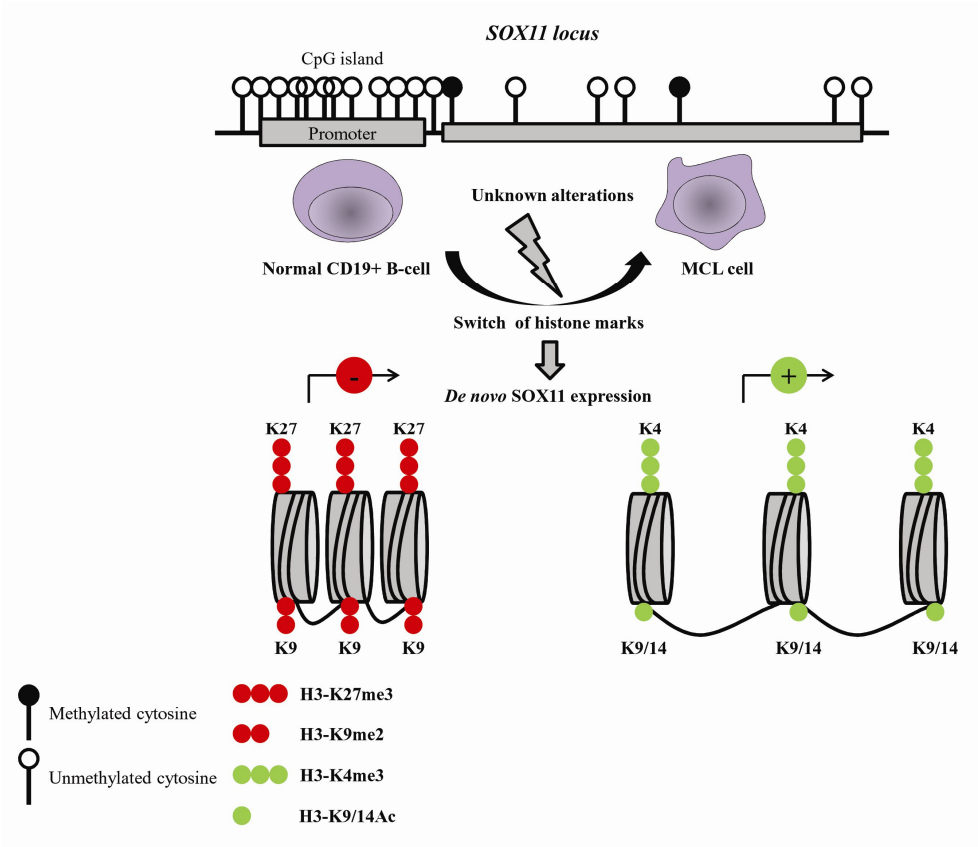

Figure 1. Hypothesis of SOX11 aberrant expression in MCL Normal CD19+ B-cell exhibits unmethylated SOX11 promoter, enrichment of repressive histone marks (H3K27me3 and H3K9me2) and do not express SOX11. In mantle cell lymphoma cell,unknown alterations cause a switch of histone marks from inactive to active ones (H3K9/14Ac and H3K4me3) resulting in an 'open' chromatin state which leads to*de novo* aberrant overexpression of SOX11 associated with aggressive phenotype.

In the case of TEL-AML1-positive B-ALLs it might bethat such fusion protein induces SOX11 expression. A recent publication has characterized the transcriptome of cord blood cells after introducing the TEL-AML1 fusion gene (Hong et al., 2008). We extracted SOX11 expression from this study and verified that its expression did not change from wild-type cord blood cells to TEL-AML1transfected cells. In the case of MCL, CCND1 expression derived from the t(11;14) translocation cannot lead to SOX11

expression, as indolent forms of MCL, that also contain the t(11;14) translocation, do not express SOX11 (Salaverria et al., 2008).

Therefore, the upstream mechanisms inducing an open chromatin conformation and subsequent oncogenic upregulation of SOX11 remain unknown.

In conclusion, our data provide a thorough investigation of SOX11 expression and epigenetic state during lymphoid development and in several lymphoid malignancies. As SOX11 is not expressed in normal lymphoid cells, its DNA hypermethylation in some neoplasms lacking SOX11 expression is most likely functionally inert, and might be associated with reducing epigenetic plasticity in tumor cells (Gal-Yam et al., 2008).

We also show that *de novo* SOX11 expression is associated with aggressive lymphoid malignancies like MCL, some ALL subtypes and a fraction of BL cases, being this effect mediated by a switch between active and repressive histone marks. Furthermore, as SOX11 is strongly expressed in ESCs, our data suggest that SOX11 expression could be associated with the acquisition of stem cell-like chromatin features, as previously proposed (Martin-Subero et al., 2009b).

At the mechanistic level, additional studies are required to elucidate which is the functional role of the illegitimate SOX11 expression in lymphoid neoplasms, and which upstream transcription factors and histone modifying enzymes are involved in this phenomenon.

NGS technology emerging in the last years has led to a better understanding of disease pathogenesis (Rossi et al., 2013). A recent study using a RNA-sequencing approach in DLBCL and FL identified an enrichment of somatic mutations affecting genes involved in transcriptional regulation and, more specifically, chromatin modification (Morin et al., 2011). MLL2, which encodes a histone methyltransferase, and MEF2B a calcium-regulated gene that cooperates with CREBBP and EP300 in acetylating histones, were found as the most frequent mutated genes in the series analyzed (Morin et al., 2011). These data have raised the hypothesis that disruption of chromatin biology might have a pivotal role in lymphomagenesis. Thus, a genetic alteration in the gene encoding an 'epigenetic enzyme' may lead to broad-spectrum changes within the epigenome, which could affect several targets, for instance if these changes cause the *de novo* expression of an oncogene then cancer may arise. NGS approach in MCL could be serving as a powerful tool to discover novel genetic alterations in this complex disease and provide

new insights into epigenome landscape which could explain such aberrant changes in gene expression, including SOX11.

4.2. Paper II

SOX11 is a new oncogene in MCL

Several recent reports have identified SOX11 as a reliable biomarker of MCL since it is expressed in ~90% of MCL (Mozos et al., 2009; Dictor et al., 2009). SOX11 is very specific for MCL as it is expressed at lower levels in a subgroup of BL and ALL, but not in other lymphoid neoplasms. SOX11 expression confers the cells a more aggressive behavior as indolent variant of MCL and normal B-cells lack the expression of this transcription factor. All these observations led to the hypothesis that SOX11 has a pivotal role in the biology of MCL and could play an oncogenic role in the pathogenesis of this disease.

In paper II, we investigated target genes and oncogenic pathways responsible for B-cell transformation and the aggressive clinical course typically associated with SOX11-high MCLs.

Towards this goal, after a precise characterization of the specificity of SOX11-antibody, we first used a ChIP-chip approach to reveal the first human genome-wide promoter analysis of SOX11 and uncovered 1133 unique genes as putative targets of this transcription factor in MCL. Furthermore, we analyzed gene expression changes associated with SOX11 short hairpin RNA knockdown to establish the specific role of SOX11 in the control of expression in MCL. GEP identified 366 genes whose expression was modulated by silencing SOX11 in MCL cell lines. Gene Ontology analyses showed that genes regulated by SOX11 in these lymphoid cells were involved in lymphocyte activation and differentiation, phosphorylation, cell cycle, immune system development, hematopoiesis, and lymphoid organ development as the top annotated functions, but also in stem cell development, apoptosis, and cell migration.

The role of different members of the SOX gene family, including SOX11, as direct regulators of differentiation program of early neural lineage development has been recently recognized in a murine model (Bergsland et al., 2011). Our ChIP-chip study confirmed that SOX11 occupied promoter sequences of target genes similar to those found in neuronal development (BTG2, MEIS1, and NREP1), but these genes were not

expressed in our lymphoid model, indicating the tissue-specific regulation of the SOX11-bound genes.

In our study, the main target genes modulated by SOX11 were involved in immune system development and hematopoiesis. PAX5, MSI2, and HSPD1 were among the most significant genes directly regulated by SOX11. Using Gene Set Enrichment Analysis (GSEA), we observed that SOX11 knockdown in MCL cells results in upregulation of gene expression signatures associated with plasma cell differentiation while suppressing the genetic programs characteristic of B-cells. Furthermore, PAX5, a key transcription factor strictly required for the establishment of B-cell identity and a major negative regulator of plasma cell differentiation, emerged as one of the most significant target genes upregulated by SOX11 in MCL.

We further validated the direct binding of SOX11 to the regulatory region of PAX5 by ChIP-qPCR in two SOX11-expressing MCL cell lines. We also verified the transcriptional effect of SOX11 on PAX5 promoter using a luciferase assay, demonstrating the specificity of SOX11 in regulating the transcription of PAX5 over the homologous protein SOX4 and mutant variants of the SOX11 protein lacking HMG or TAD. Consistently, constitutional expression of SOX11 in these tumors maintains the downstream PAX5 program. Thus, several B-cell specific genes directly activated by PAX5 were downregulated in SOX11-knockdown MCL cell lines, whereas BLIMP1 was upregulated upon SOX11 repression. Furthermore, the slight upregulation of XBP1(u) variant and immunophenotypic changes leading to downregulation of specific B-cell surface markers (CD20, CD24, IgD and IgM) in Z138 SOX11-silenced cells compared with control cells, confirmed that SOX11 downregulation is able to initiate the terminal B-cell differentiation process but is not sufficient to drive the full plasma cell program.

SOX11 is constitutively overexpressed in the vast majority of MCLs (Ek et al., 2008; Dictor et al., 2009; Mozos et al., 2009). However, recent studies have identified a subset of SOX11-negative MCLs that differs from conventional SOX11-positive tumors in their frequent hypermutated IGHV, leukemic, non-nodal presentation and more indolent clinical behavior (Orchard et al., 2003; Fernandez et al., 2010; Ondrejka et al., 2011; Navarro et al., 2012).

To investigate the potential tumorigenic ability of SOX11 *in vivo*, we studied the effect of SOX11 depletion in a MCL-xenotransplant model by inoculating CB17-SCID mice with three stably transduced shSOX11 MCL cell lines. Interestingly, we observed significative reduction in tumour growth in mice bearing silenced cells compared to scramble controls. We also observed PAX5 downregulation and BLIMP1 upregulation in immunohistochemical sections derived from SOX11-silenced tumors compared to the SOX11 positive control tumors. Moreover, we observed that SOX11-silenced tumors displayed large necrotic areas with high levels of activated cleaved caspase-3 that were minimal or not observed in SOX11-positive tumors. These results suggest that SOX11 sustains the B-cell differentiation program and tumor cell survival *in vivo* and support the implication of SOX11 expression in the aggressive behavior of these tumors.

One of the most important hallmarks of paper II is its potential clinical impact. We highlighted the relevance of our findings by integrative analyses of SOX11 shRNA knockdown induced signatures with those derived from a panel of 38 well-characterized MCL clinical samples (22 SOX11-negative and 16 SOX11-positive cases). We confirmed that the gene signatures modulated upon SOX11 silencing *in vitro* were also enriched in primary MCLs, indicating that our cell line model closely reflects the *in vivo* situation. Consistently, SOX11-positive MCL signatures were enriched in B-cell vs plasmablast and PAX5 activated gene sets, whereas the SOX11 negative MCL program was characteristically enriched in plasmablast-associated transcripts. However, the downregulation of SOX11 in both the *in vitro* model and primary tumors is not sufficient to trigger a mature plasma cell program.

These results, together with the observation that some histological examinations showed signs of focal plasmacytic differentiation and downregulation of B-cell markers expression in SOX11-negative tumors, reinforce the idea that these tumors may modulate the mature B-cell and plasmacytic differentiation programs. Conversely, SOX11 overexpression in aggressive MCL may block the cells in a mature B-cell stage, preventing their further differentiation.

The resistance of MCL to new treatments with proteasome inhibitors has been linked to the development of plasmacytic differentiation, sugesting that the findings in our study may also have implications in the design of new therapeutic strategies (Perez-Galan et al., 2011).

A common viewpoint is that the different types of mature B-cell lymphomas are blocked in a specific B-cell stage. We proposed a hypotetical model which can suggest a probable explanation about clinical heterogenity observed among SOX11-positive and SOX11-negative MCLs. The naive B-cell carrying the t(11;14) colonizes the mantle zone of the lymphoid follicle and generates an *in situ* MCL lesion. Most MCLs evolve from these cells in the marginal zone with no or limited *IGHV* somatic mutations and SOX11 expression. SOX11 overexpression in conventional MCL may block the cells in a mature B-cell stage, preventing their further differentiation through the SOX11-PAX5-PRDM1/BLIMP regulatory axis. Alternatively, some cells with the t(11;14) and lacking expression of SOX11 may enter the germinal center and undergo *IGHV* somatic hypermutation. SOX11 may modulate the mature B-cell and early plasma cell differentiation program in MCL (Figure 2).

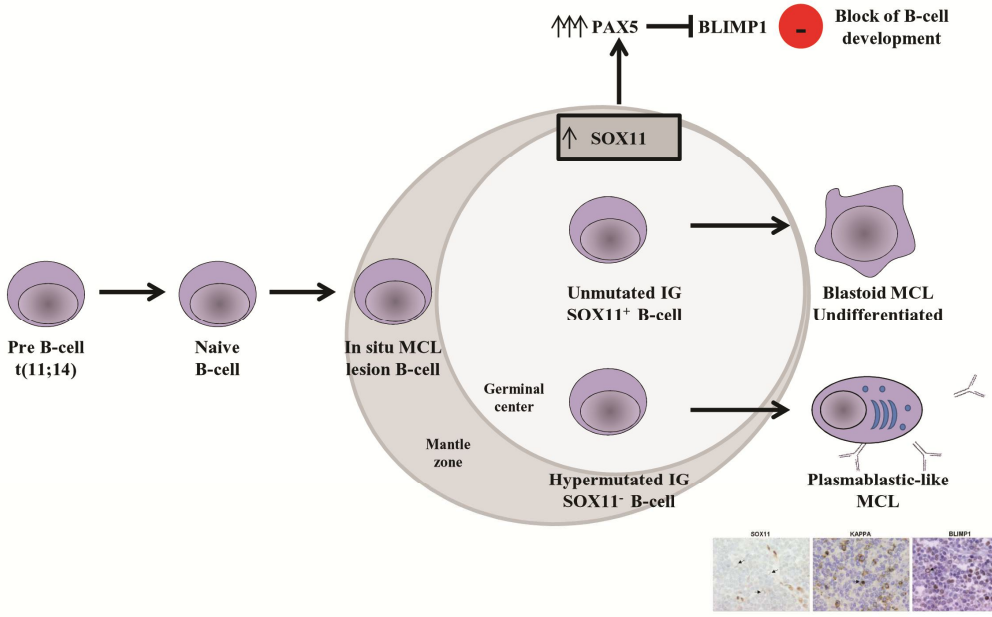

Figure 2. Hypothetical models of SOX11-positive vs SOX11 negative MCL. Modified from (Ferrando, 2013)

Mainly, SOX11 exerts its pathogenic role in MCL by maintaining constitutive expression of PAX5 and its downstrean pathway, preventing PAX5 downregulation, that is necessary to initiate the plasma cell differentiation program (Nera et al., 2006).

There has not been described any lymphopoietic function of SOX11 to date as it is not expressed in lymphoid progenitors or in mature normal B-cells. Conversely, SOX4, the SOX family member with the highest homology to SOX11, has an essential role in B-cell lymphopoiesis. Further studies will be needed to investigate whether there is a

physiologic counterpart of MCL-assosiated SOX11-PAX5-BLIMP1 axis in normal B-cells and which are the SOX factors acting upstream of this putative physiological pathway.

The significance of blocking plasma cell differentiation program as a relevant oncogenic mechanism in lymphoid neoplasias has been previously observed. The impairment of terminal B-cell differentiation caused by SOX11 overexpression in MCL may parallel the forced expression of PAX5 by the t(9;14)(p13;q32) translocation identified in some B-cell lymphomas (Busslinger et al., 1996; Iida et al., 1996; Morrison et al., 1998), and the inactivating mutations of PRDM1 in DLBCL (Mandelbaum et al., 2010; Tam et al., 2006; Pasqualucci et al., 2006).

The significant reduction on tumor growth of the SOX11-silenced cells in the xenograft experiments is consistent with the indolent clinical course of the non-nodal SOX11-negative primary MCL and highlights the implication of SOX11 expression in the aggressive behavior of conventional MCL. These results demonstrate a pivotal role of SOX11 in the growth of MCL *in vivo* suggesting its oncogenic role in the pathogenesis of classic MCL. Our hypothesis is that MCL pathogenesis is due to the combination of the deregulation of the cell proliferation by t(11;14) and cyclin D1 overexpression in early stages of the disease and the block of B-cell differentiation in a mature B-cell stage, preventing their further differentiation through the SOX11-PAX5-BLIMP1 regulatory axis (Figure 3).

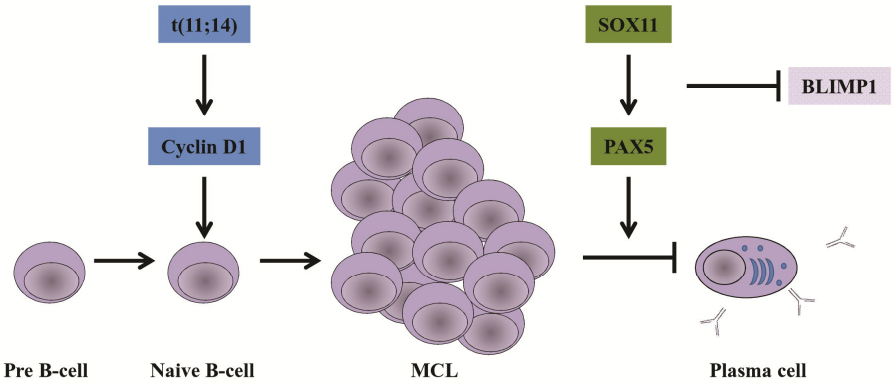

Figure 3. MCL Pathogenesis between a push of proliferation and blocking differentiation.

We identified the global transcriptional network and direct target genes regulated by SOX11 in MCL that may contribute to the development and the aggressive behavior of

this tumor. Our findings provide an improved understanding of the molecular mechanisms contributing to the pathogenesis of MCL and may have clinical implications in the diagnosis of patients and selection of therapeutic strategies more adapted to the molecular diversity of this tumor.

We described for the first time the oncogenic role of SOX11 in MCL. The expression of SOX11 in cancer was broadly described, however its function had not yet been investigated to date. High levels of SOX11 expression were detected in glioblastoma and ephitelial ovarian cancer and associated with a good prognosis in both tumors (Korkolopoulou et al., 2013; Brennan et al., 2009; Sernbo et al., 2011), suggesting its role as a tumor suppressor gene. In particular, SOX11 acts as tumor suppressor gene in glioma blocking tumorigeneis by inducing neuronal differentiation (Hide et al., 2009). The significance of SOX11 prognostic value in MCL remains under debate. Some studies have identified SOX11-negative MCLs with aggressive behavior but virtually all these cases have TP53 alterations (Royo et al., 2012; Navarro et al., 2012; Nygren et al., 2012). SOX11 negative MCLs with an aggressive behavior (Nygren et al., 2012) may correspond to a progressed or transformed stage with generalized lymphadenopathy of SOX11-negative tumors, suggesting that this phenotype may have an indolent phase and eventually some of the tumors could progress with a generalized lymphadenopathy and aggressive behavior (Jares et al., 2012).

Nearly all SOX11 positive MCLs are associated with poor prognosis (Royo et al., 2012), and in this thesis we have deciphered the structure of the SOX11-controlled oncogenic network in MCL. We have also demonstrated that aberrant *de novo* expression of SOX11 occurs in MCL, due to a switch of histone marks from inactive to active profile. SOX11-positive MCLs acquire epigenetic features similar to embryonic stem cell. Further studies will be needed to study a putative correlation between stem cell features and MCL cells. Recently, SOX11 expression was also described in breast cancer with poor prognosis and associated with embryonic mammary gene that could explain the aggressive phenotype in this type of tumor (Zvelebil et al., 2013). It is possible that SOX11 gene has different effects on tumor cells depending on the context and primary transformation mechanism. Further studies will be needed to clarify the specific mechanisms mediating the antilymphoma effect of SOX11 inactivation in MCL and which are the upstream mechanisms associated to such deregulation of B-cell differentiation.

5. CONCLUSIONS

1. SOX11 is highly expressed in ESC but it loses its expression in adult progenitor cells, including normal hematopoietic cells, suggesting that SOX11 expression in MCL could be associated with the acquisition of stem cell-like chromatin features in tumor cells.

2. SOX11 is expressed in some subtypes of ALLs (TEL-AML1-positive or with E2A rearrangements), MCLs and part of BL, but not in any other lymphoid neoplasias, including the indolent variant of MCL.

3. SOX11 is silenced in all cases showing methylation, although a wide range of samples, from normal cells to lymphoid neoplasms, are also silenced in spite of an unmethylated status of their *SOX11* promoter. This result suggests that DNA methylation does not seem to represent a mechanism leading to *de novo* SOX11 repression in lymphoid neoplasms.

4. As SOX11 is not expressed in normal lymphoid cells, the DNA promoter hypermethylation in some neoplasms lacking SOX11 expression is most likely functionally inert, and might be associated with reducing epigenetic plasticity in tumor cells.

5. SOX11 *de novo* expression is associated with aggressive lymphoid malignancies like MCL, some ALL subtypes and a fraction of BL cases, being this effect mediated by a switch between inactivating and activating histone modifications.

6. Direct target genes and transcriptional programs regulated by SOX11 in MCL were deciphered combining chromatin immunoprecipitation-microarray analysis and gene expression profiling upon SOX11 knockdown. The main pathogenic mechanism regulated by SOX11 includes the block of mature B-cell differentiation in MCL.

7. SOX11 silencing downregulates PAX5, induces BLIMP1 expression and promotes the shift from a mature B-cell into the initial plasmacytic differentiation phenotype in MCL cell lines.

8. The gene signatures modulated upon SOX11 silencing *in vitro* were also enriched in primary MCLs, indicating that our cell line model closely reflects the *in vivo* situation.

9. SOX11 overexpression in conventional MCL cases may block the cells in a mature naive stage, preventing their further differentiation through the SOX11-PAX5-PRDM1/BLIMP1 regulatory axis. Alternatively, some cells with t (11;14) lacking SOX11 expression may enter the germinal center and undergo *IGHV* somatic hypermutation.
10. SOX11 promotes tumor growth of MCL in a xenotransplant model sustaining the B-cell differentiation program and tumor cell survival *in vivo*, indicating its implication in the aggressive behavior of this tumor.
11. SOX11 is a new oncogene in MCL, therefore its silencing might represent a suitable strategy for therapeutic intervention.

6. ACKNOWLEDGMENTS

Aún no me creo que esté aquí escribiendo estas páginas después del gran esfuerzo...Tesis...una palabra que me parecía tan lejana de mi alcance.

Han pasado cuatros años desde que empecé mi aventura catalana y ahora que está a punto de concluirse un ciclo importante, no sólo para mi carrera profesional sino también a nivel personal, por todo esto quiero agradecer a las personas que han hecho posible mi llegada hasta la meta.

En primer lugar quería agradecer a la persona con la que he compartido prácticamente todo!!! Mil gracias **Jara**, por ser tan buena persona, compañera, trabajadora y consejera. Por todos los momentos que hemos compartido juntas, por todas las dificultades y las alegrías, por ser mí constante apoyo en estos años.

Gracias a **Alba** y **Cris**, por ser las primeras personas que me acogieron en este laboratorio. Gracias por estar siempre dispuestas a echarme una mano, por contestar a mis mil, y muchas veces inútiles, preguntas siempre con una sonrisa. A Cris por su extrema dulzura, por su cariño y por compartir muchas cosas de nuestras vidas personales. A Alba por darme siempre ánimo y tranquilizarme en los momentos de más agobio.

Mil gracias a todas las "super" técnicos. A **Miriam** por su alegría y disponibilidad a echarme una mano con mis experimentos, a **Noe** por su amabilidad y paciencia, a **Sara** por su generosidad y por nunca decirme no a nada y en ningún momento y finalmente a **Marta**, por haber tenido mucha paciencia conmigo, por aguantar días de mucho estrés y por traernos tanta alegría justo cuando más la necesitábamos.

Gracias a todos los pre-docs que han compartido conmigo esta maravillosa aventura durante estos años: a **Robert** por su entusiasmo y por tener siempre una explicación a cualquier duda, a **Carla** por alegrarnos tanto durante los ratos de cafés, comidas meriendas y por tener siempre algo extraordinario que contar, a **David** por su disponibilidad y por compartir el mundo "hostil" de la bioinformática y a **Ferran** por ser un excelente trabajador a pesar de su joven edad.

Gracias a **Guillem**, por su disponibilidad y ayudarnos con nuestros análisis estadísticos, por tener tanta paciencia y estar dispuesto a repetir millones de veces los análisis. Muchas gracias a los investigadores principales de nuestro grupo: a **Lluís** por estar tan

disponible a organizar y controlar todos los aspectos del laboratorio e intentar que tengamos siempre las mejores condiciones de trabajo. A **Sílvia** por ser ejemplo de tenacidad a nivel laboral, por compartir en silencio el laboratorio vacío. A **Iti** por ser tan eficiente y organizada, por ser ejemplo que se puede trabajar de mañana a tarde sin parar ni un momento.

I would like to thank Dr. Karube, for his enriching presence in our laboratory above all at scientific level. Thank you also for this extraordinary cultural exchange.

Muchas gracias al grupo "International" de Epigénetica. En primer lugar muchas gracias a **Iñaki**, el jefe, por su amabilidad, por tener interés portodos nosotros, por estar dispuesto a echarnos una mano a pesar de estar muy ocupado y por demostrarme que la investigación es algo más que un trabajo. A **Marta** y **Ana** por compartir mi condición de extranjera del laboratorio. A Marta por su alegría, sus sonrisas. A Ana por su entusiasmo y su cariño. A **Nuria** por su ejemplo de fortaleza y sus ganas de aprender siempre cosas nuevas. A **Reneé** por estar dispuesta a ayudarme con las becas, por darme buenos consejos y compartir muchas cosas personales a pesar del poco tiempo que lleva en el laboratorio. Finalmente gracias a **Giancarlo**, mi compatriota, por su amabilidad, por llevarme con paciencia a este mundo complicado de la bioinformática, por compartir muchas conversaciones sobre nuestro País, y por volvernos locos delante de un ordenador.

Muchas gracias a toda la Unidad de Genómica: **Marta**, **Pedro, Montse**, **Laura** por estar dispuestos a ayudarme y por animarme en los momentos de estrés. A **Anna** con la que he trabajado directamente, por su amabilidad, por tener siempre una explicación a cualquier duda y por tener mucha paciencia conmigo. Finalmente a **Helena** por compartir muchos momentos importantes, ser mi compañera de piso y apoyarme siempre.

Muchas gracias a las personas que han trabajado en el laboratorio, gracias a **Laura Conde** por los buenos ratos pasados juntas.

Muchas gracias al grupo de **Dolors Colomer** por pasar buenos momentos científicos juntos, en especial a **Gael** y **Patricia** con los que hemos trabajado directamente, por su amabilidad y disponibilidad a compartir sus experiencias y conocimientos.

Muchas gracias a **Carmen Muro** y **Nathalie** por llevar con extrema eficiencia toda la parte burocrática del laboratorio y hacer que todo funcione en tiempos record.

Quería agradecer a mis dos directores de tesis Elisa y Virginia, sin vosotros todo esto no hubiera sido posible. Gracias a **Virginia**, por darme la oportunidad de ser su "primera becaria", por haberme hecho aprender muchas técnicas y cosas nuevas y por haberlas aprendido juntas; gracias por haberme tratado siempre como una compañera más y no como jefa-becaria, y por hacerme crecer mucho laboralmente. Estoy convencida que esta experiencia me abrirá un buen camino en mi futuro profesional.

Muchas gracias a **Elias**, por haberme dado la oportunidad de trabajar en su brillante grupo. Gracias por la confianza, por creer en mí, por estar siempre pendiente de nuestros resultados y por animarnos siempre a mejorar. Agradezco también su capacidad de no perderse nunca ningún detalle y por ser un gran jefe.

Muchas gracias a la Lab Manager de la planta 2, **Marta Diví**, por su disponibilidad y por resolvernos rápidamente todos los problemas de laboratorio.

I would like to thank Prof. **Graziano Pesole**, Prof. **Ernesto Picardi** and Dr. **Sabino Liuni** from University of Bari (Italy) to give me the opportunity to stay in their laboratories and acquire important knowledges about the novel NGS techniques. It has been of great value for my scientific career! Thank to **Bruno** y **Giorgio**, my roommates, to have the great patience to teach bioinformatics to a biothechnologist. Thanks to **Angelica** for kindly help me with statistics and to **Nicola** to introduce me in the "Linux world".

También quería agradecer a todos mis amigos de Barcelona, que me han hecho sentir como en casa, y sufrir menos por la distancia. Gracias a **Miguel** y **Mariona** con la pequeña **Luna**, a **Paz**, **Fanny**, **Clara**, **Ricardo**, **Cesar, Lucía**, **Gemma**, **Maria** y **José Manuel** con los pequeños **Martina** y **Luis**, y a todo el grupo y a la gente de "Pacos". Gracias por cruzaros en mi camino y compartir muchas cosas importantes conmigo.

Gracias a mis compañeras de piso Suny y Lucia, por crear nuestra pequeña familia en Barcelona. **Suny** por su sabiduría y ejemplo de fortaleza personal delante de millones de dificultades. Grazie **Lu**, "la amiga de toda la vida", grazie per il tuo costante sostegno, per la tua grande disponibilità, per le lunghe chiacchierate e per non farmi sentire sola in questa città straniera.

Grazie alle mie care colleghe del CEK, **Lucia** e **Valeria**, per formare il "triangolo" Bari-Foggia-Benevento qui a Barcellona, per i momenti passati insieme davanti a un caffè, per condividere l'amore per il nostro Paese e la voglia di ritornarci.

Grazie alla mia cara amica **Maria Rita**, **Moussa** e al piccolo e dolce **Farid**. Grazie per i momenti passati insieme a Barcellona tra mille difficoltà, grazie per il tuo sostegno e per condividere con noi, nonostante la distanza, la quotidianità della vostra vita lussemburghese.

Grazie a tutti i miei cari amici di Noicattaro: **Vittoria**, **Emanuele** con i loro pargoletti **Elisa** e **Giuseppe**, **Annamaria**, **Stefano**, **Vania**, **Andrea**, **Annalinda**, e a tutto la fraternità GIFRA perché nonostante i chilometri che ci separano non avete mai fatto mancare il vostro sostegno e la vostra amicizia.

Infine vorrei ringraziare la mia famiglia. *In primis* i **miei genitori**, perché mi avete permesso di arrivare fin qui grazie ai vostri sforzi e sacrifici, per non esservi mai lamentati della mia partenza e per non avermi mai fatto mancare nulla nonostante la distanza. A mia sorella **Daniela**, per il suo affetto e per soffrire in silenzio e reciprocamente la distanza l'una dall'altra.

Alla mia "seconda" famiglia...A **Mario**, **Katia** per essere costantemente preoccupati per me e il mio lavoro. A **Lucia**, **Pino**, **Francesco** e al piccolo **Roberto**, grazie per il vostro sostegno, il vostro affetto e la pazienza di chiacchierare davanti ad un computer.

E infine grazie a colui per "colpa" del quale è iniziata la mia avventura qui a Barcellona, Grazie **Peppe** per il tuo sostegno quotidiano, per non avermi mai fatto pesare la mia scelta e per avere tanta pazienza nel sopportare la distanza. Grazie per il tuo amore incondizionato, per avermi fatto sempre sentire libera di realizzarmi professionalmente. Grazie per la forza che mi hai dimostrato e per tutti i sacrifici che hai fatto per me.

Finalmente muchas gracias a todos también a los que no he mencionado por haber hecho que lo imposible se convirtiera en realidad.

Mariella

7. REFERENCES

1. Aaboe,M., Birkenkamp-Demtroder,K., Wiuf,C., Sorensen,F.B., Thykjaer,T., Sauter,G., Jensen,K.M., Dyrskjot,L., and Orntoft,T.F. (2006). SOX4 expression in bladder carcinoma: clinical aspects and in vitro functional characterization. Cancer Res. *66*, 3434-3442.

2. Adolfsson,J., Mansson,R., Buza-Vidas,N., Hultquist,A., Liuba,K., Jensen,C.T., Bryder,D., Yang,L., Borge,O.J., Thoren,L.A., Anderson,K., Sitnicka,E., Sasaki,Y., Sigvardsson,M., and Jacobsen,S.E. (2005). Identification of Flt3+ lympho-myeloid stem cells lacking erythro-megakaryocytic potential a revised road map for adult blood lineage commitment. Cell *121*, 295-306.

3. Aggarwal,P., Vaites,L.P., Kim,J.K., Mellert,H., Gurung,B., Nakagawa,H., Herlyn,M., Hua,X., Rustgi,A.K., McMahon,S.B., and Diehl,J.A. (2010). Nuclear cyclin D1/CDK4 kinase regulates CUL4 expression andtriggers neoplastic growth via activation of the PRMT5 methyltransferase. Cancer Cell *18*, 329-340.

4. Akasaka,H., Akasaka,T., Kurata,M., Ueda,C., Shimizu,A., Uchiyama,T., and Ohno,H. (2000). Molecular anatomy of BCL6 translocations revealed by long-distance polymerase chain reaction-based assays. Cancer Res. *60*, 2335-2341.

5. Allman,D. and Pillai,S. (2008). Peripheral B cell subsets. Curr. Opin. Immunol. *20*, 149-157.

6. Allman,D., Sambandam,A., Kim,S., Miller,J.P., Pagan,A., Well,D., Meraz,A., and Bhandoola,A. (2003). Thymopoiesis independent of common lymphoid progenitors. Nat. Immunol. *4*, 168-174.

7. Alt,F.W., Yancopoulos,G.D., Blackwell,T.K., Wood,C., Thomas,E., Boss,M., Coffman,R., Rosenberg,N., Tonegawa,S., and Baltimore,D. (1984). Ordered rearrangement of immunoglobulin heavy chain variable region segments. EMBO J. *3*, 1209-1219.

8. Alt,J.R., Cleveland,J.L., Hannink,M., and Diehl,J.A. (2000). Phosphorylation-dependent regulation of cyclin D1 nuclear export and cyclin D1-dependent cellular transformation. Genes Dev. *14*, 3102-3114.

9. Andersen,C.L., Christensen,L.L., Thorsen,K., Schepeler,T., Sorensen,F.B., Verspaget,H.W., Simon,R., Kruhoffer,M., Aaltonen,L.A., Laurberg,S., and Orntoft,T.F. (2009). Dysregulation of the transcription factors SOX4, CBFB and SMARCC1 correlates with outcome of colorectal cancer. Br. J. Cancer *100*, 511-523.

10. Angelopoulou,M.K., Siakantariz,M.P., Vassilakopoulos,T.P., Kontopidou,F.N., Rassidakis,G.Z., Dimopoulou,M.N., Kittas,C., and Papalis,G.A. (2002). The splenic form of mantle cell lymphoma. Eur. J. Haematol. *68*, 12-21.

11. Argatoff,L.H., Connors,J.M., Klasa,R.J., Horsman,D.E., and Gascoyne,R.D. (1997). Mantle cell lymphoma: a clinicopathologic study of 80 cases. Blood *89*, 2067-2078.

12. Avilion,A.A., Nicolis,S.K., Pevny,L.H., Perez,L., Vivian,N., and Lovell-Badge,R. (2003). Multipotent cell lineages in early mouse development depend on SOX2 function. Genes Dev. *17*, 126-140.

13. Ballestar,E., Paz,M.F., Valle,L., Wei,S., Fraga,M.F., Espada,J., Cigudosa,J.C., Huang,T.H., and Esteller,M. (2003). Methyl-CpG binding proteins identify novel sites of epigenetic inactivation in human cancer. EMBO J. *22*, 6335-6345.

14. Baron,B.W., Nucifora,G., McCabe,N., Espinosa,R., III, Le Beau,M.M., and McKeithan,T.W. (1993). Identification of the gene associated with the recurring chromosomal translocations t(3;14)(q27;q32) and t(3;22)(q27;q11) in B-cell lymphomas. Proc. Natl. Acad. Sci. U. S. A *90*, 5262-5266.

15. Bartel,D.P. (2009). MicroRNAs: target recognition and regulatory functions. Cell *136*, 215-233.

16. Basso,K. (2009). Toward a systems biology approach to investigate cellular networks in normal and malignant B cells. Leukemia *23*, 1219-1225.

17. Basso,K. and la-Favera,R. (2010). BCL6: master regulator of the germinal center reaction and key oncogene in B cell lymphomagenesis. Adv. Immunol. *105*, 193-210.

18. Basso,K., Saito,M., Sumazin,P., Margolin,A.A., Wang,K., Lim,W.K., Kitagawa,Y., Schneider,C., Alvarez,M.J., Califano,A., and la-Favera,R. (2010). Integrated biochemical and computational approach identifies BCL6 direct target genes controlling multiple pathways in normal germinal center B cells. Blood *115*, 975-984.

19. Bea,S., Salaverria,I., Armengol,L., Pinyol,M., Fernandez,V., Hartmann,E.M., Jares,P., Amador,V., Hernandez,L., Navarro,A., Ott,G., Rosenwald,A., Estivill,X., and Campo,E. (2009). Uniparental disomies, homozygous deletions, amplifications, and target genes in mantle cell lymphoma revealed by integrative high-resolution whole-genome profiling. Blood *113*, 3059-3069.

20. Bea,S., Tort,F., Pinyol,M., Puig,X., Hernandez,L., Hernandez,S., Fernandez,P.L., van,L.M., Colomer,D., and Campo,E. (2001). BMI-1 gene amplification and overexpression in hematological malignancies occur mainly in mantle cell lymphomas. Cancer Res. *61*, 2409-2412.

21. Beltran,E., Fresquet,V., Martinez-Useros,J., Richter-Larrea,J.A., Sagardoy,A., Sesma,I., Almada,L.L., Montes-Moreno,S., Siebert,R., Gesk,S., Calasanz,M.J., Malumbres,R., Rieger,M., Prosper,F., Lossos,I.S., Piris,M.A., Fernandez-Zapico,M.E., and Martinez-Climent,J.A. (2011). A cyclin-D1 interaction with BAX underlies its oncogenic role and potential as a therapeutic target in mantle cell lymphoma. Proc. Natl. Acad. Sci. U. S. A *108*, 12461-12466.

22. Bergsland,M., Ramskold,D., Zaouter,C., Klum,S., Sandberg,R., and Muhr,J. (2011). Sequentially acting Sox transcription factors in neural lineage development. Genes Dev.*25*, 2453-2464.

23. Bergsland,M., Werme,M., Malewicz,M., Perlmann,T., and Muhr,J. (2006). The establishment of neuronal properties is controlled by Sox4 and Sox11. Genes Dev. *20*, 3475-3486.

24. Bernstein,B.E., Meissner,A., and Lander,E.S. (2007). The mammalian epigenome. Cell*128*, 669-681.

25. Bernstein,B.E., Mikkelsen,T.S., Xie,X., Kamal,M., Huebert,D.J., Cuff,J., Fry,B., Meissner,A., Wernig,M., Plath,K., Jaenisch,R., Wagschal,A., Feil,R., Schreiber,S.L., and Lander,E.S. (2006). A bivalent chromatin structure marks key developmental genes in embryonic stem cells. Cell *125*, 315-326.

26. Betticher,D.C., Thatcher,N., Altermatt,H.J., Hoban,P., Ryder,W.D., and Heighway,J. (1995). Alternate splicing produces a novel cyclin D1 transcript. Oncogene *11*, 1005-1011.

27. Bewley,C.A., Gronenborn,A.M., and Clore,G.M. (1998). Minor groove-binding architectural proteins: structure, function, and DNA recognition. Annu. Rev. Biophys. Biomol. Struct.*27*, 105-131.

28. Bibikova,M., Le,J., Barnes,B., Saedinia-Melnyk,S., Zhou,L., Shen,R., and Gunderson,K.L. (2009). Genome-wide DNA methylation profiling using Infinium(R) assay. Epigenomics.*1*, 177-200.

29. Bienvenu,F., Jirawatnotai,S., Elias,J.E., Meyer,C.A., Mizeracka,K., Marson,A., Frampton,G.M., Cole,M.F., Odom,D.T., Odajima,J., Geng,Y., Zagozdzon,A., Jecrois,M., Young,R.A., Liu,X.S., Cepko,C.L., Gygi,S.P., and Sicinski,P. (2010). Transcriptional role of cyclin D1 in development revealed by a genetic-proteomic screen. Nature*463*, 374-378.

30. Bird,A. (2002). DNA methylation patterns and epigenetic memory. Genes Dev. *16*, 6-21.

31. Blombery,P.A., Dickinson,M., and Westerman,D.A. (2013). Molecular lesions in B-cell lymphoproliferative disorders: recent contributions from studies utilizing high-throughput sequencing techniques. Leuk. Lymphoma.

32. Borriello,F., Sethna,M.P., Boyd,S.D., Schweitzer,A.N., Tivol,E.A., Jacoby,D., Strom,T.B., Simpson,E.M., Freeman,G.J., and Sharpe,A.H. (1997). B7-1 and B7-2 have overlapping, critical roles in immunoglobulin class switching and germinal center formation. Immunity.*6*, 303-313.

33. Bosch,F., Jares,P., Campo,E., Lopez-Guillermo,A., Piris,M.A., Villamor,N., Tassies,D., Jaffe,E.S., Montserrat,E., Rozman,C., and . (1994). PRAD-1/cyclin D1 gene overexpression in chronic lymphoproliferative disorders: a highly specific marker of mantle cell lymphoma. Blood*84*, 2726-2732.

34. Bracken,A.P., Pasini,D., Capra,M., Prosperini,E., Colli,E., and Helin,K. (2003). EZH2 is downstream of the pRB-E2F pathway, essential for proliferation and amplified in cancer. EMBO J.*22*, 5323-5335.

35. Brass,A.L., Kehrli,E., Eisenbeis,C.F., Storb,U., and Singh,H. (1996). Pip, a lymphoid-restricted IRF, contains a regulatory domain that is important for autoinhibition and ternary complex formation with the Ets factor PU.1. Genes Dev. *10*, 2335-2347.

36. Brass,A.L., Zhu,A.Q., and Singh,H. (1999). Assembly requirements of PU.1-Pip (IRF-4) activator complexes: inhibiting function invivo using fused dimers. EMBO J. *18*, 977-991.

37. Brennan,D.J., Ek,S., Doyle,E., Drew,T., Foley,M., Flannelly,G., O'Connor,D.P., Gallagher,W.M., Kilpinen,S., Kallioniemi,O.P., Jirstrom,K., O'Herlihy,C., and Borrebaeck,C.A. (2009). The transcription factor Sox11 is a prognostic factor for improved recurrence-free survival in epithelial ovarian cancer. Eur. J. Cancer *45*, 1510-1517.

38. Busslinger,M., Klix,N., Pfeffer,P., Graninger,P.G., and Kozmik,Z. (1996). Deregulation of PAX-5 by translocation of the Emu enhancer of the IgH locus adjacent to two alternative PAX-5 promoters in a diffuse large-cell lymphoma. Proc. Natl. Acad. Sci. U. S. A*93*, 6129-6134.

39. Butler,M.P., Iida,S., Capello,D., Rossi,D., Rao,P.H., Nallasivam,P., Louie,D.C., Chaganti,S., Au,T., Gascoyne,R.D., Gaidano,G., Chaganti,R.S., and Dalla-Favera,R. (2002). Alternative translocation breakpoint cluster region 5' to BCL-6 in B-cell non-Hodgkin's lymphoma. Cancer Res*62*, 4089-4094.

40. Cairns,B.R. (2001). Emerging roles for chromatin remodeling in cancer biology. Trends Cell Biol.*11*, S15-S21.

41. Calin,G.A. and Croce,C.M. (2006a). MicroRNA signatures in human cancers. Nat. Rev. Cancer*6*, 857-866.

42. Calin,G.A. and Croce,C.M. (2006b). MicroRNAs and chromosomal abnormalities in cancer cells. Oncogene*25*, 6202-6210.

43. Camacho,E., Hernandez,L., Hernandez,S., Tort,F., Bellosillo,B., Bea,S., Bosch,F., Montserrat,E., Cardesa,A., Fernandez,P.L., and Campo,E. (2002). ATM gene inactivation in mantle cell lymphoma mainly occurs by truncating mutations and missense mutations involving the phosphatidylinositol-3 kinase domain and is associated with increasing numbers of chromosomal imbalances. Blood *99*, 238-244.

44. Campo,E., Raffeld,M., and Jaffe,E.S. (1999).Mantle-cell lymphoma. Semin. Hematol. *36*, 115-127.

45. Casimiro,M.C., Crosariol,M., Loro,E., Ertel,A., Yu,Z., Dampier,W., Saria,E.A., Papanikolaou,A., Stanek,T.J., Li,Z., Wang,C., Fortina,P., Addya,S., Tozeren,A., Knudsen,E.S., Arnold,A., and Pestell,R.G. (2012). ChIP sequencing of cyclin

D1 reveals a transcriptional role in chromosomal instability in mice. J. Clin. Invest *122*, 833-843.

46. Chen,C.Z. (2005). MicroRNAs as oncogenes and tumor suppressors. N. Engl. J. Med. *353*, 1768-1771.

47. Chen,R.W., Bemis,L.T., Amato,C.M., Myint,H., Tran,H., Birks,D.K., Eckhardt,S.G., and Robinson,W.A. (2008). Truncation in CCND1 mRNA alters miR-16-1 regulation in mantle cell lymphoma. Blood *112*, 822-829.

48. Chen,W., Iida,S., Louie,D.C., Dalla-Favera,R. and Chaganti,R.S. (1998). Heterologous promoters fused to BCL6 by chromosomal translocations affecting band 3q27 cause its deregulated expression during B-cell differentiation. Blood *91*, 603-607.

49. Chiarle,R., Budel,L.M., Skolnik,J., Frizzera,G., Chilosi,M., Corato,A., Pizzolo,G., Magidson,J., Montagnoli,A., Pagano,M., Maes,B., De Wolf-Peeters,C., and Inghirami,G. (2000). Increased proteasome degradation of cyclin-dependent kinase inhibitor p27 is associated with a decreased overall survival in mantle cell lymphoma. Blood *95*, 619-626.

50. Chim,C.S., Wong,K.Y., Loong,F., Lam,W.W., and Srivastava,G. (2007). Frequent epigenetic inactivation of Rb1 in addition to p15 and p16 in mantle cell and follicular lymphoma. Hum. Pathol. *38*, 1849-1857.

51. Chim,C.S., Wong,K.Y., Loong,F., and Srivastava,G. (2004). SOCS1 and SHP1 hypermethylation in mantle cell lymphoma and follicular lymphoma: implications for epigenetic activation of the Jak/STAT pathway. Leukemia *18*, 356-358.

52. Ci,W., Polo,J.M., Cerchietti,L., Shaknovich,R., Wang,L., Yang,S.N., Ye,K., Farinha,P., Horsman,D.E., Gascoyne,R.D., Elemento,O., and Melnick,A. (2009). The BCL6 transcriptional program features repression of multiple oncogenes in primary B cells and is deregulated in DLBCL. Blood *113*, 5536-5548.

53. Cimmino,A., Calin,G.A., Fabbri,M., Iorio,M.V., Ferracin,M., Shimizu,M., Wojcik,S.E., Aqeilan,R.I., Zupo,S., Dono,M., Rassenti,L., Alder,H., Volinia,S., Liu,C.G., Kipps,T.J., Negrini,M., and Croce,C.M. (2005). miR-15 and miR-16 induce apoptosis by targeting BCL2. Proc. Natl. Acad. Sci. U. S. A *102*, 13944-13949.

54. Cloos,P.A., Christensen,J., Agger,K., Maiolica,A., Rappsilber,J., Antal,T., Hansen,K.H., and Helin,K. (2006). The putative oncogene GASC1 demethylates tri- and dimethylated lysine 9 on histone H3. Nature *442*, 307-311.

55. Cobaleda,C., Schebesta,A., Delogu,A., and Busslinger,M. (2007). Pax5: the guardian of B cell identity and function. Nat. Immunol. *8*, 463-470.

56. Colot,V. and Rossignol,J.L. (1999). Eukaryotic DNA methylation as an evolutionary device. Bioessays *21*, 402-411.

57. Dalla-Favera,R., Martinotti,S., Gallo,R.C., Erikson,J., and Croce,C.M. (1983). Translocation and rearrangements of the c-myc oncogene locus in human undifferentiated B-cell lymphomas. Science *219*, 963-967.

58. de Boer,C.J., Schuuring,E., Dreef,E., Peters,G., Bartek,J., Kluin,P.M., and van Krieken,J.H. (1995). Cyclin D1 protein analysis in the diagnosis of mantle cell lymphoma. Blood *86*, 2715-2723.

59. de Boer,C.J., Vaandrager,J.W., van Krieken,J.H., Holmes,Z., Kluin,P.M., and Schuuring,E. (1997). Visualization of mono-allelic chromosomal aberrations 3' and 5' of the cyclin D1 gene in mantle cell lymphoma using DNA fiber fluorescence in situ hybridization. Oncogene *15*, 1599-1603.

60. DeKoter,R.P. and Singh,H. (2000). Regulation of B lymphocyte and macrophage development by graded expression of PU.1. Science *288*, 1439-1441.

61. Del,G., I, Messina,M., Chiaretti,S., Santangelo,S., Tavolaro,S., De Propris,M.S., Nanni,M., Pescarmona,E., Mancini,F., Pulsoni,A., Martelli,M., Di,R.A., Finolezzi,E., Paoloni,F., Mauro,F.R., Cuneo,A., Gurrini,A., and Foa,R. (2012). Behind the scenes of non-nodal MCL: down-modulation of genes involved in actin cytoskeleton organization, cell projection, cell adhesion, tumour invasion, TP53 pathway and mutated status of immunoglobulin heavy chain genes. Br. J. Haematol. *156*, 601-611.

62. Delogu,A., Schebesta,A., Sun,Q., Aschenbrenner,K., Perlot,T., and Busslinger,M. (2006). Gene repression by Pax5 in B cells is essential for blood cell homeostasis and is reversed in plasma cells. Immunity. *24*, 269-281.

63. Denny,C.T., Hollis,G.F., Magrath,I.T., and Kirsch,I.R. (1985). Burkitt lymphoma cell line carrying a variant translocation creates new DNA at the breakpoint and violates the hierarchy of immunoglobulin gene rearrangement. Mol. Cell Biol. *5*, 3199-3207.

64. Di,L.L., Gomez-Lopez,G., Sanchez-Beato,M., Gomez-Abad,C., Rodriguez,M.E., Villuendas,R., Ferreira,B.I., Carro,A., Rico,D., Mollejo,M., Martinez,M.A., Menarguez,J., az-Alderete,A., Gil,J. Cigudosa,J.C., Pisano,D.G., Piris,M.A., and Martinez,N. (2010). Mantle cell lymphoma: transcriptional regulation by microRNAs. Leukemia *24*, 1335-1342.

65. Dictor,M., Ek,S., Sundberg,M., Warenholt,J., Gyorgy,C., Sernbo,S., Gustavsson,E., Abu-Alsoud,W., Wadstrom,T., and Borrebaeck,C. (2009). Strong lymphoid nuclear expression of SOX11 transcription factor defines lymphoblastic neoplasms, mantle cell lymphoma and Burkitt's lymphoma. Haematologica *94*, 1563-1568.

66. Diehl,J.A., Cheng,M., Roussel,M.F., and Sherr,C.J. (1998). Glycogen synthase kinase-3beta regulates cyclin D1 proteolysis and subcellular localization. Genes Dev. *12*, 3499-3511.

67. Dong,C., Wilhelm,D., and Koopman,P. (2004). Sox genes and cancer. Cytogenet. Genome Res. *105*, 442-447.

68. Dy,P., Penzo-Mendez,A., Wang,H., Pedraza,C.E., Macklin,W.B., and Lefebvre,V. (2008). The three SoxC proteins--Sox4, Sox11 and Sox12--exhibit overlapping expression patterns and molecular properties. Nucleic Acids Res. *36*, 3101-3117.

69. Ek,S., Dictor,M., Jerkeman,M., Jirstrom,K., and Borrebaeck,C.A. (2008). Nuclear expression of the non B-cell lineage Sox11 transcription factor identifies mantle cell lymphoma. Blood *111*, 800-805.

70. Enjuanes,A., Fernandez,V., Hernandez,L., Navarro,A., Bea,S., Pinyol,M., Lopez-Guillermo,A., Rosenwald,A., Ott,G., Campo,E., and Jares,P. (2011). Identification of methylated genes associated with aggressive clinicopathological features in mantle cell lymphoma. PLoS. One. *6*, e19736.

71. Espinet,B., Sole,F., Pedro,C., Garcia,M., Belbsillo,B., Salido,M., Florensa,L., Camacho,F.I., Baro,T., Lloreta,J., and Serrano,S. (2005). Clonal proliferation of cyclin D1-positive mantle lymphocytes in an asymptomatic patient: an early-stage event in the development or an indolent form of a mantle cell lymphoma? Hum. Pathol. *36*, 1232-1237.

72. Esteller,M. (2006). Epigenetics provides a new generation of oncogenes and tumour-suppressor genes. Br. J. Cancer *94*, 179-183.

73. Esteller,M. (2007). Cancer epigenomics: DNA methylomes and histone-modification maps. Nat. Rev. Genet. *8*, 286-298.

74. Esteller,M. (2008). Epigenetics in cancer. N Engl. J. Med. *358*, 1148-1159.

75. Esteller,M., Silva,J.M., Dominguez,G., Bonilla,F., Matias-Guiu,X., Lerma,E., Bussaglia,E., Prat,J., Harkes,I.C., Repasky,E.A., Gabrielson,E., Schutte,M., Baylin,S.B., and Herman,J.G. (2000). Promoter hypermethylation and BRCA1 inactivation in sporadic breast and ovarian tumors. J. Natl. Cancer Inst. *92*, 564-569.

76. Ewen,M.E., Sluss,H.K., Sherr,C.J., Matsushime,H., Kato,J., and Livingston,D.M. (1993). Functional interactions of the retinoblastoma protein with mammalian D-type cyclins. Cell *73*, 487-497.

77. Fabbri,M. and Croce,C.M. (2011). Role of microRNAs in lymphoid biology and disease. Curr. Opin. Hematol. *18*, 266-272.

78. Familiades,J., Bousquet,M., Lafage-Pochitaloff,M., Bene,M.C., Beldjord,K., De,V.J., Dastugue,N., Coyaud,E., Struski,S., Quelen,C., Prade-Houdellier,N., Dobbelstein,S., Cayuela,J.M., Soulier,J., Grardel,N., Preudhomme,C., Cave,H., Blanchet,O., Lheritier,V., Delannoy,A., Chalandon,Y., Ifrah,N., Pigneux,A., Brousset,P., Macintyre,E.A., Huguet,F., Dombret,H., Broccardo,C., and Delabesse,E. (2009). PAX5 mutations occur frequently in adult B-cell progenitor acute lymphoblastic leukemia and PAX5 haploinsufficiency is associated with BCR-ABL1 and TCF3-PBX1 fusion genes: a GRAALL study. Leukemia *23*, 1989-1998.

79. Feinberg,A.P. and Tycko,B. (2004). The history of cancer epigenetics. Nat. Rev. Cancer *4*, 143-153.

80. Fernandez,V., Salamero,O., Espinet,B., Sole,F., Royo,C., Navarro,A., Camacho,F., Bea,S., Hartmann,E., Amador,V., Hernandez,L., Agostinelli,C., Sargent,R.L., Rozman,M., Aymerich,M., Colomer,D., Villamor,N., Swerdlow,S.H., Pileri,S.A., Bosch,F., Piris,M.A., Montserrat,E., Ott,G., Rosenwald,A., Lopez-Guillermo,A., Jares,P., Serrano,S., and Campo,E. (2010). Genomic and gene expression profiling defines indolent forms of mantle cell lymphoma. Cancer Res. *70*, 1408-1418.

81. Ferrando,A.A. (2013). SOX11 is a mantle cell lymphoma oncogene. Blood *121*, 2169-2170.

82. Fouse,S.D., Shen,Y., Pellegrini,M., Cole,S., Meissner,A., Van,N.L., Jaenisch,R., and Fan,G. (2008). Promoter CpG methylation contributes to ES cell gene regulation in parallel with Oct4/Nanog, PcG complex, and histone H3 K4/K27 trimethylation. Cell Stem Cell *2*, 160-169.

83. Fraga,M.F., Ballestar,E., Villar-Garea,A., Boix-Chornet,M., Espada,J., Schotta,G., Bonaldi,T., Haydon,C., Ropero,S., Petrie,K., Iyer,N.G., Perez-Rosado,A., Calvo,E., Lopez,J.A., Cano,A., Calasanz,M.J., Colomer,D., Piris,M.A., Ahn,N., Imhof,A., Caldas,C., Jenuwein,T., and Esteller,M. (2005). Loss of acetylation at Lys16 and trimethylation at Lys20 of histone H4 is a common hallmark of human cancer. Nat. Genet. *37*, 391-400.

84. Fu,K., Weisenburger,D.D., Greiner,T.C., Dave,S., Wright,G., Rosenwald,A., Chiorazzi,M., Iqbal,J., Gesk,S., Siebert,R., De,J.D., Jaffe,E.S., Wilson,W.H., Delabie,J., Ott,G., Dave,B.J., Sanger,W.G., Smith,L.M., Rimsza,L., Braziel,R.M., Muller-Hermelink,H.K., Campo,E., Gascoyne,R.D., Staudt,L.M., and Chan,W.C. (2005). Cyclin D1-negative mantle cell lymphoma: a clinicopathologic study based on gene expression profiling. Blood *106*, 4315-4321.

85. Fu,M., Wang,C., Li,Z., Sakamaki,T., and Pestell,R.G. (2004). Minireview: Cyclin D1: normal and abnormal functions. Endocrinology *145*, 5439-5447.

86. Gal-Yam,E.N., Egger,G., Iniguez,L., Holster,H., Einarsson,S., Zhang,X., Lin,J.C., Liang,G., Jones,P.A., and Tanay,A. (2008). Frequent switching of Polycomb repressive marks and DNA hypermethylation in the PC3 prostate cancer cell line. Proc. Natl. Acad. Sci. U. S. A *105*, 12979-12984.

87. Gesk,S., Klapper,W., Martin-Subero,J.I., Nagel,I., Harder,L., Fu,K., Bernd,H.W., Weisenburger,D.D., Parwaresch,R., and Siebert,R. (2006). A chromosomal translocation in cyclin D1-negative/cyclin D2-positive mantle cell lymphoma fuses the CCND2 gene to the IGK locus. Blood *108*, 1109-1110.

88. Giorgetti,A., Montserrat,N., Aasen,T., Gonzalez,F., Rodriguez-Piza,I., Vassena,R., Raya,A., Boue,S., Barrero,M.J., Corbella,B.A., Torrabadella,M., Veiga,A., and Izpisua Belmonte,J.C. (2009). Generation of induced pluripotent

stem cells from human cord blood using OCT4 and SOX2. Cell Stem Cell *5*, 353-357.

89. Gladden,A.B., Woolery,R., Aggarwal,P., Wasik,M.A., and Diehl,J.A. (2006). Expression of constitutively nuclear cyclin D1 in murine lymphocytes induces B-cell lymphoma. Oncogene *25*, 998-1007.

90. Gonzalez-Zulueta,M., Bender,C.M., Yang,A.S., Nguyen,T., Beart,R.W., Van Tornout,J.M., and Jones,P.A. (1995). Methylation of the 5' CpG island of the p16/CDKN2 tumor suppressor gene in normal and transformed human tissues correlates with gene silencing. Cancer Res. *55*, 4531-4535.

91. Goossens,T., Klein,U., and Kuppers,R. (1998). Frequent occurrence of deletions and duplications during somatic hypermutation: implications for oncogene translocations and heavy chain disease. Proc. Natl. Acad. Sci. U. S. A *95*, 2463-2468.

92. Gottesfeld,J.M. and Forbes,D.J. (1997). Mitotic repression of the transcriptional machinery. Trends Biochem. Sci. *22*, 197-202.

93. Greger,V., Passarge,E., Hopping,W., Messmer,E., and Horsthemke,B. (1989). Epigenetic changes may contribute to the formation and spontaneous regression of retinoblastoma. Hum. Genet. *83*, 155-158.

94. Gronbaek,K., Straten,P.T., Ralfkiaer,E., Ahrenkiel,V., Andersen,M.K., Hansen,N.E., Zeuthen,J., Hou-Jensen,K., and Guldberg,P. (1998). Somatic Fas mutations in non-Hodgkin's lymphoma: association with extranodal disease and autoimmunity. Blood *92*, 3018-3024.

95. Gustavsson,E., Sernbo,S., Andersson,E., Brennan,D.J., Dictor,M., Jerkeman,M., Borrebaeck,C.A., and Ek,S. (2010). SOX11 expression correlates to promoter methylation and regulates tumor growth in hematopoietic malignancies. Mol. Cancer *9*, 187.

96. Guth,S.I. and Wegner,M. (2008). Having it both ways: Sox protein function between conservation and innovation. Cell Mol. Life Sci. *65*, 3000-3018.

97. Hadzidimitriou,A., Agathangelidis,A., Darzentas,N., Murray,F., fau-Larue,M.H., Pedersen,L.B., Lopez,A.N., Dagklis,A., Rombout,P., Beldjord,K., Kolstad,A., Dreyling,M.H., Anagnostopoulos,A., Tsaftaris,A., Mavragani-Tsipidou,P., Rosenwald,A., Ponzoni,M., Groenen,P., Ghia,P., Sander,B., Papadaki,T., Campo,E., Geisler,C., Rosenquist,R., Davi,F., Pott,C., and Stamatopoulos,K. (2011). Is there a role for antigen selection in mantle cell lymphoma? Immunogenetic support from a series of 807 cases. Blood *118*, 3088-3095.

98. Harris,N.L., Stein,H., Coupland,S.E., Hummel,M., Favera,R.D., Pasqualucci,L., and Chan,W.C. (2001). New approaches to lymphoma diagnosis. Hematology. Am. Soc. Hematol. Educ. Program. 194-220.

99. Hartmann,E.M., Campo,E., Wright,G., Lenz,G., Salaverria,I., Jares,P., Xiao,W., Braziel,R.M., Rimsza,L.M., Chan,W.C., Weisenburger,D.D., Delabie,J.,

Jaffe,E.S., Gascoyne,R.D., Dave,S.S., Mueller-Hermelink,H.K., Staudt,L.M., Ott,G., Bea,S., and Rosenwald,A. (2010). Pathway discovery in mantle cell lymphoma by integrated analysis of high-resolution gene expression and copy number profiling. Blood *116*, 953-961.

100. He,L. and Hannon,G.J. (2004). MicroRNAs: small RNAs with a big role in gene regulation. Nat. Rev. Genet. *5*, 522-531.

101. Heng,T.S. and Painter,M.W. (2008). The Immunological Genome Project: networks of gene expression in immune cells. Nat. Immunol. *9*, 1091-1094.

102. Herens,C., Lambert,F., Quintanilla-Martinez,L., Bisig,B., Deusings,C., and de,L.L. (2008). Cyclin D1-negative mantle cell lymphoma with cryptic t(12;14)(p13;q32) and cyclin D2 overexpression. Blod *111*, 1745-1746.

103. Herman,J.G. and Baylin,S.B. (2003). Gene silencing in cancer in association with promoter hypermethylation. N. Engl. J. Med. *349*, 2042-2054.

104. Herman,J.G., Latif,F., Weng,Y., Lerman,M.I., Zbar,B., Liu,S., Samid,D., Duan,D.S., Gnarra,J.R., Linehan,W.M., and . (1994).Silencing of the VHL tumor-suppressor gene by DNA methylation in renal carcinoma. Proc. Natl. Acad. Sci. U. S. A *91*, 9700-9704.

105. Herman,J.G., Merlo,A., Mao,L., Lapidus,R.G., Issa,J.P., Davidson,N.E., Sidransky,D., and Baylin,S.B. (1995). Inactivation of the CDKN2/p16/MTS1 gene is frequently associated with aberrant DNA methylation in all common human cancers. Cancer Res. *55*, 4525-4530.

106. Hernandez,L., Bea,S., Pinyol,M., Ott,G., Katzenberger,T., Rosenwald,A., Bosch,F., Lopez-Guillermo,A., Delabie,J., Colomer,D., Montserrat,E., and Campo,E. (2005). CDK4 and MDM2 gene alterations mainly occur in highly proliferative and aggressive mantle cell lymphomas with wild-type INK4a/ARF locus. Cancer Res. *65*, 2199-2206.

107. Hernandez,L., Fest,T., Cazorla,M., Teruya-Feldstein,J., Bosch,F., Peinado,M.A., Piris,M.A., Montserrat,E., Cardesa,A., Jaffe,E.S., Campo,E., and Raffeld,M. (1996). p53 gene mutations and protein overexpression are associated with aggressive variants of mantle cell lymphomas. Blood *87*, 3351-3359.

108. Hide,T., Takezaki,T., Nakatani,Y., Nakamura,H., Kuratsu,J., and Kondo,T. (2009). Sox11 prevents tumorigenesis of glioma-initiating cells by inducing neuronal differentiation. Cancer Res. *69*, 7953-7959.

109. Hirt,C., Schuler,F., Dolken,L., Schmidt,C.A., and Dolken,G. (2004). Low prevalence of circulating t(11;14)(q13;q32)-positive cells in the peripheral blood of healthy individuals as detected by real-time quantitative PCR. Blood *104*, 904-905.

110. Holmes,M.L., Pridans,C., and Nutt,S.L. (2008). The regulation of the B-cell gene expression programme by Pax5. Immunol. Cell Biol. *86*, 47-53.

111. Hong,D., Gupta,R., Ancliff,P., Atzberger,A., Brown,J., Soneji,S., Green,J., Colman,S., Piacibello,W., Buckle,V., Tsuzuki,S., Gottgens,B., Graves,M., and Enver,T. (2008). Initiating and cancer-propagating cells in TEL-AML1-associated childhood leukemia. Science *319*, 336-339.

112. Hoser,M., Potzner,M.R., Koch,J.M., Bosl,M.R., Wegner,M., and Sock,E. (2008). Sox12 deletion in the mouse reveals nonreciprocal redundancy with the related Sox4 and Sox11 transcription factors. Mol. Cell Biol. *28*, 4675-4687.

113. Hosokawa,Y., Joh,T., Maeda,Y., Arnold,A., and Seto,M. (1999). Cyclin D1/PRAD1/BCL-1 alternative transcript [B] protein product in B-lymphoid malignancies with t(11;14)(q13;q32) translocation. Int. J. Cancer *81*, 616-619.

114. Hu,C.C., Dougan,S.K., McGehee,A.M., Love,J.C., and Ploegh,H.L. (2009). XBP-1 regulates signal transduction, transcription factors and bone marrow colonization in B cells. EMBO J. *28*, 1624-1636.

115. Hunter,T. and Pines,J. (1994). Cyclins and cancer. II: Cyclin D and CDK inhibitors come of age. Cell *79*, 573-582.

116. Huppi,K., Volfovsky,N., Mackiewicz,M., Runfola,T., Jones,T.L., Martin,S.E., Stephens,R., and Caplen,N.J. (2007). MicroRNAs and genomic instability. Semin. Cancer Biol. *17*, 65-73.

117. Hutter,G., Scheubner,M., Zimmermann,Y., Kalla,J., Katzenberger,T., Hubler,K., Roth,S., Hiddemann,W., Ott,G., and Dreyling,M. (2006). Differential effect of epigenetic alterations and genomic deletions of CDK inhibitors [p16(INK4a), p15(INK4b), p14(ARF)] in mantle cell lymphoma. Genes Chromosomes. Cancer *45*, 203-210.

118. Iida,S., Rao,P.H., Nallasivam,P., Hibshoosh,H., Butler,M., Louie,D.C., Dyomin,V., Ohno,H., Chaganti,R.S., and Dalla-Favera,R. (1996). The t(9;14)(p13;q32) chromosomal translocation associated with lymphoplasmacytoid lymphoma involves the PAX-5 gene. Blood *88*, 4110-4117.

119. Iqbal,J., Shen,Y., Liu,Y., Fu,K., Jaffe,E.S., Liu,C., Liu,Z., Lachel,C.M., Deffenbacher,K., Greiner,T.C., Vose,J.M., Bhagavath,S., Staudt,L.M., Rimsza,L., Rosenwald,A., Ott,G., Delabie,J., Campo,E., Braziel,R.M., Cook,J.R., Tubbs,R.R., Gascoyne,R.D., Armitage,J.O., Weisenburger,D.D., McKeithan,T.W., and Chan,W.C. (2012). Genome-wide miRNA profiling of mantle cell lymphoma reveals a distinct subgroup with poor prognosis. Blood *119*, 4939-4948.

120. Iwakoshi,N.N., Lee,A.H., Vallabhajosyula,P., Otipoby,K.L., Rajewsky,K., and Glimcher,L.H. (2003). Plasma cell differentiation and the unfolded protein response intersect at the transcription factor XBP-1. Nat. Immunol. *4*, 321-329.

121. Jacobs,J.J., Kieboom,K., Marino,S., DePinho,R.A., and van,L.M. (1999). The oncogene and Polycomb-group gene bmi-1 regulates cell proliferation and senescence through the ink4a locus. Nature *397*, 164-168.

122. Jaenisch,R. and Bird,A. (2003). Epigenetic regulation of gene expression: how the genome integrates intrinsic and environmental signals. Nat. Genet. *33 Suppl*, 245-254.

123. Jankowski,M.P., Cornuet,P.K., McIlwrath,S., Koerber,H.R., and Albers,K.M. (2006). SRY-box containing gene 11 (Sox11) transcription factor is required for neuron survival and neurite growth. Neuroscience *143*, 501-514.

124. Jares,P. and Campo,E. (2008). Advances in the understanding of mantle cell lymphoma. Br. J. Haematol. *142*, 149-165.

125. Jares,P., Campo,E., Pinyol,M., Bosch,F., Miquel,R., Fernandez,P.L., Sanchez-Beato,M., Soler,F., Perez-Losada,A., Nayach,I., Mallofre,C., Piris,M.A., Montserrat,E., and Cardesa,A. (1996). Expression of retinoblastoma gene product (pRb) in mantle cell lymphomas. Correlation with cyclin D1 (PRAD1/CCND1) mRNA levels and proliferative activity. Am. J. Pathol. *148*, 1591-1600.

126. Jares,P., Colomer,D., and Campo,E. (2007). Genetic and molecular pathogenesis of mantle cell lymphoma: perspectives for new targeted therapeutics. Nat. Rev. Cancer *7*, 750-762.

127. Jares,P., Colomer,D., and Campo,E. (2012). Molecular pathogenesis of mantle cell lymphoma. J. Clin. Invest *122*, 3416-3423.

128. Jenuwein,T. and Allis,C.D. (2001). Translating the histone code. Science *293*, 1074-1080.

129. Jiang,Q., Feng,M.G., and Mo,Y.Y. (2009). Systematic validation of predicted microRNAs for cyclin D1. BMC. Cancer *9*, 194.

130. Jirawatnotai,S., Hu,Y., Michowski,W., Elias,J.E., Becks,L., Bienvenu,F., Zagozdzon,A., Goswami,T., Wang,Y.E., Clark,A.B., Kunkel,T.A., van,H.T., Xia,B., Correll,M., Quackenbush,J., Livingston,D.M., Gygi,S.P., and Sicinski,P. (2011). A function for cyclin D1 in DNA repair uncovered by protein interactome analyses in human cancers. Nature *474*, 230-234.

131. Johnson,S.M., Grosshans,H., Shingara,J., Byrom,M., Jarvis,R., Cheng,A., Labourier,E., Reinert,K.L., Brown,D., and Slack,F.J. (2005). RAS is regulated by the let-7 microRNA family. Cell *120*, 635-647.

132. Jones,P.A. and Baylin,S.B. (2007). The epigenomics of cancer. Cell *128*, 683-692.

133. Kallies,A., Hasbold,J., Fairfax,K., Pridans,C., Emslie,D., McKenzie,B.S., Lew,A.M., Corcoran,L.M., Hodgkin,P.D., Tarlinton,D.M., and Nutt,S.L. (2007). Initiation of plasma-cell differentiation is independent of the transcription factor Blimp-1. Immunity. *26*, 555-566.

134. Kamachi,Y., Cheah,K.S., and Kondoh,H. (1999). Mechanism of regulatory target selection by the SOX high-mobility-group domain proteins as revealed by comparison of SOX1/2/3 and SOX9. Mol. Cell Biol. *19*, 107-120.

135. Karpf,A.R. and Matsui,S. (2005). Genetic disruption of cytosine DNA methyltransferase enzymes induces chromosomal instability in human cancer cells. Cancer Res. *65*, 8635-8639.

136. Kerckaert,J.P., Deweindt,C., Tilly,H., Quief,S., Lecocq,G., and Bastard,C. (1993). LAZ3, a novel zinc-finger encoding gene, isdisrupted by recurring chromosome 3q27 translocations in human lymphomas. Nat. Genet. *5*, 66-70.

137. Keshet,I., Schlesinger,Y., Farkash,S., Rand,E., Hecht,M., Segal,E., Pikarski,E., Young,R.A., Niveleau,A., Cedar,H., and Simon,I. (2006). Evidence for an instructive mechanism of de novo methylation in cancer cells. Nat. Genet. *38*, 149-153.

138. Kiefer,J.C. (2007). Back to basics: Sox genes. Dev. Dyn. *236*, 2356-2366.

139. Kim,J., Sif,S., Jones,B., Jackson,A., Koipally,J., Heller,E., Winandy,S., Viel,A., Sawyer,A., Ikeda,T., Kingston,R., and Georgopoulos,K. (1999). Ikaros DNA-binding proteins direct formation of chromatin remodeling complexes in lymphocytes. Immunity. *10*, 345-355.

140. Klapper,W. (2011). Histopathology of mantle cell lymphoma. Semin. Hematol. *48*, 148-154.

141. Klein,U., Casola,S., Cattoretti,G., Shen,Q., Lia,M., Mo,T., Ludwig,T., Rajewsky,K., and Dalla-Favera,R. (2006). Transcription factor IRF4 controls plasma cell differentiation and class-switch recombination. Nat. Immunol. *7*, 773-782.

142. Klein,U. and la-Favera,R. (2008). Germinal centres: role in B-cell physiology and malignancy. Nat. Rev. Immunol. *8*, 22-33.

143. Klein,U., Tu,Y., Stolovitzky,G.A., Keller,J.L., Haddad,J., Jr., Miljkovic,V., Cattoretti,G., Califano,A., and Dalla-Favera,R. (2003). Transcriptional analysis of the B cell germinal center reaction. Proc. Natl. Acad. Sci. U. S. A *100*, 2639-2644.

144. Kolar,G.R., Mehta,D., Pelayo,R., and Capra,J.D. (2007). A novel human B cell subpopulation representing the initial germinal center population to express AID. Blood *109*, 2545-2552.

145. Komatsu,H., Iida,S., Yamamoto,K., Mikuni,C., Nitta,M., Takahashi,T., Ueda,R., and Seto,M. (1994). A variant chromosome translocation at 11q13 identifying PRAD1/cyclin D1 as the BCL-1 gene. Blood *84*, 1226-1231.

146. Korkolopoulou,P., Levidou,G., El-Habr,E.A., Adamopoulos,C., Fragkou,P., Boviatsis,E., Themistocleous,M.S., Petraki,K., Vrettakos,G., Sakalidou,M., Samaras,V., Zisakis,A., Saetta,A., Chatziandreou,I., Patsouris,E., and Piperi,C. (2013). Sox11 expression in astrocytic gliomas: correlation with nestin/c-Met/IDH1-R132H expression phenotypes, p-Stat-3 and survival. Br. J. Cancer *108*, 2142-2152.

147. Kridel,R., Meissner,B., Rogic,S., Boyle,M., Telenius,A., Woolcock,B., Gunawardana,J., Jenkins,C., Cochrane,C., Ben-Neriah,S., Tan,K., Morin,R.D., Opat,S., Sehn,L.H., Connors,J.M., Marra,M.A., Weng,A.P., Steidl,C., and Gascoyne,R.D. (2012). Whole transcriptome sequencing reveals recurrent NOTCH1 mutations in mantle cell lymphoma. Blood *119*, 1963-1971.

148. Kuhlbrodt,K., Herbarth,B., Sock,E., Enderich,J., Hermans-Borgmeyer,I., and Wegner,M. (1998). Cooperative function of POU proteins and SOX proteins in glial cells. J. Biol. Chem. *273*, 16050-16057.

149. Kuppers,R. (2005). Mechanisms of B-cell lymphoma pathogenesis. Nat. Rev. Cancer *5*, 251-262.

150. Kuppers,R. and Dalla-Favera,R. (2001). Mechanisms of chromosomal translocations in B cell lymphomas. Oncogene *20*, 5580-5594.

151. LeBien,T.W. (2000). Fates of human B-cell precursors. Blood *96*, 9-23.

152. LeBien,T.W. and Tedder,T.F. (2008). B lymphocytes: how they develop and function. Blood *112*, 1570-1580.

153. Lee,C.H., Melchers,M., Wang,H., Torrey,T.A., Slota,R., Qi,C.F., Kim,J.Y., Lugar,P., Kong,H.J., Farrington,L., van der,Z.B., Zhou,J.X., Lougaris,V., Lipsky,P.E., Grammer,A.C., and Morse,H.C., III (2006). Regulation of the germinal center gene program by interferon (IFN) regulatory factor 8/IFN consensus sequence-binding protein. J. Exp. Med *203*, 63-72.

154. Lee,C.J., Appleby,V.J., Orme,A.T., Chan,W.I., and Scotting,P.J. (2002). Differential expression of SOX4 and SOX11 in medulloblastoma. J. Neurooncol. *57*, 201-214.

155. Lefebvre,V., Dumitriu,B., Penzo-Mendez,A., Han,Y., and Pallavi,B. (2007). Control of cell fate and differentiation by Sry-related high-mobility-group box (Sox) transcription factors. Int. J. Biochem. Cell Biol. *39*, 2195-2214.

156. Leshchenko,V.V., Kuo,P.Y., Shaknovich,R., Yang,D.T., Gellen,T., Petrich,A., Yu,Y., Remache,Y., Weniger,M.A., Rafiq,S., Suh,K.S., Goy,A., Wilson,W., Verma,A., Braunschweig,I., Muthusamy,N., Kahl,B.S., Byrd,J.C., Wiestner,A., Melnick,A., and Parekh,S. (2010). Genomewide DNA methylation analysis reveals novel targets for drug development in mantle cell lymphoma. Blood *116*, 1025-1034.

157. Lessard,J. and Sauvageau,G. (2003). Bmi-1 determines the proliferative capacity of normal and leukaemic stem cells. Nature *423*, 255-260.

158. Li,J.Y., Gaillard,F., Moreau,A., Harousseau,J.L., Laboisse,C., Milpied,N., Bataille,R., and vet-Loiseau,H. (1999). Detection of translocation t(11;14)(q13;q32) in mantle cell lymphoma by fluorescence in situ hybridization. Am. J. Pathol. *154*, 1449-1452.

159. Liber,D., Domaschenz,R., Holmqvist,P.H., Mazzarella,L., Georgiou,A., Leleu,M., Fisher,A.G., Labosky,P.A., and Dillon,N. (2010). Epigenetic priming

of a pre-B cell-specific enhancer through binding of Sox2 and Foxd3 at the ESC stage. Cell Stem Cell *7*, 114-126.

160. Liu,P., Ramachandran,S., Ali,S.M., Scharer,C.D., Laycock,N., Dalton,W.B., Williams,H., Karanam,S., Datta,M.W., Jaye,D.L., and Moreno,C.S. (2006). Sex-determining region Y box 4 is a transforming oncogene in human prostate cancer cells. Cancer Res. *66*, 4011-4019.

161. Liu,Y.J. (2005). IPC: professional type 1 interferon-producing cells and plasmacytoid dendritic cell precursors. Annu. Rev. Immunol. *23*, 275-306.

162. Liu,Y.J., Grouard,G., de,B.O., and Banchereau,J. (1996). Follicular dendritic cells and germinal centers. Int. Rev. Cytol. *166*, 139-179.

163. Liu,Y.J., Zhang,J., Lane,P.J., Chan,E.Y., and MacLennan,I.C. (1991). Sites of specific B cell activation in primary and secondary responses to T cell-dependent and T cell-independent antigens. Eur. J. Immunol. *21*, 2951-2962.

164. Lo,C.F., Ye,B.H., Lista,F., Corradini,P., Offit,K., Knowles,D.M., Chaganti,R.S., and Dalla-Favera,R. (1994). Rearrangements of the BCL6 gene in diffuse large cell non-Hodgkin's lymphoma. Blood *83*, 1757-1759.

165. Loder,F., Mutschler,B., Ray,R.J., Paige,C.J., Sideras,P., Torres,R., Lamers,M.C., and Carsetti,R. (1999). B cell development in the spleen takes place in discrete steps and is determined by the quality of B cell receptor-derived signals. J. Exp. Med. *190*, 75-89.

166. Loh,Y.H., Hartung,O., Li,H., Guo,C., Sahalie,J.M., Manos,P.D., Urbach,A., Heffner,G.C., Grskovic,M., Vigneault,F., Lensch,M.W., Park,I.H., Agarwal,S., Church,G.M., Collins,J.J., Irion,S., and Daley,G.Q. (2010). Reprogramming of T cells from human peripheral blood. Cell Stem Cell *7*, 15-19.

167. Lopez,F.J., Cuadros,M., Cano,C., Concha,A., and Blanco,A. (2012). Biomedical application of fuzzy association rules for identifying breast cancer biomarkers. Med. Biol. Eng Comput. *50*, 981-990.

168. Lovec,H., Grzeschiczek,A., Kowalski,M.B., and Moroy,T. (1994). Cyclin D1/bcl-1 cooperates with myc genes in the generation of B-cell lymphoma in transgenic mice. EMBO J. *13*, 3487-3495.

169. Lu,J., Getz,G., Miska,E.A., Alvarez-Saavedra,E., Lamb,J., Peck,D., Sweet-Cordero,A., Ebert,B.L., Mak,R.H., Ferrando,A.A., Downing,J.R., Jacks,T., Horvitz,H.R., and Golub,T.R. (2005). MicroRNA expression profiles classify human cancers. Nature *435*, 834-838.

170. Lujambio,A., Ropero,S., Ballestar,E., Fraga,M.F., Cerrato,C., Setien,F., Casado,S., Suarez-Gauthier,A., Sanchez-Cespedes,M., Git,A., Spiteri,I., Das,P.P., Caldas,C., Miska,E., and Esteller,M. (2007). Genetic unmasking of an epigenetically silenced microRNA in human cancer cells. Cancer Res. *67*, 1424-1429.

171. Mack,G.S. (2006). Epigenetic cancer therapy makes headway. J. Natl. Cancer Inst. *98*, 1443-1444.

172. MacLennan,I.C. (1994). Germinal centers. Ann. Rev. Immunol. *12*, 117-139.

173. Mandelbaum,J., Bhagat,G., Tang,H., Mo,T., Brahmachary,M., Shen,Q., Chadburn,A., Rajewsky,K., Tarakhovsky,A., Pasqualucci,L., and Dalla-Favera,R. (2010). BLIMP1 is a tumor suppressor gene frequently disrupted in activated B cell-like diffuse large B cell lymphoma. Cancer Cell *18*, 568-579.

174. Martin,P., Chadburn,A., Christos,P., Weil,K., Furman,R.R., Ruan,J., Elstrom,R., Niesvizky,R., Ely,S., Diliberto,M., Melnick,A., Knowles,D.M., Chen-Kiang,S., Coleman,M., and Leonard,J.P. (2009). Outcome of deferred initial therapy in mantle-cell lymphoma. J. Clin. Oncol. *27*, 1209-1213.

175. Martin-Subero,J.I., Ammerpohl,O., Bibikova,M., Wickham-Garcia,E., Agirre,X., Alvarez,S., Bruggemann,M., Bug,S., Calasanz,M.J., Deckert,M., Dreyling,M., Du,M.Q., Durig,J., Dyer,M.J., Fan,J.B., Gesk,S., Hansmann,M.L., Harder,L., Hartmann,S., Klapper,W., Kuppers,R., Montesinos-Rongen,M., Nagel,I., Pott,C., Richter,J., Roman-Gomez,J., Seifert,M., Stein,H., Suela,J., Trumper,L., Vater,I., Prosper,F., Haferlach,C., Cruz,C.J., and Siebert,R. (2009a). A comprehensive microarray-based DNA methylation study of 367 hematological neoplasms. PLoS. One. *4*, e6986.

176. Martin-Subero,J.I., Kreuz,M., Bibikova,M., Bentink,S., Ammerpohl,O., Wickham-Garcia,E., Rosolowski,M., Richter,J., Lopez-Serra,L., Ballestar,E., Berger,H., Agirre,X., Bernd,H.W., Calvanese,V., Colquhatti,S.B., Drexler,H.G., Fan,J.B., Fraga,M.F., Hansmann,M.L., Hummel,M., Klapper,W., Korn,B., Kuppers,R., Macleod,R.A., Moller,P., Ott,G., Pott,C., Prosper,F., Rosenwald,A., Schwaenen,C., Schubeler,D., Seifert,M., Sturzenhofecker,B., Weber,M., Wessendorf,S., Loeffler,M., Trumper,L., Stein,H., Siebert,R., Esteller,M., Barker,D., Hasenclever,D., and Siebert,R. (2009b). New insights into the biology and origin of mature aggressive B-cell lymphomas by combined epigenomic, genomic, and transcriptional profiling. Blood *113*, 2488-2497.

177. Matthias,P. and Rolink,A.G. (2005). Transcriptional networks in developing and mature B cells. Nat. Rev. Immunol. *5*, 497-508.

178. McKercher,S.R., Torbett,B.E., Anderson,K.L., Henkel,G.W., Vestal,D.J., Baribault,H., Klemsz,M., Feeney,A.J., Wu,G.E., Paige,C.J., and Maki,R.A. (1996). Targeted disruption of the PU.1 gene results in multiple hematopoietic abnormalities. EMBO J. *15*, 5647-5658.

179. McManus,S., Ebert,A., Salvagiotto,G., Medvedovic,J., Sun,Q., Tamir,I., Jaritz,M., Tagoh,H., and Busslinger,M. (2011). The transcription factor Pax5 regulates its target genes by recruiting chromatin-modifying proteins in committed B cells. EMBO J. *30*, 2388-2404.

180. Medina,K.L., Garrett,K.P., Thompson,L.F., Rossi,M.I., Payne,K.J., and Kincade,P.W. (2001). Identification of very early lymphoid precursors in bone marrow and their regulation by estrogen. Nat. Immunol. *2*, 718-724.

181. Melichar,H.J., Narayan,K., Der,S.D., Hiraoka,Y., Gardiol,N., Jeannet,G., Held,W., Chambers,C.A., and Kang,J. (2007). Regulation of gammadelta versus alphabeta T lymphocyte differentiation by the transcription factor SOX13. Science *315*, 230-233.

182. Merlo,A., Herman,J.G., Mao,L., Lee,D.J., Gabrielson,E., Burger,P.C., Baylin,S.B., and Sidransky,D. (1995). 5' CpG island methylation is associated with transcriptional silencing of the tumour suppressor p16/CDKN2/MTS1 in human cancers. Nat. Med. *1*, 686-692.

183. Mikkelsen,T.S., Ku,M., Jaffe,D.B., Issac,B., Lieberman,E., Giannoukos,G., Alvarez,P., Brockman,W., Kim,T.K., Koche,R.P., Lee,W., Mendenhall,E., O'Donovan,A., Presser,A., Russ,C., Xie,X., Meissner,A., Wernig,M., Jaenisch,R., Nusbaum,C., Lander,E.S., and Bernstein,B.E. (2007). Genome-wide maps of chromatin state in pluripotent and lineage-committed cells. Nature *448*, 553-560.

184. Mitsui,K., Tokuzawa,Y., Itoh,H., Segawa,K., Murakami,M., Takahashi,K., Maruyama,M., Maeda,M., and Yamanaka,S. (2003). The homeoprotein Nanog is required for maintenance of pluripotency in mouse epiblast and ES cells. Cell *113*, 631-642.

185. Mittrucker,H.W., Matsuyama,T., Grossman,A., Kundig,T.M., Potter,J., Shahinian,A., Wakeham,A., Patterson,B., Ohashi,P.S., and Mak,T.W. (1997). Requirement for the transcription factor LSIRF/IRF4 for mature B and T lymphocyte function. Science *275*, 540-543.

186. Morin,R.D., Mendez-Lago,M., Mungall,A.J., Goya,R., Mungall,K.L., Corbett,R.D., Johnson,N.A., Severson,T.M., Chiu,R., Field,M., Jackman,S., Krzywinski,M., Scott,D.W., Trinh,D.L., Tamura-Wells,J., Li,S., Firme,M.R., Rogic,S., Griffith,M., Chan,S., Yakovenko,O., Meyer,I.M., Zhao,E.Y., Smailus,D., Moksa,M., Chittaranjan,S., Rimsza,L., Brooks-Wilson,A., Spinelli,J.J., Ben-Neriah,S., Meissner,B., Woolcock,B., Boyle,M., McDonald,H., Tam,A., Zhao,Y., Delaney,A., Zeng,T., Tse,K., Butterfield,Y., Birol,I., Holt,R., Schein,J., Horsman,D.E., Moore,R., Jones,S.J., Connors,J.M., Hirst,M., Gascoyne,R.D., and Marra,M.A. (2011). Frequent mutation of histone-modifying genes in non-Hodgkin lymphoma. Nature *476*, 298-303.

187. Morrison,A.M., Jager,U., Chott,A., Schebesta,M., Haas,O.A., and Busslinger,M. (1998). Deregulated PAX-5 transcription from a translocated IgH promoter in marginal zone lymphoma. Blood *92*, 3865-3878.

188. Mozos,A., Royo,C., Hartmann,E., De,J.D., Baro,C., Valera,A., Fu,K., Weisenburger,D.D., Delabie,J., Chuang,S.S., Jaffe,E.S., Ruiz-Marcellan,C., Dave,S., Rimsza,L., Braziel,R., Gascoyne,R.D., Sole,F., Lopez-Guillermo,A., Colomer,D., Staudt,L.M., Rosenwald,A., Ott,G., Jares,P., and Campo,E. (2009). SOX11 expression is highly specific for mantle cell lymphoma and identifies the cyclin D1-negative subtype. Haematologica *94*, 1555-1562.

189. Mullighan,C.G., Goorha,S., Radtke,I., Miller,C.B., Coustan-Smith,E., Dalton,J.D., Girtman,K., Mathew,S., Ma,J., Pounds,S.B., Su,X., Pui,C.H.,

Relling,M.V., Evans,W.E., Shurtleff,S.A., and Downing,J.R. (2007). Genome-wide analysis of genetic alterations in acute lymphoblastic leukaemia. Nature *446*, 758-764.

190. Murray,F., Darzentas,N., Hadzidimitriou,A., Tobin,G., Boudjogra,M., Scielzo,C., Laoutaris,N., Karlsson,K., Baran-Marszak,F., Tsaftaris,A., Moreno,C., Anagnostopoulos,A., Caligaris-Cappio,F., Vaur,D., Ouzounis,C., Belessi,C., Ghia,P., Davi,F., Rosenquist,R., and Stamatopoulos,K. (2008). Stereotyped patterns of somatic hypermutation in subsets of patients with chronic lymphocytic leukemia: implications for the role of antigen selection in leukemogenesis. Blood *111*, 1524-1533.

191. Navarro,A., Clot,G., Prieto,M., Royo,C., Vegliante,M.C., Amador,V., Hartmann,E., Salaverria,I., Bea,S., Martin-Subero,J.I., Rosenwald,A., Ott,G., Wiestner,A., Wilson,W.H., Campo,E., and Hernandez,L (2013). microRNA Expression Profiles Identify Subtypes of Mantle Cell Lymphoma with Different Clinicobiological Characteristics. Clin. Cancer Res.

192. Navarro,A., Clot,G., Royo,C., Jares,P., Hadzidimitriou,A., Agathangelidis,A., Bikos,V., Darzentas,N., Papadaki,T., Salaverria,I., Pinyol,M., Puig,X., Palomero,J., Vegliante,M.C., Amador,V., Martinez-Trillos,A., Stefancikova,L., Wiestner,A., Wilson,W., Pott,C., Calasanz,M.J., Trim,N., Erber,W., Sander,B., Ott,G., Rosenwald,A., Colomer,D., Gine,E., Sieberth,R., Lopez-Guillermo,A., Stamatopoulos,K., Bea,S., and Campo,E. (2012). Molecular subsets of mantle cell lymphoma defined by the IGHV mutational status and SOX11 expression have distinct biologic and clinical features. Cancer Res. *72*, 5307-5316.

193. Navarro,A., Royo,C., Hernandez,L., Jares,P., and Campo,E. (2011). Molecular pathogenesis of mantle cell lymphoma: new perspectives and challenges with clinical implications. Semin. Hematol. *48*, 155-165.

194. Nebral,K., Denk,D., Attarbaschi,A., Konig,M., Mann,G., Haas,O.A., and Strehl,S. (2009). Incidence and diversity of PAX5 fusion genes in childhood acute lymphoblastic leukemia. Leukemia *23*, 134-143.

195. Nemazee,D. and Weigert,M. (2000). Revising B cell receptors. J. Exp. Med. *191*, 1813-1817.

196. Nera,K.P., Kohonen,P., Narvi,E., Peippo,A., Mustonen,L., Terho,P., Koskela,K., Buerstedde,J.M., and Lassila,O. (2006). Loss of Pax5 promotes plasma cell differentiation. Immunity. *24*, 283-293.

197. Nera,K.P. and Lassila,O. (2006). Pax5--a critical inhibitor of plasma cell fate. Scand. J. Immunol. *64*, 190-199.

198. Nieuwenhuis,P. and Opstelten,D. (1984). Functional anatomy of germinal centers. Am. J. Anat. *170*, 421-435.

199. Nissen-Meyer,L.S., Jemtland,R., Gautvik,V.T., Pedersen,M.E., Paro,R., Fortunati,D., Pierroz,D.D., Stadelmann,V.A., Reppe,S., Reinholt,F.P., Del,F.A., Rucci,N., Teti,A., Ferrari,S., and Gautvik,K.M. (2007). Osteopenia, decreased

bone formation and impaired osteoblast developmentin Sox4 heterozygous mice. J. Cell Sci.*120*, 2785-2795.

200. Niu,H., Cattoretti,G., and la-Favera,R. (2003). BCL6 controls the expression of the B7-1/CD80 costimulatory receptor in germinal center B cells. J. Exp. Med. *198*, 211-221.

201. Niu,H., Ye,B.H., and Dalla-Favera,R. (1998). Antigen receptor signaling induces MAP kinase-mediated phosphorylation and degradation of the BCL-6 transcription factor. Genes Dev.*12*, 1953-1961.

202. Nodit,L., Bahler,D.W., Jacobs,S.A., Locker,J., and Swerdlow,S.H. (2003). Indolent mantle cell lymphoma with nodal involvement and mutated immunoglobulin heavy chain genes. Hum. Pathol.*34*, 1030-1034.

203. Norton,A.J., Matthews,J., Pappa,V., Shamash,J., Love,S., Rohatiner,A.Z., and Lister,T.A. (1995). Mantle cell lymphoma: natural history defined in a serially biopsied population over a 20-year period. Ann. Oncol. *6*, 249-256.

204. Nowling,T., Bernadt,C., Johnson,L., Desler,M., and Rizzino,A. (2003). The co-activator p300 associates physically with and can mediate the action of the distal enhancer of the FGF-4 gene. J. Biol. Chem.*278*, 13696-13705.

205. Nutt,S.L., Morrison,A.M., Dorfler,P., Rolink,A., and Busslinger,M. (1998). Identification of BSAP (Pax-5) target genes in early B-cell development by loss- and gain-of-function experiments. EMBO J.*17*, 2319-2333.

206. Nutt,S.L., Taubenheim,N., Hasbold,J., Corcoran,L.M., and Hodgkin,P.D. (2011). The genetic network controlling plasma cell differentiation. Semin. Immunol. *23*, 341-349.

207. Nygren,L., Baumgartner,W.S., Klimkowska,M., Christensson,B., Kimby,E., and Sander,B. (2012). Prognostic role of SOX11 in a population-based cohort of mantle cell lymphoma. Blood*119*, 4215-4223.

208. O'Neill,D.W., Schoetz,S.S., Lopez,R.A., Castle,M., Rabinowitz,L., Shor,E., Krawchuk,D., Goll,M.G., Renz,M., Seelig,H.P., Han,S., Seong,R.H., Park,S.D., Agalioti,T., Munshi,N., Thanos,D., Erdjument-Bromage,H., Tempst,P., and Bank,A. (2000). An ikaros-containing chromatin-remodeling complex in adult-type erythroid cells. Mol. Cell Biol.*20*, 7572-7582.

209. Okita,K., Ichisaka,T., and Yamanaka,S. (2007). Generation of germline-competent induced pluripotent stem cells. Nature*448*, 313-317.

210. Ondrejka,S.L., Lai,R., Smith,S.D., and Hsi,E.D. (2011). Indolent mantle cell leukemia: a clinicopathological variant characterized by isolated lymphocytosis, interstitial bone marrow involvement, kappa light chain restriction, and good prognosis. Haematologica*96*, 1121-1127.

211. Orchard,J., Garand,R., Davis,Z., Babbage,G., Sahota,S., Matutes,E., Catovsky,D., Thomas,P.W., Avet-Loiseau,H., and Oscier,D. (2003). A subset of t(11;14) lymphoma with mantle cell features displays mutated IgVH genes and

includes patients with good prognosis, non-nodal disease. Blood *101*, 4975-4981.

212. Ott,G., Kalla,J., Ott,M.M., Schryen,B., Katzenberger,T., Muller,J.G., and Muller-Hermelink,H.K. (1997). Blastoid variants of mantle cell lymphoma: frequent bcl-1 rearrangements at the major translocation cluster region and tetraploid chromosome clones. Blood *89*, 1421-1429.

213. Ozdag,H., Teschendorff,A.E., Ahmed,A.A., Hyland,S.J., Blenkiron,C., Bobrow,L., Veerakumarasivam,A., Burtt,G., Subkhankulova,T., Arends,M.J., Collins,V.P., Bowtell,D., Kouzarides,T., Brenton,J.D., and Caldas,C. (2006). Differential expression of selected histone modifier genes in human solid cancers. BMC. Genomics *7*, 90.

214. Pal,S., Baiocchi,R.A., Byrd,J.C., Grever,M.R., Jacob,S.T., and Sif,S. (2007). Low levels of miR-92b/96 induce PRMT5 translation and H3R8/H4R3 methylation in mantle cell lymphoma. EMBO J *26*, 3558-3569.

215. Pal,S., Yun,R., Datta,A., Lacomis,L., Erdjument-Bromage,H., Kumar,J., Tempst,P., and Sif,S. (2003). mSin3A/histone deacetylase 2- and PRMT5-containing Brg1 complex is involved in transcriptional repression of the Myc target gene cad. Mol. Cell Biol. *23*, 7475-7487.

216. Pan,G., Tian,S., Nie,J., Yang,C., Ruotti,V., Wei,H., Jonsdottir,G.A., Stewart,R., and Thomson,J.A. (2007). Whole-genome analysis of histone H3 lysine 4 and lysine 27 methylation in human embryonic stem cells. Cell Stem Cell *1*, 299-312.

217. Pasqualucci,L., Compagno,M., Houldsworth,J., Monti,S., Grunn,A., Nandula,S.V., Aster,J.C., Murty,V.V., Shipp,M.A., and la-Favera,R. (2006). Inactivation of the PRDM1/BLIMP1 gene in diffuse large B cell lymphoma. J. Exp. Med. *203*, 311-317.

218. Pasqualucci,L., Migliazza,A., Fracchiolla,N., William,C., Neri,A., Baldini,L., Chaganti,R.S., Klein,U., Kuppers,R., Rajewsky,K., and la-Favera,R. (1998). BCL-6 mutations in normal germinal center B cells: evidence of somatic hypermutation acting outside Ig loci. Proc. Natl. Acad. Sci. U. S. A *95*, 11816-11821.

219. Paun,A., Reinert,J.T., Jiang,Z., Medin,C., Balkhi,M.Y., Fitzgerald,K.A., and Pitha,P.M. (2008). Functional characterization of murine interferon regulatory factor 5 (IRF-5) and its role in the innate antiviral response. J. Biol. Chem. *283*, 14295-14308.

220. Perez-Galan,P., Mora-Jensen,H., Weniger,M.A., Shaffer,A.L., III, Rizzatti,E.G., Chapman,C.M., Mo,C.C., Stennett,L.S., Rader,C., Liu,P., Raghavachari,N., Stetler-Stevenson,M., Yuan,C., Pittaluga,S., Maric,I., Dunleavy,K.M., Wilson,W.H., Staudt,L.M., and Wiestner,A. (2011). Bortezomib resistance in mantle cell lymphoma is associated with plasmacytic differentiation. Blood *117*, 542-552.

221. Pevny,L.H. and Nicolis,S.K. (2010). Sox2 roles in neural stem cells. Int. J. Biochem. Cell Biol. *42*, 421-424.

222. Pinyol,M., Bea,S., Pla,L., Ribrag,V., Bosq,J., Rosenwald,A., Campo,E., and Jares,P. (2007). Inactivation of RB1 in mantle-cell lymphoma detected by nonsense-mediated mRNA decay pathway inhibition and microarray analysis. Blood *109*, 5422-5429.

223. Pontiggia,A., Rimini,R., Harley,V.R., Goodfellow,P.N., Lovell-Badge,R., and Bianchi,M.E. (1994). Sex-reversing mutations affect the architecture of SRY-DNA complexes. EMBO J. *13*, 6115-6124.

224. Potzner,M.R., Griffel,C., Lutjen-Drecoll,E., Bosl,M.R., Wegner,M., and Sock,E. (2007). Prolonged Sox4 expression in oligodendrocytes interferes with normal myelination in the central nervous system. Mol. Cell Biol. *27*, 5316-5326.

225. Poulat,F., Girard,F., Chevron,M.P., Goze,C., Rebillard,X., Calas,B., Lamb,N., and Berta,P. (1995). Nuclear localization of the testis determining gene product SRY. J. Cell Biol. *128*, 737-748.

226. Pridans,C., Holmes,M.L., Polli,M., Wettenhall,J.M., Dakic,A., Corcoran,L.M., Smyth,G.K., and Nutt,S.L. (2008). Identification of Pax5 target genes in early B cell differentiation. J. Immunol. *180*, 1719-1728.

227. Puente,X.S., Pinyol,M., Quesada,V., Conde,L., Ordonez,G.R., Villamor,N., Escaramis,G., Jares,P., Bea,S., Gonzalez-Diaz,M., Bassaganyas,L., Baumann,T., Juan,M., Lopez-Guerra,M., Colomer,D., Tubio,J.M., Lopez,C., Navarro,A., Tornador,C., Aymerich,M., Rozman,M., Hernandez,J.M., Puente,D.A., Freije,J.M., Velasco,G., Gutierrez-Fernandez,A., Costa,D., Carrio,A., Guijarro,S., Enjuanes,A., Hernandez,L., Yague,J., Nicolas,P., Romeo-Casabona,C.M., Himmelbauer,H., Castillo,E., Dohm,J.C., de,S.S., Piris,M.A., de,A.E., San,M.J., Royo,R., Gelpi,J.L., Torrents,D., Orozco,M., Pisano,D.G., Valencia,A., Guigo,R., Bayes,M., Heath,S., Gut,M., Klatt,P., Marshall,J., Raine,K., Stebbings,L.A., Futreal,P.A., Stratton,M.R., Campbell,P.J., Gut,I., Lopez-Guillermo,A., Estivill,X., Montserrat,E., Lopez-Otin,C., and Campo,E. (2011). Whole-genome sequencing identifies recurrent mutations in chronic lymphocytic leukaemia. Nature *475*, 101-105.

228. Qi,C.F., Xiang,S., Shin,M.S., Hao,X., Lee,C.H., Zhou,J.X., Torrey,T.A., Hartley,J.W., Fredrickson,T.N., and Morse,H.C., III (2006). Expression of the cyclin-dependent kinase inhibitor p27 and its deregulation in mouse B cell lymphomas. Leuk. Res. *30*, 153-163.

229. Quintanilla-Martinez,L., Slotta-Huspenina,J., Koch,I., Klier,M., Hsi,E.D., de,L.L., Klapper,W., Gesk,S., Siebert,R., and Fend,F. (2009). Differential diagnosis of cyclin D2+ mantle cell lymphoma based on fluorescence in situ hybridization and quantitative real-time-PCR. Haematologica *94*, 1595-1598.

230. Quintanilla-Martinez,L., vies-Hill,T., Fend,F., Calzada-Wack,J., Sorbara,L., Campo,E., Jaffe,E.S., and Raffeld,M. (2003). Sequestration of p27Kip1 protein

by cyclin D1 in typical and blastic variants of mantle cell lymphoma (MCL): implications for pathogenesis. Blood *101*, 3181-3187.

231. Raaphorst,F.M. (2005). Deregulated expression of Polycomb-group oncogenes in human malignant lymphomas and epithelial tumors. Hum. Mol. Genet. *14 Spec No 1*, R93-R100.

232. Ramirez,J., Lukin,K., and Hagman,J. (2010). From hematopoietic progenitors to B cells: mechanisms of lineage restriction and commitment. Curr. Opin. Immunol. *22*, 177-184.

233. Rawstron,A.C. (2006). Immunophenotyping of plasma cells. Curr. Protoc. Cytom. *Chapter 6*, Unit6.

234. Reik,W., Kelsey,G., and Walter,J. (1999). Dissecting de novo methylation. Nat. Genet. *23*, 380-382.

235. Reimold,A.M., Ponath,P.D., Li,Y.S., Hardy,R.R., David,C.S., Strominger,J.L., and Glimcher,L.H. (1996). Transcription factor B cell lineage-specific activator protein regulates the gene for human X-box binding protein 1. J. Exp. Med. *183*, 393-401.

236. Remenyi,A., Lins,K., Nissen,L.J., Reinbold,R., Scholer,H.R., and Wilmanns,M. (2003). Crystal structure of a POU/HMG/DNA ternary complex suggests differential assembly of Oct4 and Sox2 on two enhancers. Genes Dev. *17*, 2048-2059.

237. Reynaud,D., Demarco,I.A., Reddy,K.L., Schjerven,H., Bertolino,E., Chen,Z., Smale,S.T., Winandy,S., and Singh,H. (2008). Regulation of B cell fate commitment and immunoglobulin heavy-chain gene rearrangements by Ikaros. Nat. Immunol. *9*, 927-936.

238. Richon,V.M., Sandhoff,T.W., Rifkind,R.A., and Marks,P.A. (2000). Histone deacetylase inhibitor selectively induces p21WAF1 expression and gene-associated histone acetylation. Proc. Natl. Acad. Sci. U. S. A *97*, 10014-10019.

239. Rimokh,R., Berger,F., Delsol,G., Digonnet,I., Rouault,J.P., Tigaud,J.D., Gadoux,M., Coiffier,B., Bryon,P.A., and Magaud,J.P. (1994). Detection of the chromosomal translocation t(11;14) by polymerase chain reaction in mantle cell lymphomas. Blood *83*, 1871-1875.

240. Ripperger,T., von,N.N., Kamphues,K., Emura,M., Lehmann,U., Tauscher,M., Schraders,M., Groenen,P., Skawran,B., Rudolph,C., Gillet-Bauchu,E., van Krieken,J.H., Schlegelberger,B., and Steinemann,D. (2007). Promoter methylation of PARG1, a novel candidate tumor suppressor gene in mantle-cell lymphomas. Haematologica *92*, 460-468.

241. Rosenwald,A., Wright,G., Wiestner,A., Chan,W.C., Connors,J.M., Campo,E., Gascoyne,R.D., Grogan,T.M., Muller-Hermelink,H.K., Smeland,E.B., Chiorazzi,M., Giltnane,J.M., Hurt,E.M., Zhao,H., Averett,L., Henrickson,S., Yang,L., Powell,J., Wilson,W.H., Jaffe,E.S., Simon,R., Klausner,R.D., Montserrat,E., Bosch,F., Greiner,T.C., Weisenburger,D.D., Sanger,W.G.,

Dave,B.J., Lynch,J.C., Vose,J., Armitage,J.O., Fisher,R.I., Miller,T.P., LeBlanc,M., Ott,G., Kvaloy,S., Holte,H., Delabie,J., and Staudt,L.M. (2003). The proliferation gene expression signature is a quantitative integrator of oncogenic events that predicts survival in mantle cell lymphoma. Cancer Cell *3*, 185-197.

242. Rossi,D., Ciardullo,C., and Gaidano,G. (2013). Genetic aberrations of signaling pathways in lymphomagenesis: Revelations from nextgeneration sequencing studies. Semin. Cancer Biol.

243. Royo,C., Navarro,A., Clot,G., Salaverria,I., Gine,E., Jares,P., Colomer,D., Wiestner,A., Wilson,W.H., Vegliante,M.C., Fernandez,V., Hartmann,E.M., Trim,N., Erber,W.N., Swerdlow,S.H., Klapper,W., Dyer,M.J., Vargas-Pabon,M., Ott,G., Rosenwald,A., Siebert,R., Lopez-Guillermo,A., Campo,E., and Bea,S. (2012). Non-nodal type of mantle cell lymphoma is a specific biological and clinical subgroup of the disease. Leukemia.

244. Royo,C., Salaverria,I., Hartmann,E.M., Rosenwald,A., Campo,E., and Bea,S. (2011). The complex landscape of genetic alterations in mantle cell lymphoma. Semin. Cancer Biol. *21*, 322-334.

245. Rule,S.A., Poplar,S., Evans,P.A., O'Connor,S.J., and Owen,R.G. (2011). Indolent mantle-cell lymphoma: immunoglobulin variable region heavy chain sequence analysis reveals evidence of disease 10 years prior to symptomatic clinical presentation. J. Clin. Oncol. *29*, e437-e439.

246. Saito,M., Gao,J., Basso,K., Kitagawa,Y., Smith,P.M., Bhagat,G., Pernis,A., Pasqualucci,L., and la-Favera,R. (2007). A signaling pathway mediating downregulation of BCL6 in germinal center B cells is blocked by BCL6 gene alterations in B cell lymphoma. Cancer Cell *12*, 280-292.

247. Saito,Y., Liang,G., Egger,G., Friedman,J.M.,Chuang,J.C., Coetzee,G.A., and Jones,P.A. (2006). Specific activation of microRNA-127 with downregulation of the proto-oncogene BCL6 by chromatin-modifying drugs in human cancer cells. Cancer Cell *9*, 435-443.

248. Sakai,T., Toguchida,J., Ohtani,N., Yandell,D.W., Rapaport,J.M., and Dryja,T.P. (1991). Allele-specific hypermethylation of the retinoblastoma tumor-suppressor gene. Am. J. Hum. Genet. *48*, 880-888.

249. Salaverria,I., Royo,C., Carvajal-Cuenca,A., Clot,G., Navarro,A., Valera,A., Song,J.Y., Woroniecka,R., Rymkiewicz,G., Klapper,W., Hartmann,E.M., Sujobert,P., Wlodarska,I., Ferry,J.A., Gaulard,P., Ott,G., Rosenwald,A., Lopez-Guillermo,A., Quintanilla-Martinez,L., Harris,N.L., Jaffe,E.S., Siebert,R., Campo,E., and Bea,S. (2013). CCND2 rearrangements are the most frequent genetic events in cyclin D1(-) mantle cell lymphoma. Blood *121*, 1394-1402.

250. Salaverria,I., Zettl,A., Bea,S., Hartmann,E.M., Dave,S.S., Wright,G.W., Boerma,E.J., Kluin,P.M., Ott,G., Chan,W.C., Weisenburger,D.D., Lopez-Guillermo,A., Gascoyne,R.D., Delabie,J., Rimsza,L.M., Braziel,R.M., Jaffe,E.S., Staudt,L.M., Muller-Hermelink,H.K., Campo,E., and Rosenwald,A.

(2008). Chromosomal alterations detected by comparative genomic hybridization in subgroups of gene expression-defined Burkitt's lymphoma. Haematologica *93*, 1327-1334.

251. Salaverria,I., Zettl,A., Bea,S., Moreno,V., Valls,J., Hartmann,E., Ott,G., Wright,G., Lopez-Guillermo,A., Chan,W.C., Weisenburger,D.D., Gascoyne,R.D., Grogan,T.M., Delabie,J., Jaffe,E.S., Montserrat,E., Muller-Hermelink,H.K., Staudt,L.M., Rosenwald,A., and Campo,E. (2007). Specific secondary genetic alterations in mantle cell lymphoma provide prognostic information independent of the gene expression-based proliferation signature. J. Clin. Oncol. *25*, 1216-1222.

252. Sander,B., Flygare,J., Porwit-Macdonald,A., Smith,C.I., Emanuelsson,E., Kimby,E., Liden,J., and Christensson,B. (2005). Mantle cell lymphomas with low levels of cyclin D1 long mRNA transcripts are highly proliferative and can be discriminated by elevated cyclin A2 and cyclin B1. Int. J. Cancer *117*, 418-430.

253. Sarkar,A. and Hochedlinger,K. (2013). The sox family of transcription factors: versatile regulators of stem and progenitor cell fate. Cell Stem Cell *12*, 15-30.

254. Scaffidi,P. and Bianchi,M.E. (2001). Spatially precise DNA bending is an essential activity of the sox2 transcription factor. J. Biol. Chem. *276*, 47296-47302.

255. Schebesta,A., McManus,S., Salvagiotto,G., Delogu,A., Busslinger,G.A., and Busslinger,M. (2007). Transcription factor Pax5 activates the chromatin of key genes involved in B cell signaling, adhesion, migration, and immune function. Immunity. *27*, 49-63.

256. Schilham,M.W. and Clevers,H. (1998). HMG box containing transcription factors in lymphocyte differentiation. Semin. Immunol. *10*, 127-132.

257. Schilham,M.W., Moerer,P., Cumano,A., and Clevers,H.C. (1997). Sox-4 facilitates thymocyte differentiation. Eur. J. Immunol. *27*, 1292-1295.

258. Schilham,M.W., Oosterwegel,M.A., Moerer,P., Ya,J., de Boer,P.A., van de,W.M., Verbeek,S., Lamers,W.H., Kruisbeek,A.M., Cumano,A., and Clevers,H. (1996). Defects in cardiac outflow tract formation and pro-B-lymphocyte expansion in mice lacking Sox-4. Nature *380*, 711-714.

259. Schuettengruber,B., Chourrout,D., Vervoort,M., Leblanc,B., and Cavalli,G. (2007). Genome regulation by polycomb and trithorax proteins. Cell *128*, 735-745.

260. Sciammas,R., Shaffer,A.L., Schatz,J.H., Zhao,H., Staudt,L.M., and Singh,H. (2006). Graded expression of interferon regulatory factor-4 coordinates isotype switching with plasma cell differentiation. Immunity. *25*, 225-236.

261. Sernbo,S., Gustavsson,E., Brennan,D.J., Gallagher,W.M., Rexhepaj,E., Rydnert,F., Jirstrom,K., Borrebaeck,C.A., and Ek,S. (2011). The tumour suppressor SOX11 is associated with improved survival among high grade

epithelial ovarian cancers and is regulated by reversible promoter methylation. BMC. Cancer *11*, 405.

262. Seto,M., Yamamoto,K., Iida,S., Akao,Y., Utsumi,K.R., Kubonishi,I., Miyoshi,I., Ohtsuki,T., Yawata,Y., Namba,M., and . (1992). Gene rearrangement and overexpression of PRAD1 in lymphoid malignancy with t(11;14)(q13;q32) translocation. Oncogene *7*, 1401-1406.

263. Shaffer,A.L., Emre,N.C., Romesser,P.B., and Staudt,L.M. (2009). IRF4: Immunity. Malignancy! Therapy? Clin. Cancer Res *15*, 2954-2961.

264. Shaffer,A.L., Shapiro-Shelef,M., Iwakoshi,N.N., Lee,A.H., Qian,S.B., Zhao,H., Yu,X., Yang,L., Tan,B.K., Rosenwald,A., Hurt,E.M., Petroulakis,E., Sonenberg,N., Yewdell,J.W., Calame,K., Glimcher,L.H., and Staudt,L.M. (2004). XBP1, downstream of Blimp-1, expands the secretory apparatus and other organelles, and increases protein synthesis in plasma cell differentiation. Immunity. *21*, 81-93.

265. Shaffer,A.L., Yu,X., He,Y., Boldrick,J., Chan,E.P., and Staudt,L.M. (2000). BCL-6 represses genes that function in lymphocyte differentiation, inflammation, and cell cycle control. Immunity *13*, 199-212.

266. Shapiro-Shelef,M. and Calame,K. (2005). Regulation of plasma-cell development. Nat. Rev. Immunol. *5*, 230-242.

267. Shaughnessy,J., Jr., Gabrea,A., Qi,Y., Brents,L., Zhan,F., Tian,E., Sawyer,J., Barlogie,B., Bergsagel,P.L., and Kuehl,M. (2001). Cyclin D3 at 6p21 is dysregulated by recurrent chromosomal translocations to immunoglobulin loci in multiple myeloma. Blood *98*, 217-223.

268. Shiller,S.M., Zieske,A., Holmes,H., III, Feldman,A.L., Law,M.E., and Saad,R. (2011). CD5-positive, cyclinD1-negative mantle cell lymphoma with a translocation involving the CCND2 gene and the IGL locus. Cancer Genet. *204*, 162-164.

269. Sock,E., Rettig,S.D., Enderich,J., Bosl,M.R., Tamm,E.R., and Wegner,M. (2004). Gene targeting reveals a widespread role for the high-mobility-group transcription factor Sox11 in tissue remodeling. Mol. Cell Biol. *24*, 6635-6644.

270. Solomon,D.A., Wang,Y., Fox,S.R., Lambeck,T.C., Giesting,S., Lan,Z., Senderowicz,A.M., Conti,C.J., and Knudsen,E.S. (2003). Cyclin D1 splice variants. Differential effects on localization, RB phosphorylation, and cellular transformation. J. Biol. Chem. *278*, 30339-30347.

271. Sonoki,T., Harder,L., Horsman,D.E., Karran,L., Taniguchi,I., Willis,T.G., Gesk,S., Steinemann,D., Zucca,E., Schlegelberger,B., Sole,F., Mungall,A.J., Gascoyne,R.D., Siebert,R., and Dyer,M.J. (2001). Cyclin D3 is a target gene of t(6;14)(p21.1;q32.3) of mature B-cell malignancies. Blood *98*, 2837-2844.

272. Sparmann,A. and van,L.M. (2006). Polycomb silencers control cell fate, development and cancer. Nat. Rev. Cancer *6*, 846-856.

273. Spencer,J., Finn,T., Pulford,K.A., Mason,D.Y., and Isaacson,P.G. (1985). The human gut contains a novel population of B lymphocytes which resemble marginal zone cells. Clin. Exp. Immunol. *62*, 607-612.

274. Sridharan,R. and Smale,S.T. (2007). Predominant interaction of both Ikaros and Helios with the NuRD complex in immature thymocytes. J. Biol. Chem. *282*, 30227-30238.

275. Stolt,C.C., Lommes,P., Friedrich,R.P., and Wegner,M. (2004). Transcription factors Sox8 and Sox10 perform non-equivalent roles during oligodendrocyte development despite functional redundancy. Development *131*, 2349-2358.

276. Stolt,C.C., Schmitt,S., Lommes,P., Sock,E., and Wegner,M. (2005). Impact of transcription factor Sox8 on oligodendrocyte specification in the mouse embryonic spinal cord. Dev. Biol. *281*, 309-317.

277. Sudbeck,P. and Scherer,G. (1997). Two independent nuclear localization signals are present in the DNA-binding high-mobility group domains of SRY and SOX9. J. Biol. Chem. *272*, 27848-27852.

278. Swerdlow,S., Campo,E., Harris,N., Jaffe,E., Pileri,S., Stein,H., Thiele,J., and Vardiman,J. (2008). WHO Classification of Tumours of Haematopoietic and Lymphoid Tissues.

279. Takahashi,K. and Yamanaka,S. (2006). Induction of pluripotent stem cells from mouse embryonic and adult fibroblast cultures by defined factors. Cell *126*, 663-676.

280. Takaoka,A., Yanai,H., Kondo,S., Duncan,G., Negishi,H., Mizutani,T., Kano,S., Honda,K., Ohba,Y., Mak,T.W., and Taniguchi,T. (2005). Integral role of IRF-5 in the gene induction programme activated by Toll-like receptors. Nature *434*, 243-249.

281. Tam,W., Gomez,M., Chadburn,A., Lee,J.W., Chan,W.C., and Knowles,D.M. (2006). Mutational analysis of PRDM1 indicates a tumor-suppressor role in diffuse large B-cell lymphomas. Blood *107*, 4090-4100.

282. Teramoto,N., Pokrovskaja,K., Szekely,L., Polack,A., Yoshino,T., Akagi,T., and Klein,G. (1999). Expression of cyclin D2 and D3 in lymphoid lesions. Int. J. Cancer *81*, 543-550.

283. Tiemann,M., Schrader,C., Klapper,W., Dreyling,M.H., Campo,E., Norton,A., Berger,F., Kluin,P., Ott,G., Pileri,S., Pedrinis,E., Feller,A.C., Merz,H., Janssen,D., Hansmann,M.L., Krieken,H., Moller,P., Stein,H., Unterhalt,M., Hiddemann,W., and Parwaresch,R. (2005). Histopathology, cell proliferation indices and clinical outcome in 304 patients with mantle cell lymphoma (MCL): a clinicopathological study from the European MCL Network. Br. J. Haematol. *131*, 29-38.

284. Tong,W.G., Wierda,W.G., Lin,E., Kuang,S.Q., Bekele,B.N., Estrov,Z., Wei,Y., Yang,H., Keating,M.J., and Garcia-Manero,G. (2010). Genome-wide DNA methylation profiling of chronic lymphocytic leukemia allows identification of

epigenetically repressed molecular pathways with clinical impact. Epigenetics. *5*, 499-508.

285. Tort,F., Hernandez,S., Bea,S., Martinez,A., Esteller,M., Herman,J.G., Puig,X., Camacho,E., Sanchez,M., Nayach,I., Lopez-Guillermo,A., Fernandez,P.L., Colomer,D., Hernandez,L., and Campo,E. (2002). CHK2 decreased protein expression and infrequent genetic alterations mainly occur in aggressive types of non-Hodgkin lymphomas. Blood *100*, 4602-4608.

286. Tost,J. and Gut,I.G. (2007). DNA methylation analysis by pyrosequencing. Nat. Protoc. *2*, 2265-2275.

287. Tsuda,M., Takahashi,S., Takahashi,Y., and Asahara,H. (2003). Transcriptional co-activators CREB-binding protein and p300 regulate chondrocyte-specific gene expression via association with Sox9. J. Biol. Chem. *278*, 27224-27229.

288. Tsujimoto,Y., Gorham,J., Cossman,J., Jaffe,E., and Croce,C.M. (1985). The t(14;18) chromosome translocations involved in B-cell neoplasms result from mistakes in VDJ joining. Science *229*, 1390-1393.

289. Tsujimoto,Y., Louie,E., Bashir,M.M., and Croce,C.M. (1988). The reciprocal partners of both the t(14; 18) and the t(11; 14) translocations involved in B-cell neoplasms are rearranged by the same mechanism. Oncogene *2*, 347-351.

290. Tunyaplin,C., Shaffer,A.L., Angelin-Duclos,C.D., Yu,X., Staudt,L.M., and Calame,K.L. (2004). Direct repression of prdm1 by Bcl-6 inhibits plasmacytic differentiation. J. Immunol. *173*, 1158-1165.

291. Turner,C.A., Jr., Mack,D.H., and Davis,M.M. (1994). Blimp-1, a novel zinc finger-containing protein that can drive the maturation of B lymphocytes into immunoglobulin-secreting cells. Cell *77*, 297-306.

292. Urbanek,P., Wang,Z.Q., Fetka,I., Wagner,E.F., and Busslinger,M. (1994). Complete block of early B cell differentiation and altered patterning of the posterior midbrain in mice lacking Pax5/BSAP. Cell *79*, 901-912.

293. Vaissiere,T., Sawan,C., and Herceg,Z. (2008). Epigenetic interplay between histone modifications and DNA methylation in gene silencing. Mutat. Res. *659*, 40-48.

294. van de Wetering,M., Oosterwegel,M., van,N.K., and Clevers,H. (1993). Sox-4, an Sry-like HMG box protein, is a transcriptional activator in lymphocytes. EMBO J. *12*, 3847-3854.

295. Vastenhouw,N.L. and Schier,A.F. (2012). Bivalent histone modifications in early embryogenesis. Curr. Opin. Cell Biol. *24*, 374-386.

296. Wang,X., Asplund,A.C., Porwit,A., Flygare,J., Smith,C.I., Christensson,B., and Sander,B. (2008). The subcellular Sox11 distribution pattern identifies subsets of mantle cell lymphoma: correlation to overall survival. Br. J. Haematol. *143*, 248-252.

297. Weber,M., Hellmann,I., Stadler,M.B., Ramos,L., Paabo,S., Rebhan,M., and Schubeler,D. (2007). Distribution, silencing potential and evolutionary impact of promoter DNA methylation in the human genome. Nat.Genet. *39*, 457-466.

298. Wegner,M. (1999). From head to toes: the multiple facets of Sox proteins. Nucleic Acids Res. *27*, 1409-1420.

299. Wegner,M. (2011). SOX after SOX: SOXession regulates neurogenesis. Genes Dev. *25*, 2423-2428.

300. Wegner,M. and Stolt,C.C. (2005). From stem cells to neurons and glia: a Soxist's view of neural development. Trends Neurosci. *28*, 583-588.

301. Weigle,B., Ebner,R., Temme,A., Schwind,S., Schmitz,M., Kiessling,A., Rieger,M.A., Schackert,G., Schackert,H.K., and Rieber,E.P. (2005). Highly specific overexpression of the transcription factor SOX11 in human malignant gliomas. Oncol. Rep. *13*, 139-144.

302. Weiss,M.A. (2001). Floppy SOX: mutual induced fit in hmg (high-mobility group) box-DNA recognition. Mol. Endocrinol. *15*, 353-362.

303. Wiestner,A., Tehrani,M., Chiorazzi,M., Wright,G., Gibellini,F., Nakayama,K., Liu,H., Rosenwald,A., Muller-Hermelink,H.K., Ott,G., Chan,W.C., Greiner,T.C., Weisenburger,D.D., Vose,J., Armitage,J.O., Gascoyne,R.D., Connors,J.M., Campo,E., Montserrat,E., Bosch,F., Smeland,E.B., Kvaloy,S., Holte,H., Delabie,J., Fisher,R.I., Grogan,T.M., Miller,T.P., Wilson,W.H., Jaffe,E.S., and Staudt,L.M. (2007). Point mutations and genomic deletions in CCND1 create stable truncated cyclin D1 mRNAs that are associated with increased proliferation rate and shorter survival. Blood *109*, 4599-4606.

304. Wilson,M. and Koopman,P. (2002). Matching SOX: partner proteins and co-factors of the SOX family of transcriptional regulators. Curr. Opin. Genet. Dev. *12*, 441-446.

305. Wlodarska,I., Dierickx,D., Vanhentenrijk,V., Van,R.K., Pospisilova,H., Minnei,F., Verhoef,G., Thomas,J., Vandenberghe,P., and De Wolf-Peeters,C. (2008). Translocations targeting CCND2, CCND3, and MYCN do occur in t(11;14)-negative mantle cell lymphomas. Blood *111*, 5683-5690.

306. Wolffe,A.P. (2001). Chromatin remodeling: why it is important in cancer. Oncogene *20*, 2988-2990.

307. Wurm,A., Sock,E., Fuchshofer,R., Wegner,M., and Tamm,E.R. (2008). Anterior segment dysgenesis in the eyes of mice deficient for the high-mobility-group transcription factor Sox11. Exp. Eye Res. *86*, 895-907.

308. Xiong,Y., Connolly,T., Futcher,B., and Beach,D. (1991). Human D-type cyclin. Cell *65*, 691-699.

309. Xu,W. and Li,J.Y. (2010). SOX11 expression in mantle cell lymphoma. Leuk. Lymphoma *51*, 1962-1967.

310. Yang,X.J. (2004). The diverse superfamily of lysine acetyltransferases and their roles in leukemia and other diseases. Nucleic Acids Res. *32*, 959-976.

311. Yasuda,T., Hayakawa,F., Kurahashi,S., Sugimoto,K., Minami,Y., Tomita,A., and Naoe,T. (2012). B cell receptor-ERK1/2 signal cancels PAX5-dependent repression of BLIMP1 through PAX5 phosphorylation a mechanism of antigen-triggering plasma cell differentiation. J. Immunol *188*, 6127-6134.

312. Ye,B.H., Lista,F., Lo,C.F., Knowles,D.M., Offit,K., Chaganti,R.S., and Dalla-Favera,R. (1993). Alterations of a zinc finger-encoding gene, BCL-6, in diffuse large-cell lymphoma. Science *262*, 747-750.

313. Yin,C.C., Medeiros,L.J., Cromwell,C.C., Mehta,A.P., Lin,P., Luthra,R., and Abruzzo,L.V. (2007). Sequence analysis proves clonal identity in five patients with typical and blastoid mantle cell lymphoma. Mod Pathol. *20*, 1-7.

314. Yoshida,H., Matsui,T., Yamamoto,A., Okada,T., and Mori,K. (2001). XBP1 mRNA is induced by ATF6 and spliced by IRE1 in response to ER stress to produce a highly active transcription factor. Cell *107*, 881-891.

315. Yuan,H., Corbi,N., Basilico,C., and Dailey,L. (1995). Developmental-specific activity of the FGF-4 enhancer requires the synergistic action of Sox2 and Oct-3. Genes Dev. *9*, 2635-2645.

316. Zhao,J.J., Lin,J., Lwin,T., Yang,H., Guo,J., Kong,W., Dessureault,S., Moscinski,L.C., Rezania,D., Dalton,W.S., Sotomayor,E., Tao,J., and Cheng,J.Q. (2010). microRNA expression profile and identification of miR-29 as a prognostic marker and pathogenetic factor by targeting CDK6 in mantle cell lymphoma. Blood *115*, 2630-2639.

317. Zhao,X.D., Han,X., Chew,J.L., Liu,J., Chiu,K.P., Choo,A., Orlov,Y.L., Sung,W.K., Shahab,A., Kuznetsov,V.A., Bourque,G., Oh,S., Ruan,Y., Ng,H.H., and Wei,C.L. (2007). Whole-genome mapping of histone H3 Lys4 and 27 trimethylations reveals distinct genomic compartments in human embryonic stem cells. Cell Stem Cell *1*, 286-298.

318. Zvelebil,M., Oliemuller,E., Gao,Q., Wansbury,O., Mackay,A., Kendrick,H., Smalley,M.J., Reis-Filho,J.S., and Howard,B.A. (2013). Embryonic mammary signature subsets are activated in Brca1-/- and basal-like breast cancers. Breast Cancer Res. *15*, R25.

8. APPENDIX

Appendix I

Leukemia. 2012 Aug;26(8):1895-8

Non-nodal type of mantle cell lymphoma is a specific biological and clinical subgroup of the disease.

Royo C, Navarro A, Clot G, Salaverria I, Giné E, Jares P, Colomer D, Wiestner A, Wilson WH, Vegliante MC, Fernandez V, Hartmann EM, Trim N, Erber WN, Swerdlow SH, Klapper W, Dyer MJ, Vargas-Pabón M, Ott G, Rosenwald A, Siebert R, López-Guillermo A, Campo E, Beà S.

Mantle cell lymphoma (MCL) is an aggressive B-cell neoplasm with a median survival of the patients of 3–5 years. This aggressive behavior has been related to its genetic and molecular pathogenesis that integrates the deregulation of cell proliferation due to the t(11;14)(q13;q32) and cyclin D1 overexpression, and the accumulation of a high number of chromosomal aberrations mainly targeting genes related to DNA damage response and the cell survival pathways. Thus, it is usually recommended that patients with MCL should be treated with chemotherapeutic regimens immediately following their diagnosis. However, this attitude is being reconsidered, due in part to the increasing recognition of subsets of patients that do not need therapy for a long period of time and the observation that deferral of treatment does not seem to impair their global outcome. The identification of asymptomatic patients at diagnosis that may benefit from initial watch and wait approach is challenging because some studies have shown that intensive treatment may improve the survival of patients with MCL. Therefore, it is of paramount importance to develop clinical and biological criteria that may assist in the selection of the optimal individual management for patients with MCL.

Appendix II

Cancer Res. 2012 Oct 15;72(20):5307-16

Molecular subsets of mantle cell lymphoma defined by the IGHV mutational status and SOX11 expression have distinct biologic and clinical features.

Navarro A, Clot G, Royo C, Jares P, Hadzidimitriou A, Agathangelidis A, Bikos V, Darzentas N, Papadaki T, Salaverria I, Pinyol M, Puig X, Palomero J, Vegliante MC, Amador V, Martinez-Trillos A, Stefancikova L, Wiestner A, Wilson W, Pott C, Calasanz MJ, Trim N, Erber W, Sander B, Ott G, Rosenwald A, Colomer D, Giné E, Siebert R, Lopez-Guillermo A, Stamatopoulos K, Beà S, Campo E.

Mantle cell lymphoma (MCL) is a heterogeneous disease with most patients following an aggressive clinical course, whereas others having an indolent behavior. We conducted an integrative and multidisciplinary analysis of 177 MCL to determine whether the immunogenetic features of the clonotypic B-cell receptors (BcR) may identify different subsets of tumors. Truly unmutated (100% identity) IGHV genes were found in 24% cases, 40% were minimally/borderline mutated (99.9%-97%), 19% significantly mutated (96.9%-95%), and 17% hypermutated (<95%). Tumors with high or low mutational load used different IGHV genes, and their gene expression profiles were also different for several gene pathways. A gene set enrichment analysis showed that MCL with high and low IGHV mutations were enriched in memory and naive B-cell signatures, respectively. Furthermore, the highly mutated tumors had less genomic complexity, were preferentially SOX11-negative, and showed more frequent non-nodal disease. The best cut-off of germline identity of IGHV genes to predict survival was 97%. Patients with high and low mutational load had significant different outcome with 5-year overall survival (OS) of 59% and 40%, respectively (P = 0.004). Nodal presentation and SOX11 expression also predicted for poor OS. In a multivariate analysis, IGHV gene status and SOX11 expression were independent risk factors. In conclusion, these observations suggest the idea that MCL with mutated IGHV, SOX11-negativity, and non-nodal presentation correspond to a subtype of the disease with more indolent behavior.

Appendix III

Clin Cancer Res. 2013 Jun 15;19(12):3121-3129

microRNA Expression Profiles Identify Subtypes of Mantle Cell Lymphoma with Different Clinicobiological Characteristics.

Navarro A, Clot G, Prieto M, Royo C, Vegliante MC, Amador V, Hartmann E, Salaverria I, Beà S, Martín-Subero JI, Rosenwald A, Ott G, Wiestner A, Wilson WH, Campo E, Hernández L.

PURPOSE:

MicroRNAs (miRNA) are posttranscriptional gene regulators that may be useful as diagnostic and/or prognostic biomarkers. We aim to study the expression profiles of a high number of miRNAs and their relationship with clinicopathologic and biologic relevant features in leukemic mantle cell lymphomas (MCL).

EXPERIMENTAL DESIGN:

Expression profiling of 664 miRNAs was investigated using a high-throughput quantitative real-time PCR platform in 30 leukemic MCLs. Statistical and bioinformatic analyses were conducted to define miRNAs associated with different clinicopathologic parameters. Gene expression profiling was investigated by microarrays in 16 matching cases to study the potential genes and pathways targeted by selected miRNAs. The prognostic value of miR-34a was investigated in 2 independent series of 29 leukemic and 50 nodal MCLs.

RESULTS:

Robust consensus clustering defined 2 main MCL subgroups with significant differences in the immunoglobulin (IGHV) mutational status, SOX11 expression, genomic complexity, and nodal clinical presentation. Supervised analyses of IGHV and SOX11 categories identified 17 and 22 miRNAs differentially expressed, respectively. Enriched targets of these miRNAs corresponded to relevant pathways in MCL pathogenesis such as DNA stress response, CD40 signaling, and chromatin modification. In addition, we found 7 miRNAs showing prognostic significance independently of IGHV status and SOX11 expression. Among them, miR-34a was also

associated with poor prognosis in 2 independent series of leukemic and nodal MCL, and in cooperation with high expression of the MYC oncogene.